



UNIL | Université de Lausanne

Unicentre

CH-1015 Lausanne

<http://serval.unil.ch>

Year : 2012

SOURCE, FATE AND FUNCTION OF EARLY GLIAL CELLS EXPRESSING NKX2.1 IN MOUSE EMBRYONIC BRAINS

VALLOTON Delphine

VALLOTON Delphine, 2012, SOURCE, FATE AND FUNCTION OF EARLY GLIAL CELLS
EXPRESSING NKX2.1 IN MOUSE EMBRYONIC BRAINS

Originally published at : Thesis, University of Lausanne

Posted at the University of Lausanne Open Archive.
<http://serval.unil.ch>

Droits d'auteur

L'Université de Lausanne attire expressément l'attention des utilisateurs sur le fait que tous les documents publiés dans l'Archive SERVAL sont protégés par le droit d'auteur, conformément à la loi fédérale sur le droit d'auteur et les droits voisins (LDA). A ce titre, il est indispensable d'obtenir le consentement préalable de l'auteur et/ou de l'éditeur avant toute utilisation d'une oeuvre ou d'une partie d'une oeuvre ne relevant pas d'une utilisation à des fins personnelles au sens de la LDA (art. 19, al. 1 lettre a). A défaut, tout contrevenant s'expose aux sanctions prévues par cette loi. Nous déclinons toute responsabilité en la matière.

Copyright

The University of Lausanne expressly draws the attention of users to the fact that all documents published in the SERVAL Archive are protected by copyright in accordance with federal law on copyright and similar rights (LDA). Accordingly it is indispensable to obtain prior consent from the author and/or publisher before any use of a work or part of a work for purposes other than personal use within the meaning of LDA (art. 19, para. 1 letter a). Failure to do so will expose offenders to the sanctions laid down by this law. We accept no liability in this respect.



Département de Biologie Cellulaire et Morphologie

**SOURCE, FATE AND FUNCTION OF EARLY GLIAL CELLS
EXPRESSING NKX2.1 IN MOUSE EMBRYONIC BRAINS**

Thèse de doctorat en Neurosciences

présentée à la

Faculté de Biologie et de Médecine
de l'Université de Lausanne

par

Delphine VALLOTON

Biologiste diplômée de l'Université de Lausanne, Suisse

Jury

Prof. Philippe Maeder, Président
Dr. Cécile Lebrand, Directrice
Prof. Jean-Pierre Hornung, Co-directeur
Dr. Sonia Garel, Experte
Prof. Alexandre Dayer, Expert

Lausanne 2012

*Programme doctoral interuniversitaire en Neurosciences
des Universités de Lausanne et Genève*



**UNIVERSITÉ
DE GENÈVE**

Imprimatur

Vu le rapport présenté par le jury d'examen, composé de

<i>Président</i>	Monsieur Prof. Philippe Maeder
<i>Directeur de thèse</i>	Madame Dr Cécile Lebrand
<i>Co-directeur de thèse</i>	Monsieur Prof. Jean-Pierre Hornung
<i>Experts</i>	Monsieur Prof. Alexandre Dayer Madame Dr Sonia Garel

le Conseil de Faculté autorise l'impression de la thèse de

Madame Delphine Valloton

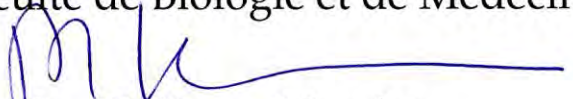
master en biologie médicale de l'Université de Lausanne

intitulée

**SOURCE, FATE AND FUNCTION OF EARLY GLIAL CELLS
EXPRESSING NKX2.1 IN MOUSE EMBRYONIC BRAINS**

Lausanne, le 31 mai 2012

pour Le Doyen
de la Faculté de Biologie et de Médecine


Prof. Philippe Maeder

ACKNOWLEDGMENTS

The first person I would like to thank a lot is of course my thesis director Cécile, who accepted to take me in her lab 5 years ago, for performing my master work first, what led then to these exciting thesis studies with a lot of sudden revivals. So, thank you, Cécile, for giving me such a great opportunity to achieve my PhD in your team. Thank you also for sharing the so many skills you possess in “Science”, for your dynamism, for your enthusiasm and tenacity, and all the time and energy you have given to offer me a favorable and prosperous thesis environment. Thanks for your availability, for the understanding you have shown and for the support you have given to me when I had doubts. Finally, thank you for this unforgettable and emotionally rich adventure.

I would like also to thank Jean-Pierre Hornung for his dedicated support and for kindly welcoming me and for sharing his lab space and equipment since the very beginning of my master until the very last moments of my PhD studies. Many thanks also for sharing your scientific knowledge and for your wise advices on many aspects of our research.

Thank you also to all the members of my master, half-thesis and thesis jury who kindly accepted to review my work many times through the last years. Thanks for the time you have offered and that you offer again, and for your scientific remarks.

Then, I would like to thank a few teams:

The Lebrand’s team in which I am proud to be the second student and maybe unfortunately... the last to end its thesis studies, and in which I feel like I had the chance to be guided by two pionnering axo... members.

Ladies first, so thanks to Christiane for her kindness and who has taken care of our psychological and unmaterial concerns with gentleness, for her technical and unmeasurable help in molecular biology; to Carine for all the working hours that you made so nice to go through, for all the fun, for all the laugh we had inside and out of the lab and for your endless creativity that just started to emerge in our first Christmas costumes and for giving me so often the account of your adventures; to Shilpi for her enormous investment and quick acclimatization in the work of the lab and for her brilliant to visionnary skills and knowledge in science, but also for many gales of laughter and for our good indian and greek food sessions.

And then the guys, so thanks to Sebastien and Mathieu who both gave me the impulse to choose the Lebrand’s team, to Belkacem who shared also with us nearly one year of its life in the lab and also many beers and parties outside of the lab.

The Hornung’s team

Thank you Dominique for your kindness, for your availability, for teaching me also a piece of your expertise in histology and thanks also for the nice chats during the long hours of dissection, cutting or mounting the brain slices. Then thanks to all the past and present members of the lab, so thank you Natacha, Peggy, Mary-Aude, Christine, Lionel, Alessandro, Julien and Alex and for all the fun we had and thank you everyone for making this journey enjoyable.

I would like also to give a special big Thanks to both teams together, for your presence and your support at all the dance shows and Christmas choreography I gave during the last five years since I think they were around 9!

Thanks also to all the members of the DBCM,

Fanny, Alain and all the members of the animal facility for taking care of our mice, Alex Sandoval and Yannick for informatical help, Eric for the printing of the posters and manuscript, Rudolf for its precious help in statistics and the secretariat team.

I would like also to thank some other people and teams that brought help in many ways
So thanks to:

Jean-Luc Martin and Hubert Fiumelli who gave me the opportunity to start in their team for my pre-master work during which I already learned a lot, and a special thank to Hubert who taught us and set up the equipment for the *In Utero* electroporation.

Jean-Yves Chatton and the CIF team for teaching me THE confocal microscopy, Christophe Lamy for helping me to give practicals in confocal microscopy and for sharing his knowledge in live imaging.

Yvan Arsenijevic for the neurosphere's technique.

Sonia Bolea, Sonia Garel, Alexandre Dayer, Denis Jabaudon, Victor Borrell, Gord Fishell, Oscar Marin, for their encouragements, advises and support.

Then I would like to thank more intimately some colleagues:

To all guys of the coffee and apero corner, thank you for your kindness, availability, happiness and humanity and for everything you have done to make the work place more warm, funny, lively and welcoming. Thank you Jannick, Nieves, Nicole, Marie, Guylène, Saska, Sanda, Maria, Francine, Shilpi, the Romanette's, Dimitri, Guy, Charles, Denis, Gilles, Alessandro, Hadi, David, Evrim...

To Peter Clarke and all the Christmas party staff:

The dancers and acrobats: Shilpi, Saska, Nicole, Franceline, Marie, Guylène, Christine, Tugce, Nieves, Jannick, Maria, Francine, Carine, Sanda, Valeria, Michel, Alex, Dimitri, Guy, Donald.

Two rock bands: A great thank to Michel Kielar our spiritual guide and musical leader, to Matthieu for the equipment and the drums, to Christophe for the guitar bass, to Mathieu and Dutch for the folk guitar and vocals and to Lily for the outstanding vocal performance.

Finally, I would like to thank my friends and family who largely contribute to this adventure.

Thank you, my Friends of Ever, Marylaure, Simone and Sonia for the years of friendship.
Thank you for being here at any time.

Thank you, my dancing friends and teachers, Jean-Philippe, Marion, Héloïse, Baronne, Alice, Gwendolyn, Marinaz, Daniela, and so many others...

Thank you, my friends from le gymnase du soir, Carine, Aurore, Amanny, Stephane, Sophie and Manu.

Thank you, my new friends, Lily, Laurent, Damien, Alex and Dutch.

Thank you, my parents and my brother, for taking care of me since ever.
Thank you, my new family.

And finally, Thank You, Mathieu, to have taken me as your Padawan in science, but more importantly to protect me, to support me, to daily share your feelings and emotions with me, and to share a big piece of life with me.

ABSTRACT

Source, fate and function of early glial cells expressing *Nkx2.1* in mouse embryonic brains

Delphine Valloton

Department of Cellular Biology and Morphology

The brain tissue is made of neuronal and glial cells generated in the germinal layer bordering the ventricles. These cells divide, differentiate and migrate following specific pathways. The specification of GABAergic interneurons and glutamatergic neurons has been broadly studied but little is known about the origin, the fate and the function of early glial cells in the embryonic telencephalon. It has been commonly accepted since long that the glial cells and more particularly the astrocytes were generated after neurogenesis from the dorsal telencephalon. However, our work shows that, unlike what was previously thought, numerous glial cells (astroglia and polydendrocytes) are generated during neurogenesis in the early embryonic stages from E14.5 to E16.5, and originate from the ventral *Nkx2.1*-expressing precursors instead.

NK2 homeobox 1 (*Nkx2.1*) is a member of the NK2 family of homeodomain-containing transcription factors. The specification of the MGE precursors requires the expression of the *Nkx2.1* homeobox gene. Moreover, *Nkx2.1* is previously known to regulate the specification of GABAergic interneurons and early oligodendrocytes in the ventral telencephalon.

Here, in my thesis work, I have discovered that, in addition, *Nkx2.1* also regulates astroglia and polydendrocytes differentiation. The use of *Nkx2.1* antibody and *Nkx2.1* riboprobe have revealed the presence of numerous *Nkx2.1*-positive cells that express astroglial markers (like GLAST and GFAP) in the entire embryonic brain. Thus, to selectively fate map MGE-derived GABAergic interneurons and glia, we crossed *Nkx2.1-Cre* mice, *Glast-Cre ERT^{+/+}* inducible mice and *NG2-Cre mice* with the Cre reporter *Rosa26-lox-STOP-lox-YFP (Rosa26-YFP)* mice.

The precise origin of *Nkx2.1*-positive astroglia has been directly ascertained by combining glial immunostaining and focal electroporation of the *pCAG-GS-EGFP* plasmids into the subpallial domains of organotypic slices, as well as, by using *in vitro* neurosphere experiments and *in utero* electroporation of the *pCAG-GS-tomato* plasmid into the ventral pallium of E14.5 *Nkx2.1-Cre⁺/Rosa-YFP^{+/+}* embryos. We have, thus, confirmed that the three germinal regions of the ventral telencephalon i.e. the MGE, the AEP/POA and the triangular septal nucleus are able to generate early astroglial cells.

Moreover, immunohistochemistry for several astroglial cells and polydendrocyte markers, both in the *Nkx2.1*^{-/-} and control embryos and in the neurospheres, has revealed a severe loss of both glial cell types in the Nkx2.1 mutants. We found that the loss of glia corresponded to a decrease of *Nkx2.1*-derived precursor division capacity and glial differentiation. There was a drastic decrease of BrdU⁺ dividing cells labeled for Nkx2.1 in the MGE*, the POA* and the septal nucleus* of Nkx2.1 mutants. In addition, we noticed that while some remaining Nkx2.1⁺ precursors still succeeded to give rise to post-mitotic neurons *in vitro* and *in vivo* in the *Nkx2.1*^{-/-}, they completely lost the capacity to differentiate in astrocytes. Altogether, these observations indicate for the first time that the transcription factor Nkx2.1 regulates the proliferation and differentiation of precursors in three subpallial domains that generate early embryonic astroglia and polydendrocytes.

Furthermore, in order to investigate the potential function of these early *Nkx2.1*-derived glia, we have performed multiple immunohistochemical stainings on *Nkx2.1*^{-/-} and wild-type animals, and *Nkx2.1-Cre* mice that were crossed to *Rosa-DTA*^{+/-} mice in which the highly toxic diphtheria toxin aided to selectively deplete a majority of the *Nkx2.1*-derived cells. Interestingly, in these two mutants, we observed a drastic and significant loss of GFAP⁺, GLAST⁺, NG2⁺ and S100β⁺ astroglial cells at the telencephalic midline and in the medial cortical areas. This cells loss could be directly correlated with severe axonal guidance defects observed in the corpus callosum (CC), the hippocampal commissure (HIC), the fornix (F) and the anterior commissure (AC).

Axonal guidance is a key step allowing neurons to form specific connections and to become organized in a functional network. The contribution of guidepost cells inside the CC and the AC in mediating the growth of commissural axons have until now been attributed to specialized midline guidepost astroglia. Previous published results in our group have unravelled that, during embryonic development, the CC is populated in addition to astroglia by numerous glutamatergic and GABAergic guidepost neurons that are essential for the correct midline crossing of callosal axons. Therefore, the relative contribution of individual neuronal or glial populations towards the guidance of commissural axons remains largely to be investigated to understand guidance mechanisms further. Thus, we crossed *Nkx2.1-Cre* mice with *NSE-DTA*^{+/-} mice that express the diphtheria toxin only in neurons and allowed us to selectively deplete *Nkx2.1*-derived GABAergic neurons. Interestingly, in the *Nkx2.1*^{-/-} mice, the CC midline was totally disorganized and the callosal axons partly lost their orientation, whereas in the *Nkx2.1Cre*⁺/*Rosa-DTA*^{+/-} and the *Nkx2.1Cre*⁺/*NSE-DTA*^{+/-} mice, the axonal organization of the CC was not affected. In the three types of mice, hippocampal axons of the fornix were not properly fasciculated and formed disoriented bundles through the septum. Additionally, the AC formation was completely absent in *Nkx2.1*^{-/-} mice and the AC was

divided into two/three separate paths in the *Nkx2.1Cre⁺/Rosa-DTA^{+/-}* mice that project in wrong territories. On the other hand, the AC didn't form or was reduced to a relatively narrower tract in the *Nkx2.1Cre⁺/NSE-DTA^{+/-}* mice as compared to wild-type AC. These results clearly indicate that midline *Nkx2.1*-derived cells play a major role in commissural axons pathfinding and that both *Nkx2.1*-derived guidepost neurons and glia are necessary elements for the correct development of these commissures.

Furthermore, during our investigations on *Nkx2.1^{-/-}* and *Nkx2.1Cre⁺/Rosa-DTA^{+/-}* mice, we noticed similar and severe defects in the erythrocytes distribution and the blood vessels network morphology in the embryonic brain of both mutants. As the Cre-mediated recombination was never observed to occur in the blood vessels of *Nkx2.1-Cre* mice, we inferred that the vessels defects observed were due to the loss of *Nkx2.1*-derived cells and not to the cells autonomous effects of Nkx2.1 in regulating endothelial cell precursors. Thereafter, the respective contribution of individual *Nkx2.1*-regulated neuronal or glial populations in the blood vessels network building were studied with the use of transgenic mice strains. Indeed, the use of *Nkx2.1Cre⁺/NSE-DTA^{+/-}* mice indicated that the *Nkx2.1*-derived neurons were not implicated in this process. Finally, to discriminate between the two *Nkx2.1*-derived glial cell populations, the GLAST⁺ astroglia and the NG2⁺ polydendrocytes, an *NG2-Cre* mouse strain crossed to the *Rosa-DTA^{+/-}* mice was used. In that mutant, the blood vessel network and the erythrocytes distribution were similarly affected as observed in *Nkx2.1Cre⁺/Rosa-DTA^{+/-}* animals. Therefore, this result indicates that most probably, the NG2⁺ polydendrocytes are involved in helping to build the vessels network in the brain.

Taken altogether, these observations show that during brain development, *Nkx2.1*-derived embryonic glial cells act as guidepost cells on the guidance of axons as well as forming vessels. Both *Nkx2.1*-regulated guidepost GABAergic neurons and glia collaborate to guide growing commissural axons, while polydendrocytes are implicated in regulating brain angiogenesis.

RESUME

Source, destin et fonction des cellules gliales précoces exprimant *Nkx2.1* dans le cerveau embryonnaire de la souris

Delphine Valloton, Département de Biologie Cellulaire et de Morphologie, UNIL.

Le tissu cérébral est composé de cellules neuronales et gliales générées dans les couches germinales qui bordent les ventricules. Ces cellules se divisent, se différencient et migrent selon des voies particulières. La spécification des interneurons GABAergiques et des neurones glutamatergiques a été largement étudiée, par contre, l'origine, le destin et la fonction des cellules gliales précoces du télencéphale embryonnaire restent peu élucidées. Depuis longtemps, il était communément accepté que les cellules gliales, et plus particulièrement les astrocytes, sont générés après la neurogénèse à partir du télencéphale dorsal. Toutefois, notre travail montre que de nombreuses cellules gliales sont générées à partir de précurseurs ventraux qui expriment le gène *Nkx2.1*, entre E14.5 et E16.5, c'est-à-dire, à des stades embryonnaires très précoces.

Le gène NK2 homéobox 1 (*Nkx2.1*) appartient à une famille de facteurs de transcription appelée NK2. Il s'agit de protéines qui contiennent un homéo-domaine. La spécification des précurseurs de la MGE requiert l'expression du gène homéobox *Nkx2.1*. De plus, la fonction du gène *Nkx2.1* dans la régulation de la spécification des interneurons GABAergiques et des oligodendrocytes dans le télencéphale ventral était déjà connue.

Au cours de mon travail de thèse, j'ai également mis en évidence que, *Nkx2.1* régule aussi les étapes de prolifération et de différenciation de divers sous-types de cellules gliales soit de type astrocytes ou bien polydendrocytes. L'utilisation d'un anticorps contre la protéine *Nkx2.1* ainsi qu'une sonde à ribonucléotides contre l'ARN messager du gène *Nkx2.1* ont révélé la présence de nombreuses cellules positives pour *Nkx2.1* qui exprimaient des marqueurs astrocytaires (comme GLAST et GFAP) dans le télencéphale embryonnaire. Afin de déterminer de manière sélective le sort des interneurons GABAergiques, des polydendrocytes et des astrocytes dérivés de la MGE, nous avons croisé soit des souris *Nkx2.1-Cre*, des souris *Glast-Cre ERT^{+/+}* inductibles ou bien des souris *NG2-Cre* avec des souris *Rosa26-lox-STOP-lox-YFP (Rosa26-YFP) Cre* rapportrices.

L'origine précise des astroglies positives pour *Nkx2.1* a été directement établie en combinant une coloration immunologique pour les glies et une électroporation focale d'un plasmide *pCAG-GS-EGFP* dans les domaines subpalliaux de tranches organotypiques, puis

également, par des cultures de neurosphères *in vitro* et des expériences d'électroporation *in utero* d'un plasmide *pCAG-GS-tomato* dans le pallium ventral d'embryons *Nkx2.1-Cre⁺/Rosa-YFP^{+/-}* au stade E14.5. Nous avons donc confirmé que les trois régions germinales du télencéphale ventral, c'est-à-dire, la MGE, l'AEP/POA et le noyau triangulaire septal sont capables de générer des cellules astrogliales.

D'autre part, l'immunohistochimie pour plusieurs marqueurs d'astrocytes ou de polydendrocytes, dans les embryons *Nkx2.1^{-/-}* et contrôles ainsi que dans les neurosphères, a révélé une sévère perte de ces deux types gliaux chez les mutants. Nous avons trouvé que la perte de glies correspondait à une diminution de la capacité de division des précurseurs dérivés de *Nkx2.1*, ainsi que l'incapacité de ces précurseurs de se différencier en cellules gliales. Nous avons en effet observé une diminution importante des cellules BrdU⁺ en division exprimant *Nkx2.1* dans la MGE*, la POA* et le noyau septal* des mutants pour *Nkx2.1*. D'autre part, nous avons pu mettre en évidence aussi bien *in vitro*, qu'*in vivo*, que certains précurseurs *Nkx2.1⁺* chez le mutant gardent la capacité à se différencier en neurones tandis qu'ils perdent celle de se différencier en cellules gliales. Prises dans leur ensemble, ces observations indiquent pour la première fois que le facteur de transcription *Nkx2.1* régule les étapes de prolifération et de différenciation des précurseurs des trois domaines subpalliaux qui génèrent les astroglies et polydendrocytes embryonnaires précoces.

Par la suite, dans le but de comprendre la fonction potentielle de ces glies précoces, nous avons procédé à de multiples colorations immunohistochimiques sur des animaux *Nkx2.1^{-/-}* et sauvages, ainsi que sur des souris *Nkx2.1-Cre* croisées à des souris *Rosa-DTA^{+/-}* dans lesquelles la toxine diphtérique hautement toxique a permis de supprimer sélectivement la majorité des cellules dérivées de *Nkx2.1*. De manière intéressante, nous avons observé dans ces deux mutants, une perte drastique et significative de cellules astrogliales GFAP⁺, GLAST⁺ et polydendrocytaires NG2⁺ et S100β⁺ dans le télencéphale, à la midline et dans les aires corticales médianes. Ces pertes ont pu être directement corrélées avec des défauts de guidage axonal observés dans le corps calleux (CC), la commissure hippocampique (HIC), le fornix (F) et la commissure antérieure (AC).

Le guidage axonal est une étape clé permettant aux neurones de former des connections spécifiques et de s'organiser dans un réseau fonctionnel. La contribution des cellules « guidepost » dans le CC et dans la AC comme médiateurs de la croissance des axones commissuraux à jusqu'à aujourd'hui été attribuée spécifiquement à des astroglies « guidepost » de la midline. Des résultats publiés précédemment dans notre groupe, ont permis de montrer que, pendant le développement embryonnaire, le CC est peuplé en plus de la glie par de nombreux neurones « guidepost » glutamatergiques et GABAergiques qui sont essentiels pour le croisement correct des axones callosaux à la midline. Ainsi, la contribution

relative des populations individuelles neuronales ou gliales pour le guidage des axones commissuraux demande à être approfondie afin de mieux comprendre les mécanismes de guidage. A ces fins, nous avons croisé des souris *Nkx2.1-Cre* avec des souris *NSE-DTA^{+/-}* qui expriment la toxine diphthérique uniquement dans les neurones et ainsi, nous avons pu sélectivement supprimer les neurones dérivés de domaines *Nkx2.1⁺*. Dans les souris *Nkx2.1^{-/-}*, nous avons découvert que le CC était désorganisé avec des axones callosaux perdant partiellement leur orientation, alors que dans les souris *Nkx2.1Cre⁺/Rosa-DTA^{+/-}* et *Nkx2.1Cre⁺/NSE-DTA^{+/-}*, l'organisation axonale n'était pas affectée. De plus, les faisceaux hippocampiques du fornix étaient défasciculés dans les trois types de mutants. Par ailleurs, la formation de la commissure antérieure (AC) était complètement absente dans les souris *Nkx2.1^{-/-}* d'une part, et d'autre part, celle-ci était divisée en deux à trois voies séparées dans les souris *Nkx2.1Cre⁺/Rosa-DTA^{+/-}*. Finalement, la AC était soit absente, soit réduite de manière ne former plus qu'un faisceau relativement plus étroit dans les souris *Nkx2.1Cre⁺/NSE-DTA^{+/-}* en comparaison avec la AC sauvage. Ces derniers résultats indiquent clairement que les cellules dérivées de *Nkx2.1* à la midline, jouent un rôle majeur dans le guidage des axones commissuraux et que, autant les neurones, que les astrocytes « guidepost » dérivés de *Nkx2.1*, sont des éléments nécessaires au développement correct de ces commissures.

En outre, lors de nos investigations sur les souris *Nkx2.1^{-/-}* et *Nkx2.1Cre⁺/Rosa-DTA^{+/-}*, nous avons remarqués des défauts sévères et similaires dans la distribution des erythrocytes et dans la morphologie du réseau de vaisseaux sanguins dans le cerveau embryonnaire des deux mutants précités. Puisque nous n'avons jamais observé de recombinaison de la Cre recombinase dans les vaisseaux sanguins des souris *Nkx2.1Cre*, nous en avons déduit que les défauts de vaisseaux observés étaient dus à la perte de cellules dérivées de *Nkx2.1*. Il existerait donc en plus de la fonction cellulaire autonome de *Nkx2.1* reconnue pour régulée directement la spécification des cellules endothéliales, une fonction indirecte de *Nkx2.1*. Afin de déterminer la contribution respective des populations individuelles neuronales ou gliales régulées par *Nkx2.1* dans la construction du réseau de vaisseaux sanguins, nous avons utilisé diverses lignées de souris transgéniques. L'utilisation de souris *Nkx2.1Cre⁺/NSE-DTA^{+/-}* a indiqué que les neurones dérivés de *Nkx2.1* n'étaient pas impliqués dans ce processus. Finalement, afin de discriminer entre les deux populations de cellules gliales dérivées de *Nkx2.1*, les astroglies et les polydendrocytes, nous avons croisé une lignée de souris *NG2-Cre* avec des souris *Rosa-DTA^{+/-}*. Dans ce dernier mutant, le réseau de vaisseaux sanguins du cortex ainsi que la distribution des erythrocytes étaient affectés de la même manière que dans le cortex des souris *Nkx2.1Cre⁺/Rosa-DTA^{+/-}*. Par conséquent, ce résultat indique que très probablement, les polydendrocytes *NG2⁺* sont impliqués dans la mise en place du réseau de vaisseaux dans le cerveau.

Prises dans leur ensemble, ces observations montrent que durant le développement embryonnaire du cerveau, des sous-populations de glies régulées par *Nkx2.1* jouent un rôle de cellules « guidepost » dans le guidage des axones, ainsi que des vaisseaux. Les polydendrocytes sont impliquées dans la régulation de l'angiogenèse tandis que, autant les neurones GABAergiques que les astrocytes collaborent dans le guidage des axones commissuraux en croissance.

LIST OF ABBREVIATIONS

5-HT3a	Serotonin receptor 3a
<i>5-HTR3a-GFP</i>	Bacterial artificial chromosome (BAC) 5-HT3a GFP transgenic mouse
AC	Anterior commissure
ACa	Anterior commissure pars anterior
ACp	Anterior commissure pars posterior
AEP	anterior entopeduncular area
AgCC	Agensis of the corpus callosum
alPCs	Astrocytic intermediate progenitor cells
Alk1/2	Activin receptor-like kinases 1/2
AMPA	α -amino-3-hydroxy-5-methyl-4-isoxazolepropionic acid receptor
Ang	Angiopoietin
AP2 γ	Activating enhancer-binding protein 2 gamma gene
<i>Ascl1(Mash1)</i>	Achaete-scute homolog 1 gene
ASMA	α -smooth muscle actin
ATP	Adenosine triphosphate
BDNF	Brain-derived neurotrophic factor
BHC	Benign hereditary chorea
bHLH	Basic helix-loop-helix
BLBP	Brain-lipid-binding-protein
BMP	Bone morphogenetic factor
BP	Basal progenitor
CAM	Cell-adhesion molecule
CaR	Cajal-Retzius
CR	Calretinin
<i>CreERTM</i>	Tamoxifen induced Cre recombinase
CC	Corpus callosum
CCi	Cingulate cortex
Cdc42	Cell division control protein 42, GTP-binding protein
CFr	Frontal cortex
CGE	Caudal ganglionic eminence
CH	Congenital hypothyroidism
CNS	Central nervous system
CNTF/LIF	Ciliary neurotrophic factor, leukemia inhibitory factor
<i>COUP-TFII (NR2F2)</i>	Chicken Ovalbumin Upstream Promoter-transcription factor 2 gene (nuclear receptor subfamily 2, group F, member 2)
CP	Cortical plate
CPN	Callosal projection neurons
CRD-Nrg1	Membrane-bound form of Neuregulin1
CSB	Corticoseptal boundary
CSPG (NG2)	Chondroitin sulfate proteoglycan
<i>Ctip2</i>	COUP-TF interacting 2 gene
<i>Cux</i>	Cut-like homeobox gene
<i>Cxcl12</i>	Chemokine (C-X-C motif) ligand 12 gene
<i>Cxcr4</i>	Chemokine (C-X-C motif) receptor gene
DCX	Doublecortin
DCC	Deleted in colorectal cancer
Dll-4	Delta-like ligand 4
DNA	Deoxyribonucleic acid
DP	Dorsal pallium
<i>Dlx</i>	Distal-less homeobox gene

E(10)	Embryonic day(10)
ECM	Extracellular matrix
ECs	Endothelial cells
EGF	Endothelial growth factor
EGFL7	EGF-like domain 7
EPCs	Endothelial precursor cells
<i>Emx</i>	Empty spiracles homeobox gene
Eng	Endoglin
Eph	Ephrin receptor
ER81 (etv1)	ETS related protein 81, ETS translocation variant 1
ErbB2	Erythroblastic leukemia viral oncogene homolog 2
ES	Embryonic stem
ET	Endothelin
<i>Fezf2</i>	Fasciculation and elongation protein zeta-2 gene
FGF	Fibroblast growth factor
<i>FOXG1</i>	Forkhead-box G1
<i>Foxp2</i>	Forkhead-box-protein P2 gene
GABAergic	γ aminobutyric acidergic
GAD 65/67	Glutamic acid decarboxylase 65/67
GC	Group-specific component (vitamin D binding protein)
GDNF	Glial cell derived neurotrophic factor
GFAP	Glial fibrillary acidic protein
GFP	Green fluorescent protein
GLAST	Astrocyte-specific glutamate and aspartate transporter
<i>Gli3</i>	Zinc finger protein GLI3 gene
GluR	Glutamate receptor
<i>GOLF</i>	guanine nucleotide binding protein, alpha stimulating, olfactory type
GPI	Glycosyl-phosphatidylinositol
GRIP	Glutamate receptor interacting protein
GS	Glutamine synthetase
<i>Gsx (Gsh)</i>	GS homeobox gene
GW	Glial wedge
<i>Hes</i>	Hairy and enhancer of split genes
<i>Hey</i>	Hairy and enhancer of split related protein
IG	Induseum griseum
Ig-Nrg1	Secreted form of Neuregulin1 with an immunoglobulin-like domain
IRGCs	Intermediate radial glial cells
ISVZ	Inner subventricular zone
IZ	Intermediate zone
JAG1	Jagged-1 protein
JAK-STAT	Janus kinase-signal transducer and activator of transcription
KO	Knockout
L1	L1CAM cell adhesion protein
LGE	Lateral ganglionic eminence
<i>Lhx</i>	LIM homeobox gene
LIS1 (PAFAH1B1)	Lissencephaly type 1 (Platelet-activating factor acetylhydrolase 1B)
<i>Lmo4</i>	LIM domain only gene 4
LOT	Lateral olfactory tract
LP	Lateral pallium
LPL	Lipoprotein lipase
MBP	Myelin basic protein
MEK/ERK	Mitogen-activated protein kinase, extracellular regulated MAP kinase
MGE	Medial ganglionic eminence

MUPP-1 (Mpdz)	Multiple PDZ domain protein
MZ	Marginal zone
MZG	Midline zipper glia
NCAM	Neural cell-adhesion molecule
NE	Neuroepithelial
<i>Nfi</i>	Nuclear factor 1 gene
<i>Ngn</i>	Neurogenin gene
NG2 (CSPG)	Nerve/glia antigen 2
<i>Nkx2.1 (TTF-1) (T/ebp)</i>	<i>NK2</i> homeobox 1, thyroid transcription factor 1 gene, thyroid-specific enhancer-binding protein
NO	Nitric oxide
NPY	Neuropeptide Y
Nrp-1/2	Neuropilin1/2 receptors
NSCs	Neural stem cells
O4	O4 antigen
<i>Olig1/2</i>	Oligodendrocyte precursor bHLH transcription factors 1/2
OLPs	Oligodendrocyte precursors
OPCs	Oligodendrocyte progenitor cells
oRG	outer radial glia
OSVZ	outer subventricular zone
<i>Otx1</i>	Orthodenticle homeobox 1 gene
P(21)	Postnatal day (21)
<i>Pax</i>	Paired box gene
RC2 (Ifaprc2)	Intermediate filament-associated protein RC2
PDGF	Platelet-derived growth factor
PDGFR α	Platelet-derived growth factor receptor alpha
PDGFR β	Platelet-derived growth factor receptor beta
Plp/Dm20	Myelin proteolipid protein
PIGF	Placental growth factor
POA	Anterior preoptic area
PP	Preplate
PSB	Pallial subpallial boundary
PV	Parvalbumin
RBP-JK	Recombination signal binding protein for immunoglobulin kappa J region
RG	Radial glial
Rig1	Retinoic acid receptor responder 1
Robo	Roundabout homolog gene
Ryk	Wnt tyrosine-kinase receptor
S1P	Sphingosin 1-phosphate
S100 β	S100 calcium-binding protein B
<i>Satb2</i>	Special AT-rich sequence-binding 2 gene
<i>SCIP(POU3f1)</i>	Suppressed cAMP-inducible POU, POU class 3 homeobox 1
Sema	Semaphorin
SEP	Septum
SGZ	Subgranular zone
Shh	Sonic hedgehog
SMAD	Mothers against DPP homolog 4
<i>Sox</i>	SRY (sex-determining region Y)-box containing gene
SP	Subplate
SST	Somatostatin
STR	Striatum
<i>Svet1</i>	Subventricular-expressed transcript 1 gene

SVZ	Subventricular zone
TAG-1 (CNTN1)	Contactin 1
<i>Tbr1</i>	T-box brain gene
<i>Tie2</i>	Endothelium-specific receptor tyrosine kinase 2
Tis21 (Btg2)	NGF-inducible protein TIS21, B-cell translocation gene 2
TGFβ1	Transforming growth factor beta1
TS	Triangular septal nucleus
<i>Unc5b</i>	Uncoordinated Netrin receptor homolog B
VEGFA	Vascular endothelial growth factor A
VEGFR	Vascular endothelial growth factor receptor
VIP	Vaso-intestinal peptide
VP	Ventral pallium
vSMCs	Vascular smooth muscle cells
VZ	Ventricular zone
Wnt	Wingless-Int
XLAG	X-linked lissencephaly with abnormal genitalia
XLMR	X-linked mental retardation
YFP	Yellow fluorescent protein

TABLE OF CONTENTS

TITLE	1
IMPRIMATUR	ERROR
! BOOKMARK NOT DEFINED.	
ACKNOWLEDGMENTS	3
ABSTRACT	5
RESUME	8
LIST OF ABBREVIATIONS	12
TABLE OF CONTENTS	16
LIST OF FIGURES	22
INTRODUCTION	23
1. Embryonic Brain Development: Neurogenesis	25
1.1 Neural induction and early patterning	25
1.2 Neurogenesis.....	26
1.2.1 Neuroepithelial cells, radial glial cells and intermediate progenitors.....	27
1.2.2 Outer radial glial cells	30
1.2.3 Symmetrical and Asymmetrical division.....	31
1.3 Dorso-ventral genetic specification and patterning.....	32
1.4 Neuronal subtype specification.....	35
1.4.1 Glutamatergic and GABAergic fate	37
1.4.2 Origin and specification of the cortical projection neurons	38
1.4.3 Origins and specification of the cortical GABAergic interneurons	39
2. Gliogenesis: The choice between glial versus neuronal fate	43
2.1 Neuronal fate.....	43
2.2 Astroglial origin and fate	44
2.2.1 Astroglial fate.....	46
2.3 Oligodendroglial origin and fate	48
2.3.1 Oligodendroglial origin	48
2.3.2 Oligodendroglial fate.....	50

2.4 Glial cell types: a matter of cell diversity	52
2.4.1 The radial glial cells.....	52
2.4.2 The mature astrocytes	52
2.4.3 The reactive astrocytes	54
2.5 The oligodendrocytes.....	55
2.6 The NG2 ⁺ polydendrocytes	55
2.6.1 Polydendrocytes identity	55
2.6.2 Polydendrocytes lineages	56
2.6.3 Integration of polydendrocytes in the neurovascular unit	59
2.6.4 Role of polydendrocytes in the synaptic responses.....	59
2.6.5 Role of polydendrocytes in axonal outgrowth.....	60
3. Nkx2.1 homeobox gene: regulation and function	61
3.1. Expression and regulation of Nkx2.1:	61
3.2 Molecular structure of the Nkx2.1 homeodomain-containing protein	62
3.3 Function of <i>Nkx2.1</i> in the specification of the precursors of the ventral telencephalon.....	64
3.4 Interneurons and oligodendrocytes specification	66
3.5 Nkx2.1-linked syndromes in humans.....	67
4. Cell Migration to the cerebral cortex	70
4.1 Cortical layers formation.....	70
4.2 Radial versus tangential neuronal migration.....	71
4.3 Cellular events of neuronal migration and nucleokinesis.....	73
4.4 Glial migration	74
5. Axonal growth and guidance	76
5.1 Mechanisms of axonal growth.....	76
5.2 Guidance cues and molecular aspects of axonal guidance.....	77
5.2.1 Ephrins	78
5.2.2 Netrins.....	79

5.2.3 Semaphorins.....	80
5.2.4 Slits.....	81
6. Development of two main telencephalic commissures:	83
6.1 Development of the Corpus Callosum	83
6.1.2 Axonal guidance in the Corpus Callosum	84
6.2 Development of the anterior commissure.....	86
6.2.1 Axonal guidance in the anterior commissure.....	86
6.3 Guidepost cells in axonal guidance	88
6.3.1 Guidepost glial and neuronal cells of the Corpus Callosum and the anterior commissure.....	89
7. Mechanisms of Brain Angiogenesis	91
7.1 Origin of the endothelial cells	91
7.2 Angiogenic growth and sprouting of the blood vessels	92
7.4 “Guidepost cells” in Angiogenesis.....	97
7.5 Differentiation and maturation of the blood vessels	97
7.6 Blood vessel formation pathologies	99
7.7 Neurovascular coupling	101
MATERIAL AND METHODS	103
Animals	103
Induction of CreERT by Tamoxifen.....	103
<i>In utero</i> electroporation.....	104
Slice cultures	104
<i>In vitro</i> focal electroporation	105
Immunohistochemistry	105
Confocal Time-Lapse Microscopy	106
BrdU tracing studies.....	107
<i>In situ</i> hybridization	107
Neurosphere generation and microscopical analysis	108
Chromatin Immunoprecipitation.....	109
Transfection of HEK293 cells.....	110
Imaging.....	111
Quantifications.....	111

RESULTS 116

SECTION 1: NKX2.1 REGULATES THE CELL FATE AND THE DIFFERENTIATION OF TRANSIENT ASTROCYTES AND POLYDENDROCYTES IN THE MOUSE EMBRYONIC TELEENCEPHALON 116

IDENTIFICATION OF ASTROGLIAL CELLS EXPRESSING NKX2.1 DURING EMBRYONIC DEVELOPMENT 117

IDENTIFICATION OF NUMEROUS EARLY AND TRANSIENT NKX2.1-DERIVED GLIAL CELL TYPES IN THE TELEENCEPHALON DURING DEVELOPMENT 119

NKX2.1-DERIVED ASTROGLIA SPATIALLY ORIGINATE FROM THREE DISTINCT SITES IN THE VENTRAL TELEENCEPHALON..... 121

NKX2.1 REGULATES THE PROLIFERATION OF VENTRAL PROGENITORS IN EMBRYOS 124

NKX2.1 CONTROLS EARLY GLIOGENESIS IN EMBRYONIC TELEENCEPHALON 126

NKX2.1 REGULATES THE DIFFERENTIATION OF NKX2.1-DERIVED EMBRYONIC ASTROGLIA 128

NKX2.1 DIRECTLY REGULATES THE EXPRESSION OF GLIAL REGULATORY GENES 130

FIGURES OF SECTION 1: 133

SECTION 2: GUIDANCE OF COMMISSURAL AXONS IN THE EMBRYONIC TELENCEPHALON: A ROLE FOR NKX2.1-POSITIVE CELLS **164**

NUMEROUS PROGENITORS AND ASTROGLIAL CELLS REGULATED BY NKX2.1 ARE STRATEGICALLY PLACED TO AID AXONAL GUIDANCE IN THE CORPUS CALLOSUM AND THE ANTERIOR COMMISSURE. 165

NKX2.1 REGULATES GABAERGIC NEURONS THAT ACT AS GUIDEPOST CELLS IN THE FORNIX AND THE ANTERIOR COMMISSURE 166

NKX2.1⁺ PRECURSORS AND *NKX2.1*-DERIVED GLIA HELP IN GUIDING THE COMMISSURAL AXONS 168

***NKX2.1*-DERIVED INTERNEURONS AND ASTROCYTES SYNERGISTICALLY COOPERATE TO GUIDE GROWING COMMISSURAL AXONS OF THE ANTERIOR COMMISSURE..... 171**

NKX2.1+ PRECURSORS FROM THE TRIANGULAR SEPTAL NUCLEUS MIGHT CHANNEL THE AXONS OF THE AC THROUGH A SLIT2-DEPENDENT MECHANISM. 172

FIGURES OF SECTION 2: **175**

SECTION 3: TRANSIENT *NKX2.1*-DERIVED POLYDENDROCYTES ARE REQUIRED FOR VESSEL NETWORK FORMATION DURING EMBRYONIC DEVELOPMENT **196**

IDENTIFICATION OF TRANSIENT *NKX2.1*-DERIVED POLYDENDROCYTES IN EMBRYONIC TELENCEPHALON 197

SPATIAL ASSOCIATION BETWEEN EMBRYONIC NKX2.1⁺ POLYDENDROCYTES AND DEVELOPING VESSELS 199

NON-CELL AUTONOMOUS FUNCTION OF NKX2.1 IN CONTROLLING BRAIN ANGIOGENESIS 200

NKX2.1 CONTROLS CORTICAL BRAIN ANGIOGENESIS VIA THE ACTION OF *NKX2.1*-DERIVED POLYDENDROCYTES 202

FIGURES OF SECTION 3:	205
DISCUSSION	224
Early subpallial origin of <i>Nkx2.1</i> -regulated astroglial cells	225
Heterogeneity and origin of the <i>Nkx2.1</i> -derived glial cells	226
The <i>Nkx2.1</i> -derived astrocyte-like cells	227
The <i>Nkx2.1</i> -derived polydendrocyte-like cells	234
The <i>Nkx2.1</i> -derived S100 β ⁺ cells	235
<i>Nkx2.1</i> -derived glial cells are transient and disappear from the pallium and then from the subpallium post-natally	236
Intrinsic regulation of Nkx2.1 ⁺ progenitors for their own division and specification into astroglia	237
Nkx2.1 binds the promotor and activates glial specific genes	239
Guidepost function of Nkx2.1 ⁺ precursors, interneurons and astroglia for commissural axons	240
Role of <i>Nkx2.1</i> -derived polydendrocytes in angiogenesis	245
CONCLUSION AND PERSPECTIVES	249
REFERENCES	251

LIST OF FIGURES

- Figure 1:** Neural induction, regional patterning and ES cell neurogenesis
- Figure 2:** Polarized features of neuroepithelial cells, radial glial cells and basal progenitors.
- Figure 3:** Lineage tree of neurogenesis without BPs.
- Figure 4:** Lineage tree of neurogenesis with BPs.
- Figure 5:** Symmetric versus asymmetric division of neuroepithelial and radial glial cells.
- Figure 6:** Genetic interactions underlying the regionalization of the mammalian telencephalon.
- Figure 7:** Key genetic pathways that interact to form and pattern the early telencephalon.
- Figure 8:** Major subtype of projection neurons within the neocortex.
- Figure 9a:** Schematic depicting how progenitors residing in the VZ and SVZ in mice produce projection neurons in an 'inside-out' fashion.
- Figure 9b:** Schematic representation of a potential model for the generation of projection neuron subtypes from progenitors.
- Figure 10:** Migration pathways of cortical interneuron subgroups from the ventral telencephalon.
- Figure 11:** Pathways regulating the neurogenesis and the astrogliogenesis by neural stem cells.
- Figure 12:** Expression of Nkx2.1 within the longitudinal organization of the brain.
- Figure 13:** 3-Dimensional structure of Nkx2.1 homeo-protein.
- Figure 14:** Production of Nkx2.1-deficient mice by homologous recombination in ES cells.
- Figure 15:** Morphological brain defects of patients with Nkx2.1 mutations.
- Figure 16:** Leading process dynamics in cortical migrating neurons.
- Figure 17:** Nucleokinesis in migrating neurons.
- Figure 18:** The structure of the growth cone.
- Figure 19:** Conserved families of guidance molecules (A) and their receptors (B).
- Figure 20:** Molecular cues controlling the pathway choices at the *Drosophila* and vertebrate midline.
- Figure 21:** Development of the Corpus Callosum in the mouse.
- Figure 22:** Two transient neuronal populations of the CC guide the pioneering axons.
- Figure 23:** Migrating guidepost cells in the developing forebrain.
- Figure 24:** Sprouting, outgrowth, guidance, lumen formation and maturation of vessels

INTRODUCTION

During the embryonic development of the human brain, in the third week the neuroectoderm generates the neural tube along the dorsal side of the embryo. Later in the fourth week, the rostral most area gives rise to three primary vesicles: the prosencephalon or future forebrain, the mesencephalon or future midbrain, and the rhombencephalon or future hindbrain. These vesicles are distributed along the rostro-caudal axis. The mesencephalon remains undivided for the rest of the neural development. In turn, the prosencephalon is divided into two additional vesicles: the telencephalon and the diencephalon. Furthermore, the rhombencephalon is separated into the metencephalon and the myelencephalon. Then, the spinal cord is formed by the caudal most part of the neural tube. The central nervous system (CNS) is formed by the encephalon and the spinal cord.

During my thesis, I have been interested by the last steps of the development of the embryonic telencephalon involving the generation of the cortical areas from its dorsal part and the differentiation of the subpallium into the septum, the striatum and the pallidum from its ventral part. The dorsal telencephalon or the pallium is anatomically divided into distinct cortices: the neocortex and the allocortex, collective term for the archicortex and the paleocortex. The neocortex is the newest part of the cerebral cortex to evolve. The archicortex corresponds to the cortex of the dentate gyrus and the hippocampus in evolved mammals. The paleocortex includes the olfactory cortex. The distinguishing feature of the neocortex in mammals is that it is formed by six layers. Each layer is then distinguished by its thickness that can vary according to its specific cytoarchitecture and connectivity. Additionally, the neocortex can also be divided following the specific functions attributed to its composing cortical areas. For example, three different functional areas have been defined: the motor, the sensory (somatosensory, visual and auditory) and the associative areas. The motor cortex is then subdivided into the primary motor, premotor and supplementary motor areas. The primary motor cortex executes the voluntary movements that are preselected by the two other aforementioned areas. Similarly, the primary sensory cortex receives the sensory inputs originating from the thalamus. Finally, the associative areas execute the complex task of processing the primary information and translating it into a meaningful perception enabling us to interact effectively and support the more evolved functions like the abstract thinking and the language. More precisely, each cortical area is also characterized by the pattern of its gene expression, its cellular composition and its connections. Together, the diverse cortical areas are integrated into functional networks with respect to their size, positioning and wiring.

The cerebral tissue is composed by two major types of cells namely the neuronal and the glial cells which are in turn subdivided into four class of glia: the astrocytes, the oligodendrocytes, the polydendrocytes and the microglia. The cortical neurons are also classified into two main types: the glutamatergic pyramidal projection neurons and GABAergic interneurons. The glutamatergic neurons are generated in the dorsal part of the telencephalon (dorsal pallium), from neuroepithelial precursors bordering the ventricles. The GABAergic interneurons originate in the ventral telencephalon from germinal zones. The former migrate radially to the cortex while the latter migrate tangentially towards the cortex. The oligodendrocytes have a very well defined function that is the myelination of the axonal tracts in the CNS, and the astrocytes play a role of intermediary in the distribution of nutriments from the blood vessels to the neurons and recently they have been shown also to participate in the modulation of the neurotransmission signaling at the synapses.

During the development of the entire nervous system, any disorganization either at the level of the precursor division, the cell type differentiation, the cell migration or any wiring defect of a network can involve severe malformations and/or neurological pathologies that can lead to behavioral troubles. Consequently, many developmental issues and syndromes have already been described involving defects in one or more developmental steps. Indeed, a precise knowledge of the mechanisms that occur during the brain formation would represent a major help in the research for new therapeutic treatments to prevent or cure the neurological disorders.

1. Embryonic Brain Development: Neurogenesis

Since several years, attempts have been made to discover and analyze the mechanisms that lead to a completely developed brain but still many questions in the field are unanswered. The challenging field of brain development awaits several scientific advances to further answer the intricacies regarding the complexity of the molecular, cellular and anatomical processes involving the transition from an embryonic stem cell to an entire functional encephalon. These mechanisms remain until now not fully understood, but they can be nevertheless classified in three major steps that transform a cluster of embryonic cells to an adult brain containing an extraordinary cellular diversity. These main events can be categorized as: 1) neural induction and early patterning; 2) neurogenesis and gliogenesis; and 3) genetic spatiotemporal specification.

1.1 Neural induction and early patterning

During embryonic development, the first step of CNS formation is the neural induction. It is characterized by the transformation of pluripotent embryonic stem (ES) cells into neural stem cells that will be committed to form progenitors with a more restricted fate that will in turn give rise to each cellular element of the nervous system.

Most of the studies about neural induction have been done first in the *Xenopus*, and second, in mouse or human *in vitro* models that require the use of ES cells. It is now generally accepted that the neural induction eventuates from a kind of “default” pathway wherein the ES cells become neural precursors in the absence of any specific instructive cue (Wilson and Houart 2004; Levine and Brivanlou 2007; Gaspard and Vanderhaeghen 2010). Indeed, it has been reported that murine ES cells begin to display neural markers after being for only few hours in culture in a minimal medium devoid of any specific signaling molecule (Smukler, Runciman et al. 2006). Moreover, the different subtypes of neuronal and glial cell lineages were similarly shown to originate from neural progenitors following the same time frame in cultured mouse ES cells than what is happening *in vivo* (Gaspard, Bouchet et al. 2008).

However, following multiple investigations on the neural induction, the “default” pathway has been attributed to the bone morphogenetic protein (BMP) inhibition (Levine and Brivanlou 2007). The regulation depends on the two antagonistic types of signaling molecules that can act on the BMP i.e. the Fibroblast Growth Factor (FGF) signaling which induces it (LaVaute, Yoo et al. 2009) and the Wingless-Int (Wnt) diffusion which antagonizes it (Fuentelba, Eivers et al. 2007; Gaspard and Vanderhaeghen 2010) (Fig. 1a). The action of

signaling cues such as, Wnts, FGFs and the retinoic acid, that are also responsible for a caudal fate acquisition induces the rostro-caudal patterning of the neuronal plate (Lee, Lumelsky et al. 2000; Wichterle, Lieberam et al. 2002; Watanabe, Kamiya et al. 2005; Borello and Pierani 2010). Furthermore, the dorso-ventral patterning of the neural plate is also regulated by morphogens like Wnt/BMP and Sonic Hedgehog (Shh) that are implicated in the arealization of the cortex (Wilson and Rubenstein 2000; Hebert and Fishell 2008; Pierani and Wassef 2009; Gaspard and Vanderhaeghen 2010) (Fig. 1a). More precisely, the ES cells have an innate rostral neural identity that is then specified into distinct progenitors following the dorso-ventral axis (Fig. 1b).

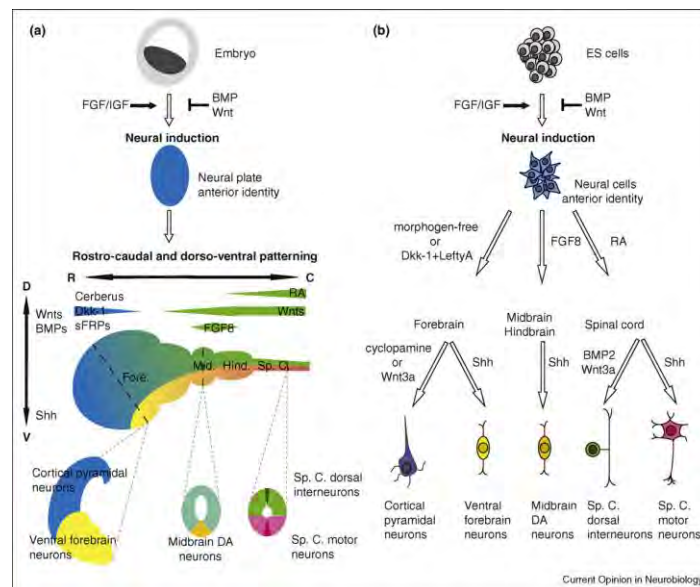


Figure 1. Neural induction, regional patterning and ES cell neurogenesis. (a) The Schema represents the neural induction and the early patterning of the neural plate and the neural tube. The neural induction is regulated by the coordinated actions of BMP, Wnt and FGF/IGF signaling pathways. The neural plate, initially of anterior identity, is then subsequently patterned by extrinsic morphogens along the rostro-caudal and the dorso-ventral axes into discrete domains. (b) ES cell neural induction and progenitor specification follow the same cues as in vivo to give rise to specific neural populations. From (Gaspard and Vanderhaeghen 2010).

1.2 Neurogenesis

As the mammalian telencephalon is formed, the dorso-ventral patterning leads to the distinction of the two main subdivisions: the dorsal and the ventral telencephalon (also subpallium), in which specific types of glia and neurons are originating. The pallium develops into the cerebral cortex, and the subpallium becomes the basal ganglia. Neurons and glia are also generated according to a specific temporal sequence. It has been stated that in the cortical VZ, the neuroepithelial stem cells are first committed to a neuronal cell fate

that is followed later by a glial commitment of the progenitors (Qian, Shen et al. 2000; Morrow, Song et al. 2001; Guillemot 2007).

In the developing brain, four distinct types of progenitors that can generate post-mitotic neurons have been defined, namely the neuroepithelial cells (NE), the radial glial cells (RG) and the intermediate or basal progenitors (BP) and more recently the outer radial glia (oRGCs) (Smart, Dehay et al. 2002; Fish, Dehay et al. 2008; Fietz, Kelava et al. 2010; Reillo, de Juan Romero et al. 2011; Wang, Tsai et al. 2011) that divide within proliferative zones bordering the ventricles (Kriegstein and Gotz 2003; Noctor, Martinez-Cerdeno et al. 2004; Gotz and Huttner 2005; Guillemot 2005; Hevner 2006; Kriegstein and Alvarez-Buylla 2009; Rowitch and Kriegstein 2010). The NE cells are considered as stem cells since they possess the ability to self-renew and are multipotent cells. Thus, the NE cells have indeed the potential to give rise either directly or indirectly (i.e. after becoming a RG cell or a basal progenitor) to all the neuronal and the glial cells of the mammalian CNS (Hevner 2006).

1.2.1 Neuroepithelial cells, radial glial cells and intermediate progenitors

Morphologically stating, the NE and the RG cells are commonly characterized by a long process that extends from the ventricular zone, where their cell body lies, towards the pial surface (Fig. 2). Consequently, the NE and the RG cells display a highly polarized organization of their components. They are oriented along the apical-basal axis and exhibit specific components on the apical side of their plasmic membrane (Huttner and Brand 1997; Kosodo, Roper et al. 2004). Both the NE and the RG contact the ventricle (Fig. 2 and 5) in which they project a single primary cilium. On the basal side, the RG cells contact the meninges, the basal lamina and the blood vessels with the endfoot of their processes (Kriegstein and Alvarez-Buylla 2009). In mice, the NE cells have the potential to generate all neuronal subtypes and the two types of macroglial cells, namely the oligodendrocytes and the astrocytes, within the entire CNS (McCarthy, Turnbull et al. 2001; Anthony, Klein et al. 2004). Between the embryonic days 10 (E10) and E12.5, they progressively adopt a RG cell fate with the onset of the neurogenesis. This time frame is appropriate as by E10 no astroglial markers can yet be detected, and by E12, most CNS regions are dominated by progenitor cells that are expressing several of the astroglial features. The RG cells and the NE progenitors share some identical features like the expression of the intermediate-filament protein Nestin, and the posttranslational modifications labeled by the RC1 and RC2 antibodies (Mori, Buffo et al. 2005).

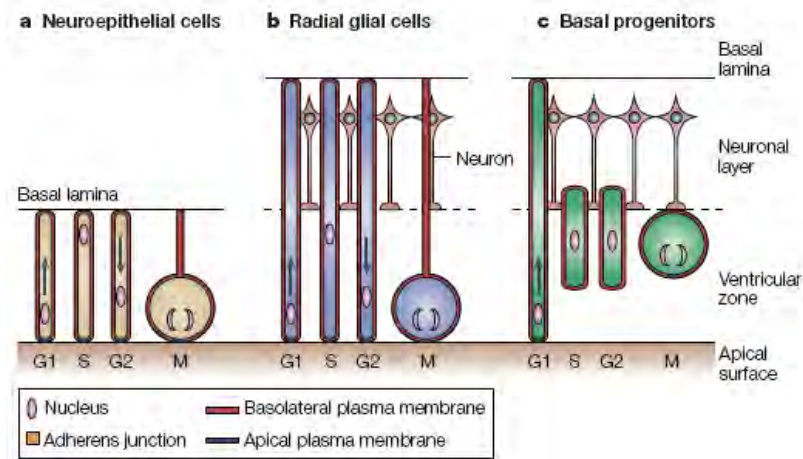


Figure 2. Polarized features of neuroepithelial cells, radial glial cells and basal progenitors. The figure summarizes the polarized organization and interkinetic nuclear migration of neuroepithelial cells, radial glial cells and basal progenitors. **(a)** In neuroepithelial cells, interkinetic nuclear migration spans the entire apical–basal axis of the cell, with the nucleus migrating to the basal side during G1 phase, being at the basal side during S phase, migrating back to the apical side during G2 phase, and mitosis occurring at the apical surface. **(b)** In radial glial cells, the basally directed interkinetic nuclear migration does not extend all the way to the basal side (that is, through the neuronal layer to their pial end-feet), but is confined to the portion of the cell between the apical surface and the basal boundary of the ventricular zone or the subventricular zone (not shown). **(c)** In basal progenitors, the nucleus migrates from the apical surface to the basal boundary of the ventricular zone (dashed line) or subventricular zone (not shown) for S phase and mitosis, and this is concomitant with the retraction of the cell from the apical surface. From (Gotz and Huttnner 2005).

In the beginning of the neurogenesis, the transformation from the NE cell identity to a distinct but related RG cell fate is characterized by the appearance of many specific features and molecules, typical from astrocytes, such as, glycogen granules, the vimentin, the glutamine synthase (GS), the tenascin-C (TN-C), the brain-lipid-binding (BLBP), the glial fibrillary acidic (GFAP) and the Ca^{2+} -binding (S100 β) proteins, as well as, the astrocyte-specific glutamate and aspartate transporter (GLAST) (Gotz and Barde 2005; Noctor, Flint et al. 2002). At the same time, the tight junctions that couple the NE cells are converted to adherent junctions and contacts are made between the RG endfeet and the endothelial cells of the blood vessels which starts to invade the parenchyma (Kriegstein and Alvarez-Buylla 2009). In the neuroepithelial cells the nuclei can migrate through the entire cortex within the the long cytoplasmic process of the cell. This process, which is called interkinetic nuclear migration, is restricted to the ventricular zone for the RG cells. Thereafter, the RG cells have a more restricted potential since they represent more fate restricted progenitors and thus, majority of them were observed to generate a single cell type only, namely the astrocytes, the oligodendrocytes or the neurons (Price and Thurlow 1988; Luskin, Parnavelas et al. 1993;

Parnavelas 1999). Indeed, the RG cells comprise heterogeneous subpopulations which originate from diverse brain regions (Kriegstein and Gotz 2003; Malatesta, Hack et al. 2003). Therefore, the RG cells are in fact a differentiated progeny of the NE precursors which display a more restricted fate, since they arise from tripotent NE cells to become unipotent RG cells (Fig. 3). One interesting feature of the RG cells is that they don't retract their long processes while dividing which can be inherited by the daughter cells and used for soma translocation (Fishell and Kriegstein 2003). This demonstrates a potential combinatorial function of being precursors and acting as guides for these cells.

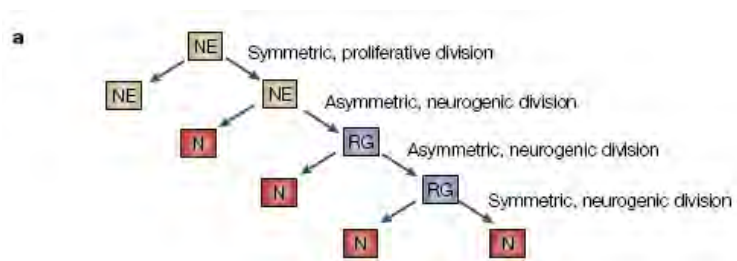


Figure 3. Lineage tree of neurogenesis without BPs. (a) The lineage trees shown provide a simplified view of the relationship between neuroepithelial cells (NE), radial glial cells (RG) and neurons (N), without basal progenitors. From (Gotz and Huttner 2005).

In addition to the above mentioned NE and the RG cells, a third type of progenitors has been described. These are named basal progenitors (BPs) or intermediate progenitor cells (IPCs) (Kriegstein and Alvarez-Buylla 2009). In contrast with the two other types of progenitors, their mitotic divisions do not take place at the apical surface of the neuroepithelium/VZ but in the upper surface of the ventricular zone (VZ) (Haubensak, Attardo et al. 2004; Miyata, Kawaguchi et al. 2004; Noctor, Martinez-Cerdeno et al. 2004). This new dividing cell layer, situated above the VZ, will form later a new mitotic cell layer called the subventricular zone (SVZ) during later stages of neurogenesis. In accordance with the migration of their nucleus to the basal neuroepithelium for S phase, they retract their extension to the apical surface. Moreover, the BPs are exhibiting frequently multipolar processes and are genetically divergent from the NE and the RG cells, since they express *Tbr2* and *Cux1* and *Cux2* for instance, and lack the expression of *GLAST* or *Pax6* (Gotz and Barde 2005). The BPs usually undergo symmetric divisions to produce two differentiated post-mitotic cells (Fig. 4) but sometimes they can also divide symmetrically to generate new BPs that will further divide again and give rise finally to four terminal post-mitotic cells (Noctor, Martinez-Cerdeno et al. 2004). The function of these BPs is, therefore, to amplify the final number of differentiated cells without decreasing the stem cell pool, since a unique progenitor can generate two post-mitotic cells (Fig. 4). At midneurogenesis, the BPs constitute more than

the half of all progenitors in the ventral pallidum, whereas in the cortex, they represent only 25% of them (Gotz and Barde 2005).

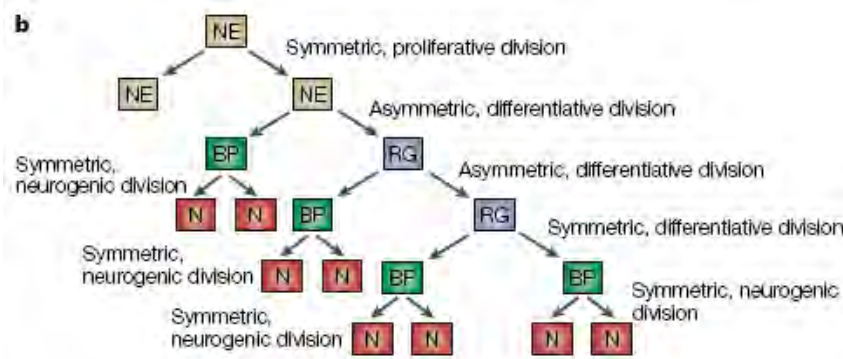


Figure 4. Lineage tree of neurogenesis with BPs. (b) The lineage trees shown provide a simplified view of the relationship between neuroepithelial cells (NE), radial glial cells (RG) and neurons (N), with basal progenitors (BP). From (Gotz and Huttner 2005).

1.2.2 Outer radial glial cells

In addition, the SVZ has been divided into an inner SVZ (ISVZ) and an outer SVZ (OSVZ) following cytoarchitectonic analyses. Historically, the OSVZ was previously described only in gyrencephalic brains of primates (Dehay and Kennedy 2007). More recently, it has been shown that both ISVZ and OSVZ could be present in lissencephalic primates (the marmoset), in gyrencephalic non primates (the ferret), as well as in rodent brains, even if the rodents haven't a cytoarchitectonically distinct OSVZ but present some extra sites of actively proliferative progenitors (Reillo and Borrell 2011; Wang, Tsai et al. 2011; Garcia-Moreno, Vasistha et al. 2012). New types of progenitor expressing Pax6, Sox2, P-Vimentin but not Tbr2 have been described in both the ISVZ and the OSVZ (Smart, Dehay et al. 2002; Fish, Dehay et al. 2008; Fietz, Kelava et al. 2010; Hansen, Lui et al. 2010; Reillo, de Juan Romero et al. 2011; Wang, Tsai et al. 2011; Kelava, Reillo et al. 2012). Furthermore, the features of this new type of RG cells situated in the superficial SVZ /IZ of mice cortex or in the OSVZ of larger brains, were further described as bipolar and termed outer radial glia (oRG) (Reillo, de Juan Romero et al. 2011; Wang, Tsai et al. 2011; Garcia-Moreno, Vasistha et al. 2012). The oRGs while having a radial glial morphology are missing the apical process, but they present a basal process which extends to the pia. Time-lapse analyses have revealed that they arise from asymmetric division of the RGCs and then, that they can self-renew and produce neuronal precursors after asymmetric cell division and therefore also increase the number of neurons (Wang, Tsai et al. 2011). The proportion of oRG has been estimated to reach 50% of the total population of progenitor cells in the human brain or in the ferret, but it may represent less than

10% in the mouse (Wang, Tsai et al. 2011). While the existence of a correlation between the oRG proportion and the gyrencephaly was previously suggested (Garcia-Moreno, Vasistha et al. 2012), recent works on mice and marmoset have both revealed that these progenitors were also present in lissencephalic species and therefore contradict these first assertions (Wang, Tsai et al. 2011; Kelava, Reillo et al. 2012). These studies altogether suggest that oRGs like-cells are not a specific feature of gyrencephaly but, that they are probably found in all mammalian brains, and that the increased number of these oRGs through evolution participated to the production of neurons and consequently contributed to the cortical amplification.

1.2.3 Symmetrical and Asymmetrical division

The apical-basal polarity of the NE and RG cells forms an essential feature for their division pattern. Within the neuroepithelial layer, the mitotic division occurs in an up and down fashion. Indeed, the movements of the NE cells nuclei during the S phase of mitosis give a pseudo-stratified aspect to the proliferative neuroepithelium. These nuclear movements start even before the onset of the neurogenesis and are called interkinetic nuclear migrations (Taverna and Huttner 2010). An internal machinery involving microtubules and actin filaments might lead to these movements of the nucleus during cell cycle progression (Gotz and Huttner 2005). Two distinct mode of division have been reported. They allow maintaining a ratio between the increasing proliferative pool and the differentiative mitoses that occur at the expense of the enhancing pool. These are termed symmetrical versus asymmetrical divisions (Fig. 5). The symmetric divisions thus, produce two daughter cells which are identical and that share a similar fate, while the unequal divisions, generate one cell strongly similar to the mother cell and another differentiated cell (Miyata, Kawaguchi et al. 2001; Noctor, Flint et al. 2001; Miyata, Kawaguchi et al. 2004).

It has been hypothesized that the two kinds of divisions can occur due to the polarized shape of the NE and the RG cells. The vertical and the horizontal planes of division of the nucleus and cytoplasm were thought to result in a symmetrical and an asymmetrical division of the progenitors respectively (Chenn and McConnell 1995; Huttner and Brand 1997). First, the cleavage planes those are parallel to the ventricular zone's apical surface (horizontal) which are rather rare, are triggered by Pax6 and result in asymmetric divisions, as the apical constituents will be inherited by one daughter cell and the basal by another involving an unequal transfer of the cellular components from the mother cell to the daughter cells (Fig. 5) (Heins, Cremsi et al. 2001). The apical components can comprise tight junctions, adherent

junctions and centrosomes whereas, the basal plasmic membrane contains constituents such as integrin α (Noctor, Martinez-Cerdeno et al. 2004; Gotz and Huttner 2005). The cleavage planes that are oriented in the radial dimension (vertical) are triggered by Emx2 and would result in symmetric divisions (equal transfer of the cellular components) (Heins, Malatesta et al. 2002; Kosodo, Roper et al. 2004). Pax6 and Emx2 transcription factors thus regulate the apt choice of cell division which regulates cell fate in a coordinated way.

Moreover, the BPs within the SVZ go through symmetrical divisions to give birth to two neurons (Noctor, Martinez-Cerdeno et al. 2004), whereas the oRG progenitors of the OSVZ divide asymmetrically to generate one new oRG daughter cell which keeps the basal process and one neuron (Hansen, Lui et al. 2010; Wang, Tsai et al. 2011).

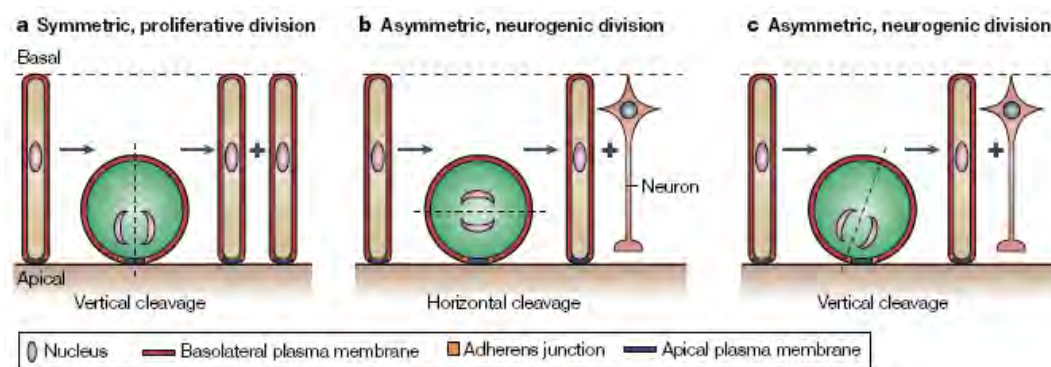


Figure 5. Symmetric versus asymmetric division of neuroepithelial and radial glial cells. The figure summarizes the relationship between apical–basal polarity, cleavage-plane orientation and the symmetric, proliferative versus asymmetric, neurogenic division of neuroepithelial and radial glial cells. For the apical–basal polarity of the plasma membrane, please refer to the key. **(a)** Vertical cleavage results in a symmetric, proliferative division. **(b)** Horizontal cleavage results in an asymmetric, neurogenic division. **(c)** Vertical cleavage results in an asymmetric, neurogenic division. From (Gotz and Huttner 2005).

1.3 Dorso-ventral genetic specification and patterning

The embryonic mammalian telencephalon displays regional differences based on morphological criteria and also exhibits distinct transcriptional patterns which allow to divide it into a dorsal and a ventral telencephalon (Puelles, Kuwana et al. 2000; Marin and Rubenstein 2001; Yun, Potter et al. 2001; Schuurmans and Guillemot 2002; Schuurmans, Armant et al. 2004; Guillemot, Molnar et al. 2006; Long, Cobos et al. 2009) (Fig. 6).

The dorsal telencephalon (pallium) is subdivided into: the dorsal pallium (Rossi, Zoico et al.), which generates the neocortex, the medial pallium (MP), which gives rise to the archicortex, as well as the lateral pallium (LP) and the ventral pallium (VP). The ventral telencephalon (subpallium) is subdivided into the lateral (LGE), the medial (MGE) and the caudal (CGE) ganglionic eminences. By contrast, the anterior entopeduncular area (AEP) and

anterior preoptic area (POA) which originate from the diencephalon are intimately linked to the other ganglionic eminences.

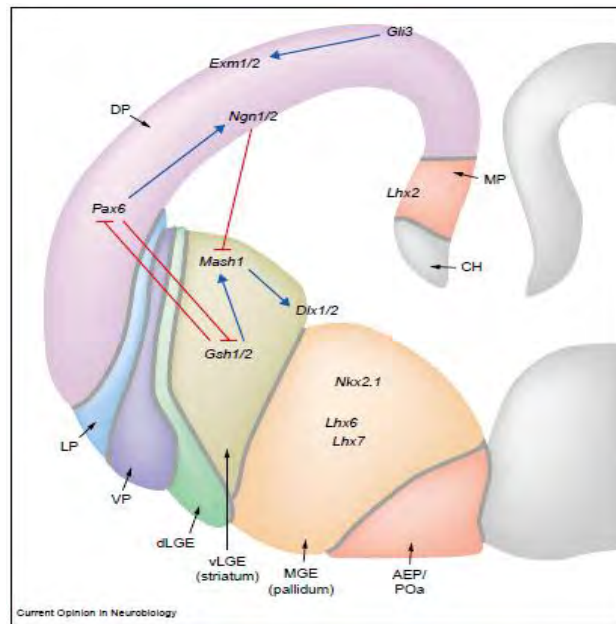


Figure 6. Genetic interactions underlying the regionalization of the mammalian telencephalon.

A schematic representation of a coronal section through the telencephalon, at E12.5, showing dorsal and ventral subdomains as defined by their unique pattern of gene expression. Dorsal telencephalic progenitors express high levels of the bHLH transcription factors *Ngn1* and *Ngn2*, and the homeodomain proteins *Emx1*, *Emx2*, and *Pax6*, whereas ventral progenitors express the bHLH protein *Mash1* and the homeodomain transcription factors *Gsh1*, *Gsh2*, *Dlx1*, *Dlx2*, *Dlx5* and *Dlx6*. The LGE can be subdivided into dLGE and vLGE compartments on the basis of higher levels of *Pax6*, *Gsh2*, *Dlx2* and *Mash1* in dLGE progenitors, and expression of *Gsh1* only in the vLGE. Progenitor populations in the MGE can be further distinguished from those in the LGE on the basis of expression of *Lhx6*, *Lhx7* and *Nkx2.1*, which also encode homeodomain transcription factors. Important cross-regulatory interactions between *Ngn1/2* and *Mash1* and *Pax6* and *Gsh2* participate in the maintenance of telencephalic progenitor identity. Arrows denote positive interactions; T-bars denote inhibitory controls. From (Schuurmans and Guillemot 2002).

As mentioned previously, early morphogens generally initiate the telencephalic subdivisions which are characterized by a precise pattern of genes expression. A territorial identity is defined and maintained by a diversity of transcription factors and their cross-regulatory interactions.

Early during embryogenesis, the dorsalizing *Gli3* and ventralizing *Shh* genes define the ventral and dorsal subdomains of the dorsal and the ventral telencephalon (Hebert and Fishell 2008). *Shh* and forkhead box G1 (*Foxg1*) are both inhibitors of *Gli3*, but they are activators of the fibroblast growth factor gene (*Fgf*). Together, FOXG1 and FGF cooperate to

produce the ventral telencephalon, as well as, many different areas of the dorsal telencephalon except some specific structures of the dorsal midline such as the cortical hem and the choroid plexus. Afterwards, the partitioning of the dorsal telencephalon is achieved by many essential genes: the dorsal midline fate is repressed by *Lhx2* and *Foxg1* and is under the regulation of BMP/WNT morphogens (Hebert and Fishell 2008) (Fig. 7). Moreover, *Gli3* activates *Emx1/2* which cooperates with *Pax6* to develop the dorsal pallium (Yoshida, Suda et al. 1997; Mallamaci, Muzio et al. 2000; Bishop, Garel et al. 2003).

Importantly, the pallial/subpallial boundary is defined as early as E9.0 by *Pax6* and *Gsx2* (*Gsh2*) through mutual cross-repressive interactions (Toresson, Potter et al. 2000; Yun, Potter et al. 2001; Carney, Cocas et al. 2009). The dorsal *Pax6* is repressed by *Gsx1/2* which promotes the ventral *Ascl1* (previously *Mash1*). Both are of crucial importance for ventralization (Corbin, Gaiano et al. 2000; Moreno, Gonzalez et al. 2009; Wang, Waclaw et al. 2009). In the ventral most part, the *Nkx2.1* transcription factor specifies the progenitors of the MGE while repressing the LGE features (see chapter 3) (Sussel, Marin et al. 1999). Then, the post-mitotically active *Lhx6/7* genes are downstream targets of *Nkx2.1*, and are required for the specification of the striatal interneurons and the migration of the cortical interneurons (Lavdas, Grigoriou et al. 1999; Alifragis, Liapi et al. 2004; Liodis, Denaxa et al. 2007; Du, Xu et al. 2008; Nobrega-Pereira, Kessarlis et al. 2008). Only recently, *COUP-TFII* (*Nr2F2*) was shown to be specifically expressed in the CGE (Kanatani, Yozu et al. 2008).

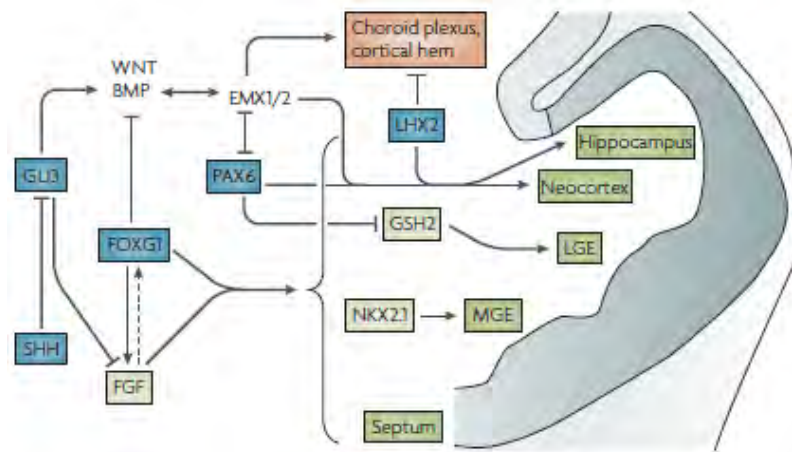


Figure 7. Key genetic pathways that interact to form and pattern the early telencephalon. Factors that act early to establish broad telencephalic regions are shown in blue. Sonic hedgehog (SHH) ventralizes the telencephalon by antagonizing the dorsalizing effect of GLI3. By repressing *Gli3*, SHH, together with forkhead box G1 (FoxG1), activates fibroblast growth factor (FGF) expression. FGF might feedback and promote *Foxg1* expression (dotted arrow). FoxG1 and FGF signaling are necessary for forming all regions of the telencephalon (shown in green), except for the dorso-medial region (shown in orange). Downstream transcription factors, such as GSH2 and NKX2.1, then form specific subdivisions. In the dorsal telencephalon, GLI3's promotion of the expression of bone morphogenetic proteins (BMPs) and Wingless/Int proteins (WNTs) is required for EMX-gene expression. The products of the EMX genes, along with PAX6 and LHX2, further subdivide the dorsal telencephalon. LGE, lateral ganglionic eminence; MGE, medial ganglionic eminence. From (Hebert and Fishell 2008).

1.4 Neuronal subtype specification

The neocortex generates pyramidal glutamatergic projection neurons that extend long distance axons toward other intracortical, subcortical or subcerebral structures. These neurons display several particular features that allow to classify them in subgroups following their morphology, their position in a specific laminar area of the cortex, their transcriptional expression pattern and finally, their function (Molyneaux, Arlotta et al. 2007). The particular connectivity of the projection neurons also depends on their positioning in the cortical layers. The neurons that are born early are situated in the deep layers V/VI and they mainly send corticofugal projections. Among them, the layer VI neurons make corticothalamic connections and the layer V pyramidal neurons send projections to subcerebral structures (corticotectal, corticopontine and corticospinal) (Fig. 8). On the contrary, the late-born neurons migrate to upper layers (II/III) and they mainly extend intracortical projections. Part of them represents the commissural neurons subtype such as the callosal projection neurons (CPN). However, the CPNs can be located within layer II/III as well as layer V and VI (Fig. 8).

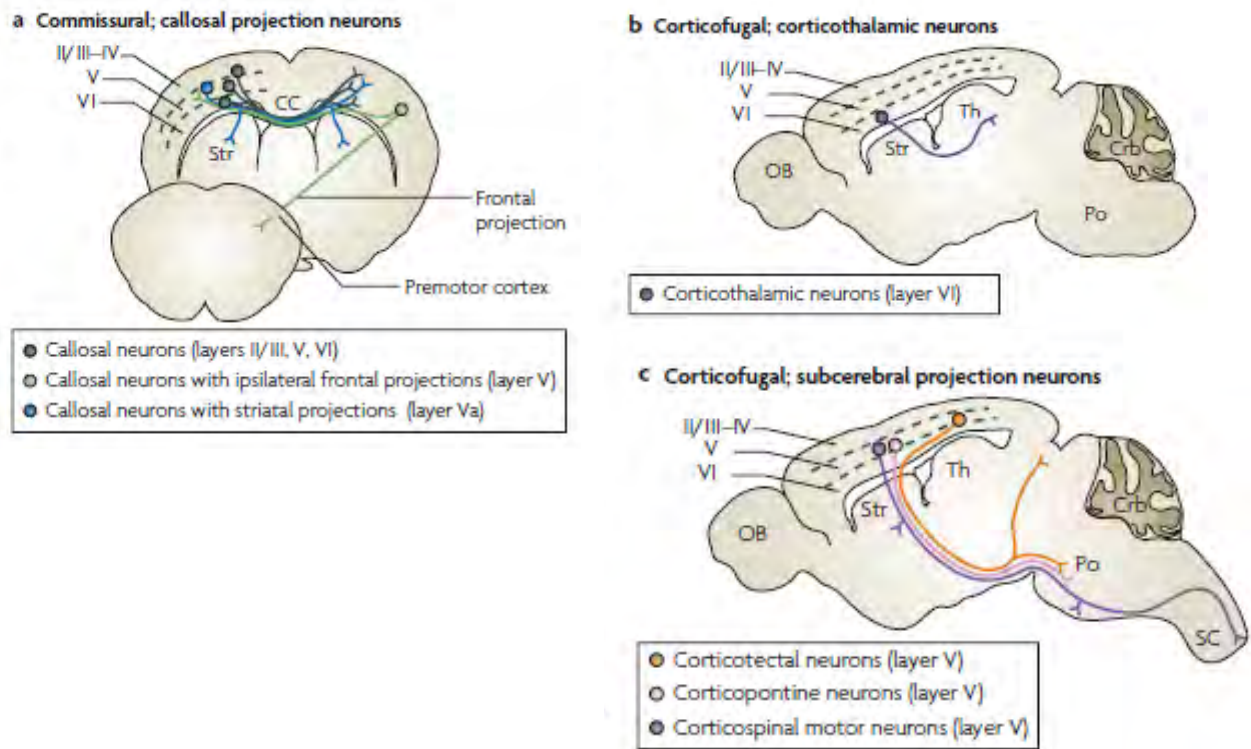


Figure 8. Major subtype of projection neurons within the neocortex. (a) Callosal projection neurons primarily located in layers II/III, V and VI which extend axons across the corpus callosum (CC). Three major types of CPN sending: 1) single projection to the contralateral cortex (black), 2) dual projections to the contralateral cortex and ipsi- or contra-lateral striatum (Str) (blue) and 3) dual projections to the contralateral cortex and ipsilateral frontal cortex (green). (b and c) Corticofugal projection neurons separate in two classes: corticothalamic projection neurons (b) which locate mainly in layer VI and project to different nuclei of the thalamus (Th) and subcerebral projection neurons (c) from layer V which project to the brainstem and the spinal cord. The latter are subdivided in: 1) corticotectal neurons (orange), visual projections to the superior colliculus with collaterals in the pons (Po), 2) corticopontine neurons (pink) with projections to the pons and 3) corticospinal motor neurons (purple) with projections to the spinal cord with collaterals to the striatum, red nucleus, pons and medulla. From (Molyneaux, Arlotta et al. 2007).

Recently, the discovery of several genes that are both layer and subtype specific increased the understanding of how the projection neuron subtypes are regulated (Molyneaux, Arlotta et al. 2007). Moreover, the same energy is employed to classify the cortical interneurons which comprise huge subtype diversity, although they represent only 20-30% of all cortical neurons. Interestingly, they exert several important functions such as the regulation of the proliferation, migration and the control of the circuitry (Ben-Ari, Khalilov et al. 2004; Levitt, Eagleson et al. 2004; Represa and Ben-Ari 2005; Wang and Kriegstein 2009). Principally, the morphology and the molecular and physiological properties of the cortical interneurons are the basic criteria for their classification (Markram, Toledo-Rodriguez et al. 2004; Monyer and Markram 2004; Flames and Marin 2005; Ascoli, Alonso-

Nanclares et al. 2008; Anastasiades and Butt 2011). Lately, the use of fate mapping techniques and transcriptional studies have allowed to elucidate the interneurons diversity (Wonders and Anderson 2006; Du, Xu et al. 2008; Xu, Tam et al. 2008; Gelman, Martini et al. 2009; Anastasiades and Butt 2011; Gelman, Griveau et al. 2011).

1.4.1 Glutamatergic and GABAergic fate

In the cerebral cortex, the excitatory glutamatergic projection neurons are generated by the progenitors of the dorsal telencephalon while the GABAergic inhibitory interneurons originate from the precursors of the ventral telencephalon (Marin, Anderson et al. 2000; Marin and Rubenstein 2001; Kriegstein and Noctor 2004; Molyneaux, Arlotta et al. 2007).

Downstream of *Pax6*, the proneural basic helix-loop-helix (bHLH) transcription factors *Ngn1/2* are responsible for the repression of the ventral signaling of *Gsx2* and *Ascl1* (*Mash1*) (Fode, Ma et al. 2000; Stoykova, Treichel et al. 2000) (Fig. 7). Then, downstream of *Ngn1/2*, the neuronal differentiation is in turn induced by the bHLH genes like *NeuroD1/2*, *Math2/3* and the T-box genes *Tbr1/2* (Hevner, Shi et al. 2001; Schuurmans, Armant et al. 2004; Guillemot, Molnar et al. 2006; Hevner 2006). In summary, this signaling cascade leads the neuroepithelial progenitors to commit and differentiate to a glutamatergic neuronal phenotype : $Pax6 \rightarrow Ngn2 \rightarrow Tbr2 \rightarrow Tbr1$ (Hevner 2006).

Similarly, in the ventral telencephalon, different transcription factors control the fate of the stem cells so that they acquire GABAergic features through a regulatory pathway. The progenitors express the proneural gene *Ascl1* (*Mash1*) that activates the *Dlx* family genes. Indeed, *Dlx5/6* are expressed throughout the ventral telencephalon (Puelles, Kuwana et al. 2000; Wilson and Rubenstein 2000; Yun, Potter et al. 2001) while *Nkx2.1* is present in the MGE progenitors (Grigoriou, Tucker et al. 1998; Marin, Anderson et al. 2000). Moreover, *Dlx2* has been shown to activate the enzyme for the GABA synthesis namely the glutamic acid decarboxylase (GAD)67 (Stuhmer, Anderson et al. 2002). Therefore, the following signaling cascade: $Gsx1/2 \rightarrow Ascl1 \rightarrow Dlx \rightarrow GAD$ regulates the specification and differentiation of the GABAergic neurons (Marin and Rubenstein 2001; Hevner 2006) (Fig. 7).

A recent study has beautifully demonstrated that, the ectopic expression of *Fezf2*, known to specify corticofugal projection neurons in the layer V, is sufficient to redirect LGE GABAergic precursors toward neurons with a glutamatergic identity and subcortical projections (Gotz 2010; Rouaux and Arlotta 2010).

1.4.2 Origin and specification of the cortical projection neurons

There are four essential early genes for the specification towards cortical projection neurons identity within the dorsal telencephalon: *Lhx2*, *Foxg1*, *Emx2* and *Pax6* that repress the ventral fate (Molyneaux, Arlotta et al. 2007; Hebert and Fishell 2008). Neurogenesis begins around E10.5 in the mouse, with the production of the primordial plexiform layer (PP) (Molyneaux, Arlotta et al. 2007). At E11.5, the multilayered neocortex derives from the PP that is split by the cortical plate. The neocortex is composed of six layers. They form in an inside-out fashion, with the later born neurons that migrate longer distances and are positioned at the periphery, followed by the early born neurons (Fig.9a).

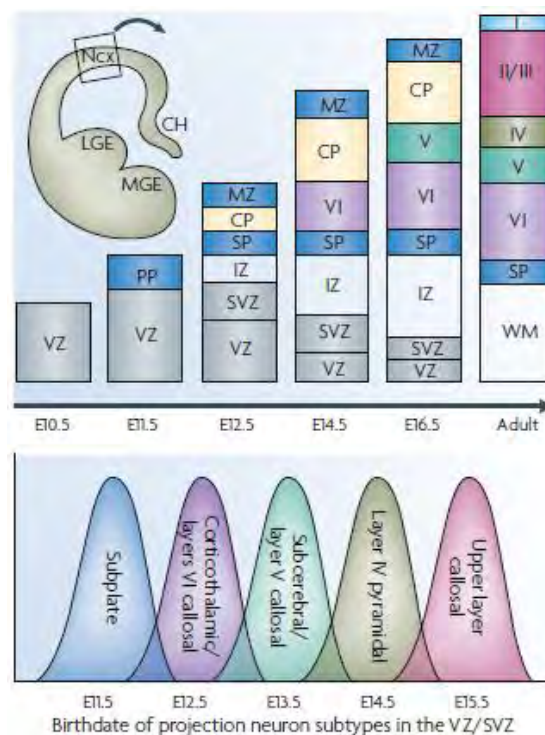


Figure 9a. Schematic depicting how progenitors residing in the VZ and SVZ in mice produce projection neurons in an ‘inside-out’ fashion. The earliest born neurons form the preplate (PP), which is later split into the more superficial marginal zone (MZ) and the deeply located subplate (SP). The cortical plate (CP), which will give rise to the multilayered neocortex, develops in between these two layers, such that later born neurons arriving at the cortical plate migrate past earlier born neurons. Different classes of projection neuron are born in overlapping temporal waves. All times listed are approximations given the neurogenic gradients that exist across the cortex, where caudomedial neurogenesis lags behind rostralateral neurogenesis. CH, cortical hem; E, embryonic day; Ncx, neocortex; IZ, intermediate zone; LGE, lateral ganglionic eminence; MGE, medial ganglionic eminence; SVZ, subventricular zone; VZ, ventricular zone; WM, white matter. From (Molyneaux, Arlotta et al. 2007).

The early progenitors generate the projection neurons that distribute in all the cortical layers, while the late progenitors are progressively restricted to the production of upper-layer neurons (Fig 9a). *In vitro* and *in vivo* studies reveal that this temporal sequence in which

projection neurons subtypes are formed is related to intrinsic factors (Shen, Wang et al. 2006; Molyneaux, Arlotta et al. 2007) (Fig. 9b). Moreover, elegant techniques using transgenic mouse lines allowing layer or lineage-restricted genes investigation and FACS-purified neuronal subtypes microarray have allowed to define multiple layer and subtype-specific genes (Gong, Zheng et al. 2003; Arlotta, Molyneaux et al. 2005; Sugino, Hempel et al. 2006; Molyneaux, Arlotta et al. 2007; Molyneaux, Arlotta et al. 2009) (see details in Fig. 9b).

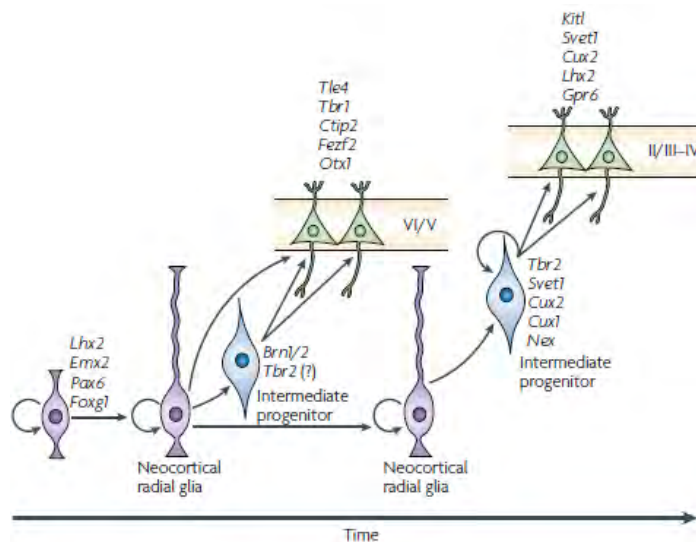


Figure 9b. Schematic representation of a potential model for the generation of projection neuron subtypes from progenitors. According to this model, the concerted action of genes such as forkhead box G1 (*FoxG1*), LIM homeobox 2 (*Lhx2*), paired box 6 (*Pax6*) and empty spiracles homologue 2 (*Emx2*) induce neuroepithelial cells to give rise to radial glial progenitors with neocortical potential. As development proceeds, radial glial progenitors located in the ventricular zone generate intermediate progenitors in the subventricular zone, which, under the influence of layer (*Svet1*, *Cux1/2*, *Lhx2*, *AP2γP2* for layers II/III to IV, *Brn2* for II-III and V, *Rorb* for layer IV and deep-layer-specific like *Opn3* for layer V and *Foxp2*, *Tbr1* for layer VI) and neuron (*Ctip2* and *Otx1* in sub-cerebral neurons of layer V and *Lmo4* and *Satb2* in callosal neurons of layers II/III and V) type-specific genes, generate deep-layer and upper-layer projection neurons. A selection of the genes with either known stage-specific functions or restricted expression is listed. From (Molyneaux, Arlotta et al. 2007).

1.4.3 Origins and specification of the cortical GABAergic interneurons

Numerous experimental approaches have confirmed the subpallial origin of cortical GABAergic neurons. For instance, dye labeling (de Carlos, Lopez-Mascaraque et al. 1996; Anderson, Mione et al. 1999; Anderson, Marin et al. 2001), retroviral lineage analysis or chimerical mice (Kriegstein and Noctor 2004) were performed. Moreover, cell transplantation paradigms and genetic fate-mapping studies indicate that the MGE and CGE are the primary source of GABAergic cortical interneurons (Lavdas, Grigoriou et al. 1999; Anderson, Marin et al. 2001; Marin and Rubenstein 2001; Nery, Fishell et al. 2002; Xu, Cobos et al. 2004; Butt, Fuccillo et al. 2005; Fogarty, Grist et al. 2007; Sousa, Miyoshi et al. 2009; Miyoshi, Hjerling-

Leffler et al. 2010; Rubin, Alfonsi et al. 2010; Rudy, Fishell et al. 2010; Vitalis and Rossier 2010; Vucurovic, Gallopin et al. 2010). In addition, it has been proposed that they might also rise in part from the LGE (Anderson, Marin et al. 2001; Inta, Alfonso et al. 2008; Vucurovic, Gallopin et al. 2010), the septum (Tagliatalata, Soria et al. 2004) and the POA (Gelman, Martini et al. 2009). The inactivation of transcription factors that regulate the differentiation (*Ascl1*, *Dlx1* and *Dlx2*) or the regionalization (*Nkx2.1*) in the ventral telencephalon have definitely confirmed the subpallial origin of the cortical GABAergic interneurons, since it leads to a strong numeric decrease of GABAergic neurons in the cerebral cortex and in the hippocampus (Anderson, Eisenstat et al. 1997; Casarosa, Fode et al. 1999; Sussel, Marin et al. 1999; Pleasure, Anderson et al. 2000; Super, Del Rio et al. 2000).

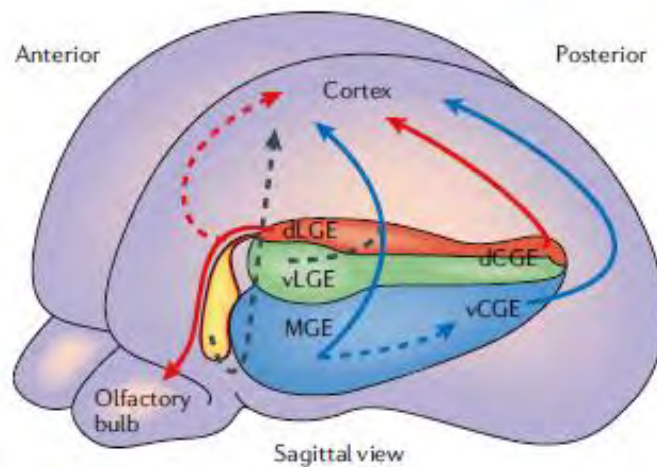


Figure 10. Migration pathways of cortical interneuron subgroups from the ventral telencephalon. Schematic illustration of established (solid arrows) and proposed (dashed arrows) pathways of migration of cortical interneurons. Blue arrows represent somatostatin (SST)- or parvalbumin (PV)-containing interneuron progenitors. Red arrows represent calretinin (CR)-containing interneuron progenitors. Black arrows represent the potential migration of cortical interneuron progenitors, the subtype of which has yet to be determined. SST and PV interneurons primarily migrate from the *Nkx2.1*-expressing MGE and from the ventral CGE (vCGE). These interneurons have also been shown to migrate caudally from the MGE into the CGE (blue shading). CR interneurons primarily arise from the dorsal CGE (dCGE). The dorsal LGE (dLGE) expresses *ER81* (red shading) and also generates CR interneurons destined for the olfactory bulb, which might contribute to the cortical CR interneuron population. Progenitors from the vLGE (green shading) also migrate to the cortex, and could represent an undetermined subgroup of cortical interneurons. Finally, *Vax1*-expressing progenitors of the septal region (yellow shading) might generate cortical interneurons of an unknown subgroup. From (Wonders and Anderson 2006).

Importantly, the MGE has been shown to give rise to half of the totality of the cortical interneurons, and to a large extent of the striatal interneurons and the pallidal neurons (Sussel, Marin et al. 1999; Wichterle, Garcia-Verdugo et al. 1999; Marin, Anderson et al. 2000; Anderson, Marin et al. 2001; Butt, Fuccillo et al. 2005; Wonders and Anderson 2006;

Nobrega-Pereira, Kessaris et al. 2008; Xu, Tam et al. 2008; Flandin, Kimura et al. 2010; Miyoshi, Hjerling-Leffler et al. 2010)(Fig.10). For years, the role of the CGE in producing cortical GABAergic neurons was underestimated. Indeed, it has been proved recently that the CGE generates 30 % of the cortical interneurons (Nery, Fishell et al. 2002; Xu, Cobos et al. 2004; Yozu, Tabata et al. 2005; Miyoshi, Hjerling-Leffler et al. 2010; Rubin, Alfonsi et al. 2010; Vucurovic, Gallopin et al. 2010). However, by using both a Cre-subtractive mouse model for LGE/CGE-derived cortical interneurons and a 5-HT3A-GFP mouse that reliably labels CGE-derived embryonic neocortical interneurons, it has been proved that the CGE-derived cortical neurons differ from those coming from the MGE (Yau, Wang et al. 2003; Niquille, Garel et al. 2009; Rubin, Alfonsi et al. 2010; Vucurovic, Gallopin et al. 2010).

Additionally, the LGE generate only a small quantity of cortical interneurons but is the main source for the olfactory bulb and striatal projection neurons (Wichterle, Garcia-Verdugo et al. 1999; Anderson, Marin et al. 2001; Wichterle, Turnbull et al. 2001; Stenman, Toresson et al. 2003; Yun, Garel et al. 2003). *In vitro* studies have reported some LGE-derived interneurons migration towards the neocortex (Anderson, Marin et al. 2001; Jimenez, Lopez-Mascaraque et al. 2002). Moreover, during early postnatal ages, 5-HT3-GFP interneuron precursors that may initially derive from the LGE, have been shown to again divide within the rostral migratory stream (RMS) and the white matter and then migrate to the cortex (Dayer, Jenny et al. 2008; Inta, Alfonso et al. 2008). On the contrary, several *in vivo* fate mapping experiments counter argue that the cortical interneurons do not originate from the LGE (Wichterle, Turnbull et al. 2001; Nery, Fishell et al. 2002; Butt, Fuccillo et al. 2005).

The CGE and MGE-derived interneurons are molecularly distinct (Valcanis and Tan 2003; Butt, Fuccillo et al. 2005; Xu, Tam et al. 2008). Indeed, *Nkx2.1* is required to specify PV-, SST- and neuropeptide Y (NPY)-expressing interneurons in the MGE and to direct them towards the cortex or the striatum (Sussel, Marin et al. 1999; Marin, Anderson et al. 2000; Anderson, Marin et al. 2001; Wonders and Anderson 2006; Du, Xu et al. 2008; Nobrega-Pereira, Kessaris et al. 2008) (Fig.10). Then, two downstream targets of *Nkx2.1*, *Lhx6/7*, specify the striatal interneurons and additionally, *Lhx6* is involved in the migration of cortical interneurons, too (Alifragis, Liapi et al. 2004; Liodis, Denaxa et al. 2007; Du, Xu et al. 2008; Fragkouli, van Wijk et al. 2009). Furthermore, the *Dlx* family of transcription factors also has diverse functions, since *Dlx5/6* regulates the development of PV-containing interneurons (Wang, Dye et al. 2010) while *Dlx1/2* controls the interneuron migration (Anderson, Eisenstat et al. 1997; Anderson, Marin et al. 2001). The *Dlx* family is also involved in the specification of CR-positive CGE-derived interneurons (Xu, Cobos et al. 2004). In addition to the spatial origin, the timing of specification is important for the regulation of intrinsic properties of

mature GABAergic neurons (Butt, Fuccillo et al. 2005; Miyoshi, Butt et al. 2007; Miyoshi and Fishell 2010; Miyoshi, Hjerling-Leffler et al. 2010).

The preoptic area (POA) was additionally shown to give rise to cortical interneurons which derive from *Nkx5.1*-expressing progenitors. They preferentially populate the superficial layers I and II (Gelman, Martini et al. 2009). Finally, the cortical SVZ and some specific cortical regions might serve as supplementary origin for the postnatal interneurons (Letinic, Zoncu et al. 2002; Dayer, Cleaver et al. 2005; Dayer, Jenny et al. 2008).

2. Gliogenesis: The choice between glial versus neuronal fate

As already mentioned, it is accepted that the diverse cell types of the mammalian CNS are produced in a sequential time frame by cell type selection or commitment in a defined order. The neurons are first to arise and then they are followed by the oligodendrocytes and finally the astrocytes. Many recent studies have focused their interest on the mechanisms that lead to the cell fate instruction wherein several extracellular molecules or epigenetic mechanisms, as well as, intrinsic signaling cues are involved. Generally, the signaling pathways are complex, they modulate several transcription factors, they intermingle and their effects can change according to the cellular environment and/or the developmental stage (Guillemot 2007).

2.1 Neuronal fate

The neuronal fate is instructed by Wnt, PDGF and Pax6 which display multiple roles in the time course of development (Bertrand, Castro et al. 2002; Guillemot 2005; Guillemot 2007).

- For instance, Wnt induces: (1) at early stages (<E13.5), the CNS formation and its patterning, it promotes dorsal and prevents ventral identity, and it promotes the proliferation of progenitors and (2), at late stages (>E13.5), it promotes neurogenesis by a cell cycle cessation and then the neuronal differentiation. This indicates that Wnt signaling has a function in the commitment of multipotent progenitors into neurons. The proneural downstream effectors of Wnt are the bHLH Ngn-1 and Ngn-2 that are directly activated by the canonical pathway.

-Additionally, PDGF also instructs the neuronal fate via the MEK-ERK pathway that will phosphorylate transcription factors of the CAAT/enhancer –binding protein /C/EBP) family and lead to the activation of neuronal genes such as T α 1 for α -tubulin (Guillemot 2007).

-In addition, Pax6 is a key factor for neurogenic instruction in the CNS. If Pax6 is no more expressed anywhere in the dorsal telencephalon, the number of cortical precursors are increased and the projection neurons are no longer produced (Fishell and Kriegstein 2003) (Gotz and Barde 2005). It functions as a patterning factor by influencing the fate of progenitors via modulation of activity of pro-neuronal genes like *Ngns* and *Mash1*.

2.2 Astroglial origin and fate

2.2.1 Astroglial origin

- **Date of birth:** Birth-dating experiments using thymidine analogues have shown that most glial cells are generated at late embryogenesis (from E16) and first postnatal weeks (Angevine and Sidman 1961; Berry and Rogers 1965; Lent et al. 1990; Jacobson 1991). However, due to the use of markers that labeled the cells at exit of the cell cycle it is possible that the timing for astrogliogenesis has been overvalued. It is mainly accepted that by the end of the embryonic period, at E18 in the mouse, the RG cells of the entire CNS, only transform to astrocytes that then start to proliferate (Schmechel and Rakic 1979; Pixley and de Vellis 1984). First, the RG cells initiate major morphological changes in their shape from bipolar to unipolar, which does not contact the ventricles anymore, and then to multipolar form with a regressing radial process to terminate their transformation in an astrocytic morphology (Takahashi, Misson et al. 1990; Mission, Takahashi et al. 1991; Kriegstein and Alvarez-Buylla 2009).

- Radial glia heterogeneity and unipotent precursors:

The heterogeneity of RG cells seems to be related to the regionalization of the developing CNS, since only the RG of the LGE contain the retinol-binding protein-1 (RBP-1) and Gsh2 for instance, and those of the MGE are labeled for Olig2 (Malatesta, Hack et al. 2003; Pinto and Gotz 2007), and Pax6 is only expressed in the dorsal telencephalic RG cells. In the ventral telencephalon, at midneurogenesis only few of RG generate neurons (Kriegstein and Gotz 2003; Malatesta, Hack et al. 2003; Gotz and Barde 2005; Gotz and Huttner 2005; Pinto and Gotz 2007). The few neurons that are generated by the RG cells of the ventral telencephalon represent either a specific subpopulation of interneurons that migrates to the olfactory bulb (Malatesta, Hack et al. 2003) and another population of MGE-derived Olig2- and Mash1-positive RG cells that might be at the origin of GABAergic neurons migrating tangentially to the cortex (Kriegstein and Gotz 2003). Therefore, while at midneurogenesis most of the projection neurons are originating from the RG of the dorsal telencephalon, the GABAergic neurons of the subpallium probably arise from BPs instead of RG cells. By contrast, the latter were observed to give birth to oligodendrocytes (Malatesta, Hack et al. 2003). As a consequence, this implies that the fate of the RG cells and their progeny differs in the ventral and in the dorsal telencephalon and thus, a kind of regionalization exists in this type of progenitors.

Moreover, it has been shown that at the onset of neurogenesis, many molecules, such as, Mnb (from the *Drosophila Minibrain* gene), Tis21, ephrin B1 and Xl α s (extra-large G protein α -subunit) were expressed in only some dividing NE cells, which might represent some early marker for neurogenic RG cells and therefore, attest for some early heterogeneity in the RG cell population (Kriegstein and Gotz 2003). This heterogeneity has also been reported for neurons (Long, Cobos et al. 2009), for oligodendrocytes (Kessaris, Fogarty et al. 2006; Kessaris, Pringle et al. 2008) and recently also for mature astrocytes in the spinal cord (Hochstim, Deneen et al. 2008). It is still unclear whether glial cells are generated from bipotent or multipotent progenitors (Rowitch and Kriegstein, 2010). *In vitro* analyses propose a model of bipotent oligodendrocytes and astrocytes precursors (Raff et al, Nature, 1983). By contrast, several investigations using retroviral lineage markers found that in the cortex, a single RG cell clone was giving rise to a homogenous neuronal (in 34% of the cases) or glial (in 47% of the cases) population (Price and Thurlow 1988; Grove, Williams et al. 1993; Luskin, Parnavelas et al. 1993; Costa, Bucholz et al. 2009) Contrastingly, only 10% of the RG progenitors were able to generate a mixed population of neurons and glia (Parnavelas, Barfield et al. 1991; Levison and Goldman 1993; Parnavelas 1999). In conclusion, RG cells seem to contain intrinsic information about the fate of their progeny and mediate the direct transmission of patterning in the neuronal or glial fates and thus, contribute to the neuronal and glial diversity of the CNS (Pinto and Gotz 2007).

Thereafter, some astrocytes might proliferate locally and therefore, form a type of intermediate progenitors referred to as astrocytic intermediate progenitor cells (aIPC) (Kriegstein and Alvarez-Buylla 2009) that will further give rise to a new astroglial population postnatally. Whether the aIPCs derive from RG cells or from early NE progenitors, is not well defined.

-Sites of origin:

Astrocytes are believed to originate from two different sources: from the RG of the dorsal telencephalon (Misson et al, glia; Price and Thurlow 1988; Shcmechel and rakic, 1979) and from migratory progenitors that reside in the dorsolateral SVZ and that, from this SVZ region, colonize the white matter and the cerebral cortex. The dorsolateral SVZ have been found to be derived from Dlx2 precursors and therefore may originate at first from the subpallium (Marshall and Goldman 2002). The RG cells remain during the entire period of neurogenesis

and are finally transformed into mature astrocytes (Schmechel and Rakic 1979; Pixley and de Vellis 1984; Mission, Takahashi et al. 1991; Mori, Buffo et al. 2005).

However, how newborn astrocytes migrate and whether they can be dispersed tangentially is not yet known (Rowitch and Kriegstein, 2010). While tangential migration has been observed in the striatum for the parenchymal astrocytes (Kriegstein and Alvarez-Buylla 2009), a recent study on spinal cord astrocytes suggests that such a mechanism might be very rare (Hochstim, Deneen et al. 2008). This implies that astrocytes may inherit positional information directly from their original RG progenitors array (Rakic 1988).

The astroglial differentiation is commonly described following the expression of markers such as GFAP and S100 β (Pixley and de Vellis 1984; Gotz and Barde 2005; Gotz and Huttner 2005). However, the signaling routes that lead to the astrocytic commitment and differentiation are tremendously complex.

2.2.1 Astroglial fate

-Notch signaling:

In the dorsal pallium, the Notch signaling regulates the temporal switch from neurogenesis to gliogenesis (Guillemot 2007). To initiate this regulation, the Notch acts on the GFAP promoter and its downstream effectors, the *Hes* genes. These genes then inhibit in turn the activation of the proneural bHLH factors (Guillemot 2007; Rowitch and Kriegstein 2010). In addition, the entrance into some gliogenic pathways for promoting the astrocyte development relies on JAK-STAT signalling, BMP morphogens and CoupTF transcription factors (Gaspard and Vanderhaeghen 2010) which in turn activate other downstream transcription factors like STATs, SMADs and RBP-JK (Fig.11).

Firstly, the Notch pathway is known to be responsible for the maintenance of an undifferentiated state of the NE progenitors, and subsequently to promote the transformation of NE into RG cells and finally to drive the differentiation of the latter into astrocytes (Anthony, Mason et al. 2005) (Fig. 11).

- At the onset of neurogenesis (E10-E12), Notch signaling will play an important role in the transformation of NE into RG, by directly activating the BLBP and the Neuregulin receptor ErbB2 that are important to promote the radial glia phenotype and the *Hes1/Hes5* transcriptional repressors that maintained RG cells undifferentiated.

- At the onset of astroglialogenesis (>E17), Notch might activate the GFAP promoter: directly via a transcriptional complex involving the notch intracellular domain (Notch-ICD) that causes the CLS to switch from a repressor form to an activator form of the GFAP

promoter; indirectly via an interaction with the Hes1/Hes5 proteins that promote astrogliogenesis in the retina and might exert the same action in the telencephalon after (1) repressing the proneuronal Ngn-1/Ngn-2 and Mash1 targets and (2) activating the JAK/STAT pathway (Guillemot 2005; Guillemot 2007; Kessaris, Pringle et al. 2008) (Fig.11b). JAK/STAT is one of the main processes involving astroglial fate determination through activation of the GFAP promoter. Indeed, the GFAP promoter contains a binding site for phosphorylated STAT1 and STAT3 which can also bind to cofactors of the p300/CREB-binding protein (CBP), forming a large complex with the RNA polymerase II that will increase the transcription (Kessaris, Pringle et al. 2008).

-BMP signaling:

Besides, the BMPs have also been described as astrocytic promoters (Guillemot 2005; Guillemot 2007; Kessaris, Pringle et al. 2008; Rowitch and Kriegstein, 2010) (Fig.11).

In late progenitor cultures (>E14) in which they are shown to work in a synergistic manner with:

(1) the JAK/STAT pathway via smad1/sm4 that bind and promote to the GFAP promoter activity; (2) the Notch pathway with Smad1 forming a complex with Notch-ICD and other co-activators of Hes5; (3) by the induction of Id proteins sequester E proteins that block the proneuronal activity of neurogenins and Mash1.

In addition, the BMPs are also known to promote astrogliogenesis in the adult SVZ which is balanced by Noggin that promotes neurogenesis through a BMP inhibition. Moreover, BMPs and Shh have been shown to have antagonistic effects. Indeed, BMPs can induce astroglial specification and repress oligodendrocytes formation *in vitro*, while the contrary is true for Shh (Kessaris, Pringle et al. 2008).

-FGF2 and EGF signaling:

Furthermore, FGF2 and EGF are mainly involved in the proliferation of telencephalic progenitors, but can, at a higher concentration either promote oligodendrocytes genesis (see above) or in combination with other signals promote astrocytic genesis (Guillemot 2007)(Fig.11). Finally, EGF receptor is asymmetrically allocated to the daughter cell of some progenitors and therefore leads to the diversification of the precursor identity (Sun, Goderie et al. 2005).

From E14, some gliogenic signals like the cytokines (CNTF, LIF, IL-6 and cardiotrophin-1), the BMPs or the EGF can induce a premature differentiation of astrocytes by binding to cell surface receptors, indicating that at this stage the progenitors have the ability to respond to these molecules. A negative feedback might be exerted by the newly born neurons

since they can produce these signals and thus, they might promote the switch from neurogenesis to gliogenesis, too. Remarkably, at the onset of gliogenesis, the progenitors return to a symmetrical mode of division (Guillemot 2007)(Fig.11).

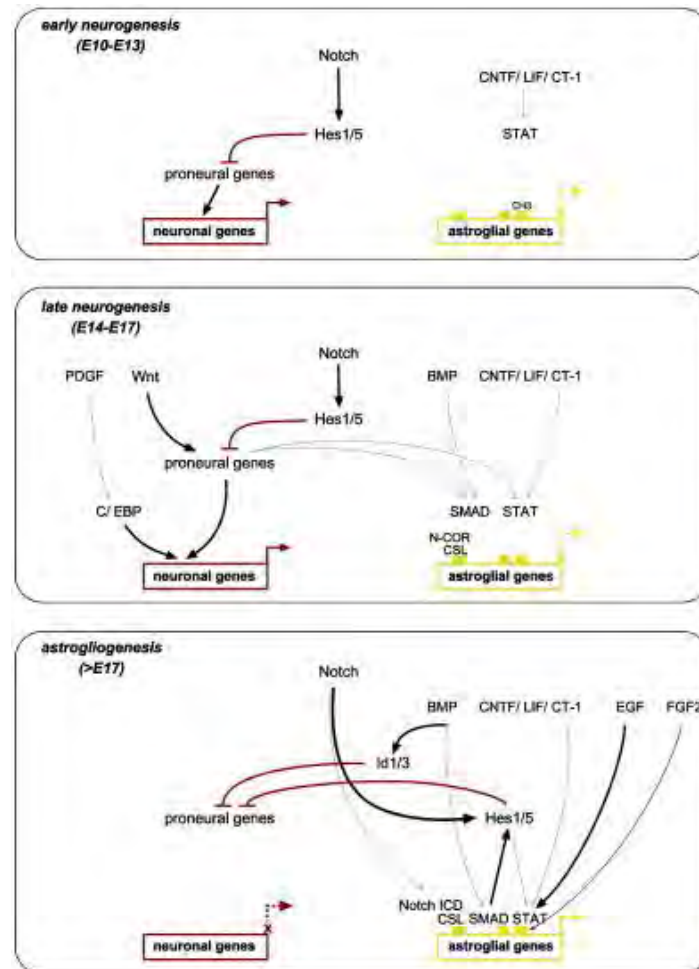


Figure 11. Pathways regulating the neurogenesis and the astroglialogenesis by neural stem cells. Synergistic and antagonistic interactions between multiple extracellular signals and transcription factors determine whether progenitors adopt a neuronal or an astroglial fate. Thick black arrows represent transcriptional activations, thick red lines represent transcriptional repressions, thin grey arrows represent non-transcriptional positive interactions and thin grey lines non-transcriptional negative interactions. From (Guillemot 2007)

2.3 Oligodendroglial origin and fate

2.3.1 Oligodendroglial origin

The controversial origin of oligodendrocyte progenitors (OLPs) or oligodendrocyte precursor cells (OPCs) in the forebrain, has been studied by Kessaris and colleagues (Kessaris, Fogarty et al. 2006; Kessaris, Pringle et al. 2008). The oligodendrocytes were first identified into

preparations of rat optic nerves, and they were believed to originate equally from all the germinal zones of the embryonic telencephalon (Kessaris, Pringle et al. 2008). However, several works have shown that the MGE and AEP precursors express Shh and its receptor Patched (Kaptchuk, Kelley et al.), as well as Olig2 which strongly suggest that OLPS may originate from these regions (Spassky, Heydon et al. 2001; Tekki-Kessaris, Woodruff et al. 2001). In accordance with these observations, a stream of migrating OLPS generated at E12.5 and expressing the platelet-derived growth factor α (PDGFR α) was observed originating from the corresponding regions and entering the cerebral cortex at E16.5 (He, Ingraham et al. 2001) (Marshall and Goldman 2002). Finally, using an elegant transgenic Cre-lox fate mapping approach, Kessaris and colleagues could show that three consecutive functionally equivalent waves of telencephalic OLPS were generated from three different germinal sites. At E12.5, a first wave of OLPS was arising from *Nkx2.1*-positive precursors of the MGE and AEP. By E15, a second wave of OLPS was arising from *Gsh2*-positive precursors of the LGE and CGE. Finally, a third additional source of *Emx-1*-positive OLPS was shown to derive from cortical precursors at birth. This study suggests that at birth the total population of cortical OLPS is composed of two ventral and one dorsal originating population of cells (Kessaris, Fogarty et al. 2006; Kessaris, Pringle et al. 2008). 10 days after birth, the ventral telencephalon contained the three OLPS populations, and 30 days after, the entire telencephalon was populated only by *Gsh-2* or *Emx-1*-derived oligodendrocytes (Kessaris, Fogarty et al. 2006; Kessaris, Pringle et al. 2008). Therefore, the *Nkx2.1*-derived OLPS were transient in nature and disappeared totally from the telencephalon 30 days after birth.

Postnatally, in addition to the RG cells of the VZ, the type B cells or the SVZ astrocytes continue to generate oligodendrocytes, in addition to neurons (Kriegstein and Alvarez-Buylla 2009), via the intermediate progenitor cells (Fogarty, Richardson et al. 2005) (Casper and McCarthy 2006). Surprisingly, some oligodendrocyte progenitor cells have also been extracted from the cortical marginal zone (MZ) and have been observed to generate clones containing astrocytes and oligodendrocytes *in vitro* (Kriegstein and Alvarez-Buylla 2009). However, some fate-mapping experiments indicate that these MZ OLPS are also ultimately derived from the VZ. Therefore, it seems that the oligodendrocytes are originating from the RG cells of the VZ of both the ventral and the dorsal telencephalon (Kriegstein and Alvarez-Buylla 2009).

Furthermore, new evidences have shown that the mature myelinating oligodendrocytes, that express the myelin basic protein (MBP), are also generated from some of NG2-positive cells (see below) that are considered as OLPS (Reynolds and Hardy 1997) (Butt, Hamilton et al. 2005; Haber, Vautrin et al. 2009). The NG2-labeled cells lying in the

nascent white matter also expressed some oligodendrocyte specific markers after birth (Levine, Stincone et al. 1993). In addition, time-lapse confocal microscopy unraveled that the NG2-expressing cells were relatively stable and non-motile cells. However, the proportion of cells that differentiate into premyelinating oligodendrocytes, characterized by the expression of 2',3'-cyclic nucleotide 3'-phosphodiesterase (CNP), and the transitional oligodendrocytes, displayed a high density of processes and OLG-growth cones, but were negative for NG2 labeling. Also, the premyelinating CNP-positive cells were displaying very dynamic extensions and retractions of their actin-containing processes (Haber, Vautrin et al. 2009).

Nevertheless, the mechanisms that regulate OLPs migration from the SVZ towards the white matter and the differentiation into mature oligodendrocytes which myelinate axons are still not well defined in the postnatal brain. Only one study has been documented showing the chemotactic and chemokinetic effects exerted by endothelin-1 (ET-1), an astrocytic soluble signal on proliferation, differentiation and migration of OLPs. The OLPs express both the G-protein-coupled ET_A and ET_B receptors (Gadea, Aguirre et al. 2009) and the effects mediated via their activation were studied both *in vitro* and *in vivo*. Interestingly, PDGF as well as FGF were seen to increase the expression of ET receptors in cultured OLPs. The ET-1-dependent signaling was observed to promote the migration of these cells while inhibiting their differentiation.

2.3.2 Oligodendroglial fate

The neuroepithelial precursor cells (NPCs) generate the vast diversity of neurons and glial cells populating the mature CNS. The morphogens, like Sonic hedgehog (Shh), FGF-2, insulin-like growth factor-1 (IGF-1) and members of the bone morphogenetic protein (BMP) family, have been documented to transmit positional information to the NEPs to help them adopt specific oligodendroglial cell fate. The specification is defined through several pathways involving combinatorial expression of various transcription factor genes.

Induction of oligodendrogenesis:

Through Shh-dependent pathway:

The oligodendrocyte precursor bHLH transcription factors 1 (Olig1) and 2 (Olig2) mark the entire oligodendrocyte lineage from the very early stages, and their transcripts can be seen in the spinal cord from E9 onwards. The morphogenetic gradient formed by the Shh triggers their expression in the spinal cord and the ventro-medial telencephalon too (see also chapter 3.3 on *Nkx2.1*-regulated oligodendrocytes specification) (Takebayashi, Nabeshima et al. 2002;

Kessaris, Pringle et al. 2008). Additionally, the neuroepithelial cells in the ventral spinal cord of the *Olig2*^{-/-} mice failed to differentiate into oligodendrocytes and instead displayed expression of an astrocytic marker, S100 β (Takebayashi, Nabeshima et al. 2002). Recent evidences have also shown that *Olig1*, which was previously believed to be unessential, functions as a key regulator of the oligodendrocyte maturation and myelinogenesis. Moreover, the embryos lacking function of both *Olig1* and *Olig2* genes, displayed complete absence of the oligodendrocytes, in the entire CNS (Zhou and Anderson 2002; Kessaris, Pringle et al. 2008). Shh also triggers the expression of other homeobox genes such as *Nkx6.1*, *Nkx6.2* and *Nkx2.2* which play a role in oligodendrocytic production and their maturation within the spinal cord via regulating the expression of *Olig2* in a dose-dependent manner (Vallstedt, Muhr et al. 2001; Vallstedt, Klos et al. 2005).

Through Shh-independent pathway:

However, the NEPs from the Shh-null mice, could still potentiate the generation of OLPs, thus, demonstrating the presence of a Shh-independent pathway for the oligodendrocyte specification. Supportingly, if the NEPs from the spinal cord were cultured in presence of FGF-2 and cyclopamine (inhibitor of Hh signaling), they generated OLPs (Kessaris, Jamen et al. 2004; Kessaris, Pringle et al. 2008). Secondly, evidences have also shown that IGF-1 also influences oligodendrocytic specification. Though the contribution of IGF-1 has not yet been conclusive, there have been studies demonstrating its importance towards oligodendrocyte maturation (Ye, Li et al. 2002). Thirdly, the *Sox* gene family (*Sox8*, *Sox9* and *Sox 10*), have also been rendered necessary for the proper oligodendrocyte development (Kessaris, Pringle et al. 2008). Fourthly, *Mash1* (or *Ascl-1*) which is co-expressed with *Olig2* in the AEP/MGE, has also been shown to be present in a population of migrating OLPs and in a portion of oligodendrocytes of the olfactory bulbs. The pups deficient in *Mash1* expression, show severely reduced numbers of oligodendrocytes in the olfactory bulb (Parras, Hunt et al. 2007). Finally, the Delta-Notch signaling has also been shown to be essential at early stages for OLPs production whereas, at later stages, Notch has been shown to prevent their maturation *in vitro* (Kessaris, Pringle et al. 2008).

Inhibition of oligodendrogenesis:

The members of the BMP family have been shown to act as negative regulators of oligodendrocyte specification and differentiation. The neural stem cells from the forebrain or the spinal cord failed to develop any oligodendrocytes when cultured in the presence of BMPs, even if Shh or FGF-2 were present (Vallstedt, Klos et al. 2005). *In vivo* studies performed with chicken spinal cord corroborated these findings, and displayed inhibition of

OLP development upon BMP ectopic expression (Mekki-Dauriac, Agius et al. 2002). The inhibitory effect is mediated via sequestration of Olig proteins and the bHLH cofactors required for interaction with the target genes (Samanta and Kessler 2004). Supportingly, incorporation of the BMP antagonist, Noggin, accelerated oligodendrocyte production (Mekki-Dauriac, Agius et al. 2002).

2.4 Glial cell types: a matter of cell diversity

2.4.1 The radial glial cells

See paragraphs 1.2.1 and 2.2.1.

2.4.2 The mature astrocytes

The astrocytes were first described more than one century ago. They were visualized by Golgi staining as “star-like” cells and were initially considered, as “a glue” for the scaffolding of the neurons, which was unable to communicate (Kimelberg 2004; Volterra and Meldolesi 2005). It is now known that adult astrocytes, which represent 20-50% of the total amount of cells of the brain, exert multiple functions such as, to provide a structural support to the neurons, to regulate the water and ion balance, to maintain the blood-brain-barrier, to regulate the cerebral blood flow, to provide nutrients, to participate in the cell signaling via calcium fluxes, to produce neuropeptides, to modulate the synaptic transmissions and to release gliotransmitters such as glutamate, ATP and D-serine either through exocytosis or through volume-regulated anion channels (VRACs) and gap junctions (Volterra and Meldolesi 2005).

Ramón y Cajal was first using the term “ependimoglia” to refer to radial glial cells and “neuroglia” to refer to astrocytes, and he was also the first scientific to consider that neuroglial cells were originating from the ectoderm (Kimelberg 2004). Then, del Río Hortega, showed that in the third element constituted by oligodendroglia and microglia, the latest was from mesodermal origin and therefore, the name neuroglia was replaced by oligodendroglia and astroglia (Kimelberg 2004). These two groups are forming the category of macroglia, from ectodermal origin, in opposition to the microglia which has a mesodermal origin (Kimelberg 2004).

Now, within the astroglial group, the mature astrocytes can be divided into two types namely fibrous and protoplasmic (Kimelberg 2004). The first category of astrocytes is found in the white matter and exhibits a star-like shape with dense processes constituted by intermediate filaments bundles that are stained by the GFAP (glial fibrillary acidic protein) marker. The second category is found in the grey matter, has a more bushy-like shape and

unsheathes the synapses and contacts the blood vessels with numerous thin processes (Kimelberg 2004; Kessaris, Pringle et al. 2008; Rowitch and Kriegstein 2010). Consequently, the second category of astrocytes has been called: GFAP-negative protoplasmic astrocytes (Kessaris, Pringle et al. 2008).

Therefore, categories of mature astrocytes have been defined according to other molecular markers, the filling of their cell body and processes with dyes, or according to their electrophysiological profile (Kimelberg 2004). Within the additional molecular markers known to be expressed in astrocytes, there are the calcium-binding protein S100 β (Ludwin, Kosek et al. 1976), the glutamine synthetase (GS) enzyme, the glutamate and aspartate astrocyte-specific transporter (GLAST), the fibroblast growth factor receptor 3 (Fgfr3), and the water-channel aquaporin-4 (Aqp4) (Malatesta, Hack et al. 2003; Kimelberg 2004; Gotz and Huttner 2005; Volterra and Meldolesi 2005; Kessaris, Pringle et al. 2008).

On the other side, the electrophysiological investigations done on astrocytes have first revealed that they were exhibiting a “passive” profile lacking voltage-gated currents. More extensive and recent studies have then lead to the existence of a more “complex” physiology including Na⁺ and K⁺ currents and were also called as variably rectifying astrocytes (VRA) or outward rectifying astrocytes (ORA), but this more complex profile has been then associated to early post-natal astrocytes implicating that probably the mature astrocytes, which are intensively coupled by gap junctions, should present a more passive electrophysiological phenotype (Kimelberg 2004; Zhou, Schools et al. 2006; Kessaris, Pringle et al. 2008).

Moreover, studies using *GFAP-Cre* transgenic mice suggested that some GFAP⁺ cells were typical protoplasmic astrocytes with passive electrical profile and gap junction coupling, whereas some others were identified by low GFAP expression, a complex electrical profile, the presence of AMPA receptors and no gap junctions (Kimelberg 2004; Volterra and Meldolesi 2005).

Importantly, the astrocytes are now considered as “excitable” since they exhibit [Ca²⁺]_i oscillations and transients in response to chemical signals from neurons or spontaneously. Astrocyte excitation has been observed in several circuits in the entire brain following release of glutamate, dopamine, acetylcholine, noradrenaline, GABA, ATP, NO and BDNF by neurons (Volterra and Meldolesi 2005). Moreover, astrocytes display highly dynamic and plastic processes which encompass the synapses and confirm the astroglial nature of the third element of the tripartite synapses. Finally, the spontaneous excitation of astrocytes can lead to the excitation of neurons. According to the new insights emerging on astrocytes, these cells are now seen as polyvalent and playing a role in nearly all processes occurring in the brain (Volterra and Meldolesi 2005).

2.4.3 The reactive astrocytes

Generally, the mature astrocytes are quiescent but they can start to proliferate after brain injury. Genetic fate-mapping and cell-type-specific viral targeting have now provided new evidences that show that quiescent astrocytes start to divide and express GFAP, Vimentin and Nestin after brain injuries due to neurodegenerative diseases, ischemic damages or stab wounds. Thus, astrocytes can contribute to reactive gliosis that surrounds axotomized and dying neurons (Kimelberg 2004; Kang and Hebert 2011). Therefore, these cells are proliferating GFAP-positive cells, called as reactive astrocytes (Kimelberg 2004; Kessaris, Pringle et al. 2008; Buffo, Rite et al. 2008). They begin to increase their expression of cytokines, chemokines and extracellular matrix molecules (Kang and Hebert 2011).

Interestingly, the $Olig2^+/NG2^+$ progenitors have been observed to proliferate and give rise to reactive astrocytes in the cortex in response to stab wound or cryo-injuries (Kang and Hebert 2011). In a genetic fate-mapping study, using *Olig2-Cre ERTTM* inducible mice, Kouko Tatsumi and colleagues could demonstrate that the Shh regulated *Olig2*-derived $NG2^+$ cells could give rise to bushy-like GFAP⁺ reactive astrocytes forming scars in the adult injured cerebral cortex (Tatsumi, Takebayashi et al. 2008). Moreover, another fate-mapping study using a *Nestin-Cre ERTTM* inducible strain coupled to a BrdU-labeling showed that after P10, $NG2^+$ polydendrocytes originating from adult SVZ, which is also dependent on Shh signaling, were the major proliferative cells to give rise to reactive gliosis after a stab wound injury (Burns, Murphy et al. 2009; Kriegstein and Alvarez-Buylla 2009).

The precise role of these reactive astrocytes in the pathogenesis of CNS diseases has only recently started to emerge. For instance, in pathological conditions such as ischemia or traumatic injury, reactive astrocytes and microglia start to form clusters of reactive gliosis in which abnormal interactions between the two types of cells results in massive $TNF\alpha$ (tumor necrosis factor α) release and neurotoxic levels of glutamate release (Volterra and Meldolesi 2005). Moreover, in brain tumors such as gliomas, the communication properties of astrocytes are impaired in such a way that the excessive release of glutamate is reinforced by a lack of its uptake. In some cases of AIDS, the microglia can be affected by the HIV virus which causes dysregulation of astrocytes and finally a massive and cytotoxic release of $TNF\alpha$ and glutamate, too.

Finally, whether the reactive astrogliosis that appears in neurodegenerative diseases is more beneficial or detrimental is still a matter of debate (Okada, Nakamura et al. 2006; 2011; Kang and Hebert 2011). However, the response of reactive astrogliosis to pathologies might also serve to protect the still intact tissue of the CNS from secondary lesions by forming a scar

which isolate the damaged area and thus prevent the spread of the toxic inflammatory response out from the damaged tissue into the intact area (Kimelberg 2004).

2.5 The oligodendrocytes

The morphologically diverse shapes of the oligodendrocytes, acquired during differentiation into promyelinating (or premyelinating) oligodendrocytes, have been extensively studied at diverse developmental stages. First, they differentiate into motile premyelinating oligodendrocytes with many branching processes and oligodendrocyte-growth cones (OLG-growth cones). Then, as soon as they form at least one myelin sheath, they are named as transitional oligodendrocytes due to presence of both ensheathing and non-ensheathing processes. The transitional cells display reduced number of radial processes and increased myelin internodes. Finally, they are termed as mature myelinating oligodendrocytes when they comprise of ensheathing processes only that connect cell bodies and myelin internodes. These initiator processes spirally ensheath the target axons, thus, leading to the formation of the myelin sheath turns (Hardy and Friedrich 1996; Haber, Vautrin et al. 2009).

2.6 The NG2⁺ polydendrocytes

2.6.1 Polydendrocytes identity

Polydendrocytes were first identified in the early 1980s using a rabbit serum raised against rat brain tumour cells different from typical neuronal or glial cells (Nishiyama et al., 2009). After the identification of NG2 (nerve/glial antigen-2), an integral membrane chondroitin sulphate proteoglycan (CSPG-4), as one of the epitopes recognized by the serum, a new line of research aims to clarify the identity of these NG2-expressing cells. The mammalian NG2 protein is encoded by one gene containing multiple exons that generate 2327 amino acids. The NG2 protein is a part of the neurexins family constituting of cell adhesion molecules containing a large extracellular domain, one transmembrane domain and a small intracellular domain containing a type I PDZ (*Post-synaptic density 95/Zonula-occludens-1*) sequence and several threonines that can be phosphorylated. It contains also a type II PDZ domain, a SH2 (*Src Homology type 2*) domain and a WW binding motif which are all implicated in intracellular interactions or signaling. In addition, the extracellular domain can be cleaved by proteases and is delivered in the extracellular matrix for signaling (Trotter, Karram et al. 2010). The type I PDZ domain binds to MUPP-1, GRIP and Syntenin-1. GRIP, in turn, binds to the GluR2/3 subunits of the AMPA and glutamate receptors expressed by the NG2 cells in

response to glutamate release by neurons which can then influence oligodendrocytic differentiation. Moreover, Syntenin works as a connector to the cytoskeleton which can thus, influence NG2⁺ cells migration (Trotter, Karram et al. 2010).

NG2⁺ cells have been at first considered as OLPs (see paragraph 2.3.1. and below). In addition, a fraction of the NG2-positive cells do not appear to divide and neither generate mature oligodendrocytes (Trotter, Karram et al. 2010) and remain NG2-positive resident cells in the rodent adult CNS. For this reason, the NG2⁺ cells comprise a unique population of cells which has been called either polydendrocytes (Nishiyama, Watanabe et al. 2002; Nishiyama, Komitova et al. 2009; Trotter, Karram et al. 2010) or synantocytes (Butt, Hamilton et al. 2005; Wigley and Butt 2009) and the term OLP has been reserved specifically for the cells that generate oligodendrocytes. Finally, the NG2⁺ polydendrocytes are genetically different from the fibrous and protoplasmic astrocytes, the microglia and the mature oligodendrocytes too, which suggests that they are forming a fourth major type of glial cells in the CNS (Nishiyama et al., 2009).

Studies on the polydendrocytic morphology using dye-filling strategies have revealed that they have a simpler shape than the protoplasmic astrocytes with multiple thin processes. The processes of polydendrocytes are more smooth and straight than those of the microglial cells, although they are also closely associated to the latter. Immunolabeling studies have unraveled that NG2⁺ polydendrocytes do not express any of the astrocytic markers such as GFAP and GLAST (Nishiyama, Watanabe et al. 2002). By contrast, some studies revealed that polydendrocytes express some astrocytic markers such as the GS at low levels and S100β. Ultrastructurally, the polydendrocytes are distinct from astrocytes since they have electron dense cytoplasm and nucleus, and also lack glycogen granules and intermediate filaments. The nucleus of NG2⁺ cells also displays different shapes; it can either have a smooth contour with clumped chromatin or have a lighter irregular shape with a dispersed chromatin (Nishiyama, Komitova et al. 2009).

2.6.2 Polydendrocytes lineages:

- Oligodendroglial fate of polydendrocytes (see paragraph 2.3.1 and below):

It is generally accepted that polydendrocytes constitute OLPs:

- NG2 is expressed in OLPs that differentiate into mature oligodendrocytes *in vitro*. They most probably correspond for a part to the oIPCs (oligodendrocyte intermediate progenitor cells) but however, unlike the actively dividing IPCs, they are found in the white matter and the grey matter, where they are quiescent or where they divide symmetrically (Kriegstein and

Alvarez-Buylla 2009). There are recent evidences which show that NG2⁺ progenitors are derived from the SVZ postnatally (Aguirre, Dupree et al. 2007) but paradoxically, other studies have shown that the IPCs of the SVZ do not express NG2 and that NG2 is only expressed in the parenchyma surrounding the SVZ (Trotter, Karram et al. 2010).

- *In vitro* and *in vivo* studies have revealed that PDGFR α and NG2 co-localize in almost 100% of the cases and that they are downregulated at the same time when O4 (marker for oligodendrocyte precursors) starts to be expressed (Trotter, Karram et al. 2010). Nevertheless, NG2 becomes only detectable at E15, *in vivo*, on PDGFR α ⁺ cells, when they exit the VZ and is never seen in PDGFR α ⁺ cells inside the VZ. In addition, most polydendrocytes in the CC and the cortex labeled for PDGFR α , start to express the immature oligodendrocyte antigen O4 during the first postnatal week (Nishiyama, Komitova et al. 2009). The function of PDGFR α ⁺/NG2⁺ cells as OLPs was established by demonstrating that the loss of PDGFR α ⁺ cells resulted in disappearance of mature oligodendrocytes.

- NG2⁺ cells express Olig1 and Olig2 that are required for the differentiation of oligodendrocytes (paragraph 2.3.2).

- Cell grafting experiments have shown that NG2⁺ cells give birth to myelinating oligodendrocytes when grafted in an environment missing myelinating cells (Franklin, 1997).

- Finally, genetic fate-mapping with *NG2-Cre* mice unraveled that the oligodendrocytes of both the grey and the white matter in the forebrain and the spinal cord are derived from polydendrocytes (Nishiyama, Komitova et al. 2009).

- Interestingly, in the peripheral nervous system (PNS), NG2 is also present in the immature Schwann cells (Trotter, Karram et al. 2010).

- Astroglial fate of polydendrocytes:

As discussed previously (paragraph 2.2.1), while *in vitro* studies have unraveled the capacity for OLPs to generate astrocytes in addition to oligodendrocytes (Raff, Miller et al. 1983), this has never been reproduced in *in vivo* physiological conditions. Type-2 astrocytes from OPCs are considered as an *in vitro* artifact. However, many studies suggest that polydendrocytes might be bipotential astroglial progenitors when transplanted in a glia-depleted environment (Franklin, Bayley et al. 1995; Windrem, Nunes et al. 2004). In addition, fate-mapping studies using *NG2-Cre/lacZ/eGFP* mice indicated that NG2-expressing cells in the grey matter of the ventral posterior but not of the dorsal anterior forebrain give rise to more than 40% of protoplasmic astrocytes (Nishiyama et al, 2009). Interestingly, these NG2⁺ cells exhibited intermediate morphological and antigenic characteristics of polydendrocytes with a weak expression of NG2 and of protoplasmic astrocytes with a weak expression of GLAST (Zhu, Bergles et al. 2008). However, the progeny of polydendrocytes in white matter were either

polydendrocytes or oligodendrocytes but not astrocytes (Nishiyama, Komitova et al. 2009), suggesting that fibrous astrocytes in the white matter originate only from the dorsal RG or from the SVZ, without going through the polydendrocyte stage (paragraph 2.2.1).

While some studies have shown that the downregulation/cytoplasmic translocation of Olig2 is crucial for the astrocytic fate decision, other works using *Olig2-Cre* mice indicate that white matter astrocytes arise from *Olig2*-derived cells (Masahira, Takebayashi et al. 2006). However, as Olig2 is widely expressed in proliferative zones and since its expression is not restricted only to oligodendrocyte cells (Ligon, Kesari et al. 2006), it is possible that white matter astrocytes are derived from early progenitor cells expressing Olig2 but not NG2. In accordance with these observations, the inhibition of Olig2 in GFAP⁺ RG, but not in polydendrocytes, interfere with the genesis of white matter astrocytes (Cai, Chen et al. 2007). Nuclear Olig2 and BMPs seem to have opposite effects in maintaining the balance between oligodendrocyte versus astrocyte differentiation (see paragraph 2.2.1 and 2.3.2). BMPs increase the expression of ID2/ID4 (bHLH proteins lacking a DNA-binding domain) that repress Olig2 by sequestering them and prevent them from forming functional heterodimers. By this mechanism, the endogenous BMPs inhibitor Noggin might inhibit the differentiation of polydendrocytes into astrocytes in the dorsal grey and white matter, even in the injured brain. However, several studies have suggested that proliferating polydendrocytes in response to cortical brain injuries or motor neuron degeneration give birth to astrocytes (see paragraph 2.4.3).

It remains to define whether polydendrocytes are bipotential cells capable of generating both oligodendrocytes and protoplasmic astrocytes or if they form a heterogeneous population with distinct committed progenitor cells giving rise to oligodendrocytes and astrocytes.

- Neuronal fate of polydendrocytes:

The question of whether polydendrocytes are multipotent progenitor cells that can generate neurons as well as oligodendrocytes remains controversial due to many discrepancies between studies. *In vitro* studies using rat optic nerve suggested that OLPs are able to generate oligodendrocytes, astrocytes as well as neurons (Raff, Miller et al. 1983; Rao and Mayer-Proschel 1997). In the *Cnp-eGFP* mice, eGFP⁺/NG2⁺ cells were shown to give rise to neurons in culture or after transplantation. By contrast, NG2⁺/DsRed⁺ cells purified from perinatal *NG2DsRedBAC*-transgenic mouse brains were never found to give rise to neurons in culture.

In vivo, NG2 was detected in the mature cerebral cortex in some GABAergic neuronal cells that had just incorporated BrdU (Dayer, Cleaver et al. 2005). Using *Olig2-Cre ERTTM/Rosa-YFP* or *NG2-Cre/Z/eGFP* transgenic adult mice, the YFP or the GFP signals

were never detected in any neuronal cells, while using *PDGFR α -Cre/Rosa-YFP* transgenic mice, a small number of YFP⁺ neurons were detected in the piriform cortex (Nishiyama, Komitova et al. 2009; Rivers, Young et al. 2008). The discrepancy between studies may be due to the transient neuronal expression of Cre, or possibly NG2 in neurons rather than by lineage progression from polydendrocytes to neurons. Further studies are however required to determine to which extent the normal fate of polydendrocytes can give birth to neurons.

2.6.3 Integration of polydendrocytes in the neurovascular unit

The function of the non-proliferating NG2⁺ glia of the adult CNS still remains to be elucidated. To this purpose, their integration with the neurons, astrocytes and vasculature has been studied. It has been observed that some polydendrocytes and astrocytes were apposed to one another like “sister cells” and that they possess large areas of contact between their cell bodies and processes which intermingle extensively (Wigley and Butt 2009). Inside these contact areas, the synaptophysin is expressed which indicates a potential vesicular communication between the two cells. In addition, both polydendrocytes and astrocytes extend processes towards the blood vessels, but only the astrocytes form perivascular endfeet. By contrast, the polydendrocytes contact the pericytes and may, therefore, also play a role in regulating the blood flow (Wigley and Butt 2009). Importantly, the pericytes also express the NG2 proteoglycan, and the close physical association seen between the polydendrocytes and the pericytes may also suggest a lineage relationship (Wigley and Butt 2009).

2.6.4 Role of polydendrocytes in the synaptic responses

The distribution of the polydendrocytes, that represent 5-10% of the total cells (Trotter, Karram et al. 2010), has been shown to be uniform between the white and the grey matter of the CNS. The NG2⁺ processes were observed to have direct contacts with neuronal synapses, although the NG2⁺ membranes appeared to lack “postsynaptic specializations” (Nishiyama, Watanabe et al. 2002; Wigley and Butt 2009). In the white matter, some perpendicular NG2⁺ cells were also seen to contact astrocytes through their processes (Trotter, Karram et al. 2010). Recent findings have shown that polydendrocytes depolarize in response to glutamate and might correspond to “complex cells” displaying a set of voltage-dependent Na⁺ and K⁺ conductances (Kimmelberg 2004; Trotter, Karram et al. 2010).

It has been established that only few (less than 20) of the synaptic contacts between neurons and polydendrocytes are electrophysiologically active. The NG2⁺ cells form specific points of synaptic contacts whereas the astrocytes form ensheathed pre- and post-synaptic

boutons (Wigley and Butt 2009). Nevertheless, the intimate associations between astrocytes and polydendrocytes were shown to allow a glia-to-glia neurotransmitter-dependent, via ATP and glutamate release, calcium wave signaling (Hamilton, Hubbard et al. 2009). The NG2⁺ polydendrocytes also express AMPA-type glutamate and GABA receptors which allow them to respond to neuronal release of GABA and glutamate (Trotter, Karram et al. 2010). Surprisingly, it has been found that a subpopulation of NG2⁺ cells in the white matter were able to elicit action potentials (Trotter, Karram et al. 2010).

2.6.5 Role of polydendrocytes in axonal outgrowth

It was first speculated that the NG2 proteoglycan, as well as, NG2⁺ cells were repulsive and inhibitory for the axonal outgrowth *in vivo* (Dou and Levine 1994; Chen, Negra et al. 2002; Chen, Ughrin et al. 2002; Nishiyama, Komitova et al. 2009). On the contrary, more recent investigations in the spinal cord have demonstrated that after injury, the axons were regenerated through a dense population of permissive NG2⁺ cells (Jones, Sajed et al. 2003). Moreover, there is no variation in axonal responses in NG2 knockout mice after spinal cord transection (de Castro, Tajrishi et al. 2005). Finally, the NG2⁺ cells *in vitro* were shown not to repel but to promote the axonal outgrowth (Yang, Suzuki et al. 2006; Nishiyama, Komitova et al. 2009). In this study, cultured hippocampal neurons were observed to actively contact the NG2⁺ cells with their growth cones, like *in vivo*, where the growing callosal axons were also seen to contact the polydendrocytes through multiple filopodia (Yang, Suzuki et al. 2006). Interestingly, the level of NG2 proteoglycan expression *in vitro* was not seen to affect the capacity of the growing axons to adhere and to extend on an NG2⁺ cells layer. Therefore, these results strongly suggest that a function of the polydendrocytes could be to offer a positive substrate for promoting axonal growth during development or after injury (Nishiyama, Komitova et al. 2009).

3. *Nkx2.1* homeobox gene: regulation and function

3.1. Expression and regulation of *Nkx2.1*:

The *Nkx2.1* gene is a member of NK2 family of homeodomain-containing protein. The invertebrate NK2 or vnd (ventral nervous system defective) family of genes has been first analyzed in *Drosophila* (Kim and Nirenberg 1989; Guazzi, Price et al. 1990). In the vertebrate, the *Nkx2* subfamily has strong homology to NK2/vnd since it is expressed in the ventral precursors of the embryonic CNS. *Nkx2.1* is also called TTF-1 for thyroid transcription factor 1 or T/ebp for thyroid-specific enhancer binding protein since it regulates the transcription of many genes of the thyroid gland (Guazzi, Price et al. 1990; Lazzaro, Price et al. 1991; Sussel, Marin et al. 1999). During embryonic development, *Nkx2.1* transcription factor is additionally expressed in the lung parenchyma where it activates pulmonary-surfactant genes (Boggaram 2009), and in the pituitary gland (Hamdan, Liu et al. 1998). In the embryonic forebrain, *Nkx2.1* is one of the earliest expressed genes. The detection of its transcripts begins at the one somite stage in the hypothalamic primordium and is clearly detected at seven somites stage in the basal ganglia primordium (Shimamura, Hartigan et al. 1995). From E10.5, expression of *Nkx2.1* is found in the rostrobasal telencephalon that further develops in the medial ganglionic eminence (MGE), the preoptical area (POA), the entopeduncular area (AEP), the septum (SEP), and parts of the amygdala (Dickson 2002; Chilton 2006; Dickson and Zou 2010). Although *Nkx2.2* and *Nkx2.9* are expressed along the entire longitudinal axis of the CNS, *Nkx2.1* is strictly expressed in the forebrain.

In the murine embryos, *Nkx2.1*, like several other *Nkx2* genes, is expressed in the ventral midline of the neuroectoderm, while other *Nkx2* genes are primarily expressed in mesendodermal organs such as the heart and the gut (Pabst, Herbrand et al. 2000). As depicted in figure 15, Sonic hedgehog (Shh) is one of the major secreted signal that drives the formation of organized ventral midline structures (Rubenstein, Martinez et al. 1994; Gulacsi and Anderson 2006). This molecule has previously been shown to be expressed in domains that match the *Nkx2.1* pattern of expression in the ventral forebrain. Moreover, the use of homozygous Shh mouse mutants unraveled the fact that *Nkx2.1* is activated by Shh signaling, since the depletion of Shh leads to the dorsalization of the ventral precursors (Chiang, Litingtung et al. 1996; Gulacsi and Anderson 2006). On the contrary, overexpression of Shh before E11.5, involves the ventralization of dorsal precursors and the expansion of *Nkx2.1*-expressing precursors to dorsal regions (Gulacsi and Anderson 2006). Finally, during neurogenesis, it has been demonstrated that Shh signaling is required to maintain the fate of

Nkx2.1 precursors (Xu, Wonders et al. 2005; Gulacsi and Anderson 2006). In addition, evidences are also showing that *Nkx2.1* expression might be directly or indirectly modulated by the fibroblast growth factor Fgf8 (Shimamura and Rubenstein 1997) and/or by bone morphogenetic proteins (BMPs) that act as dorsalizing molecules (Furuta, Piston et al. 1997; Gulacsi and Anderson 2006).

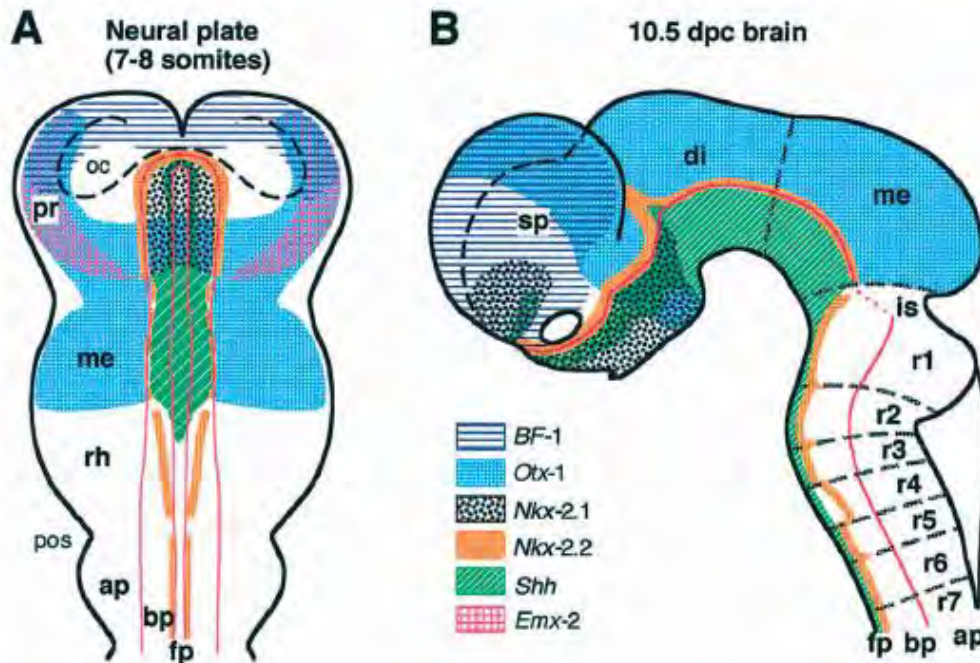


Figure 12. Expression of Nkx2.1 within the longitudinal organization of the brain.

The schematic shows the expression of early gene expression patterns comprising *Nkx-2.1* and *Shh* that underline a longitudinal and transverse organization in the neural plate and neural tube. (A) The neural plate at the 7-to 8-somite stage. (B) The brain at E10.5. *Shh* and *Nkx-2.1* are both expressed in the basal ganglia primordia of the prosencephalon and in the basal plate of the secondary prosencephalon following distinct anteroposterior and dorsoventral distribution. Their expression in these primordia begins after the neural tube formation and is found in tissue that originates from the alar region of the neuralplate. (ap) alar plate; (bp) basal plate; (di) diencephalon; (fp) floor plate; (is) isthmus; (me) mesencephalon; (oc) optical cup; (pr) prosencephalon; (rh) rhombencephalon; (r1-7) rhombomeres; (sp) secondary prosencephalon. From (Shimamura et al. 1995).

3.2 Molecular structure of the Nkx2.1 homeodomain-containing protein

Nkx2.1 gene is situated on chromosome 14 in humans and chromosome 12 in mice (Guazzi, Price et al. 1990). It is organized in two introns and three exons that codes for a 372 amino acid polypeptide that shapes in a helix-turn-helix homeodomain-containing transcription factor (Hamdan, Liu et al. 1998) (Fig.13). In humans, the gene encodes two major transcripts of 371 and 401 amino acids, whose functional significance is still unknown (Breedveld, van Dongen et al. 2002). *Nkx2.1* exerts its transcriptional activity by a direct binding of the homeodomain to the DNA, on the promoter sequences of many different genes (Guazzi, Price

et al. 1990; Sussel, Marin et al. 1999; Lonigro, Donnini et al. 2001). Nkx2.1 is a phospho-protein regulated by a protein kinase A, and its binding to DNA is under a redox control (De Felice, Damante et al. 1995; Ghaffari, Zeng et al. 1997). Moreover, activation of the transcription is driven by two transactivation domains, situated on either side just up and downstream of the homeodomain (De Felice, Damante et al. 1995; Guazzi, Price et al. 1990). Translocation of the protein is insured by a nuclear localization signal (NLS) sequence located at the N-terminus of the homeodomain. However, the homeodomain itself is required for the proper translocation of the protein to the nucleus, and thus, it has been speculated that it has an additional small NLS necessary for the transport (Ghaffari, Zeng et al. 1997).

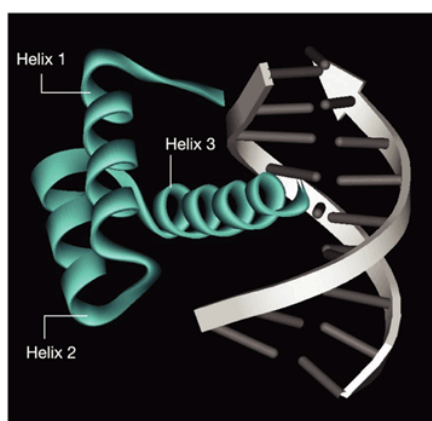


Figure 13. 3-Dimensional structure of Nkx2.1 homeo-protein.

Schematic representation of the Nkx2.1 helix-loop-helix protein and the way it can directly interact within the wide groove of the DNA helix. From (Nature,2000).

It has been reported *in vitro*, that Nestin, an intermediate filament protein of the cytoskeleton in the neuroepithelial precursors, might be a downstream regulated target of *Nkx2.1* (Lonigro, Donnini et al. 2001). More precisely, Nestin is one of the earliest specific markers to be expressed in the embryonic CNS and it is quickly down-regulated after birth, since it is replaced by the glial fibrillary acidic protein (GFAP) in the mature astrocytes and by the neurofilaments in the adult neurons (Lonigro, Donnini et al. 2001). Briefly, in these experiments where NIH3T3 or COS-7 mouse embryonic fibroblast cell line were used, the morphology of the cells was changed to a more elongated shape when *Nkx2.1* was overexpressed and the endogenous *Nestin* gene was also up-regulated showing a strong immunolabeling in the nucleus for Nkx2.1 protein and in the cytoplasm for Nestin protein. In conclusion, the authors propose that Nestin could be an effector through which Nkx2.1 could control the organogenesis of the forebrain by a direct DNA binding of Nkx2.1 on a specific enhancer sequence of *Nestin* gene (Lonigro, Donnini et al. 2001).

Nkx2.1 activates the expression of pulmonary surfactant protein A (SP-A), B (SP-B), C (SP-C), and also secretory protein genes in Clara cells (epithelial cells). The surfactant proteins are indispensable to prevent the lungs from collapsing during the expiration. The alveolar type II cells that secrete these proteins, also perform multiple functions like transport of ions and water across the epithelium, produce molecules during immune responses or inflammation, and proliferate after injury (Kolla, Gonzales et al. 2007). After hormonal treatments, DNA microarray analysis found that the lysosomal-associated membrane protein 3 (LAMP3) for cell proliferation, carcinoembryonic antigen-related cell adhesion 6 (CEACAM6) for signal transduction and cell-cell signaling, endothelin 3 (EDN3) for signal transduction and cell-cell signaling, solute carrier family 39 (SLC39A8) for metal ion transport, fibulin 5 (FBLN5) for cell-matrix adhesion, laminin alpha 3 (LAMA3) for cell adhesion, and others were all *Nkx2.1* target genes responsible for type II cells differentiation (Kolla, Gonzales et al. 2007).

Recently, a genome-wide analysis has been proceeded to find the transcriptional targets of *Nkx2.1* in normal bronchiolar and epithelial cells of the lung and in lung adenocarcinoma cells (Tagne, Gupta et al. 2012). In this study, a plethora of genes such as Notch1, E2f3, Cyclin B1, Cyclin B2 and c-Met, involved in cell proliferation has been found to be bound by *Nkx2.1* and to be expressed in lung development and tumors (Tagne, Gupta et al. 2012).

In the thyroid gland, *Nkx2.1* is known to activate the transcription of the thyroglobulin, the thyroperoxydase and the thyrotropin receptor (TSH) (Lazzaro, Price et al. 1991; Kimura, Hara et al. 1996; Ghaffari, Zeng et al. 1997).

3.3 Function of *Nkx2.1* in the specification of the precursors of the ventral telencephalon

One of the major functions known for *Nkx2.1* gene in the brain is to specify the identity of the neuroepithelial precursors of the MGE which, then give rise to the pallidum (Sussel, Marin et al. 1999) and cortical GABAergic interneurons. In addition to the MGE, and as mentioned above, *Nkx2.1* also regulates the identity of pre-mitotic and post-mitotic cells of the POA, AEP, SEP, and amygdala, which suggests that it can maintain the identity of differentiated cells (Sussel, Marin et al. 1999).

A knock-out mouse containing a disruption of *Nkx2.1* gene has been produced by using a gene targeting strategy in murine embryonic stem (ES) cells (Kimura, Hara et al. 1996) (Fig. 14). Briefly, a genomic DNA clone containing the *Nkx2.1* gene has been isolated

by screening and the coding sequence was used in a targeting vector transfected by electroporation into ES cells. The ES cells colonies containing the disrupted copies of the gene were then injected into the blastocysts of the mice.

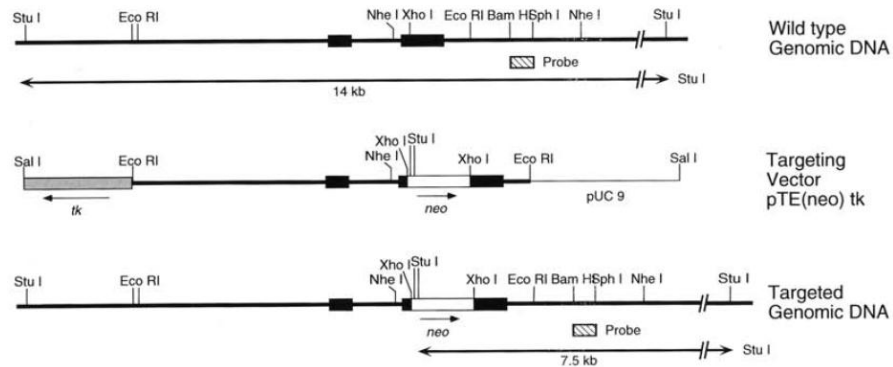


Figure 14. Production of *Nkx2.1*-deficient mice by homologous recombination in ES cells.

The schematic shows the mouse *Nkx2.1* gene, the targeting vector, and the targeted allele. The coding region of the gene is shown by solid boxes. The insertion of a pMCl-neomycine-coding cassette (*neo*) in the second exon of *Nkx2.1* genomic DNA drives to the production of a shorter transcript of 7.5 kb which leads to the disruption of the first helix of the protein. From (Kimura et al. 1996).

The heterozygous (*Nkx2.1*^{+/-}) animals were mated and produced litters with 25 % of pups dead at birth corresponding to the *Nkx2.1*^{-/-} mice. It has been shown that the former developed normally while the latter were smaller and were lacking parts of the ventral forebrain, the pituitary, the thyroid gland and the lungs (Kimura, Hara et al. 1996) (Fig15). In the *Nkx2.1*^{-/-} forebrain, the abnormalities were limited to the ventral regions. The septum was reduced and the pallidum was respecified to a more dorsal fate since the precursors of the mutant MGE (labeled MGE*) adopted an LGE identity and therefore generated striatal-like structures (Sussel, Marin et al. 1999). Interestingly, between E8.5 and E11.5, *Shh* expression was reduced in the mutant to a trace level in the rostral midline and *Pax6*, which is normally repressed by *Shh* and which inhibits *Nkx2.1* in dorsal regions such as the LGE and the cortex (Chiang, Litingtung et al. 1996; Ericson, Rashbass et al. 1997; Sussel, Marin et al. 1999), expands its pattern of expression to the mutated MGE*, where it overlaps *Nkx2.1* expression. Moreover, the mutated MGE* also lacks the expression of MGE-specific genes *Lhx6* and *Lhx7* while it starts to express other specific genes from the LGE such as, *SCIP* or *GOLF*. Anatomically, from E12.5 to E15.5, the sulcus that separates the MGE from the LGE is totally missing creating a single ganglionic eminence (Sussel, Marin et al. 1999). Additionally, the anterior commissure failed to cross the midline, and the bed nucleus of stria terminalis was also missing. More caudally, in the POA and the hypothalamic region, the deformities were

signaled only in the ventro-medial areas, and further posteriorly, the structures that originate from the hypothalamic neuroepithelium were developing normally (Kimura, Hara et al. 1996). From the limit between the diencephalon and the mesencephalon, continuous malformations were observed. Importantly, the third ventricle was not reaching the floor of the diencephalon, the hypothalamic nuclei were reduced and the pre-mammillary, arcuate, supramammillary nuclei, as well as the mammillary body, were absent. Finally, the anterior, intermediate and posterior pituitary were completely missing, involving a reduced development of the adrenal glands probably due to the absence adrenocorticotropin hormone (Kimura, Hara et al. 1996). In the mesencephalon of *Nkx2.1*^{-/-} mice, the dopaminergic (DA) neurons that have axons labeled by the tyrosine hydroxylase (TH) and that normally send their ascending projections to the ipsilateral striatum were observed to project axons on the contralateral striatum, creating an ectopic commissure in the midline of the caudal hypothalamus (Marin, Baker et al. 2002; Kawano, Horie et al. 2003). In addition, the third ventricle was lacking a proliferative neuroepithelium, which was visualized by the absence of PCNA and Nestin labeling, and in that region, labeling for two repellent molecules; semaphorin 3A and Slit2; was also strongly reduced (Marin, Baker et al. 2002; Kawano, Horie et al. 2003).

3.4 Interneurons and oligodendrocytes specification

As mentioned before (paragraph 1.4.3 and 3.3), *Nkx2.1* specifies the neuroepithelial precursor cells of the VZ, basal precursors of the SVZ and post-mitotic cells in the mantle of the MGE (Sussel, Marin et al. 1999)(see also figure 10). It has been shown through the use of several experimental techniques that, during embryonic ages, MGE-derived precursors were giving birth either to GABAergic interneurons or to oligodendrocytes that migrate tangentially towards the cortex (Kimura, Hara et al. 1996; Lavdas, Grigoriou et al. 1999; Sussel, Marin et al. 1999; Marin, Anderson et al. 2000; Anderson, Marin et al. 2001; Marin and Rubenstein 2001; Marin, Baker et al. 2002; Schuurmans and Guillemot 2002; Guillemot, Molnar et al. 2006; Kessaris, Fogarty et al. 2006; Liodis, Denaxa et al. 2007; Du, Xu et al. 2008; Kessaris, Pringle et al. 2008; Nobrega-Pereira, Kessaris et al. 2008; Xu, Tam et al. 2008; Fragkouli, van Wijk et al. 2009; Flandin, Kimura et al. 2010; Marin, Valiente et al. 2010; Rubin, Alfonsi et al. 2010).

By the mutation of *Nkx2.1* which regulates the regionalization of the ventral telencephalon, the subpallial origin of the cortical GABAergic interneurons has been demonstrated, since there was a strong loss of these neurons in the cortex and the hippocampus (Anderson, Eisenstat et al. 1997; Casarosa, Fode et al. 1999; Sussel, Marin et al. 1999; Pleasure, Anderson et al. 2000; Super, Del Rio et al. 2000). First, it has been shown that

the *Nkx2.1*⁺ MGE was generating PV-, SST- and neuropeptide Y (NPY)-expressing interneurons of the cortex, the striatum and the pallidum (Sussel, Marin et al. 1999; Wichterle, Garcia-Verdugo et al. 1999; Marin, Anderson et al. 2000; Anderson, Marin et al. 2001; Butt, Fuccillo et al. 2005; Wonders and Anderson 2006; Nobrega-Pereira, Kessarlis et al. 2008; Xu, Tam et al. 2008; Flandin, Kimura et al. 2010; Miyoshi, Hjerling-Leffler et al. 2010). Second, among the two targets of *Nkx2.1*, *Lhx6/7* specifies the interneurons of the striatum and *Lhx6* regulates their migration to the cortex (Alifragis, Liapi et al. 2004; Liodis, Denaxa et al. 2007; Du, Xu et al. 2008; Fragkouli, van Wijk et al. 2009).

As previously described, Kessarlis and colleagues (Kessarlis, Fogarty et al. 2006) have demonstrated that the OLPs in the telencephalon, are characterized by three origin sites and waves of migration (see chapter 2.3.1 on oligodendroglial fate). To this purpose, they made transgenic Cre-lox fate mapping studies and they could show that there are three consecutive waves of OLPs in the telencephalon during development. By the use of *Nkx2.1-Cre*⁺/*Rosa-YFP* mice, the authors could confirm that the first wave of OLPs migration is arising at E12.5 from the *Nkx2.1*-expressing precursors of the VZ of the MGE and the AEP. Postnatally and in adult forebrain (P30), the *Nkx2.1*-derived population declined to a very low level, leaving the entire telencephalon populated only by *Gsh2* or *Emx-1*-derived oligodendrocytes (Kessarlis, Fogarty et al. 2006). In accordance with these results, early markers for OLPs (*Olig2* and *PDGFR* α) disappeared from the telencephalon of *Nkx2.1*^{-/-} mice. In this study the authors were able to rescue a partially normal phenotype by infecting *Nkx2.1*^{-/-} mice with a virally-induced expression vector for *Shh*. In addition, they discovered that all the telencephalic regions of both wild-type and *Nkx2.1*^{-/-} animals were competent to produce oligodendrocytes *in vitro* (Nery, Wichterle et al. 2001).

3.5 Nkx2.1-linked syndromes in humans

As mentioned previously, in the mouse, homologous disruption of *Nkx2.1* leads to the development of a hypoplastic lung, agenesis of the thyroid on one hand, and on the other hand, basal ganglia and pituitary agenesis, leading to death at birth of the pups. In humans, it has been reported following recombination and FISH analysis that *Nkx2.1* (*TTF-1*) gene situated on chromosome 14, was associated with benign hereditary chorea (BHC) (Breedveld, van Dongen et al. 2002). BHC is an autosomal dominant movement disorder with high level of phenotypic variability from one family to another or between individuals of the same family. The prevalence of BHC has been estimated at 1:500,000 (Kleiner-Fisman and Lang 2007). The disorder has been linked to a deletion of 1.2 Mb containing the *Nkx2.1* gene, but also, to single nucleotide mutations causing an amino-acid substitution. The mutations were

usually located in helix 3 of the protein which binds inside the wide groove of the DNA helix (see figure 13). Moreover, it has also been reported that in a patient with BHC, functional analysis of the mutation showed that it affected the cellular localization of the protein. Indeed, the mutated protein was found in the cytoplasm instead of in the nucleus (Provenzano, Veneziano et al. 2008). The loss of one allele has been linked to chorea phenotype, which suggests, that haploinsufficiency is enough to induce the disease. The symptoms begin to manifest at the age of 2 years but show a really mild progression until adulthood where the choreic movements tend to decrease. The patients show only mild mental retardation with no intelligence deterioration like in Huntington's disease. In addition, other symptoms such as, dysarthria, axial dystonia, myoclonic jerks or gait disturbances were reported. The movements have been described as quick and unpredictable, involving the face, the tongue and the limbs (Kleiner-Fisman and Lang 2007). The fact that the symptoms appear early during childhood and progressively disappear with aging indicates that the disorder is due to a developmental issue in the brain (Breedveld, van Dongen et al. 2002).

In *Nkx2.1*^{-/-} mice telencephalon, since the neurons of the globus pallidus are not properly differentiated and connected, and that, GABAergic neurons migration to the cortex is reduced; this alteration might result in a decreased inhibition of the outflow from the thalamus to the cortex, which could finally lead to produce choreic movements (Kimura, Hara et al. 1996). However, the hemizygous *Nkx2.1* mice (*Nkx2.1*^{+/-}) develop normally, although behavioral disorders linked to neurological defects have never been studied in details. Furthermore, new evidences have shown that *Nkx2.1* continues to be expressed throughout adult mice brains. In addition to the hypothalamus and other diencephalic structures, *Nkx2.1* expression is maintained in the telencephalon, in cholinergic and GABAergic neurons of the globus pallidus and striatum (Magno, Catanzariti et al. 2009) (Fig15). Therefore, it is reasonable to assess that haploinsufficiency might affect the prenatal differentiation of these neurons, as well as their adult maturation and integration into neuronal circuits (Magno, Catanzariti et al. 2009).

In addition, *Nkx2.1* (*TTF-1*) plays a crucial role in the organogenesis of epithelial cells of the thyroid and the lung (Lazzaro, Price et al. 1991; Kimura, Hara et al. 1996; Ghaffari, Zeng et al. 1997; Hamdan, Liu et al. 1998; Sussel, Marin et al. 1999; Pabst, Zweigerdt et al. 1999; Lonigro, Donnini et al. 2001). An *in vitro* culture system for studying human fetal lung type II cell differentiation has been used. By this mean, the developmental and hormonal effects of *Nkx2.1* isoforms and their potential different role in lung development has been assessed (Kolla, Gonzales et al. 2007). In the *Nkx2.1*^{-/-} mice, it has been described that the thyroid degenerates from E12/E13 through apoptosis, while *Nkx2.1*^{+/-} mice suffer from hypothyroidism (Kusakabe, Kawaguchi et al. 2006). To understand the role of *Nkx2.1* in the

adult thyroid, the authors used a thyroid follicular cell-specific conditional knockout mouse line called as *Nkx2.1(fl/fl);TPO-Cre* that expressed the Cre recombinase under the human thyroid peroxidase (TPO) promoter. This study demonstrated that *Nkx2.1* is required for the maintenance of the cytoarchitecture and the function of adult thyroids (Kusakabe, Kawaguchi et al. 2006). Thereafter, *Nkx2.1* haploinsufficiency in humans has also been related to congenital hypothyroidism (CH) (Krude, Schutz et al. 2002) (Fig 15). This disease has been first attributed to the lack of thyroid hormone during development and has been finally linked to the deletion or mutation of *Nkx2.1* gene. Some patients with CH were also suffering from associated symptoms such as, choreoathetosis, muscular hypotonia and pulmonary troubles (Krude, Schutz et al. 2002). Therefore, mutations in the human *Nkx2.1* gene results in a complex disorder comprising multiple neurological, respiratory and thyroid dysfunctions.

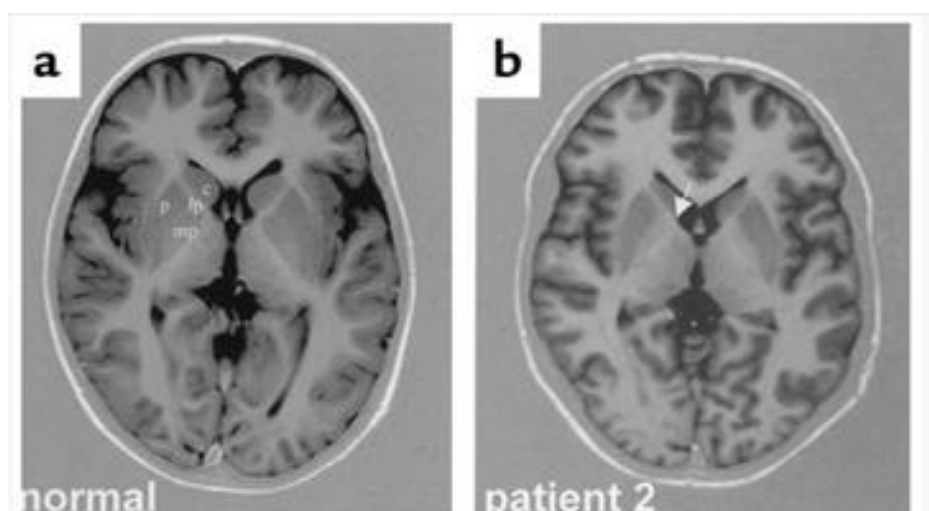


Figure 15. Morphological brain defects of patients with *Nkx2.1* mutations.

(a) MRI view of a normal patient. The white matter maturation is complete and the medial and lateral parts of the pallidum are clearly distinguishable. (c) caudate; (p) putamen; (lp) lateral part of the pallidum; (mp) medial part of the pallidum. (b) A comparable level of MRI section of patient 2 shows a hypoplastic pallidum with a lack of differentiation into medial and lateral part (arrow). The putamen and the caudate nucleus are normal, the brain maturation is normal, and there is no malformation of the cortex. From (Krude et al., 2002)

The combination of the three symptoms due to a heterozygous mutation in the *Nkx2.1* gene in one patient has received the name of Brain-Lung-Thyroid syndrome. Since the patient died at the age of 23 years from a large cell lung carcinoma, giving a name to the syndrome might help further recognition of this complex disorder and a might bring a better understanding of its pathophysiological basis and the consequences of a reduced level of the protein during the fetal development (Willemsen, Breedveld et al. 2005; Kleiner-Fisman and Lang 2007).

4. Cell Migration to the cerebral cortex

In the genesis of the brain, the cell migration is a mechanism of major importance since both the neuronal and the glial cells are generally originating in places situated far away from the site they finally stay in. The complex architecture of the mammalian forebrain involves really complicated migratory pathways required to achieve such a degree of organization and wiring. The neuronal and the glial cells are generated into the germinal zones (VZ/SVZ) and then travel through long distances before they manage to reach their final destination. To achieve this, they use two main modes of migration: the radial and the tangential migration (Marin, Plump et al. 2003; Noctor, Martinez-Cerdeno et al. 2004; Metin, Baudoin et al. 2006; Wonders and Anderson 2006; Marin, Valiente et al. 2010).

4.1 Cortical layers formation

In the dorsal telencephalon, the VZ/SVZ generates the glutamatergic pyramidal projection neurons which usually reach their final layer in the cerebral cortex by radial migration. By contrast, in the the ganglionic eminences, the VZ/SVZ gives rise to GABAergic interneurons that reach their final destinations through tangential migration (Corbin, Nery et al. 2001; Marin and Rubenstein 2001; Marin and Rubenstein 2003; Kriegstein and Noctor 2004; Rakic 2007). Nevertheless, it can happen that the neurons switch from one mode of migration to the other according to the phase of migration they are in (Nadarajah and Parnavelas 2002; Ang, Haydar et al. 2003; Tanaka, Nakaya et al. 2003; Tanaka, Maekawa et al. 2006). The glutamatergic and the GABAergic neurons which are generated at the same time but which use different routes and different modes of migration, are finally located in the same cortical layer, since glutamatergic neurons control GABAergic interneurons distribution. This environmental regulation has been nicely demonstrated by the group of Paola Arlotta, where they show that the identity of the projection neurons can inform specific subpopulations of interneurons for their laminar positioning. To this purpose, they used *Fezf2*^{-/-} mice in which the subcerebral projection neurons are replaced by callosal projection neurons, which leads to abnormal distribution of GABAergic interneurons and aberrant electrical activity of the cortex (Miller 1986; Ang, Haydar et al. 2003; Kriegstein and Noctor 2004; Lodato, Rouaux et al. 2011).

First, around E10, the transient PP layer is occupied by radially migrating pyramidal neurons coming from the dorsal telencephalon and by Cajal-Retzius (CaR) cells which migrate tangentially and originate from different germinal sites in the pallium such as the cortical hem, the choroid plexus, the pallial/subpallial border (PSB) and the pallial domain of the septum (Takiguchi-Hayashi, Sekiguchi et al. 2004; Bielle, Griveau et al. 2005; Yoshida, Assimacopoulos et al. 2006). Afterward, the PP is split into two: 1) the marginal zone (MZ) or the layer I situated at the pial surface and 2) the subplate (SP), by a new cohort of neurons migrating from the dorsal pallium and that will intercalate to form the cortical plate (CP). These neurons migrate radially in an inside out fashion, to subsequently form the cortical layers II to VI, in such a way that the early generated neurons populate the deeper layers while the later are finally located in the upper layers (Rakic, Stensas et al. 1974; Marin, Plump et al. 2003; Marin and Rubenstein 2003; Rakic 1972; Campbell and Gotz 2002; Tabata and Nakajima 2003; Noctor, Martinez-Cerdeno et al. 2004; Rakic 2007)(Fig. 9a).

4.2 Radial versus tangential neuronal migration

By a combination of different experimental approaches such as immunohistochemistry, electron microscopy, and time-lapse video imaging on organotypic slice cultures, the pyramidal neurons were observed to be guided along the RG cells to undergo their radial migration (Tabata and Nakajima 2003; Noctor, Martinez-Cerdeno et al. 2004) (Fig.16B). First, they migrate radially from the VZ to the SVZ. In a second phase, they shortly adopt a multipolar shape and are able to migrate tangentially since they are not attached to RG cell processes (Marin, Valiente et al. 2010). Third, several neurons pass through a phase in which they extend a process back to the ventricular zone in which they translocate their cell body (Marin and Rubenstein 2001; Marin, Plump et al. 2003; Kriegstein and Noctor 2004; Metin, Baudoin et al. 2006; Marin, Valiente et al. 2010). Then, the neurons take a multipolar shape followed finally by a bipolar morphology with a leading process which remains in close contact with the radial glial process to move radially to the cortical MZ where their migration is finished. During this last phase, the neurons exhibit the migratory features of radially guided cells.

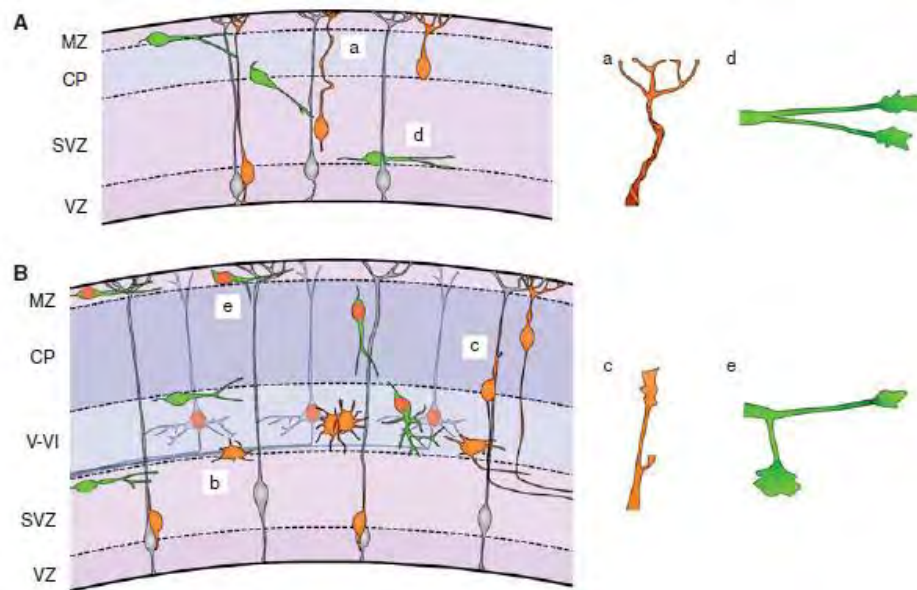


Figure 16. Leading process dynamics in cortical migrating neurons. (A) Early generated pyramidal cells migrate, independent of radial glia fibers, by translocating their soma toward the meninges using a springlike mechanism (a). (B) As the cerebral cortex grows, the distance between the ventricular zone (VZ) and the marginal zone (MZ) increases, and pyramidal cells use locomotion to reach the cortical plate (CP). Pyramidal cells go through a multipolar state (b) before attaching to the radial glial process and continue their migration toward the cortical plate (c). Cortical interneurons initially migrate tangentially through the cortex in defined streams (A and B), without invading the cortical plate. Then, eventually, they move radially to allocate in a particular cortical layer. The leading process of these cells develops several branches, which are used to modify their trajectory (d and e). Projection neurons and interneurons born at the same time end up occupying the same layers (red colored nuclei represent cells born at the same time). (SVZ) subventricular zone; (VZ) ventricular zone; (V–VI) cortical layers V and VI. From (Marin, Valiente et al. 2010).

It has been demonstrated by several experiments that the cortical GABAergic neurons are mainly generated from the MGE and the LGE/CGE (see paragraph 1.4.2) and then migrate tangentially toward the cerebral cortex (Anderson, Marin et al. 2001; Marin and Rubenstein 2001). After the peak of MGE-derived interneurons are produced, from E14.5 to E16.5, the cortical interneurons originate from the CGE and they reach the MZ only two days later. Interestingly, the PV-expressing interneurons coming from the MGE exhibit an “inside-out” pattern whereas the CR-positive interneurons originating from the CGE mostly occupy the superficial cortical layers independent of their birthdates (Ward, Jiang et al. 2005; Metin, Baudoin et al. 2006; Okada, Keino-Masu et al. 2007; Martini, Valiente et al. 2009).

4.3 Cellular events of neuronal migration and nucleokinesis

The migrating neurons are displaying a highly polarized structure identical to the growing axons, since they possess a “growth cone like” structure termed as a leading process. This leading process is able to sense the guidance molecules present in the extracellular environment and to drive the migration of the neuron (Metin, Baudoin et al. 2006; Higginbotham and Gleeson 2007; Marin, Valiente et al. 2010). Generally, the tangentially migrating interneurons exhibit a branched leading process which seems to adopt a shape in relation to its guidance role (Bellion, Baudoin et al. 2005; Schaar and McConnell 2005). Then, the cell body which follows the leading process migrates by a mechanism that is called nucleokinesis. This movement is characterized by the translocation of the nucleus and its perinuclear material within the leading process (Rivas and Hatten 1995; Tsai and Gleeson 2005) (Fig 17). First, the leading process is extended and the centrosome and the organelles move within it causing its swelling close to the nucleus (Bellion, Baudoin et al. 2005; Schaar and McConnell 2005). Then, the nucleus is pulled by its microtubular attachment to the centrosome (Marin, Valiente et al. 2010) while it is additionally pushed by an actin/myosin interplay (Reiner, Carrozzo et al. 1993; Sapir, Elbaum et al. 1997; Francis, Koulakoff et al. 1999; Gleeson, Lin et al. 1999; Kerjan and Gleeson 2007). The last step is the removal of the trailing process, and finally, this three-steps-mechanism is repeated many times allowing the progression of the migrating cell.

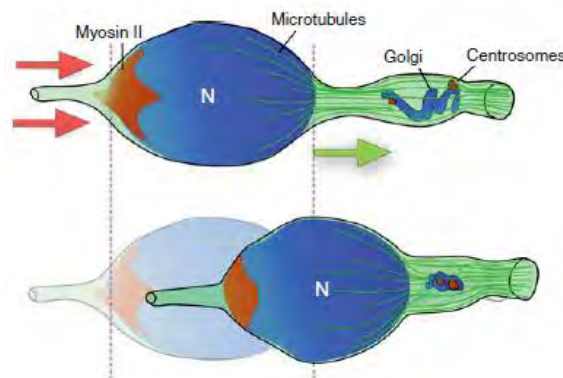


Figure 17. Nucleokinesis in migrating neurons. Nucleokinesis involves both perinuclear and nucleus translocation. First, the perinuclear dilatation containing the centrosome and the Golgi apparatus move forward. The perinuclear microtubular cage (in green) pulls the nucleus forward until reaching the swelling. Forward pulling forces (green arrow) are complemented by myosin II at the rear, which generates pushing forces (red arrows) to move the nucleus in its characteristic saltatory pattern of nucleokinesis. Many motor proteins and other proteins related to the cytoskeleton are implicated in the process. (N) Nucleus. From (Higginbotham and Gleeson 2007).

4.4 Glial migration

Also it is a less well understood mechanism, the glial cells also migrate long distances throughout the developing CNS. We now know that the astrocytes, the oligodendrocytes and the polydendrocytes are dispersed everywhere in the adult CNS (see paragraphs 2.5 and 2.6 on oligodendrocytes and polydendrocytes). Many studies on glial cells migration have been done in the rat optic nerve since this structure lacks neuronal cell bodies (Tsai and Miller 2002). The use of DiI and UV-thymidine-dimer (TD) labeling confirmed that the OLPs found in the nerve were originating from the floor of the third ventricle and had migrated all the distance from there through the optic nerve towards the retina (Sugimoto, Taniguchi et al. 2001; Tsai and Miller 2002). Later, Netrin-1 and Semaphorin 3A were shown to act as gradients of chemorepellent molecules from the chiasm for the oligodendro- and astro- glial precursors found in the optic nerve, therefore indicating that glial cells respond to similar guidance cues than do the neurons (Sugimoto, Taniguchi et al. 2001; Tsai and Miller 2002). Similarly, in the spinal cord, studies revealed that the OPCs were responsive to Netrin-1 (Sugimoto, Taniguchi et al. 2001; Tsai and Miller 2002).

However, how newborn astrocytes migrate and whether they can be dispersed radially, tangentially, or both is controversial (Rowitch and Kriegstein 2010). It has been commonly accepted that the RG cells of the cerebral cortex were transformed into mature astrocytes which were “migrating” by translocating their cell body along their long processes which were then retracted (Schmechel and Rakic 1979; Pixley and de Vellis 1984; Mission, Takahashi et al. 1991; Mori, Buffo et al. 2005).

In the contrary, transplantation of cultured astrocytes, and *in vitro* studies on cortical slices have shown that astrocytes are usually first migrating tangentially along the white matter tracts, and then they were observed to move radially through the grey matter (Zhou and Lund 1992; Hatton, Nguyen et al. 1993; Jacobsen and Miller 2003; Rowitch and Kriegstein 2010). Others retroviral labeling experiments, were indicating that astrocytic cells coming from the same clone were observed within radial columns and/or within tangential axonal tracts (Gray and Sanes 1991). Therefore, the mode of astrocyte migration is most probably variable according to the diverse regions of the CNS. For instance, it has been shown in the striatum, that the glial precursors were using two almost perpendicular paths for their migration (Kakita and Goldman 1999; Tsai and Miller 2002). While tangential migration has been observed in the striatum for the parenchymal astrocytes (Kriegstein and Alvarez-Buylla 2009), a recent study on spinal cord astrocytes suggests that such a mechanism might be very rare (Hochstim, Deneen et al. 2008). This implies that astrocytes may also inherit positional information directly from their original RG progenitors array (Rakic 1988). Interestingly, it

has been observed in the parietal cortex of rats, that the newborn astrocytes follow an inside-out pattern of laminar birth dating which is also followed by neurons (Ichikawa, Shiga et al. 1983).

5. Axonal growth and guidance

The functionality of the CNS requires in part an extremely precise wiring whose events mainly occur during the embryonic and the early postnatal ages. The projection neurons are called so because of their axonal extensions that can sometimes become relatively long, allowing them to communicate with their targets located in diverse structures. The newly grown axons are guided by extracellular molecules (Buck and Zheng 2002; Schaefer, Kabir et al. 2002; Zhou, Waterman-Storer et al. 2002; Chilton 2006; Lowery and Van Vactor 2009; Raper and Mason 2010) that act on a very sensitive and dynamic structure called the growth cone (Lowery and Van Vactor 2009) to direct them toward their respective targets.

5.1 Mechanisms of axonal growth

During the CNS development, the neurons extend a long process at the tip of which is formed an extremely motile structure, the growth cone (Fig. 18). The constant remodeling of the cytoskeleton inside the growth cones is responsible for its high motility. The extension occurs after the polymerization of stable microtubules form the axon shaft while both the actin filaments and the dynamic microtubules give the growth cone its shape in addition to controlling its outgrowth (Goldberg and Burmeister 1986; Suter and Forscher 2000; Buck and Zheng 2002; Schaefer, Kabir et al. 2002; Zhou, Waterman-Storer et al. 2002; Lowery and Van Vactor 2009; Raper and Mason 2010). The growth cone can be subdivided into three principal regions: 1) a central or (C)-domain which contains a bundle of stable microtubules entering this region from the axon shaft, numerous organelles and the central actin bundles; 2) a peripheral or (P)-domain composed of finger-like protrusions of bundled actin filaments and dynamic microtubules, and flattened veil-like membrane extensions containing a mesh of unbundled actin filaments, forming two structures that are respectively called the filopodia and the lamellipodia; and 3) a transition or (T)-zone separating the two formers.

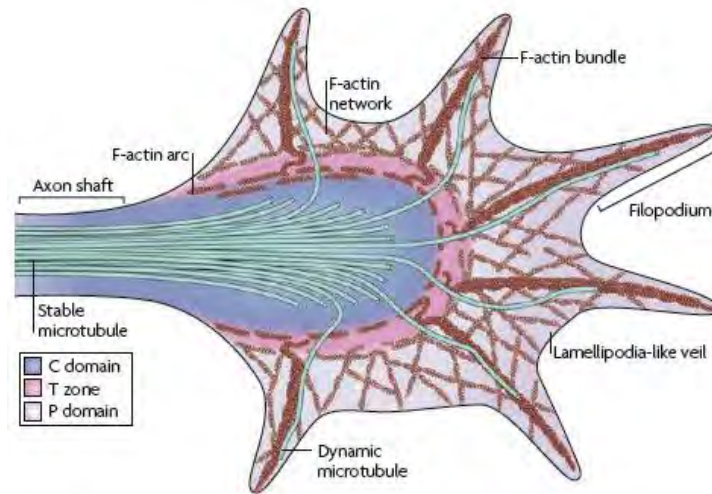


Figure 18. The structure of the growth cone. The structure of the growth cone is fundamental to its function. The leading edge consists of dynamic, finger-like filopodia that explore the path ahead, separated by sheets of membrane between the filopodia called lamellipodia-like veils. The cytoskeletal elements in the growth cone underlie its shape, and the growth cone can be separated into three domains based on cytoskeletal distribution. The peripheral (P) domain contains long, bundled actin filaments (F-actin bundles), which form the filopodia, as well as mesh-like branched F-actin networks, which give structure to lamellipodia-like veils. Additionally, individual dynamic ‘pioneer’ microtubules (MTs) explore this region, usually along F-actin bundles. The central (C) domain encloses stable MTs that enter the growth cone from the axon shaft. Finally, the transition (T) zone sits at the interface between the P and C domains, where actomyosin contractile structures (actin arcs) lie perpendicular to F-actin bundles. The dynamics of these components determine growth cone shape and movement. From (Lowery and Van Vactor 2009).

Through the influence of environmental cues, the growth cone progress and drives the axonal outgrowth by modulating its cytoskeleton in three subsequent steps known as: protrusion, engorgement and consolidation (Goldberg and Burmeister 1986; Suter and Forscher 2000; Lowery and Van Vactor 2009)

5.2 Guidance cues and molecular aspects of axonal guidance

All along their way, the axons are guided towards their final destinations by environmental guidance molecules which can be either attractive or repulsive and which can act either through short or long distances (Goodman and Shatz 1993; Tessier-Lavigne and Goodman 1996). Previously, it has been postulated that the growth cone was directed according to the intrinsic property of the guiding molecule. However, it has become rapidly obvious that the response of the growth cones was mediated by their characteristics at the moment when they encounter a specific cue. Therefore, the response of a growth cone to the same cue can be in opposite ways along its travel (Stein and Tessier-Lavigne 2001; Keleman, Rajagopalan et al. 2002; Keleman, Ribeiro et al. 2005; Chilton 2006; Lin and Holt 2007). Moreover, it seems

possible that different combinations of the ligands and their receptor/coreceptor complexes, which can also vary with their alternative splicing and their post transcriptional modifications, can result in numerous variations of signals. Finally, several studies have unraveled that the answer of the growth cone is modulated by the downstream signaling and the phosphorylation states that can change with time (Ming, Song et al. 1997; Dickson 2001; Lebrand, Dent et al. 2004).

Among numerous guidance factors, the neuronal cell adhesion molecules (CAMs) form a distinguished class since they have been shown to mediate the outgrowth and guidance of neurites by direct contacts triggering attraction or repulsion (Walsh and Doherty 1997; Stoeckli 1998; Stoeckli and Landmesser 1998; Schaefer, Kamiguchi et al. 1999; Schmid and Maness 2008). The CAMs belong to three families with structural variants: 1) integrins, 2) cadherins, and 3) IgCAMs. They can work as guidance cues or receptors, and can usually bind to the members of the same family. In addition, the more important well-known guidance factors are the four “classical” families of the Netrins, the Slits, the ephrins and the Semaphorins described below, and some other molecules like secreted morphogens, neurotrophic factors and neurotransmitters (Gundersen and Barrett 1979; Walsh and Doherty 1997; Dickson 2002; Xiang, Li et al. 2002; Brunet, Weigl et al. 2005; Chilton 2006; Zou and Lyuksyutova 2007; Sanchez-Camacho and Bovolenta 2009; Bashaw and Klein 2010; Evans and Bashaw 2010).

5.2.1 Ephrins

The ephrin ligands and their respective Eph receptors are divided into two families termed A and B. Usually, A or B ligands bind preferentially to their A or B receptors, respectively (Pasquale 2005; Egea and Klein 2007; Scicolone, Ortalli et al. 2009). However, both A and B classes of ephrins can activate EphA4 and EphB2 receptors (Himanen and Nikolov 2003; Himanen and Nikolov 2003). The ephrin-A ligands (A1–A6) possess a glycosylphosphatidylinositol (GPI)-anchor and the ephrin-B ligands (B1–B3) have a transmembrane domain. Besides, the Eph receptors (A1-A10; B1-B6) are tyrosine kinase receptors (Fig. 19). Interestingly, the binding of ephrin-B to EphB receptor and ephrin-A to EphA receptor can both induce either forward or backward signaling (Rashid, Upton et al. 2005; Egea and Klein 2007; Bush and Soriano 2009) and the Ephrins/Eph interactions can also induce both attractive and repulsive activity. For instance, they have been shown to influence the topography of retinotectal/collicular projections (McLaughlin, Hindges et al. 2003; Scicolone, Ortalli et al. 2009) since EphAs and ephrin-As are involved in the rostro-caudal axis topography whereas EphBs and ephrin-Bs are implicated in the dorso-ventral axis topography (Yates, Roskies et al. 2001; McLaughlin, Hindges et al. 2003).

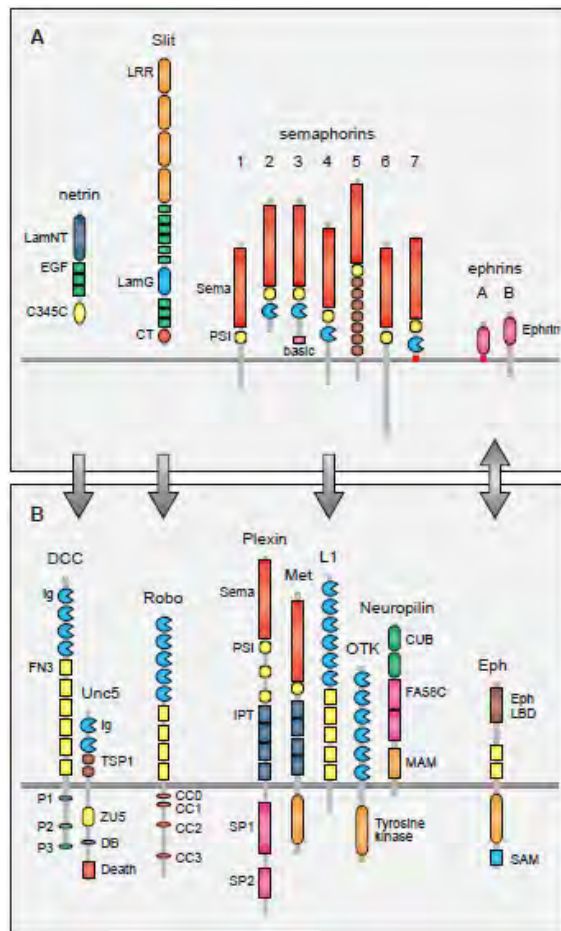


Figure 19. Conserved families of guidance molecules (A) and their receptors (B). Domain names have been taken from SMART (<http://smart.embl-heidelberg.de>). P1 to P3, DB (DCC-binding), CC0 to CC3, and SP1 and SP2 indicate conserved regions in the cytoplasmic domains of DCC, UNC-5, Robo, and Plexin receptors, respectively. From (Dickson 2002).

5.2.2 Netrins

Several studies have been focused on the mechanisms which allow the axons from the dorsal spinal cord to grow ventrally and to cross the midline. In the mice, Netrin-1 and 2 were found to be secreted by the floor plate and thus to exert the main attractive effect (Kennedy, Serafini et al. 1994; Serafini, Kennedy et al. 1994) (Fig. 19 and 20) through their binding to the Deleted in Colorectal Cancer (DCC) receptor (Keino-Masu, Masu et al. 1996). By contrast, UNC-5, another receptor for the Netrins, induces the repulsive activity of the Netrins, either alone or by interacting with DCC (Colamarino and Tessier-Lavigne 1995). The Netrins are involved in long range signaling (Winberg, Mitchell et al. 1998; Yee, Simon et al. 1999) and participate in the formation of many commissures such as decussations in the spinal cord (Serafini, Colamarino et al. 1996; Fazeli, Dickinson et al. 1997; Shu, Valentino et al. 2000; Ren, Anderson et al. 2006).

5.2.3 Semaphorins

The large family of the Semaphorins includes eight classes of membrane-bound and secreted molecules in which beginning from the third until the seventh class belongs to the vertebrates (Zhou, Gunput et al. 2008) (Fig. 19). The best characterized are the class-III Semaphorins (Sema3A-3G) that are active in the axonal guidance. They have been mainly described as repellents (Fan and Raper 1995; Raper 2000; Potiron and Roche 2005; Mann and Rougon 2007; Derijck, Van Erp et al. 2010; Schwarz and Ruhrberg 2010). The repulsion functions with the binding of the Semaphorins to the Neuropilin receptor dimers composed of Nrp-1 and Nrp-2. These two receptors can form homodimeric complexes and can be bound by the Sema3A and the Sema3F respectively, whereas the heterodimer Nrp-1/Nrp-2 is bound by Sema3C (Chen, Chedotal et al. 1997; He and Tessier-Lavigne 1997). However, the Nrp-1/2 receptors alone are not able to transduce a signal since they are missing a cytosolic signaling domain. Therefore, the Class-III Semaphorin can transduce a signal by forming two receptors complexes: either Nrps with Plexins or Nrps with adhesion molecules such as L1 or NrCAM (Tamagnone, Artigiani et al. 1999; Castellani, Chedotal et al. 2000; Rohm, Ottemeyer et al. 2000; Falk, Bechara et al. 2005). In vitro cultures of DRG neurons have shown that the DRG neurons are becoming sensitive to Sema3A and Sema3E when they express Nrp-2, but either Nrp-1/Nrp-2 hetero-oligomers or Nrp-2 homo-oligomers function as receptors for Sema3A and Sema3E. Therefore, Sema3A and Sema3E probably have roles in repulsing Nrp-2⁺ axons in some regions of the embryo (Takahashi, Nakamura et al. 1998). Besides, Sema3B and Sema3F-induced effects in the guidance of the AC, have been shown to be mediated by the association of Nrp-2 and NrCAM (Sahay, Molliver et al. 2003; Falk, Bechara et al. 2005). Interestingly, the Sema3C is able to attract cortical axons through the CC, dopaminergic projections toward the dorsal thalamus and GABAergic septo-hippocampal projections (Bagnard, Lohrum et al. 1998; Bagnard, Thomasset et al. 2000; Pascual, Pozas et al. 2005; Hernandez-Montiel, Tamariz et al. 2008). The semaphorins are responsible for axonal guidance within several important tracks such as the anterior commissure, the corticospinal projections and the limbic system (Castellani, Chedotal et al. 2000; Sahay, Molliver et al. 2003; Falk, Bechara et al. 2005) or in the local patterning within the olfactory bulb (Takeuchi, Inokuchi et al. 2010).

5.2.4 Slits

The chemorepellents Slits were first discovered in the fruit fly *Drosophila* together with their receptors Robos and their interactions with the Netrins. These studies allowed to better understand the signaling in many midline processes (Dickson 2001; Andrews, Barber et al. 2007; Dickson and Zou 2010; Ypsilanti, Zagar et al. 2010)(Fig. 19 and 20). For example, the Slits are expressed by the glial cells of the midline (Rothberg, Jacobs et al. 1990) to repel the non-crossing and the commissural axons that have already crossed the midline which express the Robo receptors. Consistent with this process, the commissural axons in the *Slit* mutants are stuck at the midline. In normal conditions, the commissural axons are allowed to cross since they express low to high levels of Robo according to the pre- or post-crossing location of their growth cones. To this purpose, the repulsive effect of Slits is inhibited as the axons cross by the Commissureless (Comm) protein which is expressed and helps to sequester the Robo receptor inside the internal endosomes (Keleman, Ribeiro et al. 2005)(Fig. 20). In the vertebrates, the Slits/Robos have redundant functions (Brose, Bland et al. 1999; Long, Sabatier et al. 2004) since the telencephalic commissures are impaired in double *Slit1/2* knockout mice (Bagri, Marin et al. 2002; Plump, Erskine et al. 2002) and since the spinal commissural axons are stuck at the midline only in the triple *Slit1/2/3* knockout mice (Long, Sabatier et al. 2004). Similarly, in the mammals, the equivalent of Comm protein, *Rig1*, is highly expressed in the precrossing axons and prevents the repulsion by Slit signaling (Sabatier, Plump et al. 2004). After crossing, Slits additionally respond to Semas, in order to maintain a good distance between the commissural axons and the midline (Zou, Stoeckli et al. 2000). Finally, the post-crossing axons are also desensitized to Netrin attraction by a direct intracellular interaction between the Robo and the DCC receptors (Stein and Tessier-Lavigne 2001).

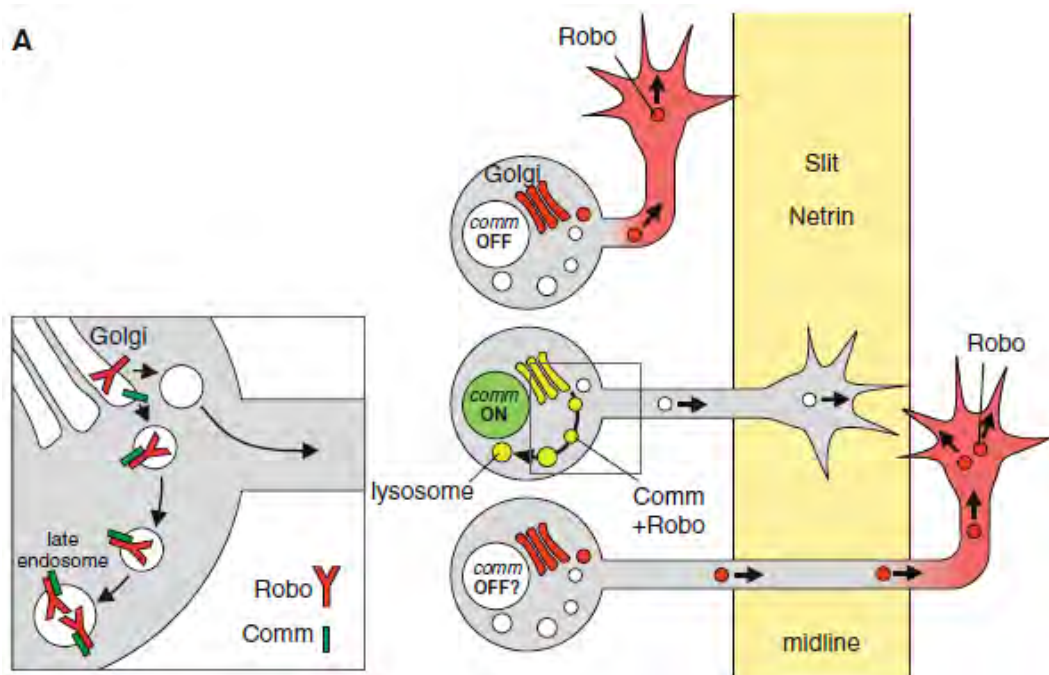


Figure 20. Molecular cues controlling the pathway choices at the *Drosophila* and vertebrate midline. (A) Comm regulates Robo1 trafficking and midline crossing. Model for the sorting action of Comm on Robo1; inset to the left shows enlarged view of the boxed region. In an ipsilateral neuron (top), Comm is absent and Robo1 is inserted into the growth cone, ensuring midline repulsion by Slit. In a commissural neuron (middle), Comm is present and diverts Robo1 to the endosomes, making the growth cone insensitive to Slit. After crossing (bottom), Comm is reduced and Robo1 begins to accumulate in the contralateral axon segment, potentially preventing the growth cone from crossing again. From (Dickson and Zou 2010).

6. Development of two main telencephalic commissures: the Corpus Callosum and the Anterior Commissure

The mammalian brain contains three major interhemispheric commissures. The biggest one, that is only present in mammals, is named the corpus callosum (CC), and the two others are the anterior commissure (AC) and the hippocampal commissure (HIC). The CC allows the connection of more than 200 million CPN linking the two hemispheres of the cerebral cortex and which are necessary for complex associative functions.

6.1 Development of the Corpus Callosum

The CC starts to be formed around E15.5, when the pioneering CPN coming from both hemispheres send their first axons towards the contralateral hemisphere and are about to cross the midline. The first axons termed callosal projections that cross the midline are coming from the cingulate cortex (CCi). They might play a role of pioneers by guiding the callosal axons that originate from other cortical areas (Koester and O'Leary 1993; Ozaki and Wahlsten 1998; Rash and Richards 2001). The callosal axons are following a trajectory composed of three segments: 1) they originate from the neocortex and they turn medially towards the midline when they penetrate the IZ, (2) they cross the midline at the corticoseptal boundary and (3) they turn again dorsally to reach the cortex in the homotopic contralateral region (Yorke and Caviness 1975; Richards, Plachez et al. 2004) (Fig. 21). Although the regulation of the navigation of the callosal axons at the midline starts to be well defined, the mechanisms that control the targeting of the contralateral cortex still need to be clarified. Yet, only one study has been published about some radial glial cells that guide the callosal projections within the contralateral hemisphere (Norris and Kalil 1991). Finally, around postnatal day 21 (P21), the last exuberant callosal projections are refined and the pattern of projection of the callosal axons is established (Clarke and Innocenti 1986; Innocenti and Price 2005).

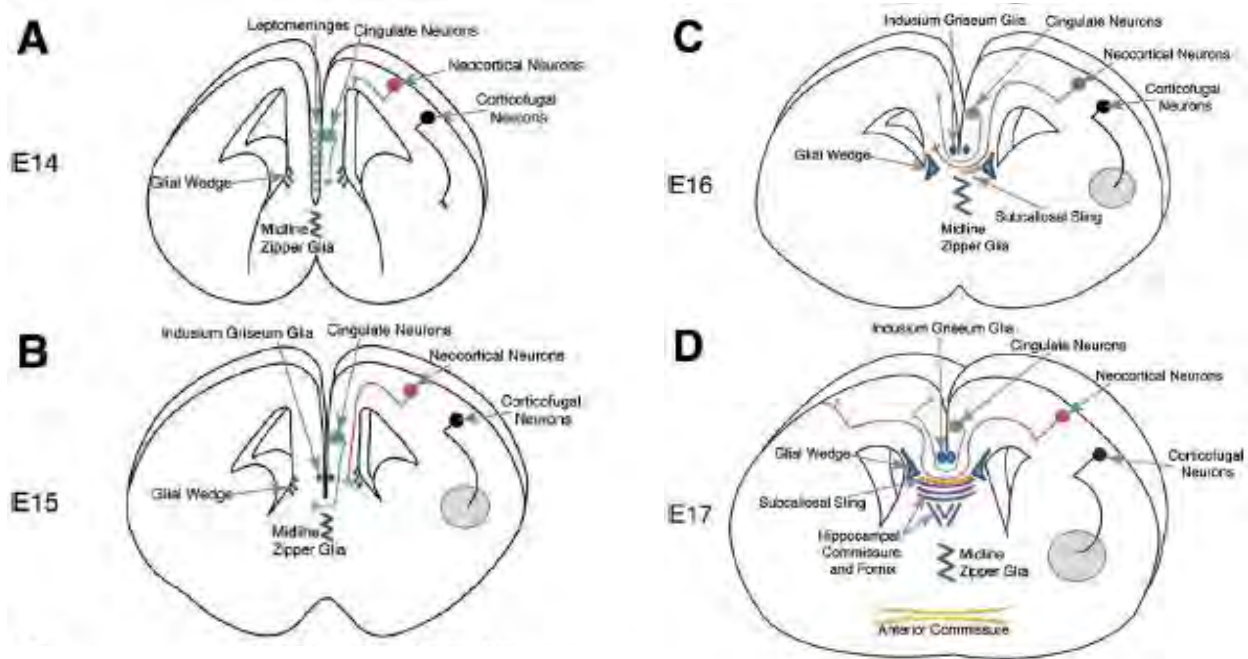


Figure 21. Development of the Corpus Callosum in the mouse brain. (A) Callosal formation firstly requires the establishment of a substrate, which is achieved through the fusion of the telencephalic midline. This involves either the elimination or exclusion of the leptomeninges found between the hemispheres. (B) The pioneers of the corpus callosum originate from the cingulate cortex (medial-most part of the cortex) and reach the midline between embryonic days 14 (E14) and E15. (C) Axons from the neocortex then grow along the pathway defined by the pioneers, expanding the corpus callosum by E17. (C) On arrival of callosal axons at the midline, midline cellular populations (glial wedge, induseum griseum and the subcallosal sling) and the extracellular cues that they secrete, assist in the turning and channeling of these axons across the midline. (D) Axon guidance of the caudal corpus callosum may also be facilitated by the hippocampal commissure. After the axons have entered the contralateral hemisphere, they traverse dorsolaterally before innervating homotopic areas of the contralateral cortex. From (Donahoo and Richards 2009)

6.1.2 Axonal guidance in the Corpus Callosum

The molecular and cellular mechanisms involved in the targeting and the crossing of the midline have revealed several short and long range signaling cues necessary for the formation of the CC. The guidance of the callosal axons has been shown to rely on the four classical families of guidance molecules (Lindwall, Fothergill et al. 2007) such as Slits, Netrins, Semaphorins and ephrins. Among these, *Slit2* is expressed by the glia of the IG and by the radial glial cells (Shu and Richards 2001). It acts by channeling the callosal axons which express the *Robo1* receptor (Shu and Richards 2001; Andrews, Liapi et al. 2006; Unni, Piper et al. 2012). These results have been confirmed by the use of *Slit2* and *Robo1* knockout mice which exhibit misrouting of the callosal axons (Bagri, Marin et al. 2002; Shu, Sundaresan et al. 2003; Andrews, Liapi et al. 2006; Lopez-Bendito, Flames et al. 2007; Unni, Piper et al. 2012).

Moreover, mutant mice for Netrin1 and/or DCC have been shown to be acallosal indicating that the Netrin/DCC signaling pathway is also required for the callosal axon guidance (Serafini, Colamarino et al. 1996; Fazeli, Dickinson et al. 1997; Shu, Valentino et al. 2000; Ren, Anderson et al. 2006).

In addition, another study has revealed that the Nrp-1 receptor is essential for the proper navigation of the callosal axons while the postulated Semaphorin candidate for its activity was still unidentified (Gu, Rodriguez et al. 2003). Therefore, a mutant mouse for the Nrp-1 receptor (*Nrp-1^{Sema-}*) has been generated. Thanks to this mutation, the interactions between Sema and Nrp-1 were abolished, and mild to severe callosal guidance defects were observed. These results strongly suggest that Semaphorins/Nrp-1 interactions are essential for the formation of the CC. More recently, Mathieu Niquille in our group has demonstrated by using mutant analyses and *in vitro* transplantation techniques that two transient populations of CC neurons were exerting an attractive influence on the pioneering callosal axons. Briefly, one population of GABAergic Mash-1-positive interneurons and one population of calretinin-positive glutamatergic neurons expressing the Semaphorin 3C were observed. Indeed, the guidance cue Sema3C has been demonstrated to be attractive via its signaling on the axonal Nrp-1 receptor (Niquille, Garel et al. 2009) (Fig. 22).

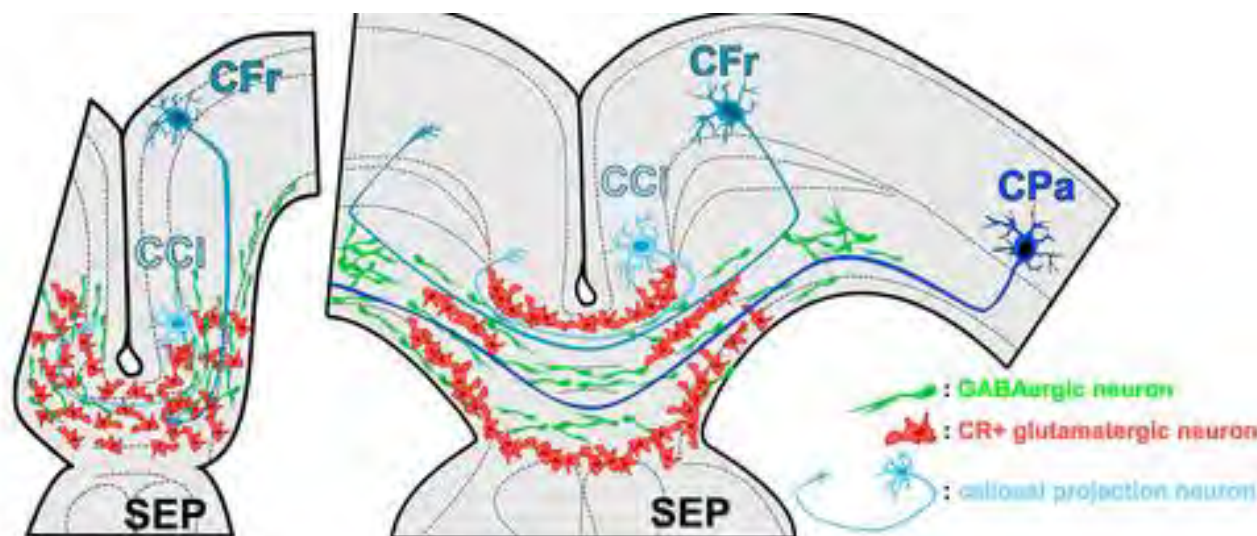


Figure 22. Two transient neuronal populations of the CC guide the pioneering axons. Schematic drawing representing the complementary organization of CR+ glutamatergic neurons (in red) and of GAD67/Mash1-GFP GABAergic interneurons (in green) in the CC at E16.5 (left) and E18.5 (right). The pioneer callosal axons originating from the cingulate (CCi) cortex (light blue), as well as the later-growing callosal axons from the frontal (sky blue) and the parietal cortices (dark blue) are represented and are seen to navigate through the CC neurons. From (Niquille, Garel et al. 2009).

Finally, the ephrins family of guidance cues and their corresponding Eph receptors, have been found to be crucial partners in the guidance of the callosal axons. For instance, the ephrinB1-B3, the EphA4-A5 and the EphB1-B3 receptors were reported (Hu, Yue et al. 2003; Bush and Soriano 2009). Interestingly, some morphogens like the Wnts have been shown to play a role of guidance molecule through the Ryk and the Frizzled receptors (Keeble, Halford et al. 2006; Wang, Zhang et al. 2006; Li, Hutchins et al. 2009) and therefore influence the CC axons trajectories (Li, Hutchins et al. 2009).

6.2 Development of the anterior commissure

Among the three major fiber tracts of the mammalian forebrain, the anterior commissure (AC) is situated more ventrally close to the rostral most part of the third ventricle. It is formed by three components: 1) the anterior limb or anterior pars (ACa), which links the olfactory bulbs, the olfactory peduncles and the anterior piriform cortex (olfactory lobe), 2) the posterior limb or posterior pars (ACp), which interconnects the posterior piriform cortex, the rhinal fissure, parts of the amygdala, and a small part of the neocortex (temporal lobe), 3) the stria terminalis, which connects the major part of the amygdala and the nucleus of the lateral olfactory tract (Lent and Guimaraes 1990; Pires-Neto and Lent 1993; Pires-Neto, Braga-De-Souza et al. 1998; Falk, Bechara et al. 2005). Despite the complexity of all the fibers that compose it, they all converge towards the midline to fasciculate in a dense bundle and cross it at the same dorsoventral plane to reach their final position in the opposite hemisphere. The AC starts to develop during embryonic ages by pioneering axons that cross the midline from E13.5 to E14. Then, they are followed by subsequent waves of growing commissural axons that widen the path of the AC (Lent and Guimaraes 1990; Pires-Neto and Lent 1993; Pires-Neto, Braga-De-Souza et al. 1998; Falk, Bechara et al. 2005).

6.2.1 Axonal guidance in the anterior commissure

Multiple studies using mice mutants lacking guidance factors from the Netrins, Semaphorins and ephrins families and their respective receptors have unraveled their role in channeling the AC tracts. The role of the Semaphorins and their receptor has been assessed through the use of Nrp-2 mutants in which the loss of this receptor was leading to an almost complete absence of AC (Chen et al, 2000; Sahay, Molliver et al. 2003). Similar defects including defasciculation and axonal tracts that fail to cross the midline were obtained after inactivation of the Sema3F that is known to bind to Npn-2 receptor (Falk, Bechara et al. 2005). Briefly, Sema3F has been detected in the developing preoptic area (POA), and in the striatum. Nrp-2 was robustly expressed on the AC, the stria terminalis and the fasciculus retroflexus axons. Therefore, both Nrp-2 and Sema3F null mice presented a similar disorganized decussation of the AC (Sahay,

Molliver et al. 2003). An additional knockout for *Sema3B* confirmed its role in the correct positioning of the two anterior (ACa) and posterior (ACp) limbs of the AC (Falk, Bechara et al. 2005). More precisely, the *Sema3B* has been shown to repel axons from the ACp and to attract axons from the ACa, while the *Sema3F* revealed only a repellent activity on both type of axons (Falk, Bechara et al. 2005). Moreover, labeling for *Sema3B* was also found in the SVZ bordering the lateral ventricles and into ventral regions, therefore, playing a role in the dorsoventral and mediolateral positioning of the ACa and a repulsive action on the ACp (Falk, Bechara et al. 2005).

Besides, it has been demonstrated that the development of the ACp required the *EphB2* receptor expression just ventral and lateral to the commissural midline in order to prevent the aberrant projection of ACp axons in the ventral forebrain (Ho, Kovacevic et al. 2009). Furthermore, the *EphA4* receptor has been shown to be expressed adjacent to the AC tract and in two lateral triangular regions between the ACa and the ACp, to restrict the ACp axons to their tract, to prevent them from entering the ACa and to intermingle with the ACa axons (Ho, Kovacevic et al. 2009). In *EphA4* knockout mice, the ACa was also observed to be displaced laterally from the midline. Finally, by the use of double knockout mice for *EphA4/EphB2*, it has been observed that a part of the ACa axons were misdirected to the ACp tract, allowing to conclude that both receptors are needed for the proper guidance of the AC (Ho, Kovacevic et al. 2009). Consistent with these results, both the ligands *ephrinB1* and *B2* were observed to be expressed in the ACa and the ACp (Ho, Kovacevic et al. 2009).

Additionally to the four classical families of guidance factors, few extracellular matrix (ECM) adhesion molecules might be involved in the embryonic formation of the AC (Pires-Neto, Braga-De-Souza et al. 1998). In hamster embryos, at pre-crossing stages, a horse-shoe pattern of tenascin expression was spanning, on horizontal sections, the midline region and the SVZ laterally. Later, when the AC fibers cross the midline, the external walls of the AC bundle were displaying a complex molecular pattern, where high levels of laminin and fibronectin were detected, whereas the tenascin expression was declining rapidly (Pires-Neto, Braga-De-Souza et al. 1998). Finally, at post-crossing stages, when the AC axons reach their targets and start arborizing, the midline tunnel of fibronectin and laminin expression decreases importantly. These data strongly suggest that this temporal expression of ECM molecules may offer an appropriate substrate for the growth of the AC axons through the midline (Pires-Neto, Braga-De-Souza et al. 1998).

6.3 Guidepost cells in axonal guidance

In order to help and direct the growth of the axonal projections through long distances and across a complex environment, several intermediate targets called guidepost cells break the travel into smaller steps by secreting guidance factors (Bentley and Caudy 1983; Bentley and Caudy 1983; Tessier-Lavigne and Goodman 1996; Dickson and Zou 2010).

In the mammalian forebrain, the first guidepost functions have been reported for the CD44-expressing neurons in the guidance of the retinal axons in the optic chiasm (Sretavan, Pure et al. 1995), second, for the Cajal-Retzius neurons and the Reelin in the development of the hippocampal projections (Del Rio, Heimrich et al. 1997) and finally for the glial cells that surround the CC, for the formation of this commissure. Intriguingly, several studies have illustrated nicely how the migrating neurons can play the role of guidepost cells and therefore how the neuronal migration and the axonal guidance can become two simultaneous coordinated mechanisms (Niquille, Garel et al. 2009; Marin, Valiente et al. 2010) (Fig. 23). For instance, the presence of migrating guidepost neurons has been demonstrated for the axonal pathfinding of thalamocortical projections and for the lateral olfactory tract (LOT). The development of the lateral olfactory tract relies on earlier born (E10.5) neurons which originate from progenitors of the dorsal telencephalon and which form a migratory stream toward the LOT (Yorke and Caviness 1975; Richards, Plachez et al. 2004) (Fig. 23A). Then, the LOT guidepost neurons direct the olfactory growing axons to the piriform cortex (Sato, Hirata et al. 1998) (Fig. 23A'). Similarly, during embryonic development, part of the LGE-derived GABAergic neurons migrate ventrally to the LGE/MGE boundary and thus, create a kind of permissive corridor in which the thalamic axons will grow towards the neocortex (Lopez-Bendito, Cautinat et al. 2006; Bielle, Marcos-Mondejar et al. 2011)(Fig. 23C-C'). Finally, Mathieu Niquille, in our group, has recently demonstrated that in addition to the guidepost glial cells surrounding the CC in the IG, the GW and the sling (Fig 23 B-B'), two transient populations of guidepost migrating neurons were also populating the developing CC in order to help guiding the axons across the midline (Fig 23) (Niquille, Garel et al. 2009).

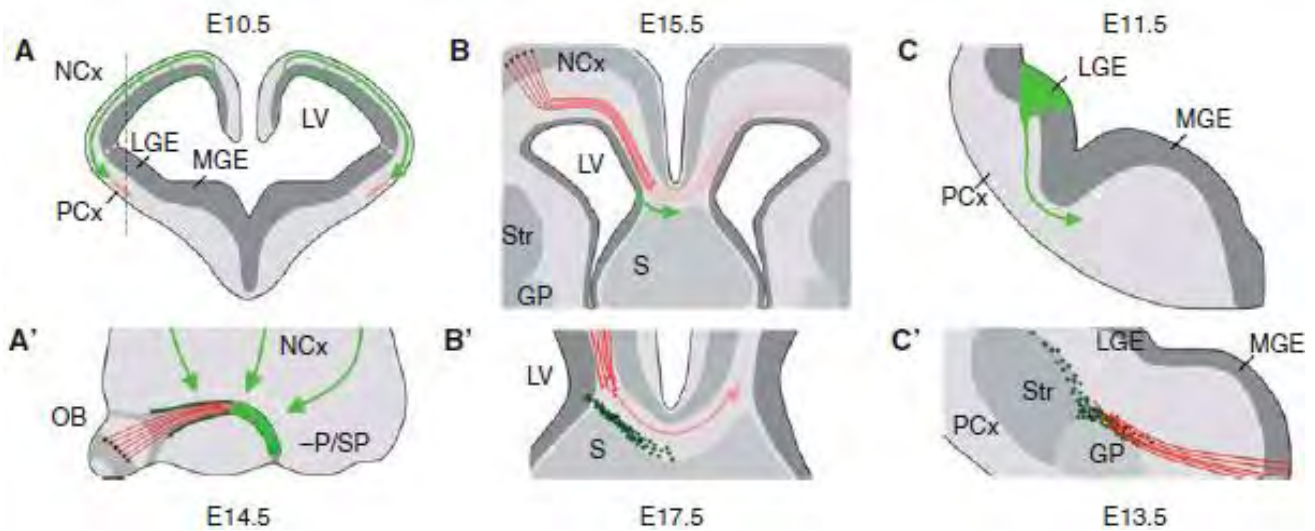


Figure 23. Migrating guidepost cells in the developing forebrain. (A, A') LOT cells are generated early in development at the ventricular zone of the neocortex. They migrate tangentially to the piriform cortex, where they arrive at 3–4 days in advance to the olfactory axonal tract. (B, B') Glial sling cells derive from the ventricular zone in the medial neocortex at E15.5. They migrate towards the midline to contribute to the formation of the corpus callosum through signaling that involves Slit2. (C, C') A subpopulation of LGE-derived interneurons migrates ventrally, forming a cellular corridor that expresses CRD-NRG1. These guidepost cells are required for the migration of thalamocortical axons as they extend through the basal telencephalon on their way to the cortex. (GP) globus pallidus; (LGE) lateral ganglionic eminence; (LV) lateral ventricle; (MGE) medial ganglionic eminence; (NCx) neocortex; (OB) olfactory bulb; (PCx) piriform cortex; (P/SP) pallium-subpallium boundary; (S) septum; (Str) striatum. From (Donahoo and Richards 2009).

6.3.1 Guidepost glial and neuronal cells of the corpus callosum and the anterior commissure

During the early developmental stages, the glial cells which surround the CC are believed to represent the major population of guidepost cells involved in the guidance of the growing callosal axons (Riederer and Innocenti 1992; Shu, Li et al. 2003; Riederer, Berbel et al. 2004; Ren, Anderson et al. 2006; Jovanov-Milosevic, Petanjek et al. 2010). The early astroglial cells composing the glial sling form a kind of bridge structure, at the midline, between the two lateral ventricles. It has been hypothesized that this structure is required for the proper fusion of the two hemispheres and the guidance of the pioneering callosal axons (Meyer and Goffinet 1998; Meyer, Soria et al. 1998). Additionally, other glial guidepost cells around the corpus callosum have been reported: the radial glial cells of the glial wedge (GW), the astrocytes forming the midline zipper glia (MZG) and glial cells composing the induseum griseum (IG)

(Shu and Richards 2001; Shu, Butz et al. 2003; Shu, Li et al. 2003; Shu, Puche et al. 2003; Shu, Sundaresan et al. 2003; Richards, Plachez et al. 2004) (Fig. 23). The current guidance model stipulates that the glial cells of the GW, the glial sling and the IG secrete guidance molecules which channel the commissural axons along the correct pathway (Shu and Richards 2001; Shu, Sundaresan et al. 2003). Moreover, some controversial studies have also showed that the glial sling was containing a majority of guidepost neurons rather than glial cells (Shu, Li et al. 2003). However, at that time, no clear function for these migrating neurons has been proposed.

As mentioned above, two transient populations of neurons have been identified by our group inside the CC: the glutamatergic calretinin-positive neurons which express the Sema3C and the GABAergic interneurons which both act as guidepost cells for the growing callosal axons while the CC is forming (Niquille, Garel et al. 2009) (Fig. 22).

During AC formation, at early embryonic stages (E12-E13), before the first AC pioneer axons have reached the midline, a kind of bridge structure has also been described between the hemispheres. This structure has been revealed by CSPG (NG2) labeled cells spanning the entire rostro-caudal axis across the interhemispheric fissure (Lent and Guimaraes 1990; Pires-Neto and Lent 1993; Pires-Neto, Braga-De-Souza et al. 1998; Falk, Bechara et al. 2005). At the crossing stage (E13.5-E14), the CSPG staining has also been identified scattered in the central part of the AC bundle revealing the positioning of some CSPG cells in that region. Moreover, in the same region, the GFAP also starts to be expressed. After the first AC axons have crossed the midline (E14.5-E16), the GFAP staining becomes denser and forms like a tunnel surrounding the AC bundle. These results strongly suggest that two glial cell populations, the CSPG and the GFAP cells, may act as guidepost cells to channel the AC axons (Lent and Guimaraes 1990; Pires-Neto, Braga-De-Souza et al. 1998).

7. Mechanisms of Brain Angiogenesis

7.1 Origin of the endothelial cells

The amazing complexity of the body architecture of the mammals requires for its maintenance a specialized system to bring nutrients, gases, water, signaling molecules and circulating cells from one organ to another. This communication and circulating system is composed of two tubular networks called blood vessels network and lymphatic vessels network. In the present work, only the blood vessels network formation in the brain will be described. The set of molecular and cellular mechanisms involved in the development of the blood vessels and capillaries are called vasculogenesis and angiogenesis. The vasculogenesis comprises the steps in which the primitive mesodermal cells transform into endothelial cells. The angiogenesis refers to the proliferation and the migration of endothelial cells in the tissues (Larrivee, Freitas et al. 2009). Many important diseases are directly linked to dysfunctions or malformations of the blood vessels network. For instance, insufficient blood supply can cause tissue ischemia, whereas, on the contrary, a dense angiogenesis can promote the growth of tumors in the case of cancers. Therefore, a good knowledge and the capacity to control angiogenesis could bring inestimable therapeutic benefits.

The blood vessels are formed by endothelial cells (ECs). Early in embryogenesis, these ECs themselves originate from mesoderm-derived endothelial precursor cells (EPCs) also called as angioblasts. These angioblasts form aggregates called blood islands. Finally, these clusters of EPCs fuse and form the primary capillary plexuses in the yolk-sac and the embryo and then organize them into hierarchical structures. Afterwards, other circulating EPCs will be incorporated into the growing blood vessels (Adams and Alitalo 2007).

The blood circulation is generated by the heart beating and the blood flows from the heart, through the arteries, into arterioles and capillaries. The capillaries form dense and complex network in the tissues and organs compositely called as anastomosis. These anastomosed networks allow the exchange of gases and nutrients between the blood and the tissue, before the blood returns to the heart via the venules, the veins and then the lungs to be refilled with oxygen. While the organs such as the brain are developing, the transport of the blood is increased by the arteries and the veins that expand through circumferential growth (Adams and Alitalo 2007).

The current model of telencephalic angiogenesis stipulates that the pial plexuses encompassing the neural tube grow radial sprouts that will enter the parenchyma to construct a

vascular network in response to the growing metabolic needs of the neural tissue (Vasudevan, Long et al. 2008). Besides, a ventral periventricular vascular plexus was also observed from E10 and was starting to form branches that were entering the lateral pallium (Hiruma, Nakajima et al. 2002). Then, from E10 to E11, this periventricular network was growing towards the dorsal telencephalon to progressively develop in a ventro-lateral to dorso-medial gradient. Thin branches started to elongate from the periventricular plexus to join the pial plexuses. The origin of the ventral vessels was found in a basal vessel within the basal ganglia primordium. This basal vessel was probably originating from the pharyngeal arch arteries (Hiruma, Nakajima et al. 2002). It was then hypothesized that the pial plexuses were developing in a venous network whereas the periventricular plexus was forming an arterial network (Vasudevan, Long et al. 2008). Recent findings in the mice telencephalon, suggest that the cerebral angiogenesis develops in a ventral-to-dorsal fashion through gradients generated by some regionalized and specific homeobox transcription factors (Vasudevan, Long et al. 2008). During embryogenesis, the regional patterning of the telencephalon due to differential expression of transcription factors has been shown to instruct the vascular development. Indeed, the angiogenesis of the periventricular vessels is controlled cell autonomously by homeobox transcription factors from the ventral telencephalon such as *Nkx2.1*, *Dlx1/2* at first and then from the dorsal telencephalon by factors such as *Pax6* (Vasudevan and Bhide 2008; Vasudevan, Long et al. 2008). Based on this work, it has been proposed that embryonic cerebral vascularization in the telencephalon is intrinsically regulated.

7.2 Angiogenic growth and sprouting of the blood vessels

The sprouting of the growing blood vessels is induced first by a selection of some particular ECs. These specific ECs are called tip cells, since their function is to lead the growing sprouts. The tip cells proliferate minimally, while the subjacent ECs called stalk cells proliferate extensively (Adams and Alitalo 2007). Sprouting is regulated by the balance between the pro-angiogenic signals, like VEGF, and molecules that promote quiescence, such as tight pericyte contacts, some extracellular matrix cues or VEGF inhibitors (Fig. 24).

The stimulation of the angiogenic growth is mediated by many signaling factors. One major molecule implicated in the blood vessels morphogenesis is the vascular endothelial growth factor A (VEGFA) (Adams and Alitalo 2007). It belongs to a larger family of angiogenic regulators including VEGFB, C and D, as well as, the placental growth factor (PlGF). At different developmental ages, VEGFA plays multiple roles such as, the chemotaxis and the differentiation of EPCs, the proliferation of ECs and their organization into vascular structures and finally, the angiogenic remodeling of the capillaries (Adams and Alitalo 2007).

Interestingly, the alternative splicing of VEGFA can produce an isoform that have an antagonist anti-angiogenic effect. Therefore, the balance between these two properties can regulate the blood vessels outgrowth and patterning. VEGFA can bind to its receptors VEGFR1 and 2. Binding to the tyrosine kinase VEGFR2 can induce ECs proliferation, differentiation and sprouting (Fig. 24a and b).

In the mouse brain, the Notch receptors and their ligand Delta-like 4 (Dll-4) are essential signaling molecules that regulate sprouting during vasculogenesis and angiogenesis. Dll-4 is expressed in the tip cells while Notch is activated in the neighboring ECs to suppress their sprouting ability. Indeed, it has been demonstrated that a reduction of these signals leads to the formation of new tip cells and significant increase of sprouting and branching. More precisely, in selected ECs, VEGFA induces the expression of Dll-4, which in turn activates Notch in the direct adjacent cells (Fig. 24a) (Adams and Alitalo 2007). Notch signaling suppresses then the expression of VEGFR2 in these cells. As an EC is selected to be transformed into a tip cell, it has to change its behavior and phenotype to become motile, invasive and it has to switch its apical-basal polarity. Since these tip cells express VEGFR2, their guidance is controlled by the presence of a gradient of VEGFA in the extracellular matrix, acting like a chemoattractant for the filopodia of the extending tip cells (Fig. 24b) (Adams and Alitalo 2007).

While the arteries and the veins are growing, they are progressively covered by vascular smooth muscles cells (vSMCs) and by pericytes that encircle the capillaries. Both the vSMCs and the pericytes are forming what is called: the mural cells (Adams and Alitalo 2007). The pericytes are mesenchyme-derived cells that make direct contacts with the ECs through numerous long processes expressing adhesion molecules and that stabilize the endothelial layer (Fig.24) (Adams and Alitalo 2007). Their morphology and density depends on the tissue specificity (Hellstrom, Kalen et al. 1999). The physical contact between the pericytes and the ECs is believed to establish a non-sprouting quiescence. However, new evidences show that the pericytes might contribute to the early growth of the blood vessels by stimulating and guiding the ECs through VEGF signaling (Virgintino, Girolamo et al. 2007).

Moreover, angiogenesis can be affected by many other factors composing the extracellular matrix which surround the growing vasculature (see below and Fig. 24) (Adams and Alitalo 2007).

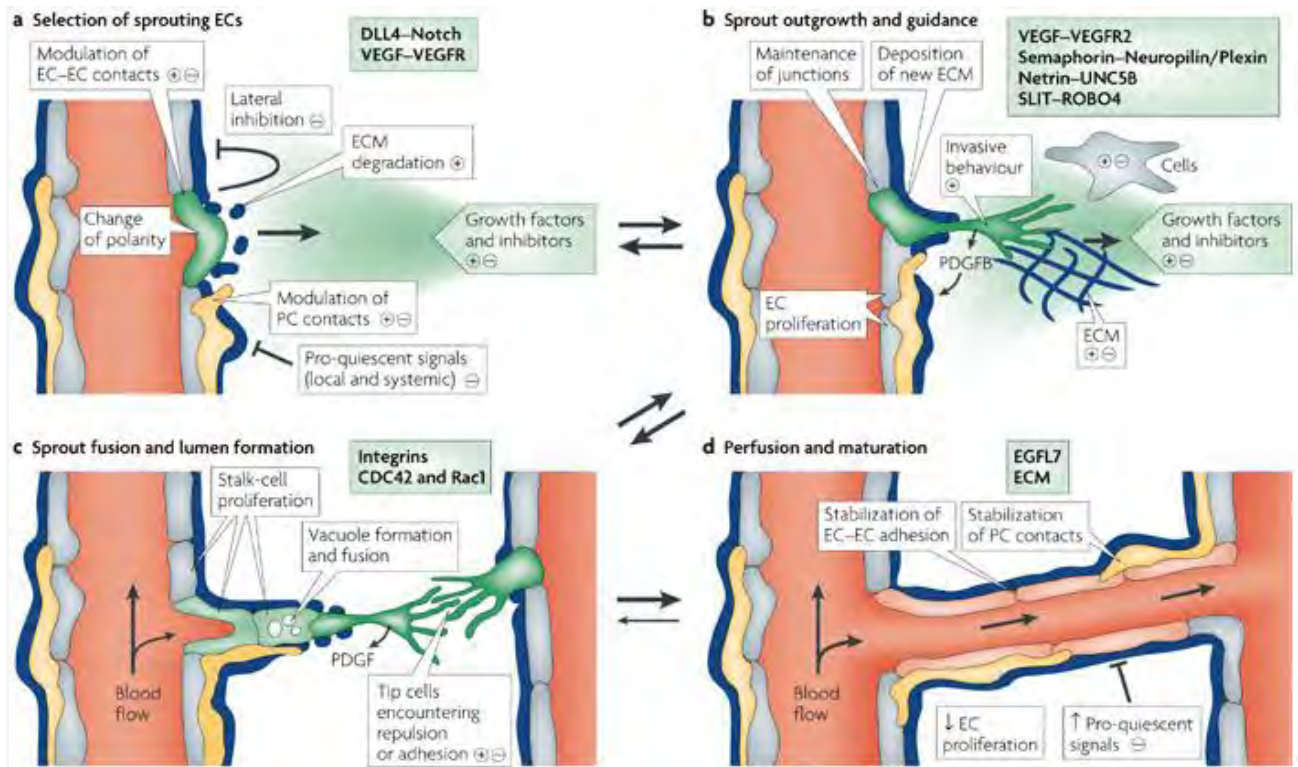


Figure 24. Sprouting, outgrowth, guidance, lumen formation and maturation of vessels.

(a) Sprouting is controlled by the balance between pro-angiogenic signals, such as VEGF, and factors that promote quiescence, such as tight pericyte (yellow) contacts, certain extracellular matrix molecules or VEGF inhibitors. In conditions that favor angiogenesis, some ECs can sprout (green), whereas others fail to respond (grey). Sprouting requires the flipping of apical–basal polarity, the induction of motile and invasive activity, the modulation of cell–cell contacts and local matrix degradation. (b) The growing EC sprout is guided by VEGF gradients. Other signals may include attractive or repulsive matrix cues and guidepost cells in the tissue environment. Release of PDGFB by the tip cells promotes the recruitment of PCs to new sprouts. EC–EC junctions need to be maintained after lumen formation to prevent excessive leakage. (c) Adhesive or repulsive interactions that occur when tip cells encounter each other regulate the fusion of adjacent sprouts and vessels. Lumen formation in stalk ECs involves the fusion of vacuoles but other mechanisms may also contribute. (d) Fusion processes at the EC–EC interface establish a continuous lumen. Blood flow improves oxygen delivery and thereby reduces pro-angiogenic signals that are hypoxia-induced. Perfusion is also likely to promote maturation processes such as the stabilization of cell junctions, matrix deposition and tight PC attachments. Growth factor withdrawal can trigger sprout retraction and endothelial apoptosis. DLL4, delta-like-4 ligand; EGFL7, epidermal growth factor ligand-7; ROBO4, roundabout homologue-4; VEGFR2, VEGF receptor-2. From (Adams, and Alitalo 2007).

7.3 Neurovascular guidance molecules

During angiogenesis, the tip cells are dynamic and motile structures including filopodia that explore and respond to attractive or repulsive signals. In this way, they behave similarly than the axonal growth cones and share morphological features with them (Fig. 24b and c). Therefore, it has been hypothesized that the axons and the blood vessels might develop and navigate through identical mechanisms (Eichmann, Makinen et al. 2005). In this field, the growing axons reach their final targets via attractive or repulsive cues expressed by guidepost cells or extracellular matrix substrates, which involve contact, or act via soluble diffusing molecules. Some of these guidance signals can also be involved in the angiogenesis (Eichmann, Makinen et al. 2005; Larrivee, Freitas et al. 2009).

For example, the Semaphorins, a family of axonal guidance molecules which can bind to their receptors, the Neuropilins (Nrp1 and Nrp2), as well as the VEGF, might be involved in the selection of responsive ECs. Indeed, Nrp1 can bind to VEGF₁₆₄ and not to VEGF₁₂₀ which can suggest the existence of a selective mechanism between the different ECs. The Neuropilins are transmembrane receptors that can homo- or hetero-dimerize with other receptors like the Plexins and the VEGFR. Both Nrps can display various splicing forms, including soluble inhibitory forms (Eichmann, Makinen et al. 2005; Larrivee, Freitas et al. 2009). They are important for vascular development and differentiation, and play different roles in the tumorigenesis.

Moreover, the platelet-derived growth factor B (PDGFB) is expressed in the growing sprouts by the tip cells that recruit the pericytes expressing the PDGF receptor β (PDGFR β) (Fig. 24b). PDGFB has also been shown to play a role in the proliferation of the mural cells which display the highest rate of division between E11.5 and E14.5 in the brain. Recent analysis suggests that the ECs of the capillaries produce PDGFB which signals to the neighboring mural cells progenitors which express PDGFR β , and promotes their co-migration along the angiogenic sprouts (Hellstrom, Kalen et al. 1999). The recruitment of these cells insures the stabilization of new growing vessels. In addition to Neuropilins, the Semaphorins, that represent either long range diffusible molecules or short range membrane bound molecules, can react with the Plexin family of transmembrane protein. It has been demonstrated that PlexinD1 was expressed by the tip cells and that the secreted Sema3E was able to interact with it, independent of the Neuropilins (Hellstrom, Kalen et al. 1999). Therefore, the coexpression of these receptors (Nrps, Plexin, and VEGFR) suggests that there might be multiple ways of signaling through Semaphorins and VEGFs in the ECs (Eichmann, Makinen et al. 2005; Larrivee, Freitas et al. 2009).

Additionally, the Netrin transmembrane receptor Unc5B is strongly expressed in the sprouting capillaries and arterial tip cells (Fig. 24b) (Eichmann, Makinen et al. 2005; Larrivee, Freitas et al. 2009). The Netrins are a family of secreted molecules. Netrin-1, Netrin-3, and β -Netrin/Netrin-4 have been identified in the mammals. They can be attracting or repelling cues in the axonal guidance. The stimulation of the tip cells by its ligand Netrin-1 leads to the retraction of their filopodia which indicates a negative regulation of vessels outgrowth by the Netrin-1/Unc5B interaction. Similarly, Netrin-4 may also be a negative regulator of the angiogenesis (Eichmann, Makinen et al. 2005; Larrivee, Freitas et al. 2009).

Furthermore, the Slits are large secreted glycoproteins that might also be involved in angiogenesis, since Robo4, one of their receptor, is essential for the proper patterning of the blood vessels (Fig. 24b) (Adams and Alitalo 2007). The Slits were first described as repulsive guidance molecules in the CNS development. Two Slit shorter fragments have also been observed, with one fragment being more diffusible than the other. In the mammals, three Slit (Slit1, Slit2, and Slit3) proteins and four Robo (Robo1, Robo2, Robo3/Rig-1, and Robo4/magic Roundabout) receptors have been found. Robo4 was the only receptor to be observed in murine and tumoral endothelial stalk cells (Fig. 24b) (Adams and Alitalo 2007). Controversial results have been found with Slit2, which has been shown to inhibit ECs migration in mouse embryos via its binding to Robo4, and by contrast, to promote it via its interaction with Robo1 in tumoral cells (Carmeliet and Tessier-Lavigne 2005). In addition, a Robo1/Robo4 heterodimerization has been recently reported *in vitro* (Larrivee, Freitas et al. 2009). Nevertheless, in any mutants for Robo receptors or for Slits, no developmental vascular defects have ever been described.

A short range family of guidance cues namely the ephrins A1-A5 and B1-B3, and their respective receptors namely EphA1-A8 and EphB1-B6, are also implicated in the vascular development. Briefly, the ephrinB2-EphB4 interactions and bidirectional signaling are essential to prevent the mixing of arterial and venous ECs, but their repellent activity might also serve to guide ECs migrating through the tissue boundaries during the formation of intersomitic vessels. However, new evidences suggest on the contrary that ephrinB2-Eph might induce angiogenetic sprouting *in vivo* (Eichmann, Makinen et al. 2005). In addition, their expression in adjacent ECs and vSMCs may help in establishing a contact-dependent communication (Carmeliet and Tessier-Lavigne 2005).

7.4 “Guidepost cells” in Angiogenesis

As previously mentioned, the endothelial tip cells are playing a similar role in angiogenesis than the axonal growth cones in axonal guidance. But do they also respond to matrix cues or signals secreted by guidepost cells (Fig. 24b). In the retina, the astrocytes begin to express VEGF at birth to stimulate the ECs to sprout from the optic nerve (Larrivee, Freitas et al. 2009). Besides, new evidences show that the pericytes might contribute to the early growth of the blood vessels by stimulating and guiding the ECs through VEGF signaling (Virgintino, Girolamo et al. 2007). Furthermore, recent evidences have shown that the guidepost key player in angiogenesis might be the macrophage. The early embryonic macrophages travel from the yolk sac and colonize the embryonic brain even before the vascularization is built. It has been shown that VEGF signaling was in a large part responsible for the sprouting of tip cells, but how the tip cells of neighbouring nascent vessels can fusion to form new circuits remained to be clarified. Moreover, macrophages have been shown to be implicated in developmental and in pathological angiogenesis in several diseases (Fantin, Vieira et al. 2010). Intriguingly, the subpopulation of macrophages that promote tumor angiogenesis and which express the angiopoietin receptor Tie2 and the Sema3 receptor Nrp-1, has been shown to be largely expressed during the brain vascularization and to promote vascular anastomosis in physiological developmental conditions (Fantin, Vieira et al. 2010). By using transgenic mice, in which the hematopoietic transcription factor PU.1 was mutated, and which were lacking macrophages, it has been demonstrated that these cells might act as “guidepost cells” to help for the fusion of tip cells. Indeed, in these mice, the blood vessels were making fewer intersections (Fantin, Vieira et al. 2010). Moreover, the matrophages were observed to localize at vessels junctions and to interact with the endothelial tip cells, by forming sort of bridges in order to align them and to prepare them for the fusion (Fantin, Vieira et al. 2010).

7.5 Differentiation and maturation of the blood vessels

The development of a mature blood vessel network involves many other mechanisms such as, EC proliferation and migration of stalk cells behind the tip cells, extension of filopodia also by the stalk cells, suppression of motile, explorative behavior of the tip cells when they find the counterparts of other growing sprouts, adhesive interactions and establishment of junctions between ECs and repulsion between incompatible parts of the vasculature. Thereafter, the initiation of the blood flow will be triggered by the formation of a lumen in between the vascular walls (Fig. 24c and d) (Adams and Alitalo 2007). Very little is known about this process, but there have been evidences about pinocytosis and vacuole formation followed by intra- and inter-cellular fusion of the large vacuoles. The integrins, the small GTPases Cdc42

and Rac1 play a role in the lumen formation which is followed by the tubulogenesis. EGFL7 (EGF-like domain-7) is believed to suppress the adhesion of the ECs to the extracellular matrix. It is also thought that some circulating angioblasts may be integrated between the ECs to either form new sprouts or to enlarge the vessel diameter (Fig. 24c and d) (Adams and Alitalo 2007).

During the entire embryonic and perinatal development of the vascular network, the arteries and the veins are differentiated through a mechanism termed as arteriovenous differentiation. The arteries are specified by a concentric layer of vSMCs, by extracellular matrix (ECM) molecules, and by elastic fibers which allows them to resist being squashed and the pressure of the pulsatile blood flow. By contrast, the veins are surrounded by fewer vSMCs and they contain valves that open unidirectionally to prevent blood backflow (Adams and Alitalo 2007). Molecularly, the Notch pathway and its downstream targets namely, Hey and Hes, are also extensively involved in the differentiation of the arteries. In addition, the arterous endothelium expresses the transmembrane protein ephrin-B2 while the receptor Eph-B4 is specifically expressed in the venous endothelium. Similarly, Nrp1 is found in arteries whereas Nrp2 is restricted to the veins. Moreover, the orphan nuclear receptor COUP-TFII, is specific to the venous endothelium and inhibits the Notch signaling while the two forkhead box transcription factors FoxC1 and FoxC2 are required to enhance the expression of Notch ligand Dll-4 and promote arterial identity (Adams and Alitalo 2007).

The final maturation and quiescence of the vessels network is triggered by the oxygen delivery and the recruitment of the mural cells which are accompanied by the progressive arrest of ECs proliferation. The incorporation of mural cells implies the direct covering of the ECs by pericytes in the capillaries, whereas, in bigger vessels like arteries and veins, the ECs are first encircled by basement membrane and then are recovered by vSMCs (Adams and Alitalo 2007). The pericyte population is largely heterogeneous and can be labeled by several markers such as, the proteoglycan NG2, the intermediate filament protein desmin, the α -smooth-muscle actin (ASMA) and the regulator of G-protein signaling (RGS5). The proliferation of mural cells, their migration and their incorporation around the vessels is regulated by PDGFR β , a tyrosine kinase receptor, through its binding by PDGFB or D in mice. The lack of PDGFR β signaling leads first, to pericytes loss and secondary, to capillary dilation (microaneurysm) and rupture (Hellstrom, Kalen et al. 1999). Then, the differentiation of the mural cells is mostly due to the activity of the transforming growth factor β 1 (TGF β 1) which triggers signals mostly through two Activin receptor-like kinases (Alk-1 and Alk-5). These receptors have opposite effects, since signaling through Alk-5 promotes the mural cells differentiation and the maturation of blood vessels, while activation of Alk-1 inhibits these

processes (Gaengel, Genove et al. 2009). Furthermore, the secreted growth factors Angiopoietins (Ang ligands) and their tyrosine kinase Tie receptors also promote angiogenesis and the association of the pericytes to the ECs. For instance, Ang1 is expressed by the mural cells and might mediate their adhesion to the ECs, whereas Ang2, its antagonist, is expressed predominantly by the ECs. Both Ang1 and Ang2 can bind Tie2 receptor to either promote or repress angiogenic or inflammatory responses depending on the tissue in which they are expressed (Adams and Alitalo 2007). In addition, Ang1 and Ang4 have recently been shown to activate Tie1 and to amplify its signal by heterodimerization with Tie2. The latter is present in the embryonic and adult quiescent ECs, as well as in the bone marrow-derived macrophages (Fantin, Vieira et al. 2010). The expression of Tie1 starts later, and continues during adulthood. The loss of Tie2 during late embryonic ages leads to ECs apoptosis demonstrating that it is essential for their survival (Gaengel, Genove et al. 2009). Finally, the extracellular lipid sphingosine-1-phosphate (S1P) which binds to G-protein-coupled receptors, and that originate in majority from the platelets, is indispensable for the blood vessels maturation. On the five S1P₁₋₅ receptors, the S1P₅ receptor is expressed exclusively in the CNS (Gaengel, Genove et al. 2009). The cell adhesion molecule N-Cadherin, which connects the ECs and the pericytes, has been shown to be relocalized to specific regions of the plasma membrane following S1P/S1P₁ signaling which is of critical importance for the adhesion mechanisms between the mural cells and the ECs (Gaengel, Genove et al. 2009).

7.6 Blood vessel formation pathologies

Many genes involved in human cardiovascular pathologies linked to developmental defects were identified with the use of transgenic mice strains. For example, it has been observed in both PDGFB and PDGFR β mutants that the loss of pericytes or vSMCs leads to excessive sprouting, microaneurysms, leakage and hemorrhages with no distinguishable phenotypes between the two mutants (Hellstrom, Kalen et al. 1999). Similarly, the loss of ephrin-B2 protein from the mural cells causes strong defects in the shape of the blood vessels. Again, the blocking of Notch signaling or the reduced expression of Dll-4, results in a dramatic increase of sprouting and branching. In opposition, the Nrp-1 knockout mice which are embryonically lethal, exhibit defects in their vascular patterning linked to defects in the extension of the ECs filopodia and in their migration. By contrast, the arteriovenous differentiation in Nrp-2 knockouts is normal; anyway, their lymphatic vessels have malformations (Eichmann, Makinen et al. 2005; Larrivee, Freitas et al. 2009). Moreover, the loss of PlexinD1 causes aberrant sprouting of intersegmental vessels, which indicates that the Semaphorins have a repulsive activity on the ECs. Additionally, the loss of function of Unc5B in mice leads to

increased sprouting of ECs and increased capillary branching, whereas their stimulation with the ligand Netrin-1 leads to the retraction of the filopodia of the tip cells (Eichmann, Makinen et al. 2005; Larrivee, Freitas et al. 2009). However, in mice deficient for Netrin-1, no vascular defects have been reported. Generally, knockout mice that lack any component of the Notch pathway (Notch1 and/or Notch4, JAG1 or Dll-4, Hey1 or Hey2) present severe vascular defects and die before birth. Interestingly, when COUP-TFII is inactivated in mice, the veins acquire an arterial identity. In mice that lack TGF β 1, Alk5 or Alk1(activin-receptor-like kinase-1), a dramatic vascular phenotype in the yolk sac, the placenta and the embryo is observed, and defects in hematopoiesis usually lead to death between E9.5 and E11.5. Moreover, embryos that lack Alk1 make large connections between arteries and veins (Gaengel, Genove et al. 2009). Finally, the Tie-1 knockout mice die perinatally and display oedema and hemorrhaging, while ablation of the Tie-2 receptor or its ligand Ang-1 leads to severe defects in angiogenesis, remodeling and maturation processes (Hellstrom, Kalen et al. 1999).

In humans, a point mutation in the Tie-2 receptor causes a venous disease in which the patients have thin-walled and dilated veins and the mutations of Alk1 gene or of Eng (endoglin) gene cause a disorder in which the capillary are dilated presenting local arteriovenous network malformations and bleeding. This disease is named hereditary hemorrhagic telangectasia (Adams and Alitalo 2007). In addition, mutations in Notch3 gene cause a severe disorder called CADASIL for cerebral autosomal dominant arteriopathy with subcortical infarcts and leukoencephalopathy. The patients present vascular lesions which result in the degenerescence of vSMCs causing strokes and dementia. In mice defective for Notch3, only the final maturation of the vSMCs of the arteries is not achieved and shows instead a venous pattern of maturation (Gaengel, Genove et al. 2009).

Therefore, a refine regulation of the signaling pathways involved in both vasculogenesis and angiogenesis processes, is of primordial importance during the entire embryonic brain development and perinatally.

7.7 Neurovascular coupling

Neurovascular coupling (functional hyperemia) is defined by the ability of the CNS to elicit some regionalized changes in the blood flow in response to the neuronal activity to match the metabolic needs of the latter (Zonta, Angulo et al. 2003; Cauli, Tong et al. 2004; Metea and Newman 2006; Metea and Newman 2007). The variations of the blood flow in the brain can be visualized by functional magnetic resonance imaging (fMRI) or by positron emission tomography (PET) scan (Metea and Newman 2006). These techniques are usually employed to diagnose diseases in humans. The cellular and molecular mechanisms that regulate neurovascular coupling have been only recently and partially unraveled. It is generally accepted that the neurovascular unit is composed of three main actors: the blood vessels, the neurons and the glial cells which play a role of intermediary between the two others (Zonta, Angulo et al. 2003; Cauli, Tong et al. 2004; Metea and Newman 2006; Metea and Newman 2007). Neurovascular coupling has been studied extensively in *in vitro* preparations of rat cortical slices or of the mammalian retina, since the retinal neurons can be stimulated naturally by flashes of light (Metea and Newman 2006; Metea and Newman 2007). The regional regulation of the blood flow is mediated by either vasodilatation or vasoconstriction of the blood vessels via the vSMCs surrounding the arteries or the pericytes encircling the capillaries (Zonta, Angulo et al. 2003; Cauli, Tong et al. 2004; Metea and Newman 2006; Metea and Newman 2007).

Following light stimulation, both vasoconstriction and vasodilatation responses were observed. In addition, some sphincter-like contractions at vessel branch points were elicited (Metea and Newman 2006). In the CNS, the glial cells (Müller's glia in the retina or astrocytes in the cortex) cannot fire action potential, but they are able to respond to neurotransmitters release from the neurons, such as the glutamate, by increasing their intracellular level of Ca^{2+} and by releasing their own transmitters (Volterra and Meldolesi 2005). Then, in certain regions of the brain, this mechanism can be correlated with vasomotor responses of the neighboring blood vessels. The glial cells have been shown to release some vasoactive factors in response to the local neuronal activity (Zonta, Angulo et al. 2003). For instance, they might induce the production of arachidonic acid metabolites such as prostaglandins, epoxyeicosatrienoic acids (EETs) and 20-hydroxyeicosatetraenoic acid (20-HETE) (Zonta, Angulo et al. 2003; Metea and Newman 2006; Metea and Newman 2007). The prostaglandins can be either vasoconstricting or vasodilating, and the two last metabolites are believed to mediate the dilation and the constriction of the blood vessels respectively. Therefore, they can play a key role in the glial control of the blood flow (Metea and Newman 2006; Metea and Newman 2007). Moreover, the extracellular level of nitric oxide (NO) in the retina has also

been suggested to determine which process between vasoconstriction or vasodilatation will be dominant. Increasing NO levels was favoring vasoconstriction, while reducing it was favoring vasodilatation (Metea and Newman 2006; Metea and Newman 2007). Finally, when the communication between neurons and glia is interrupted through the blockage of purinergic receptors, the vasomotor responses induced by the neurons are abolished, whereas the responses induced by the glia are maintained (Metea and Newman 2006; Metea and Newman 2007). Additionally, when the neurotransmitters release is inhibited by incubation into tetanus toxin, the vasomotor responses to glial Ca^{2+} waves were conserved. This indicates that the glial cells are an essential intermediary in the neurovascular coupling (Metea and Newman 2006; Metea and Newman 2007).

Intriguingly, in addition to the glial cells, some specific subpopulations of cortical GABAergic interneurons have been hypothesized to play a major role in neurovascular coupling (Cauli, Tong et al. 2004; Kocharyan, Fernandes et al. 2008). Indeed, during the last decade, patch-clamp recordings were used in acute rat cortical slice preparations to show that the evoked firing of one single interneuron could either lead to the vasoconstriction or to the vasodilatation of the adjacent capillaries (Cauli, Tong et al. 2004; Kocharyan, Fernandes et al. 2008). Afterwards, vasomotor interneurons were identified by their localization, their morphologies and their GAD65 and/or GAD67 labeling. Then, the expression of vasoactive intestinal peptide (VIP), nitric oxide synthase (NOS), neuropeptide Y (NPY) and somatostatin (SOM) was revealed. It was observed that these interneurons were establishing close contacts with the cortical micro-arteries and that they were receiving subcortical afferents from cholinergic (ACh) and serotonergic (5-HT) pathways (Cauli, Tong et al. 2004; Kocharyan, Fernandes et al. 2008). Moreover, analysis of the astrocytic processes, the ECs and the vSMCs which surround the blood vessels showed that they exhibit some neuropeptide receptors such as VIP, SOM and cholecystokinin (CCK) receptors. Altogether, these observations lead to suggest that a subset of cortical GABAergic interneurons could act as integrators, since they transform the neuronal signals into regional vascular responses (Cauli, Tong et al. 2004; Kocharyan, Fernandes et al. 2008).

MATERIAL AND METHODS

Animals

All studies on mice of either sex have been performed in compliance with the national and international guidelines. For staging of embryos, midday of the day of vaginal plug formation was considered as embryonic day 0.5 (E0.5). Wild-type mice maintained in a C57Bl/6 genetic background were used for developmental analysis of the CC. We used wild-type ($^{+/+}$), heterozygous ($^{+/-}$) and homozygous mutant *Nkx2.1* mice (Flames et al., 2007; Kimura et al., 1996; Sussel et al., 1999), which are referred as *Nkx2.1* $^{+/+}$, *Nkx2.1* $^{+/-}$ and *Nkx2.1* $^{-/-}$ in this work. We used heterozygous *GAD67-GFP* knock-in mice, described in this work as *GAD67-GFP* mice (Tamamaki, Yanagawa et al. 2003). *GAD67-GFP* embryos could be recognized by their GFP fluorescence. PCR genotyping of these lines was performed as described previously (Lopez-Bendito et al., 2006). Heterozygous embryos did not show any phenotype and were used as controls. We used *Nkx2.1-Cre* (Kessar, Fogarty et al. 2006; Mori, Tanaka et al. 2006; Fogarty, Grist et al. 2007; Zhu, Bergles et al. 2008; Rubin, Alfonsi et al. 2010), *GLAST-Cre ERTTM* (Jackson Laboratory: Tg(Slc1a3-cre/ERT)1Nat/J), *Olig2-Cre ERTTM* (Takebayashi, Nabeshima et al. 2002) and *NG2-Cre* (Jackson Laboratory: B6;FVB-Tg(Cspg4-cre)1Akik/J) (Zhu, Bergles et al. 2008) transgenic mice that have been described previously. The reporter mouse *Rosa26R-Yellow fluorescent protein (YFP)* (Srinivas, Watanabe et al. 2001) was used to reliably express YFP under the control of the Rosa26 promoter upon Cre-mediated recombination. Embryos were recognized by their YFP fluorescence. The reporter *Rosa26:lacZ/DT-A* (*Rosa-DTA*) mouse line (Brockschneider et al., 2006) was used to conditionally express the cytotoxic diphtheria toxin polypeptide toxic fragment A (DTA) allele under the control of ubiquitously active Rosa26 promoter. The neuron-specific enolase (NSE)-stop-DTA (*NSE-DTA*) mice (Kobayakawa et al., 2007) were used to induce the expression of highly potent diphtheria toxin fragment A (DTA) from neuron-specific enolase locus, and resulted in specific ablation of neurons.

Induction of CreERT by Tamoxifen

Tamoxifen (20 mg/ml, Sigma, St Louis, MO) was dissolved at 37°C in 5 ml corn oil (Sigma, St Louis, MO) pre-heated at 42°C for 30 minutes. A single dose of 4 mg (250-300 μ l) was administered to pregnant females by oral gavage. For embryos younger than E10.5, a dose of 3 mg or less was administered.

***In utero* electroporation**

To perform *in utero* electroporation, we adapted our protocol from the one described previously (Cancedda, Fiumelli et al. 2007). E14.5 timed-pregnant *Nkx2.1^{+/-}/GAD67-GFP*, *Nkx2.1Cre/Rosa-DTA:GAD67-GFP*, *Nkx2.1Cre/NSE-DTA:GAD67-GFP* and *Nkx2.1Cre⁺/Rosa-YFP* mice were anesthetized with isoflurane (3.5% during induction and 2.5% during surgery) and embryos were exposed within the intact uterine wall after sectioning the abdominal wall. The DNA solution containing the expression vector encoding the red fluorescent protein (*pCAG-IRES-Tomato*) (2 mg/ml) together with the dye Fast Green (0.3 mg/ml; Sigma, St. Louis, MO) was pressure injected focally (1–2 μ l) into the lateral ventricle of embryos through a glass micropipette using a PicoSpritzer III (Parker Hannifin, Cleveland, OH). Each embryo, while still being within the uterus, was placed between tweezer-type electrodes (System CUY-650P5 Nepa Gene Co, Chiba, Japan) and was electroporated with five electrical square unipolar pulses (amplitude: 45 V; duration: 50 ms; intervals: 950 ms) powered by a BTX electroporator apparatus (model BTX ECM 830; Harvard Apparatus, Holliston, MA). By orienting the tweezer-type electrodes, we were able to preferentially electroporate dorsal pallium precursors that give rise in part to pyramidal callosally-projecting neurons (Borrell, Yoshimura et al. 2005) or ventral pallium precursors that give rise in part to embryonic glial cells. The embryos were quickly placed back into the abdominal cavity and the muscular and skin body wall layers were sutured. The embryos were allowed to develop until E16.5.

Slice cultures

For E14.5 to E16.5 CC slice cultures, we used an *in vitro* model of CC organotypic slices that has been previously described (Niquille, Garel et al. 2009). Embryos were dissected in ice cold dissecting medium (MEM Gibco ref 11012-044 with 15 mM glucose and 10 mM Tris pH7-9). Brains were isolated and embedded in 3% low-melting point agarose (Invitrogen). 250 μ m thick coronal sections were made using a vibratome and slices at the level of the CC were collected in cold dissecting medium. CC slices were cultured on nucleopore Track-Etch membrane (1 μ m pore size; Whatman) or millicell inserts (0.4 μ m pore size; Millipore) in slice culture medium (SCM) (BME/HBSS (Invitrogen) supplemented with 1% glutamine, 5% horse serum, and Pen/Strep (Lopez-Bendito, Cautinat et al. 2006).

***In vitro* focal electroporation**

We applied an *in vitro* focal electroporation method using a Nepagene apparatus to transfect an expression vector into telencephalic slices (Stuhmer, Anderson et al. 2002). E14.5-E16.5 organotypic coronal slices from *WT* embryos were obtained as described above. The expression vectors encoding the green (*pCAG-IRES-EGFP*) or the red (*pCAG-IRES-Tomato*) fluorescent proteins were electroporated at a concentration of 1mg/ml in sterile PBS 1X (Sigma, St. Louis, MO). Expression vectors were focally injected through a glass micropipette into the LGE or the MGE using a PicoSpritzer III (Parker Hannifin, Cleveland, OH) and the slices were electroporated between platinum Petri-dish and cover square platinum electrodes (System CUY-700-1 and CUY-700-2; Nepa Gene Co, Chiba, Japan) with two unipolar square pulses (amplitude: 100 V; duration: 5 ms; intervals: 500 ms) generated by a CUY21EDIT Electroporator (Nepa Gene Co, Chiba, Japan).

Immunohistochemistry

Embryos were collected after caesarean section and quickly killed by decapitation. Their brains were dissected out and fixed by immersion overnight in a solution of 4% paraformaldehyde in 0.1 M phosphate buffer (pH 7.4) at 4°C. Postnatal mice were profoundly anaesthetized and perfused with the same fixative, and their brains post-fixed for 4 hours. Brains were cryoprotected in a solution of 30% sucrose in 0.1 M phosphate buffer (pH 7.4), frozen and cut in 50 µm-thick coronal sections for immunostaining.

Mouse monoclonal antibodies were: BrdU (Monosan, Am. Uden, Netherlands), Nestin (Pharmingen), GFAP (Chemicon), α -tubulin (SY Synaptic System) and β III-tubulin (Promega). Rat monoclonal antibodies were: Lymphocyte antigen76 (Ter119) (Lifespan Bioscience); L1 (Chemicon, Temecula, CA), PDGFR α (BD Bioscience); PECAM (CD31) (BD Pharmingen); SNAP25 (Stemberger Monoclonal Inc., BA). Rabbit polyclonal antibodies were: Calbindin (Swant, Bellinzona, Switzerland); Calretinin (Swant, Bellinzona, Switzerland); cleaved-caspase 3 (Chemicon); GFAP (DAKO, Carpinteria, CA); GFP (Molecular Probes, Eugene, OR); NG2 (Chemicon); Nkx2.1 (Biopat, Caserta, Italy); Olig2 (Millipore); PH3 (Upstate), S100 β (Swant), GABA (Sigma, St Louis, MO); NPY (Sigma, St Louis, MO) and RFP (Labforce MBL). Goat polyclonal antibodies were: Calretinin (Swant, Bellinzona, Switzerland); Nrp-1 (R&D System, Minneapolis, MN) and PDGFR β (R & D Systems). Guinea pig antibody was: GLAST (Chemicon, Temecula, CA) Chicken antibody was: GFP (Aves); biotin-conjugated antibodies were: Isolectine Ig-IB4 (Molecular probes), PECAM (CD31) (BD Pharmingen).

a) Fluorescence immunostaining was performed as follows: unspecific bindings were blocked during preincubation and incubations after adding 2% normal horse serum in PBS 1X solution with 0.3% Triton X-100. The primary antibodies were detected with Cy3-conjugated (Jackson ImmunoResearch laboratories, West Grove, PA) and Alexa488-, Alexa594- or Alexa647-conjugated antibodies (Molecular Probes, Eugene, OR). Sections were counterstained with Hoechst 33258 (Molecular Probes), mounted on glass slides and covered in Mowiol 4-88 (Calbiochem, Bad Soden, Germany).

b) DAB immunostaining was performed as follows: Endogenous peroxidase reaction was quenched with 0.5% hydrogen peroxide in methanol, and unspecific binding was blocked by adding 2% normal horse serum during preincubation and incubations in the Tris-buffered solutions containing 0.3% Triton X-100. The primary antibodies were detected with biotinylated secondary antibodies (Jackson ImmunoResearch, West Grove, PA) and the Vector-Elite ABC kit (Vector Laboratories, Burlingame, CA). The slices were mounted on glass slides, dried, dehydrated, and covered with Eukitt.

c) DAB immunostaining was adapted for erythrocytes staining as follows: Endogenous peroxidase reaction was directly used to visualize the erythrocytes. Therefore, no hydrogen peroxide was added. No primary, nor any secondary antibody, was used. Sections were rinsed in a Tris-buffered solution and preincubated for 10 minutes in 0.05% DAB diluted in 0.1 M Tris buffer. The reaction was started with the same solution supplemented with 0.5% H₂O₂ and stopped with 0.1 M Tris buffer after 10 minutes. The slices were mounted on glass slides, dried, dehydrated, and covered with Eukitt.

Confocal Time-Lapse Microscopy

For imaging neurons, slices were cultured on nucleopore Track-Etch membranes (1 μm pore size; Whatman) in tissue dishes containing 3ml of SCM medium (BME/HBSS supplemented with glutamine, 5% horse serum and Pen/Strep). CC GABAergic interneuron migration paths and dynamics were studied in coronal CC slices of GAD67-GFP, *Nkx2.1^{-/-}/GAD67-GFP*, *Nkx2.1Cre⁺/Rosa-DTA:GAD67-GFP* and *Nkx2.1Cre⁺/NSE-DTA:GAD67-GFP* transgenic mice from E14.5 to E18.5. To visualize callosal axons, the plasmid encoding the red fluorescent protein (*pCAG-IRES-Tomato*) was electroporated *in utero* into the dorsal telencephalon progenitors of E14.5 embryos that generate callosally projecting neurons. We imaged growth cone dynamics and outgrowth properties of frontal callosal axons that were found to grow continuously from the lateral extension of the CC to the midline after E16.5. After 15-20 hrs in culture, slices were placed in an open perfusion chamber on the stage of an upright Leica SP5 confocal microscope. Temperature was maintained at 37°C with the aid of a microscope incubator system (Life Scientific, Switzerland) and slices were perfused with

SCM medium containing a gas mixture of 5% CO₂/ 95% O₂. GAD67-GFP positive CC neurons and callosal axons labelled with Tomato were imaged with a 20X, a 40X, or a 60X immersion lens at 15 or 20 minute intervals using the fast scan function of the Leica SP5 confocal microscope resonant scanner. Image captures and all peripherals were controlled with Leica software. Pictures were processed and converted into *.AVI movies using Imaris and Metamorph 6.0. Migration parameters (basal rate of migration, frequency and duration of the intervening pauses) were determined by measuring movements every 15-20 minutes during 5 hours while the neurons were migrating through the CC white matter. Using the tracking function of Metamorph software 6.0, a total of 70 GAD67-GFP neuron traces were analyzed at E14.5 and at E16.5; and 35 traces at E17.5.

BrdU tracing studies

To label cells in the S-phase of the cell cycle at the suitable embryonic stages (E12.5, E14.5 and E16.5), the pregnant female mice were injected intraperitoneally with a solution of 8 mg/ml of 5-bromo-2'-deoxyuridine (BrdU; Sigma, St Louis, MO) in PBS (0.15 M NaCl, 0.1 M phosphate buffer, pH = 7.4) to a final concentration of 50 mg/kg body weight. To trace the division rate of the subpallial precursors, the pregnant females were sacrificed 2 hours post-injection. To trace the date of genesis of the CC astroglial cells, the pregnant females were sacrificed when embryos were E18.5. The BrdU was revealed by DAB or fluorescence immunostaining (as mentioned above) after a treatment with 2 M HCl for 30 min at room temperature.

***In situ* hybridization**

Sema 3A plasmid was linearized with Not1 (New England Biolabs) for antisense RNA synthesis by T3 polymerase (Promega). Sema3C plasmid was linearized with EcoRI (New England Biolabs) for antisense RNA synthesis by T7 polymerase (Promega) and with XhoI (New England Biolabs) for sense RNA synthesis by T3 polymerase (Promega). TAG-1 plasmid was linearized with XbaI (New England Biolabs) for antisense RNA synthesis by T3 polymerase (Promega) and with HindIII (New England Biolabs) for sense RNA synthesis by T7 polymerase (Promega). NrCAM plasmid was linearized with EcoRI (New England Biolabs) for antisense RNA synthesis by T7 polymerase (Promega). EphA4, Npn-1, EphB1 plasmids were linearized with SacI (New England Biolabs) for antisense RNA synthesis by T3 polymerase (Promega). ephrinB2 and ephrinA3 plasmid were linearized with BamH1 (New England Biolabs) for antisense RNA synthesis by Sp6 polymerase (Promega). ephrinB3

plasmid was linearized with HindIII (New England Biolabs) for anti-sense RNA synthesis by T7 polymerase (Promega). ephrinA1 plasmid, EphA3 and EphA5 were linearized with KpnI (New England Biolabs) for antisense RNA synthesis by T7 polymerase (Promega). ephrinA4 plasmid and EphB3 were linearized with SacII (New England Biolabs) for antisense RNA synthesis by T3 polymerase (Promega). ephrinA5 plasmid was linearized with BamHI (New England Biolabs) for antisense RNA synthesis by T7 polymerase (Promega). Slit2 plasmid was linearized with XbaI (New England Biolabs) for antisense RNA synthesis by T7 polymerase (Promega). For *in situ* hybridization, brains were dissected and fixed by immersion overnight at 4°C in a solution containing 4% paraformaldehyde (Amselgruber, Buttner et al.) in PBS. 100 µm free-floating vibratome sections were hybridized with digoxigenin-labeled cRNA probe as described before (Garel, Marin et al. 1997). To combine *in situ* hybridization and immunofluorescence, Fast Red (Potiron and Roche) was used as an alkaline phosphatase fluorescent substrate.

Neurosphere generation and microscopical analysis

The protocol has been adapted from Arsenijevic *et al.*, 2001.

a) Primary culture and sphere passaging

The brains of embryos at developmental stage E14.5 were collected as described above. They were carefully removed from the skull into ice-cold sterile dissecting medium (MEM 1X) complemented with Glucose 1M (5ml/100ml). Thereafter, the brains were embedded in low melting point Agarose 3% (LMP-Agar, Gibco) at 37°C, and cut into 250 µm thick slices using a vibratome (Leica© VT 1000 S). The sections were collected in the ice-cold dissecting medium. The areas of interest (MGE, POA and SEP) were dissected out using two tungsten needles under a stereomicroscope (Leica© MZ16F). The dissected pieces of tissue were then collected into 1ml ice-cold sterile Hormone Mix Medium (MHM 1X) supplemented with Penicillin (50 U/ml) and Streptomycin (50 U/ml) (GIBCO). The Hormone Mix Medium is a growing medium containing DMEM and F-12 nutrient (1:1), glucose (0.6%), glutamine (2 mM), sodium bicarbonate (3 mM), HEPES buffer (5 mM), transferrin (100 mg/ml), insulin (25 µg/ml), progesterone (20 nM), putrescine (60 µM), selenium chloride (30 nM) (Avery, Kaur et al.). Brain tissue pieces were mechanically dissociated under sterile conditions with a fire-polished pipette in the Hormone Mix Medium. The pipette was rinsed before the dissociation of each new region.

The dissociated cells were then grown in Hormone Mix Medium complemented with Pen/Strep and EGF in 6-well dishes (Nunclon Surface, NUNC Brand Products, Nalge Nunc International) at a concentration of around 10^4 - 10^5 cells per 1 ml and 4 ml per dish. After 6-7

days *in vitro* (DIV) at a temperature of 37°C in a 5% CO₂ atmosphere, the sphere cultures were expanded. Primary spheres were dissociated mechanically and cells were plated at the density of 2x10⁶ cells for 40 ml in a flask (Nunclon Surface, NUNC Brand Products, Nalge Nunc International). Sphere passages were done every 7 DIV, by spheres dissociation and transfer of 2x10⁶ cells to a new 40 ml flask.

b) Differentiation of spheres

After 7 DIV, the neurospheres of optimum size were chosen under a stereomicroscope (Nikon©) to be transferred individually and plated onto poly-L-ornithine coated coverslips in 24-well plates (Nunclon Surface, NUNC Brand Products, Nalge Nunc International). Each coverslip contained about ten spheres and 1 ml of Hormone Mix Medium supplemented with Pen/Strep and 2% fetal bovine serum (FBS).

c) Immunofluorescence on differentiated Neurospheres

After 7 DIV, the neurospheres were fixed in 4% PFA for 20 minutes and permeabilized with 0.3% triton/PBS1X for 3 minutes. Coverslips were incubated with primary antibodies diluted in PBS containing 10% NHS for 2 hours at room temperature, followed by secondary fluorescent antibodies for 45 minutes at 37° and Hoechst staining for 5 minutes.

Chromatin Immunoprecipitation

Chromatin immunoprecipitation was conducted on E14.5 and E16.5 brain samples according to the instructions provided by the manufacturer (Upstate, 17-295), using a mouse anti-Nkx2.1 monoclonal antibody (MS699-P, Lab Vision).

A 391 bp PCR fragment of the *Lhx6* promoter that includes a consensus Nkx2.1 binding sequence at position –240 bp relative to the putative translational start site was identified using primers 5'-ttgtaccgagagtaggagaagg and 5'-gtcctaactttgtagtggcattt.

Two fragments of the *GFAP* promoter that include a consensus Nkx2.1 binding sequence were found to be positive binding targets. 1) A 412 bp PCR fragment at position –4227 bp relative to the putative translational start site was identified using primers 5'-cagcctggggtatataagtctgtc and 5'-tctctgattctccatttcctatc. 2) A second 216 bp PCR fragment at position –4753 bp relative to the putative translational start site was identified using primers 5'-ctgtagggaagactcagctcat and 5'-tggagtctgaagtagatgttctc.

A 363 bp PCR fragment of the *GLAST* promoter that includes a consensus Nkx2.1 binding sequence at position –3550 bp relative to the putative translational start site was identified using primers 5'-acaactactctaaaaggccacac and 5'-agattgagagcaagatgaggaact.

A 417 bp PCR fragment of the *S100β* promoter that includes two consensus Nkx2.1 binding sequences, separated by 70 nucleotides, at positions –5245 bp and -5322 bp relative to the putative translational start site was identified using primers 5'-gtattcttgactcacaacactcg and 5'-agaatgggatctgtgttctaaag.

Two fragments of the *Olig2* promoter that include a consensus Nkx2.1 binding sequence were found as putative Nkx2.1 binding targets. 1) A 340 bp PCR fragment at position –965 bp relative to the putative translational start site was identified using primers 5'-cagatccagtttctcagcttggta and 5'-ccggagagctatttcaatacagt. 2) A 334 bp PCR fragment at position -6680 bp relative to the putative translational start site was identified using primers 5'-catctggacagacaatacacaca and 5'-gagtacacagacagaccagagaa.

A 205 bp PCR fragment of the *NG2* promoter that includes a consensus Nkx2.1 binding sequence at position –5186 bp relative to the putative translational start site was identified using primers 5'-aaaatcagatcctcccactgtag and 5'-tttaggacttcaggattccctta.

Primers against two fragments of the *Neurogenin2* promoter region, comprising of the core Nkx2.1 binding consensus sequence (tcaag), were made. 1) Primers 5'-cgggattctgactctcactaattc and 5'-aatggttctaaagctcctgttgg were designed to amplify a 410 bp PCR fragment with the core consensus Nkx2.1 binding sequence at position –668 bp relative to the putative translational start site. 2) Primers 5'-cgggattctgactctcactaattc and 5'-aatggttctaaagctcctgttgg were designed to amplify another 352 bp PCR fragment with the core consensus Nkx2.1 binding sequence at position –4073 bp relative to the putative translational start site.

Transfection of HEK293 cells

A suspension of HEK-293 cells adapted to serum-free growth medium was plated at 1×10^6 cells in 4 ml media in a 60mm plate. For formation of the transfection complexes, 3:1 ratio of FuGENE® HD Transfection Reagent (μ l) : plasmid DNA (μ g) was prepared and used for transfection. The study was performed by co-transfecting an expression plasmid for constitutive over-expression of Nkx2.1 (*pCAG-Nkx2.1-IRES-Tomato*) or a control plasmid (*pCAG-IRES-Tomato*) with the test plasmid containing the promoter region tagged to a reporter gene (like *pDRIVE-mGFAP* or *pNG2-eGFP*). Transfection complexes were formed by mixing 2 μ g of each of the two plasmids with 12 μ l of Fugene transfection reagent and 188 μ l of Optimem reduced serum media. The mix was incubated at room temperature for 20 minutes and thereafter, added to the cell plates. The cell plates were kept in the 37°C incubator and gene expression analysis was done after 24-48 hours of transfection (time of expression after transfection varied depending on strength of promoter in plasmid).

Imaging

DAB stained sections were imaged with a Zeiss© Axioplan2 microscope equipped with 10×, 20×, 40× or 100× Plan-NEOFLUAR objectives and coupled to a CCD camera (Axiocam MRc 1388x1040 pixels). Fluorescent-immunostained sections were imaged using confocal microscopes (Zeiss LSM 510 Meta, Leica SP5 or Zeiss Qasar 710) equipped with 10×, 20×, 40×oil Plan-NEOFLUAR and 63×oil, 100×oil Plan-Apochromat objectives. Fluorophore excitation and scanning were done with an Argon laser 458, 488, 514 nm (blue excitation for GFP and Alexa488), with a HeNe laser 543 nm (green excitation for Alexa 594, CY3 and DiI), with a HeNe laser 633 nm (excitation for Alexa 647 and CY5) and a Diode laser 405 nm (for Hoechst-stained sections). Z-stacks of 10-80 planes were acquired for each coronal section in a multitrack mode avoiding crosstalk. Z-stacks of 10-20 sections were acquired for each section for the creation of isosurfaces with Imaris 7.2.1 software (Bitplane Inc.).

All 3D Z stack reconstructions and image processings were performed with Imaris® 7.2.1 software. To create real 3D data sets we used the mode “Surpass”. The generation of isosurfaces (object defining a surface surrounding voxels located between two threshold values) allowed us to visualize the contours of cells, of blood vessels and of growth cones. The colocalization between two fluorochromes was calculated and visualized by creating a yellow channel. Figures were processed in Adobe Photoshop© CS2 and CS4 and schematic illustrations were produced using Adobe Illustrator© CS2 and CS4.

Quantifications

a) CC, CCi and AC GABAergic neuronal population analysis

In 50 µm coronal sections of *Nkx2.1^{+/+}:GAD67-GFP*, *Nkx2.1^{-/-}:GAD67-GFP*, *Nkx2.1-Cre⁺/Rosa-DTA:GAD67-GFP* and *Nkx2.1-Cre⁺/NSE-DTA:GAD67-GFP* embryos, GABAergic neurons of the CC, the CCi and the AC were counted at E18.5 as the number of cells labeled for the GFP from at least 2 sections per condition. To study the density of GABAergic neurons through the CC, the CCi and the AC, the values were quantified on 4 planes of the CC, the CCi and the AC section stacks and were reported per surface unit (number of cells/mm²). The cell densities were determined in two CC areas (medial and lateral) and in the entire CC area (total). Based on our work, we considered that the CC is divided into two regions: medial and lateral. The medial part is bordered dorsally by the IG and the longitudinal fissure and ventrally by the glial wedge and the dorsal limit of the septum. The lateral part comprises the white matter bordered by the cingulate cortex dorsally, and by the ventricular zone between the glial wedge and the medio-dorsal angle of the lateral ventricle towards the ventricular side. For the AC, the quantifications were performed in the

medial part (including both anterior and posterior limb) that was divided into three zones. For the CCI, the quantifications were done in one region comprising the cingulate bundle (CI). The quantifications were done using the Imaris® 7.1 software.

b) *Astroglial cell population analysis*

In 50 µm thick brain sections of *Nkx2.1^{+/+}*, *Nkx2.1^{+/-}* and *Nkx2.1^{-/-}* embryos at E18.5, the astroglial cells that were labeled for GFAP or S100β were counted in the CC, CCI, CFI, CPA, CPF, MGE, MZG and POA regions from at least 4 brains per condition. S100β staining labeled the astroglial cell bodies while GFAP principally labeled the cell processes. The cell densities were reported per surface unit area (number of cells/mm²). The quantification was done using Neurolucida 9.0 and Neurolucida 9.0 Explorer© software.

In 50 µm thick brain sections of *Nkx2.1^{+/+}*, *Nkx2.1^{-/-}*, and *Nkx2.1-Cre⁺/Rosa-DTA* embryos at E18.5, the astroglial cells that were labeled for Olig2 or both Olig2 and GLAST were counted in the CC mid and CC side, the CI and the AC from at least 2 brains per condition. Olig2 staining labeled the glial cell bodies while GLAST labeled both the cell bodies and processes. The cell densities were determined in the medial and lateral part of the CC, the CI and the AC. The cell densities were reported per volume unit (number of cells/mm³). The quantification was done using Imaris® 7.2.1 software.

c) *Nkx2.1⁺ BrdU⁺ GLAST⁺ precursors and post-mitotic glia division analyses*

Pregnant *Nkx2.1^{+/-}* female mice were injected intraperitoneally with a solution of 8 mg/ml of 5-bromo-2'-deoxyuridine in PBS to a final concentration of 50 mg/kg body weight. To trace the division rate of the subpallial precursors, the pregnant females were sacrificed 2 hours post-injection. Embryos were collected after caesarean section and quickly killed by decapitation. Their brains were dissected out and fixed by immersion overnight in a solution of 4% paraformaldehyde in 0.1 M phosphate buffer (pH 7.4) at 4°C. In 50 µm thick brain sections of *Nkx2.1^{+/+}* and *Nkx2.1^{-/-}* embryos at E16.5, *Nkx2.1⁺* cells, BrdU⁺ dividing cells and GLAST⁺ precursors or post-mitotic astroglial cells of the MGE, POA and TS were counted in the VZ, SVZ and in the parenchyma of each region, from at least 2 brains per condition. *Nkx2.1* and BrdU staining labeled the cell bodies while GLAST labeled both the cell bodies and processes. The percentage of *Nkx2.1*-derived dividing precursors or post-mitotic glial cells, were determined as follows: In each sub region, and for each condition, a sample of at least four different Z-stacks was acquired at 100x magnification by using a Leica SP5 confocal microscope. The Z-stacks comprised of 10 planes that were acquired in a multitrack mode avoiding any crosstalk. Thereafter, in order to exclude the possibility of quantifying the

same cells more than once, snapshots of only 3 planes (from the acquired 10 planes), were taken with Imaris® 7.2.1 software (Bitplane Inc.) and analyzed.

The quantification of Nkx2.1, BrdU, GLAST and Hoechst staining was done on each snapshot separately by using NeuroLucida© 9.0 and NeuroLucida 9.0 Explorer© software.

d) *Neurospheres Self-renewal analysis*

Individual primary neurospheres derived from the MGE and the POA of wild-type and *Nkx2.1*^{-/-} E14.5 brains were tested for their capacity to self-renew and expand. Single primary neurospheres were dissociated by mechanical action and single stem cells were transferred into 96-well plates (Nunclon Surface, NUNC Brand Products, Nalge Nunc International) containing 200 µl of MHM 1X in the presence of EGF. The number of secondary spheres derived from the stem cells was counted in each well after 10 DIV.

e) *Neurospheres differentiation analysis*

MGE- and POA-derived neurospheres were obtained from *Nkx2.1*^{+/+} and *Nkx2.1*^{-/-} E14.5 embryos. After 7 DIV, the neurospheres were differentiated and immunostained as mentioned above. Two different brains were used for each condition and were labeled for Nkx2.1, GFAP and βIII tubulin. Cell nuclei were counterstained with Hoechst. For each condition, a total of at least 5 different Z-stacks in 5 different neurospheres were acquired at 100x magnification by using a Leica SP5 microscope. The percentage of *Nkx2.1*⁺/*GFAP*⁺ differentiated astrocytes and *Nkx2.1*⁺/*βIII tubulin*⁺ differentiated neurons were counted directly on the Z-stacks by using Imaris® 7.2.1 software.

f) *Cell death analysis*

In brain sections of *Nkx2.1*^{+/+} and *Nkx2.1*^{-/-} embryos at E16.5, apoptotic cells labeled for either cleaved-caspase 3 or for TUNEL were counted in the the CC, MGE, and POA from at least 2 brains per condition. 50 µm thick brain sections were used for cleaved-caspase 3 staining whereas 10 µm thick brain sections were utilized for TUNEL staining. Cell nuclei were counterstained with Hoechst. For each condition, at least 5 different Z-stacks were obtained at 100x magnification by using a Leica SP5 microscope. The number of apoptotic nuclei were counted and reported as an absolute number per section (the surface area of one section was 24119.332 µm²). The quantification was done using NeuroLucida 9.0 and NeuroLucida 9.0 Explorer© software.

g) *NG2-Cre recombination level analysis*

In 50 µm thick brain sections of *NG2-Cre⁺/Rosa-YFP* embryos at E18.5, NG2⁺ polydendrocytes of the CC (midline) CI, CCi and AC labeled for the YFP and NG2 were counted from 3 brains per condition. For each condition, at least 2 different Z-stacks were obtained at 63x magnification by using a Leica SP5 microscope. The percentage of Cre-mediated recombination within the NG2 cells was calculated as follows: 100/ (NG2⁺ cells * YFP⁺ cells). The quantification was done using Imaris® 7.2.1 software.

h) *loss of NG2⁺ cells analysis*

In 50 µm thick brain sections of *NG2-Cre⁻/Rosa-DTA* and *NG2-Cre⁺/Rosa-DTA* embryos at E18.5, the loss of NG2⁺ polydendrocytes in the CC (medial and lateral), CI, CCi and AC labeled for NG2 were counted from 3 brains per condition. Cell nuclei were counterstained with Hoechst. For each condition, at least 2 different Z-stacks were obtained at 63x magnification by using a Leica SP5 microscope. The percentage of loss of the NG2⁺ cells was reported as a cell density (number of NG2⁺ cells/mm³). The quantification was done using Imaris® 7.2.1 software.

i) *Erythrocytes distribution analysis*

In 50 µm thick brain sections of WT, *Nkx2.1^{-/-}*, *Nkx2.1-Cre⁺/Rosa-DTA*, *Nkx2.1-Cre⁺/NSE-DTA* and *NG2-Cre⁺/Rosa-DTA* embryos at E18.5, DAB stained erythrocytes (see immunohistochemistry section 'c' in material and methods) were counted in a predetermined region comprising of the entire CC, CI and CCi from at least 4 brains per condition. The erythrocytes were counted as a cluster when more than 5 consecutive erythrocytes were closely apposed to each other, while the individual erythrocytes which were well separated from one another were counted separately. The quantification was done using Neurolucida 9.0 and Neurolucida 9.0 Explorer© software.

j) *Blood vessels morphology analysis*

In 50 µm thick brain sections of WT, *Nkx2.1^{-/-}*, *Nkx2.1-Cre⁺/Rosa-DTA*, *Nkx2.1-Cre⁺/NSE-DTA*, *NG2-Cre⁺/Rosa-DTA* embryos at E18.5, DAB staining for PECAM was used to label the endothelial cells of the blood vessels. The blood vessels morphology was analysed in a predetermined region comprising of the entire CC, CI and CCi from at least 4 brains per condition, by using the axonal tracing tool of Neurolucida 9.0 and Neurolucida 9.0 Explorer© software. This tool allows to trace and to calculate the number of individual trees, the number

of nodes, the number of branches, the length, the surface and the volume of the blood vessels network for each condition.

Statistical analysis

The results from all quantifications were analyzed with the aid of Statview© software (SAS Institute Inc.). For all analysis, values from at least three independent experiments were first tested for normality. Values that followed a normal distribution were compared using Student's *t*-test. Values that did not follow a normal distribution were compared using Mann-Whitney and Kolmogorov-Smirnov non-parametric tests.

RESULTS

SECTION 1:

NKX2.1 REGULATES THE CELL FATE AND THE DIFFERENTIATION OF TRANSIENT ASTROCYTES AND POLYDENDROCYTES IN THE MOUSE EMBRYONIC TELENCEPHALON

IDENTIFICATION OF ASTROGLIAL CELLS EXPRESSING NKX2.1 DURING EMBRYONIC DEVELOPMENT

Nkx2.1 has been found to be essential for the proper specification of the medial ganglionic eminence (MGE), the anterior entopeduncular area (AEP) and the anterior preoptic area (POA) (Sussel, Marin et al. 1999). In *Nkx2.1*^{-/-} mice, the progenitors originating from the MGE and the AEP are re-specified to a more dorsal fate and are comparable to lateral ganglionic eminence (LGE) progenitors (Sussel, Marin et al. 1999). Moreover, the ventral-to-dorsal re-specification of the *Nkx2.1* domain in the subpallium of *Nkx2.1*^{-/-} mice results in a drastic loss of GABAergic interneurons (~50%) in the neocortex and the hippocampus indicating that most of these cells are derived from *Nkx2.1*⁺ precursors (Pleasure, Anderson et al. 2000) (Sussel, Marin et al. 1999). In addition to giving rise to GABAergic interneurons, *Nkx2.1*-derived precursors also produce transient oligodendrocytes that migrate tangentially from the ventral MGE and the AEP to the cerebral cortex (Nery, Wichterle et al. 2001) (Kessaris, Fogarty et al. 2006).

Interestingly, the use of the Nkx2.1 antibody and RNA riboprobes, from embryonic day 16.5 (E16.5) to E18.5, revealed the presence of numerous cells in the dorsal telencephalon that expressed the subpallial transcription factor Nkx2.1. Nkx2.1⁺ cells were observed at the CC midline, in regions surrounding the CC: the indusium griseum (IG), the glial sling (GS) and the midline zipper glia (MZG), and in the hippocampal commissure (Fig. 1a1 and not shown). Through these regions, Nkx2.1 was detected in many cells that may either correspond to transient GABAergic interneurons previously identified by our group (Niquille, Garel et al. 2009) or to migrating oligodendrocytes originating from the MGE (Nery, Wichterle et al. 2001; Kessaris, Fogarty et al. 2006). Additionally, Nkx2.1 was also expressed in multiple cells populating the ventral telencephalic regions: the septum (SEP), the striatum and the anterior commissure (AC) (Fig. 1a1 and not shown). Consequently, in order to discern and characterize the observed multitude of Nkx2.1⁺ cells, we made use of several transgenic mice and antibodies that could be employed to specifically label the distinct neuronal and glial subtypes that populate the embryonic telencephalon.

To ascertain if Nkx2.1 is expressed by GABAergic interneurons, we used a *GAD67-GFP* mouse line, in which the green fluorescent protein (GFP) is consistently expressed in

GABAergic neurons (Donahoo and Richards 2009). We found that, at E16.5, none of the $Nkx2.1^+$ cells of the CC and the surrounding areas corresponded to $GAD67-GFP^+$ interneurons (Fig. 1a1-a2; open arrowheads) in accordance with the previously observed results documenting the down-regulation of $Nkx2.1$ expression in GABAergic interneurons migrating from the MGE to the cortex (Nobrega-Pereira, Kessaris et al. 2008). Additionally, $Nkx2.1^+$ cells did not correspond to oligodendrocytes, identified by the expression of the transcription factor *Olig2* (Oligodendrocyte precursor bHLH transcription factors 2), either (not shown). Surprisingly, while astrocytes of the CC are believed to originate from the dorsal telencephalon (Smith et al., 2006), we found that numerous $Nkx2.1^+$ cells, that have originated from the subpallium, of the CC and the surrounding areas expressed markers like GLAST (Astrocyte-specific glutamate and aspartate transporter), Nestin (intermediate filament) and GFAP (glial fibrillary acidic protein) that are specific for post-mitotic astrocytes at this age in the CC (Shu, Puche et al. 2003) (Fig. 1b1-b2, white arrowheads and not shown). However, $Nkx2.1$ was never detected in any radial glial cells of the glial wedge (GW) and of the dorsal telencephalon ventricular zone labeled for the same astrocytic markers (not shown). After post-natal day 0 (P0), $Nkx2.1$ was strongly down-regulated and not detected anymore by immunohistochemistry in the astroglial cells of the telencephalon (not shown).

Thereafter, we aimed to further characterize the properties and the precise cellular identities of the glial cells that converge to the embryonic inter-hemispheric commissures. Thus, to selectively fate map astroglial cells, we crossed $GLAST-Cre$ ERT^{TM} (Jackson Laboratory: Tg(Slc1a3-cre/ERT)1Nat/J) inducible mice with the reporter $Rosa26-lox-STOP-lox-YFP$ ($Rosa26-YFP$) mice (Srinivas, Watanabe et al. 2001). Using $GLAST-Cre^+/Rosa-YFP$ mice, we were able to trace the early astroglial cells present outside the germinal zones and within all the midline telencephalic commissures from E16.5 to E18.5 (Fig. 1c1-c3 and 1d1-d3, white arrowheads). Many of the early astroglial cells visualized by the YFP signal and GLAST staining, co-expressed $Nkx2.1$, implying that the identity of these GLAST-derived GFP^+ astroglial cells was probably regulated by $Nkx2.1$ and that they were generated from E14.5 to E16.5 in the ventral telencephalon when the recombination was induced (Fig. 1c2-c3, 1d2-d3). Some $GLAST^+/Nkx2.1^+$ cells were not labeled by the YFP signal, indicating that either they have been generated prior to the induction of recombination or that the Cre recombinase could not be successively expressed in all $GLAST^+/Nkx2.1^+$ cells (Fig. 1c2-c3, 1d2-d3, open arrowheads). Additionally, we also crossed the $NG2-Cre$ mice (Jackson Laboratory: B6;FVB-Tg(Cspg4-cre)1Akik/J) with the reporter $Rosa-YFP$ mice (Srinivas, Watanabe et al. 2001). Nerve/glial antigen 2 (NG2) is a chondroitin sulfate proteoglycan utilized as a marker for polydendrocytes that are considered as oligodendrocyte progenitor cells and constitute a population of cells different from neurons, mature oligodendrocytes,

astrocytes and microglia (Nishiyama, Watanabe et al. 2002; Nishiyama, Komitova et al. 2009). We found that the NG2⁺ polydendrocytes visualized by the YFP signal did not express the Nkx2.1 protein and were different from the GLAST⁺ astroglial cells (Fig. 2c1-c3, open arrows).

Thus, these results directly suggest that there are different intermingled populations of astroglial cells in the telencephalon of which some subpopulations express the Nkx2.1 transcription factor, and subsequently, raising the possibility that presumably Nkx2.1 could have been down-regulated in the other glial cells as soon as they achieved their differentiation.

IDENTIFICATION OF NUMEROUS EARLY AND TRANSIENT NKX2.1-DERIVED GLIAL CELL TYPES IN THE TELEENCEPHALON DURING DEVELOPMENT

In order to trace the diverse types of cells generated by the Nkx2.1⁺ subpallial domains within the entire telencephalon from E14.5 to birth, we made use of the *Nkx2.1-Cre* mice (Xu, Tam et al. 2008) crossed with the *Rosa-YFP* reporter mice (Srinivas, Watanabe et al. 2001). We verified the existence of *Nkx2.1*-derived YFP⁺ astrocytes expressing GLAST or GFAP within the AC, the septum (MZG) and the striatum from E16.5 to E18.5 (Fig. 3d1-d4 and 3e1-e4, white arrowheads). Unfortunately, the Cre-mediated recombination did not occur sufficiently enough in the GLAST⁺/GFAP⁺ astrocytes of the CC and the surrounding regions that were labeled for Nkx2.1 by immunostaining or by *in situ* hybridization, and thus, the YFP was not found to be expressed in the GLAST⁺/GFAP⁺ astroglial cells of the CC (Fig. 3a3 and 3e2, open arrowheads).

We also observed the existence of *Nkx2.1*-derived YFP⁺ cells expressing NG2, Olig2 or S100β⁺ throughout the commissures (CC, HIC, AC), in midline cortical area, in the septum and in the striatum from E16.5 to E18.5 (Fig. 3a1-a4, 3b1-b2, 3c1-c2 and 3d1-d4, white arrowheads). Complementary analyses using *NG2-Cre⁺/Rosa-YFP* mice showed that all NG2-derived YFP⁺ polydendrocytes were Olig2⁺, and additionally, some of them were also S100β⁺, thus, confirming that part of the *Nkx2.1*-derived Olig2⁺ and S100β⁺ cells corresponded to a sub-population of polydendrocytes (Fig. 2d1-d3, 2e1-e3 and Supplementary Fig. S1). Interestingly we observed that the YFP signal was also detected in a GLAST⁺ population of astrocytes, in the commissures and the cerebral cortex, which co-expressed Olig2 and were different from the GLAST⁺/GFAP⁺ astrocytes that were previously described (Fig. 3f1-f2, arrowheads). Indeed, the use of *Olig2-Cre ERTM/Rosa-YFP* mice (Takebayashi, Nabeshima et al. 2002), confirmed that during embryonic development some of the telencephalic GLAST⁺ astrocytes co-expressed Olig2 (Fig. 3g1-g2, white arrowheads). However, in the telencephalon of *Nkx2.1-Cre⁺/Rosa-YFP* mice, we noticed the additional presence of Olig2⁺ cells that were

not expressing the YFP, thereby, suggesting that glial cells other than the *Nkx2.1*-derived glia may also express Olig2 embryonically (Fig. 3c1-c2, open arrowheads). In the AC of *Nkx2.1-Cre⁺/Rosa-YFP* embryos, the YFP signal was seen to be expressed in both GLAST⁺ astrocytes and NG2⁺ polydendrocytes (Fig. 3d1-d4) and importantly, both populations appeared to be exclusively non-overlapping. Thus, the *Nkx2.1*-derived YFP⁺ glia that did not express NG2 expressed GLAST, and vice-versa (Supplementary Fig. S1). Moreover, while all the *Nkx2.1*-derived NG2⁺ polydendrocytes expressed Olig2 only part of *Nkx2.1*-derived GLAST⁺ astrocytes expressed Olig2. Finally, only *Nkx2.1*-derived NG2⁺ polydendrocytes but not GLAST⁺ astrocytes expressed S100β⁺. In accordance with the subpallial origin of the early telencephalic astroglia and polydendrocytes, transcription factors specific of the dorsal telencephalon (*Emx-1* and *Tbr1*) were never detected in any of the described glial cells at embryonic ages (not shown). Therefore, based on our careful analysis with the astroglial and polydendrocytic markers together with the various transgenic mouse lines, we have shortlisted the *Nkx2.1*-derived glial cells into four major categories, namely, the astrocyte-like glial cells that are GLAST⁺/GFAP⁺/Olig2⁻/Nkx2.1⁺ and those that are GLAST⁺/GFAP⁻/Olig2⁺/Nkx2.1⁺; polydendrocyte-like cells that are NG2⁺/Olig2⁺/S100β⁺ and those that are NG2⁺/Olig2⁻/S100β⁻ (Supplementary Fig. S1).

The temporal profile of the embryonic GLAST⁺ and GFAP⁺ astroglial cells co-expressing Nkx2.1 was studied in the embryonic CC and its surrounding regions (IG and GS) by performing 5-bromo-2'-deoxy-uridine (BrdU) injections at E12.5, E14.5 and E16.5 in wild-type (WT) mice and brains were processed for BrdU immunostaining at E18.5 (Supplementary Fig. S2a-d). The bulk of the Nkx2.1⁺/GLAST⁺ astroglial cells were generated between E14.5 and E16.5 (Supplementary Fig. S2b-c and S2e-f), and very few of those that were born at E12.5 were co-labelled for BrdU at E18.5 (Supplementary Fig. S2a and S2d). Thus, the astroglial embryonic cells of the CC and the HIC are generated primarily between E14.5 and E16.5. This is in perfect accordance with the results showing that the origin of GFAP⁺ astroglial cells at the midline in the CC occurs between E14.5 and E16.5 (Supplementary Fig S2e and S2f) and (Silver, Edwards et al. 1993; Shu, Puche et al. 2003). Also, similar birth-dating results were obtained for the glial cells present in the other telencephalic regions (AC, septum and striatum) too (not shown).

Thereafter, in order to ascertain the survival of these *Nkx2.1*-derived glial cells, we made use of the *Nkx2.1-Cre⁺/Rosa-YFP* mice and stained the brains at different post-natal stages. While the number of *Nkx2.1*-derived glia in the CC continued to increase through P0 to P2, we observed a drastic decrease by P8 for all the different *Nkx2.1*-derived glial populations (GLAST⁺/GFAP⁺ and GLAST⁺/Olig2⁺ astrocytes and S100β^{or+}/Olig2⁺/NG2⁺ polydendrocytes) in the dorsal telencephalon (Supplementary Fig. S3a1-e2). Only rare,

S100 β ⁺ or Olig2⁺, *Nkx2.1*-derived glia still remained (Supplementary Fig. S3c2-d2). However, in the subpallium (septum, striatum and AC), many *Nkx2.1*-derived astroglia, expressing all types of glial markers, could still be visualized until P14 (not shown and Supplementary Fig. S3a3-e3, S3f-j). Thus, implying that the *Nkx2.1*-derived glia in the CC constitute a transient population and disappear completely by P8 from the dorsal pallium while they still continue to exist in the AC and the subpallium post-natally.

Our results, therefore, demonstrate that in embryos, glial cells of the telencephalon are more heterogeneous and are generated much earlier than previously thought. Specifically, different transient astrocyte-like or polydendrocyte-like glial cell subpopulations occupy the entire telencephalon and are derived from Nkx2.1⁺ progenitors of the ventral telencephalon. Interestingly, this study unravels that *Nkx2.1*-derived astrocytes and polydendrocytes of the embryonic telencephalon are generated principally from E14.5 to E16.5. Therefore, contrary to the idea that gliogenesis starts only after the end of neurogenesis at E17 (Schmechel and Rakic 1979; Pixley and de Vellis 1984; Mission, Takahashi et al. 1991; Guillemot 2005), we characterized a new gliogenesis step that occurs in the ventral telencephalon in the same time frame as that of late neurogenesis, and generates transient embryonic glia cells.

***NKX2.1*-DERIVED ASTROGLIA SPATIALLY ORIGINATE FROM THREE DISTINCT SITES IN THE VENTRAL TELECEPHALON**

Nkx2.1 has been shown to be expressed by subpallial progenitors of the MGE, the AEP/POA, the septum and the CGE in the telencephalon of embryonic mice in a subdomain that may correspond to the caudal part of the MGE (Sussel, Marin et al. 1999; Marin and Rubenstein 2001; Yun, Potter et al. 2001; Flames, Pla et al. 2007). It has also been shown that cells expressing Nkx2.1 are found in the septum, the hypothalamus and the Amygdala (Xu, Tam et al. 2008). These studies have majorly focused on the Nkx2.1⁺ precursors in the MGE and have shown that they give rise to GABAergic interneurons or oligodendrocytes (Sussel, Marin et al. 1999; Marin and Rubenstein 2001; Nery, Wichterle et al. 2001; Kessar, Fogarty et al. 2006; Guillemot 2007). We, thus, focused our study on the Nkx2.1⁺ subpallial domains that could potentially generate the transient embryonic glial cells we have identified, at E14.5 and E16.5, since our birth-dating experiments indicated that *Nkx2.1*-derived embryonic glial cells were generated during this period of time (Supplementary Fig. S2). In order to determine the possible sites of origin of the Nkx2.1⁺ embryonic astroglia, we performed double immunohistochemical staining for Nkx2.1 and several astroglial markers and looked at their co-expression in the subpallial domains. This analysis was complicated by the fact that radial glial precursors in the VZ and basal precursors in the subventricular zone (SVZ), while

expressing at first various astroglial markers like Nestin, GLAST and GFAP, can later give rise to neurons as well as to glia (Malatesta, Hack et al. 2003; Gotz and Huttner 2005; Mori, Tanaka et al. 2006). However, it is generally accepted that cells expressing these markers can be considered as astroglial cells as soon as they escape the germinal ventricular and subventricular zones (Schmechel and Rakic 1979; Pixley and de Vellis 1984; Mission, Takahashi et al. 1991; Sultana, Sernett et al. 2000). Therefore, we not only focused our attention on germinal precursors co-expressing Nkx2.1 and astroglial markers, but also, on cells co-expressing these markers and localized at a distance from the germinal zones.

First, we intended to show that the radial glial cells and the basal progenitors of the MGE and the AEP/POA were regulated by Nkx2.1. This was demonstrated by a double immunohistochemical labeling for Nkx2.1 and several astroglial markers like Nestin, GLAST and GFAP (Supplementary Fig. S4a1-b3 and not shown). Indeed, we found that as early as E14.5, the radial glial precursors co-expressed Nkx2.1 and GLAST and finally, by E16.5, they co-expressed Nkx2.1 and GFAP (not shown and Supplementary Fig. S4a-b). The colocalized glial cells were found in the VZ of different subpallial germinal regions, namely the MGE (Supplementary Fig. S4a1-a3) and the AEP/POA (Supplementary Fig. S4b1-b3). Surprisingly, a third region localized in the septum called the triangular septal nucleus (ts) also contained numerous Nkx2.1⁺ cells labeled for the astroglial markers (Supplementary Fig. S4a1 and S4b1). The Nkx2.1⁺ cells of the septal nucleus formed a triangular structure with a germinal aspect bordering the third ventricle and localized in the septum directly under the hippocampal commissure. Moreover, the basal progenitors in the SVZ of the MGE co-expressed the same astrocytic markers. At more caudal levels, radial glial cells expressing Nkx2.1 were also detected in the VZ of the caudal part of the MGE (Flames, Pla et al. 2007), as well as, in the preoptic area bordering the third ventricle (Supplementary Fig. S4b3). Thus, these results imply that the Nkx2.1⁺ precursors of the MGE, the AEP/POA and the septal nucleus are potentially capable of producing GLAST⁺ or GFAP⁺ astrocytes. Thereafter, in order to demonstrate that these three sites give rise to mature Nkx2.1⁺ astrocytes, we investigated the colocalization profile of Nkx2.1 with GLAST or GFAP in a region called as mantle, situated beyond the SVZ (Supplementary Fig. S4a1-a3). This region of the mantle is known to contain post-mitotic neurons expressing different transcription factors than in the germinal zones (like Dlx5/Dlx6) and markers for mature neurons (like β III-tubulin and SCG10) (Casarosa, Fode et al. 1999; Marin and Rubenstein 2001). Interestingly, we found numerous mature Nkx2.1⁺ astrocytes expressing GLAST or GFAP in the ganglionic mantle zone, as well as in the lateral part of the POA (LPOA), far from the VZ (Supplementary Fig. S4a1-a3 and S4b1-b3, arrowheads in b3). We also noticed the presence of numerous mature Nkx2.1⁺ astroglial cells in migratory streams linking the three sites described previously, and that contained Nkx2.1⁺

progenitors. We could observe a flux of Nkx2.1⁺ astroglial cells migrating from the MGE towards the POA (* in Supplementary Fig. S4a1, S4a2 and S4b1), or from the POA towards the MGE (** in Supplementary Fig. S4a1-a3 and S4b1-b2, arrowheads in S4a3), and finally, from the septal nucleus towards the AEP/POA (***) in Supplementary Fig. S4a1 and S4b1). In addition, numerous Nkx2.1⁺ migrating astroglial cells originating most probably from the MGE or the AEP/POA were dispersed in the entire hypothalamus and striatum (not shown).

Thereafter, we used the *GLAST-Cre⁺/Rosa-YFP* mice to investigate if the GLAST-derived YFP⁺ astrocytes also originate from any of the three same sites as mentioned above. The Cre-mediated recombination was induced at E15, in accordance with the time of development, and several GLAST-derived YFP⁺ cells were observed to originate from the MGE, the AEP/POA and from the septal nucleus (not shown and Supplementary Fig. S4c1-c4). These cells were also seen to migrate to the parenchymal regions such as the striatum and to the AC (Supplementary Fig. S4d1-d2 and not shown). Consistent with our previous experiment, these GLAST-derived YFP⁺ cells, generated at E15, constituted a sub-population of astrocytes and co-expressed Nkx2.1 and GLAST (arrowheads) in the MGE (Supplementary Fig. S4e1-e2), the LPOA (Supplementary Fig. S4f1-f2) and the septal nucleus (Supplementary Fig. S4g1-g2). However, some of the GLAST-derived YFP⁺ cells observed outside the germinal zones were not co-expressing GLAST and thus, may also correspond to GABAergic interneurons (Supplementary Fig. S4e1-e2). Finally, some GLAST⁺ glial cells co-expressing Nkx2.1 were not positive for the YFP signal, thus, implying that these cells might have been born before the recombination event was induced, or that the Cre recombinase could not be successively expressed in all GLAST⁺ cells (Supplementary Fig. S4g1-g2, open arrowheads). Additionally, we also made use of the *NG2-Cre⁺/Rosa-YFP* mice and observed that some of the NG2-derived YFP⁺ polydendrocytes originated from the Nkx2.1⁺ precursors of the MGE or the POA, while expressing Nkx2.1 just after they exit the VZ (Fig. 2a1-a3), were not seen to express Nkx2.1 any more after they have migrated far from the VZ (Fig. 2b1-b3).

Thereafter, the precise origin of Nkx2.1⁺ glia was directly visualized by combining the aforementioned glial immunostaining with focal electroporation of a *pCAG-GS-EGFP* plasmid into subpallial domains of organotypic slices of WT embryonic brains. The focal injections were delivered into the three Nkx2.1-regulated subpallial ventricular regions namely the MGE, the septal nucleus and the AEP/POA at both E14.5 and E16.5, and the migration pathways of glia originating from the subpallial domains were analyzed after 3 days *in vitro* (3DIV). The glial cells were identified by staining with the astrocytic markers, GLAST or GFAP. In E14.5 and E16.5 embryonic brain slices, the *in vitro* focal injection and electroporation of the *pCAG-GFP* plasmid into the MGE, the septal nucleus or the AEP gave rise to GLAST⁺ or GFAP⁺ astroglial cells that could be seen migrating to the striatum and to

the dorsal telencephalic regions (Fig. 4a1-a3, 4b1-b3 and not shown). Upon injecting the *pCAG-GFP* plasmid into the POA in the E16.5 embryonic brain slices, many GFAP⁺ glial cells could be visualized migrating outside the VZ to the LPOA (Fig. 4c1-c3). Furthermore, we also confirmed our results by performing *in utero* injection and electroporation of the *pCAG-GS-tomato* plasmid into the ventral telencephalon of E14.5 *Nkx2.1-Cre⁺/Rosa-YFP* embryos and indeed, many *Nkx2.1*-derived YFP⁺ and GLAST⁺ glial cells could be seen migrating from the AEP region to the striatum, mantle zone and the AC (Fig. 4d1-d3). We observed similar results with the POA where the glial cells were seen at the LPOA, and with the septal nucleus too where the glial cells were seen in the septum and the CC (not shown).

The pattern of *Nkx2.1* expression, shows that it is mainly expressed in subpallial regions known to contain pluripotent or unipotent precursors expressing astroglial markers in mammalian telencephalon, as well as, in post-mitotic migrating glial cells. These results together with the fate mapping analysis using electroporation indicates that the telencephalic embryonic *Nkx2.1*-derived astroglia and polydendrocytes originate and migrate from three distinct *Nkx2.1*⁺ domains of the ventral telencephalon: the MGE, the AEP/POA and the septal nucleus.

NKX2.1 REGULATES THE PROLIFERATION OF VENTRAL PROGENITORS IN EMBRYOS

The aforesaid results showed that *Nkx2.1* is expressed in ventral glial precursors of the MGE, AEP/POA and septal nucleus and thus, we wanted to determine if *Nkx2.1* regulates the proliferation of the embryonic glial cells. We investigated if *Nkx2.1* controls the cell proliferation *in vivo* by using two different markers of cell division: the PH3, for phosphorylated histone 3, a metaphase chromosomal marker and the BrdU. The rate of cell proliferation was studied in WT and *Nkx2.1^{-/-}* mice from E12.5 to E16.5, with a principal attention at E16.5 when the bulk of embryonic telencephalic glia is generated. The immunohistochemical staining for PH3 in subpallial domains did not indicate any significant difference in the mitosis of cell precursors between the *Nkx2.1^{-/-}* and the WT mice (data not shown). By contrast, the study with BrdU revealed some differences between WT and *Nkx2.1^{-/-}* mice characterized by a different repartition of precursor cells division in the mutant MGE (named MGE*) from E12.5 to E16.5 (Supplementary Fig. S5a to S5d). In the mutant MGE*, we observed a marked reduction in the BrdU⁺ basal progenitors of the SVZ compared to the WT MGE (Supplementary Fig. S5; compare S5a3 to S5b3 and S5c3 to S5d3). This observed difference may be attributed to the fact, that has been shown before, that although a MGE-like structure forms in the mutant, it has been re-specified to a more dorsal LGE-like fate (Sussel

et al., 1999). In any case, the change of the morphological appearance of the MGE* VZ and the decreased number of basal progenitors in the MGE* SVZ suggests that the progenitors of the MGE* do not develop normally.

To determine if there was a decrease in *Nkx2.1* precursor cell division in the mutant MGE*, POA* and ts*, we performed BrdU injections at E16.5 in both WT and *Nkx2.1*^{-/-} mice, and studied the rate of cell proliferation one hour after the injections by staining for BrdU together with the antibody against Nkx2.1. Both, the mutated and the WT, Nkx2.1 proteins are similarly recognized by the anti-Nkx2.1 antibody indicating that the mutated protein conserves an intact epitope enough for recognition (Corbin, Rutlin et al. 2003). In the WT brains, both in the VZ and SVZ of the MGE, POA and ts, numerous Nkx2.1⁺ precursors were co-labeled with BrdU (Fig. 5a, white arrowheads, Fig. 5e3 and not shown). Contrastingly, a severe decrease in the number of Nkx2.1⁺ cells and of Nkx2.1⁺/BrdU⁺ dividing cells was observed in the VZ and SVZ of the *Nkx2.1*^{-/-} MGE* and POA* and in the VZ of the *Nkx2.1*^{-/-} ts* compared to the WT (Fig. 5b, white arrowheads and Fig. 5e1 and 5e3). On the other hand, we observed numerous BrdU⁺ dividing precursors that did not express the mutated Nkx2.1 in the mutant MGE*, POA* and ts* (Fig. 5b1-b3; open arrowheads and not shown). In the *Nkx2.1*^{-/-}, upon looking at the total number of BrdU⁺ dividing cells, we only noticed a slight decrease in the mutant MGE*, a significant increase in the POA* and a constant division rate in the ts* (Fig 5e2). Using a well characterized stem cell proliferation assay (Arsenijevic et al., 2001), we confirmed that the neuronal stem cell population of the mutant *Nkx2.1*^{-/-} MGE*, POA* and ts* was still able to self-renew in a similar manner than the corresponding WT stem cells (Supplementary Fig. S5e-g). This was due to the fact that the proliferation rate in the mutant *Nkx2.1*^{-/-} MGE*, POA* and ts* was only affected for the Nkx2.1⁺ progenitors but not for the Nkx2.1⁻ progenitors (Fig 5e4 and 5e5). Therefore, the replacement of Nkx2.1⁺ precursors, by Nkx2.1⁻ precursors with a LGE identity, in the *Nkx2.1*^{-/-} MGE* may explain the presence of numerous dividing Nkx2.1⁻ precursors in the mutant MGE*. Similarly, other Nkx2.1⁻ precursors were able to replace the Nkx2.1⁺ precursors in the *Nkx2.1*^{-/-} mutant POA* and the ts*. Indeed, we noticed a significant increase in the rate of proliferation of Nkx2.1⁻ precursors in the *Nkx2.1*^{-/-} mutant POA* too (Fig. 5e5).

Thereafter, we performed double immunohistochemical staining for Nkx2.1 and for the radial glia/astrocytic marker, GLAST on coronal sections of the MGE in both WT and *Nkx2.1*^{-/-} mutant mice brains at E16.5. In the VZ, the SVZ and the mantle zone of the WT MGE, many GLAST⁺ precursors and astroglial cells co-expressed Nkx2.1 (Fig. 5c, white arrowheads) whereas in the germinal and mantle zones of the MGE* of *Nkx2.1*^{-/-} mice, only few GLAST⁺ precursors expressed Nkx2.1 (Fig. 5d). Consequently, the quantitative analyses revealed a drastic and significant decrease of the Nkx2.1⁺/GLAST⁺ precursors in the VZ, SVZ

and of the $Nkx2.1^+/GLAST^+$ astrocytes in the parenchyma (striatum, LPOA/LH, septum) of the $Nkx2.1^{-/-}$ subpallium as compared to the WT (Fig. 5e6). Thus, these results suggest that the absence of $Nkx2.1$ results in $Nkx2.1^+$ precursors losing their capacity to give rise to $Nkx2.1^+$ astrocytes in the mice brains.

Altogether, these observations indicate that the transcription factor $Nkx2.1$ regulates the proliferation of the original $Nkx2.1^+$ precursors in the MGE, the POA and the septal nucleus, the three subpallial domains that potentially generate early embryonic glia

NKX2.1 CONTROLS EARLY GLIOGENESIS IN EMBRYONIC TELEENCEPHALON

In order to investigate the function of $Nkx2.1$ in regulating embryonic gliogenesis, we performed immunohistochemistry for several glial markers ($GLAST$, $GFAP$, $S100\beta$ and $NG2$) in WT and $Nkx2.1^{-/-}$ embryos (Fig. 6). In the control mice, $GLAST^+$ or $GFAP^+$ astroglial cells, and $NG2^+$ or $S100\beta^+$ polydendrocytes were clearly visible from E16.5 to E18.5 in the telencephalic commissures (CC, HIC and AC) and their surrounding regions, in the medial cortical area as well as in the septum (Fig. 6a-c and 6g). In contrast, we observed a complete loss of astroglial cells and of polydendrocytes in all commissures and in the medial cortical areas in the $Nkx2.1^{-/-}$ mice (Fig. 6d-f and 6h). However, $Nkx2.1$ inactivation did not affect the organization of astroglia within the GW, in accordance with the absence of $Nkx2.1$ expression in these cells (Fig. 6d and 6e1-e2). Quantitative measurements made with the three markers, $GFAP$ (Fig. 6i), $S100\beta$ (Fig. 6j) confirmed the complete loss of astroglia and polydendrocytes in the midline dorsal telencephalic areas. Analysis with $GFAP$ showed the complete disappearance of $GFAP^+$ astrocytes in the CC and its surrounding areas (IG, GS and MZG) in the $Nkx2.1^{-/-}$ embryos (Fig. 6i). Interestingly, analysis with $GFAP$ also revealed the loss of a subpopulation of $GFAP^+$ radial glial cells within the mutant POA* (not shown) and MGE* VZ (Fig. 6e3). Additionally, there was a complete loss of $NG2^+$, $S100\beta^+$ polydendrocytes in the medial cortical areas (the cingulate cortex (CCi) and the frontal cortex (CFr)) and the septum of $Nkx2.1^{-/-}$ embryos (Fig. 6f, 6h, 6j and not shown). By contrast, there were no significant differences in the lateral cortical areas (parietal cortex (CPa) and pyriform cortex (CPf)) as well as in the striatum (STR) (Fig. 6j and not shown). This indicated the heterogeneity between embryonic glial cells expressing various glial markers, of which some are controlled by $Nkx2.1$. Furthermore, the identification of three different $Nkx2.1$ -derived glial cell populations, two astrocyte-like populations expressing $GLAST$ only ($GLAST^+/Olig2^-$) or co-expressing both glial markers ($GLAST^+/Olig2^+$) and one polydendrocyte-like population expressing $Olig2$ only ($GLAST^-/Olig2^+$), prompted us to investigate in details the function of $Nkx2.1$ in these different glial cell types (Supplementary Fig. S6). Also, we already know that

all the NG2⁺ polydendrocytes co-express the oligodendroglial marker, Olig2 in addition, and thus, part of those that are referred to as Olig2⁺/GLAST⁻ could be inferred as Olig2⁺/NG2⁺/GLAST⁻ glial cells. To this purpose, we performed immunostaining for Olig2 and GLAST on telencephalic sections from WT and *Nkx2.1*^{-/-} mice (Supplementary Fig. S6a and S6b). At the *Nkx2.1*^{-/-} CC midline, a significant reduction in the cell density of GLAST⁺/Olig2⁻ astrocytes was observed when compared to the WT, while no evident differences were detected for GLAST⁺/Olig2⁺ astroglial cell densities (Supplementary Fig. S6b2 and S6c). However, in the lateral CC and the cingulate bundle, we observed a marked decrease in the GLAST⁺/Olig2⁺ astroglia in the absence of Nkx2.1 (Supplementary Fig. S6b3-b4 and S6c). This indicates that the GLAST⁺/Olig2⁺ astroglial population is heterogeneous and that only a part of these cells are under the regulation of Nkx2.1. Similarly, the Olig2⁺/GLAST⁻ glial population that we know to correspond for a part to *Nkx2.1*-derived polydendrocytes was only significantly decreased in the CC at the midline (Supplementary Fig. S6b2 and S6c). This suggests that yet another population of Olig2⁺ cells, different from *Nkx2.1*-derived NG2⁺ polydendrocytes, occupied the lateral CC regions and the cortex during development.

Furthermore, in order to exclude the possibility of cell death being the central reason for the marked decrease in the number of glial cells we observed, we analyzed the WT and *Nkx2.1*^{-/-} brains at E16.5 for cleaved-caspase 3, a key biomarker for apoptosis (Supplementary Fig. S7a and S7b), and by terminal deoxynucleotidyl transferase-mediated dUTP-biotin nick end labeling (TUNEL) assay which detects DNA fragmentation that results from apoptosis (Supplementary Fig. S7c and S7d). The activation of cleaved-caspase 3 was detected by indirect immunofluorescence using primary antibody against the cleaved-caspase 3. The DNA binding dye, Hoechst was also used to visualize the pyknotic nuclei and in addition, to determine if there are any differences in nuclear size or nuclear morphology between the WT and mutant brains (Supplementary Fig. S7). The quantification of the absolute number of dying cells, labeled by the cleaved-caspase 3 (Supplementary Fig. S7e), and by TUNEL staining (Supplementary Fig. S7f), revealed no significant differences between the *Nkx2.1*^{-/-} brains and the WT brains in any of the observed telencephalic regions namely the CC, the MGE, the POA or the septum. The size and morphology of the nuclei was comparable in both WT and mutant brains, with no stark differences observed.

These results show, for the first time, that early gliogenesis is a process under the regulation of Nkx2.1. The observed loss of astrocytes and polydendrocytes, in the *Nkx2.1*^{-/-} telencephalon, was not due to the glial cell death but due to the lack of *Nkx2.1*-derived glial generation in the absence of *Nkx2.1*⁺ precursor proliferation. In addition, the loss could also be potentially attributed to the incapacity of *Nkx2.1*-derived glia to differentiate.

NKX2.1 REGULATES THE DIFFERENTIATION OF *NKX2.1*-DERIVED EMBRYONIC ASTROGLIA

Our studies elucidating the precise pattern of Nkx2.1 expression in embryos at E16.5 have unraveled that, this transcription factor is expressed in subpallial precursors, as well as, in post-mitotic astroglia. The role of Nkx2.1 in regulating the differentiation of *Nkx2.1*-derived astroglia was further investigated *in vivo* by using *Nkx2.1*^{-/-} mutant mice (Fig. 7). We studied the characteristics of Nkx2.1⁺ mature astroglia and postmitotic neurons, in regions far from the germinal zones, by using the astrocytic marker GLAST and the specific neuronal marker βIII-tubulin, respectively. We looked carefully at all the regions, that we have reported, containing Nkx2.1⁺ cells, and especially at the migratory streams, since they most probably contained cells that undergo final differentiation. As previously shown, numerous Nkx2.1⁺ mature astroglia expressing GLAST were observed far from the germinal zones within commissures and adjacent areas, within numerous migratory routes and throughout the septum, the striatum as well as the hypothalamus of WT embryonic brains (Fig. 1a1, Supplementary Fig. S4a to S4b and Fig. 6a). Additionally, precocious observations made *in vivo* indicated that Nkx2.1 was expressed at high levels in the nuclei of differentiated neurons and astroglia (Fig. 7a2, open arrowheads). Interestingly, in the caudal POA, we also discovered the presence of Nkx2.1 within the cytosol of cells that morphologically resembled neurons and expressed the post-mitotic neuronal marker βIII-tubulin instead of GLAST (Fig. 7b, open arrows). On the contrary, in *Nkx2.1*^{-/-} embryos, the astroglia labeled for the mutated Nkx2.1 protein were never detected in any of the telencephalic brain areas or the migratory pathways (Fig. 7c2). These observations, thus, confirm the definitive loss of astroglial cells after Nkx2.1 inactivation. However, in the caudal POA of *Nkx2.1*^{-/-} embryos, we could still detect the post-mitotic neurons labeled for βIII-tubulin, but not GLAST, co-expressing the mutated Nkx2.1 protein in their processes and within the cytoplasm (Fig. 7c2 and 7d; open arrows). Hence, indicating that some post-mitotic neurons continued to be generated and achieved differentiation in the absence of the active form of Nkx2.1. Altogether, these observations indicated that the transcription factor *Nkx2.1* is indispensable for the genesis and the differentiation of *Nkx2.1*-derived astroglia in embryos.

Since, we observed impaired differentiation of *Nkx2.1*-derived glia in the absence of *Nkx2.1* *in vivo* (Fig. 7), we aimed to analyse the specification of *Nkx2.1* precursors generating early glial cells by observing the MGE- and the POA-derived neurospheres differentiation at E14.5 prior to the appearance of *Nkx2.1*-derived glia at the midline of the telencephalon. After 7 DIV, WT MGE and POA neurospheres were able to differentiate and generate three cell types of the brain (Arsenijevic, Villemure et al. 2001) which were GFAP⁺ mature astrocytes (Fig. 7e1-e2), β III-tubulin⁺ post-mitotic neurons (Fig. 7f) and the NG2⁺ or PDGFR α ⁺ (platelet-derived growth factor alpha receptor) polydendrocytes (not shown). β III-tubulin⁺ post-mitotic neurons were seen to form distinct neuronal clusters throughout the spheres (Fig. 7f) whereas the GFAP⁺ astrocytes were observed to be uniformly dispersed on the entire surface of the spheres (Fig. 7e1-7e2). The quantification based on GFAP and β III-tubulin staining indicated that precursors within WT neurospheres generated around 70% of astroglia and 25 % of neurons (not shown). Using immunohistochemistry for *Nkx2.1*, we found that in the neurospheres derived from WT MGE and the POA, *Nkx2.1* was present in the nucleus of about 50% of the GFAP⁺ astroglia (Fig. 7e1-7e2; white arrowheads, Fig. 7i and not shown). Moreover, a strong *Nkx2.1* signal was also detected in about 80% of the β III-tubulin⁺ neurons (Fig. 7f; white arrows and inset). Thereafter, *in vitro* differentiation of E14.5 *Nkx2.1*^{-/-} mutant MGE*, POA*-derived neurospheres revealed that, in absence of *Nkx2.1*, the progenitors did differentiate into GFAP⁺ astroglia (Fig. 7g1-7g2), as well as postmitotic β III-tubulin⁺ neurons (Fig. 7h). However, the quantification of the *Nkx2.1*⁺ astroglia indicated that the *Nkx2.1* loss in the mutant MGE* and POA* neurospheres induced a significant decrease of *Nkx2.1*⁺/GFAP⁺ astroglia, but no change was observed for the β III-tubulin⁺ neurons that were faintly labeled for the mutant *Nkx2.1* protein (Fig. 7g2, open arrowheads and Fig. 7h, open arrows). Quantification of these results confirmed that while more than 50% of differentiated GFAP⁺ astroglia expressed *Nkx2.1* in WT neurospheres, less than 10% of GFAP⁺ astroglia expressed *Nkx2.1* in mutant neurospheres (Fig. 7i). It indicates that in *Nkx2.1*^{-/-} mutant MGE* and POA* neurospheres, *Nkx2.1*⁺ precursors have nearly completely lost the capacity to differentiate into *Nkx2.1*-derived astroglia. On the other hand, *Nkx2.1*^{-/-} MGE* and POA* neurospheres were still able to generate a similar number of neurons expressing the mutant *Nkx2.1* protein (Fig. 7i).

Thus, our *in vitro* and *in vivo* analysis of the *Nkx2.1*^{-/-} and control embryos corroborates our results about the new subpallial origin for astroglial cells in the embryonic brain, and furthermore, shows the major contribution of the *Nkx2.1* gene in regulating astroglial cell specification.

NKX2.1 DIRECTLY REGULATES THE EXPRESSION OF GLIAL REGULATORY GENES

It is clear from our above mentioned results that the astroglial cell populations of the embryonic telencephalon are derived from *Nkx2.1*⁺ progenitors, and *Nkx2.1* regulates the precursor cells proliferation and differentiation. Moreover, there have been few studies that have brought forth the role of NK2 transcription factor family in regulating various genes either through activation or repression. For example, it is also known that *Nkx2.1* directly activates the transcription of differentiation-specific genes in the thyroid and the lung (Nobrega-Pereira, Kessarlis et al. 2008; Reillo, de Juan Romero et al. 2011). Additionally, *Nkx2.2*, another member of the NK2 family, has been discovered to act as a transcriptional repressor through its interaction with either *Groucho-4* or *Arx* (Griveau, Borello et al. 2010; Mastracci, Wilcox et al. 2011). Thus, likewise, in order to ascertain the direct binding interaction of the transcription factor *Nkx2.1* with the promoter sequences of the various glial regulatory genes in the brain, we performed chromatin immunoprecipitation assay on lysates of E14.5 and E16.5 embryonic brains. Firstly, we searched for the consensus NK2 family binding sequence [GNNCACT(T/C)AAGT(A/G)(G/C)TT] (Guazzi, Price et al. 1990) in the upstream promoter regions of the various regulatory genes namely *GLAST*, *GFAP*, *S100β*, *NG2*, *Olig2* and *Ngn2*. In the absence of the complete consensus binding sequence, the core binding sequence T(C/T)AAG was chosen for analysis. As a positive control, we also included *Lhx6* in our analysis for which the exact site for the binding of transcription factor is already known (Duan, Wang et al. 2011). Secondly, after shortlisting the position of consensus binding sites, primers for the sequence flanking all the shortlisted consensus binding sites (up to three) were made. We then performed the PCR on the crosslinked and sonicated DNA pulled down using an anti-*Nkx2.1* monoclonal antibody. The amplification of one or two *Nkx2.1* consensus binding sequences located in the respective PCR products within the various regulatory glial genes were positive for the brain samples chromatin immunoprecipitated with the *Nkx2.1* antibody, except those that were chosen for *Ngn2* (Fig. 8 a1-a7). *Ngn-2* is a transcription factor of the dorsal telencephalic precursors, and our aforementioned results have clearly specified that *Nkx2.1* regulates the precursors in the MGE, the POA and the ts, thus, it is possible that *Nkx2.1* doesn't regulate the *Ngn2* gene directly. Also, the amplification of the PCR product comprising of the already known *Nkx2.1* consensus binding sequence within the *Lhx6* promoter was positive upon immunoprecipitation with the anti-*Nkx2.1* antibody (Fig. 8 a6). The consensus binding sequences that could positively be pulled down with the anti-*Nkx2.1* sequence contained at least the core sequence. The PCR fragment(s) amplified for the *GLAST* promoter contained TCAAGTnCTT, for the

GFAP promoter contained CACTCAAGT and CTCAAGT, for the S100 β promoter contained ACTCAAG and TCAAGT, for the NG2 promoter contained CAAGTGGT and GNNCANTCAAGTAG and for the Olig2 contained TCAAGTA and CTCAAGTGGT, as the consensus sequence. Thus, these results imply that Nkx2.1 binds the promoter regions of various glial regulatory genes containing the above mentioned highly conserved consensus binding sequence *in vivo*. Identical results were also obtained for the same glial regulatory genes in the E14.5 brain samples.

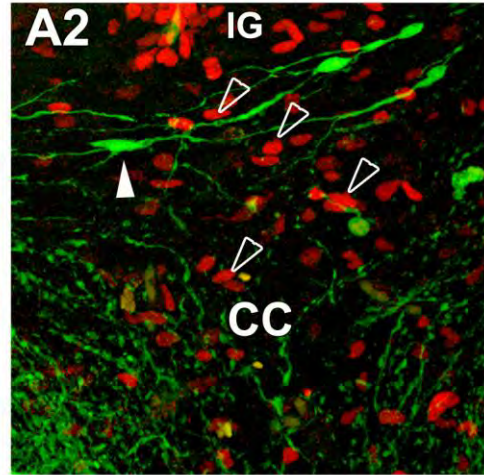
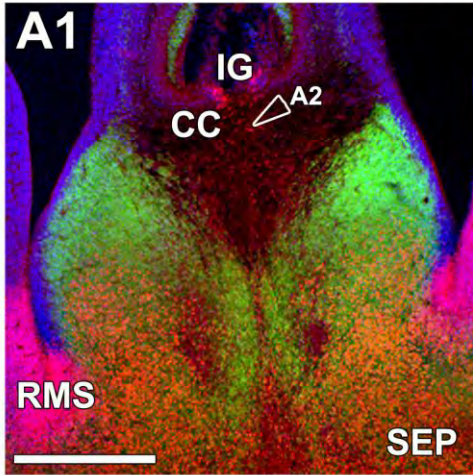
Thereafter, to determine the direct influence of the binding of Nkx2.1 to these upstream consensus binding sequences towards the transcription of these glial regulatory genes, we performed co-transfection studies in the HEK293 cells. We made use of the expression plasmid *pDRIVE-mGFAP* which contains the LacZ reporter under the control of the mouse upstream -1679 bp GFAP promoter sequence, and the *pCAG-Nkx2.1-IRES-Tomato* plasmid constitutively over-expressing the Nkx2.1 protein tagged to the Tomato reporter under the control of the *pCAG* promoter. Co-transfection of both these plasmids in the HEK293 cells resulted in robust expression of the LacZ reporter (Fig. 8 b1-b3). Contrastingly, almost no expression was apparent upon transfection of the *pDRIVE-mGFAP* plasmid with the control *pCAG-IRES-Tomato* plasmid lacking the *Nkx2.1* cDNA (Fig. 8 c1-c3). Thus, these results directly suggest that the activation of the *GFAP* promoter fragment requires the presence of Nkx2.1.

These results, altogether, show that during embryonic development midline glial cells of the telencephalon originate from the ventral telencephalon instead of the dorsal telencephalon. While the *Nkx2.1* homeobox gene is known to be required for the specification of GABAergic interneurons in the ventral telencephalon, we have found that, in addition, it regulates glial (astrocytes and polydendrocytes) proliferation and differentiation.

FIGURES of section 1:

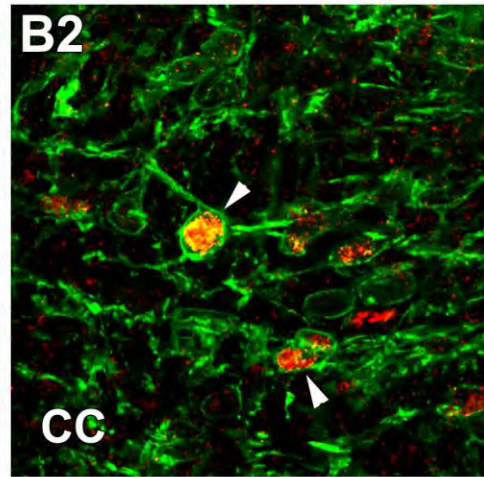
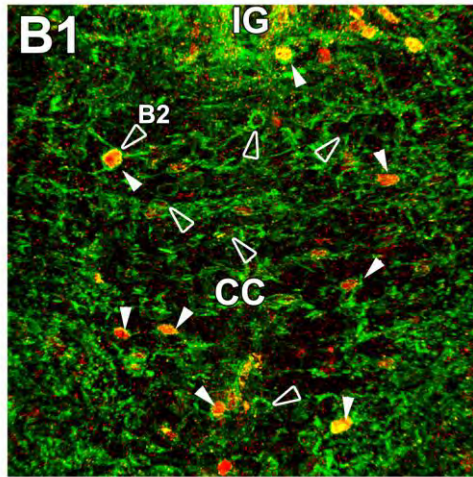
E16.5 / **Nkx2.1** / **Hoechst**

GAD67-GFP+



E16.5 / **GLAST** / **Nkx2.1**

Wild-type



E18.5 / **Nkx2.1** / **GLAST** / **Hoechst**

GLAST-Cre ERT+/Rosa-YFP

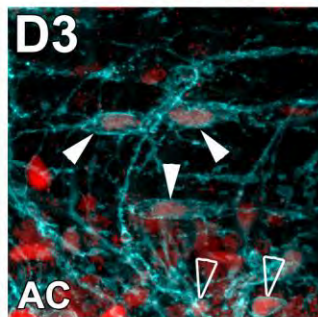
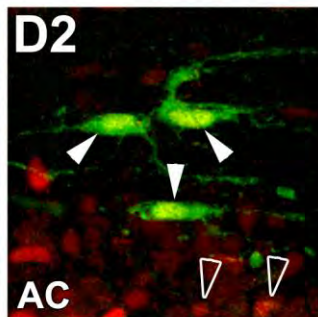
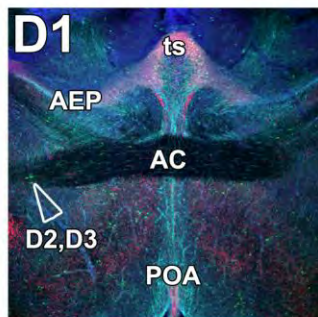
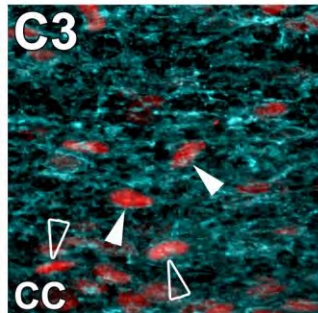
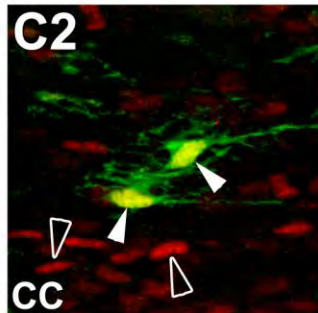
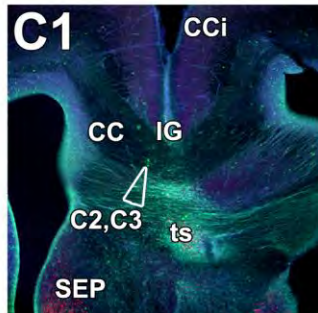


Figure 1. The Nkx2.1-positive cells of the CC are glial cells.

(A-B) Double immunohistochemistry for the GFP and Nkx2.1 (**A1-A2**) on coronal CC sections from *GAD67-GFP*⁺ mice at E16.5, and for GLAST and Nkx2.1 (**B1-B2**) on coronal sections from wild-type mice at E16.5.

(C-D) Triple immunohistochemistry for the YFP, Nkx2.1 and GLAST on coronal CC and AC sections from *GLAST-Cre ERT*⁺/*Rosa-YFP* (**C1-C3** and **D1-D3**) mice at E18.5. Cell nuclei were counterstained in blue with Hoechst (**A1**, **C1** and **D1**). Colocalization between the green and the red channel is highlighted in yellow (**B1-B2**, **C2** and **D2**). **A2**, **B2**, **C2**, **C3**, **D2** and **D3** are higher power views of the CC and AC regions indicated by an open arrowhead in **A1**, **B1**, **C1** and **D1**, respectively.

(A-B) At E16.5, Nkx2.1 labelling (in red) is found in many cell nuclei in the medial part of the CC (open arrowheads in **A2**). Most of the *GAD67-GFP*⁺ interneurons (in green) populating this region are not labelled by Nkx2.1 (white arrowhead in **A2**). At this age, colocalization reveals that most of the Nkx2.1-expressing nuclei belong to cells that express glial markers like GLAST (white arrowheads and colocalization in **B1** and **B2**). **(C-D)** The Cre-mediated recombination was initiated under the control of the inducible GLAST promoter at E16, and the GLAST-derived cells were visualized (in green) with the YFP signal. Some GLAST⁺ glial cells (in light blue) of the CC (**C1-C3**) and the AC (**D1-D3**) co-expressed Nkx2.1 (in red). Some of the GLAST⁺/Nkx2.1⁺ glia were not labelled by the YFP signal and might have been generated before the recombination was induced (open arrowheads in **C2**, **C3**, **D2** and **D3**). **(AC)** anterior commissure; **(CC)** corpus callosum; **(CCi)** cingulate cortex; **(IG)** induseum griseum; **(RMS)** rostral migratory stream; **(SEP)** septum; **(ts)** triangular septal nucleus.

Bar = 675 µm in **C1** and **E1**; 450 µm in **A1**; 67 µm in **A2** and **B1**; 40 µm in **C2**, **C3**, **D2** and **D3**; 30 µm in **B2**.

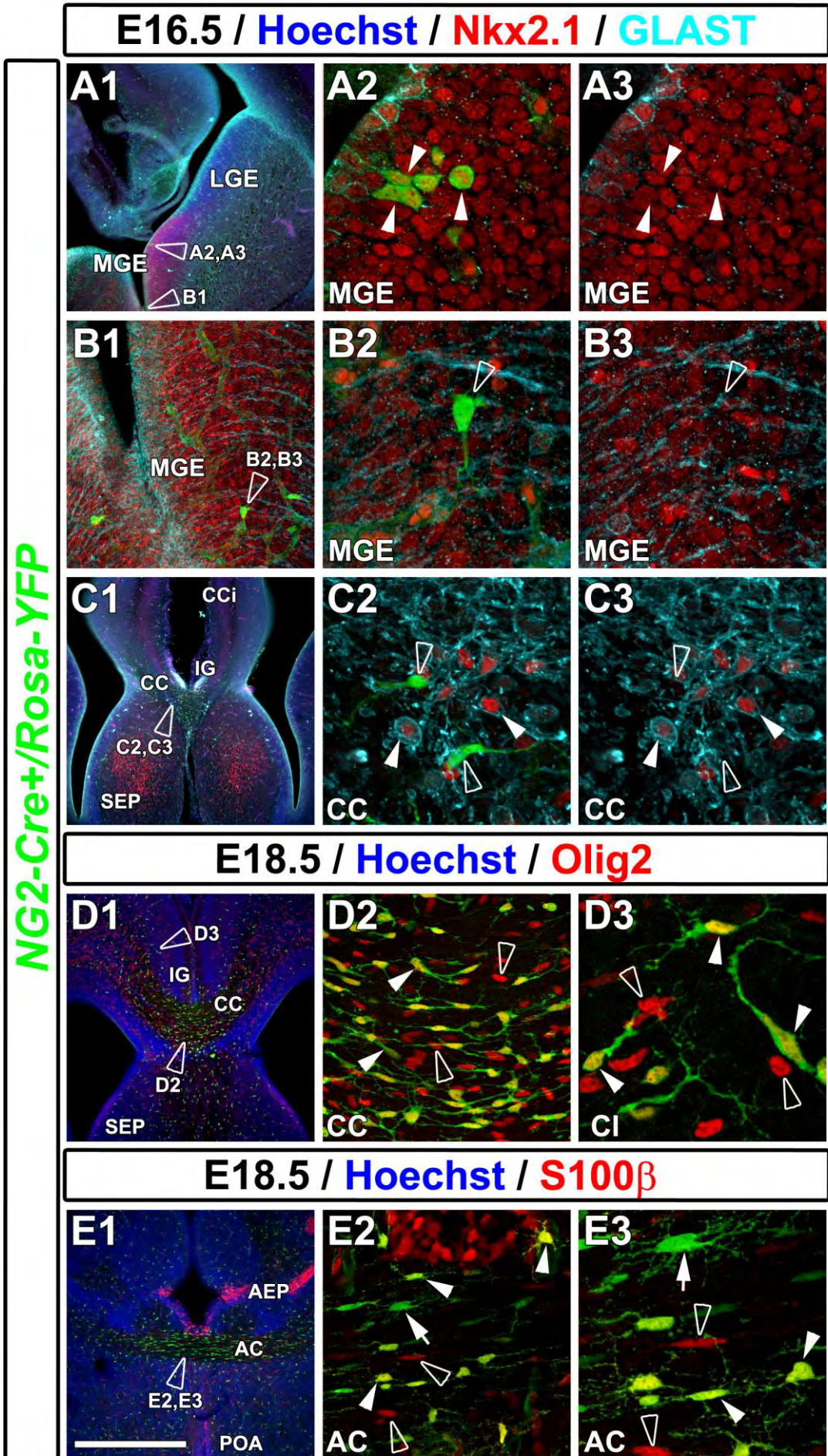


Figure 2. Fate-mapping study of *Nkx2.1*-regulated NG2⁺ polydendrocytes using the *NG2-Cre⁺/Rosa-YFP* reporter mice.

(A-C) Triple immunohistochemistry for the YFP, *Nkx2.1* and GLAST on coronal sections from *NG2-Cre⁺/Rosa-YFP* mice at E16.5. (D-E) Double immunohistochemistry for the YFP and Olig2 (D1-D3) and for the YFP and S100 β (E1-E3) on CC and AC coronal sections from *NG2-Cre⁺/Rosa-YFP* mice at E18.5. Cell nuclei were counterstained in blue with Hoechst (A1, C1, D1 and E1). A2, A3, B2, B3, C2, C3, D2, D3, E2 and E3 are higher power views of the regions shown in A1, B1, C1, D1 and E1, respectively. (A-C) At E16.5, NG2⁺ polydendrocytes visualized by the YFP signal are originating from *Nkx2.1*⁺ subpallial sites such as the MGE (A1-A3 and B1-B3). The colocalization between *Nkx2.1* (in red) and the YFP signal (in green) is observed in few cells in the SVZ of the MGE (white arrowheads in A2 and A3) but as soon as the NG2⁺ cells start to differentiate and migrate, *Nkx2.1* is down-regulated and is no more visible (open arrowheads in B2-B3 and C2-C3). By contrast, *Nkx2.1* is still expressed in GLAST⁺ glial cells within the CC midline (white arrowheads in C2 and C3).

(D1-D3) At E18.5, all the NG2-derived polydendrocytes also co-expressed Olig2 (white arrowheads in D2 and D3), while not all Olig2⁺ cells expressed NG2 (open arrowheads in D2 and D3). (E1-E3) Many, though not all (white arrows in E2 and E3), post-mitotic NG2⁺ cells are co-labelled by S100 β (white arrowheads in E2 and E3). Moreover, some S100 β ⁺ progenitor cells of the AEP/POA VZ, as well as few post-mitotic S100 β ⁺ cells of the AC are not co-expressing NG2 (open arrowheads in E2 and E3).

(AC) anterior commissure; (AEP) anterior entopeduncular area; (CC) corpus callosum; (CCi) cingulate cortex; (CI) cingulate bundle; (IG) induseum griseum; (MGE) medial ganglionic eminence; (POA) preoptic area; (SEP) septum.

Bar = 675 μ m in A1, C1, D1 and E1; 160 μ m in B1, 100 μ m in D2 and E2, 40 μ m in A2, A3, B2, B3, C2, C3, D3 and E3.

Nkx2.1-Cre+/Rosa-YFP

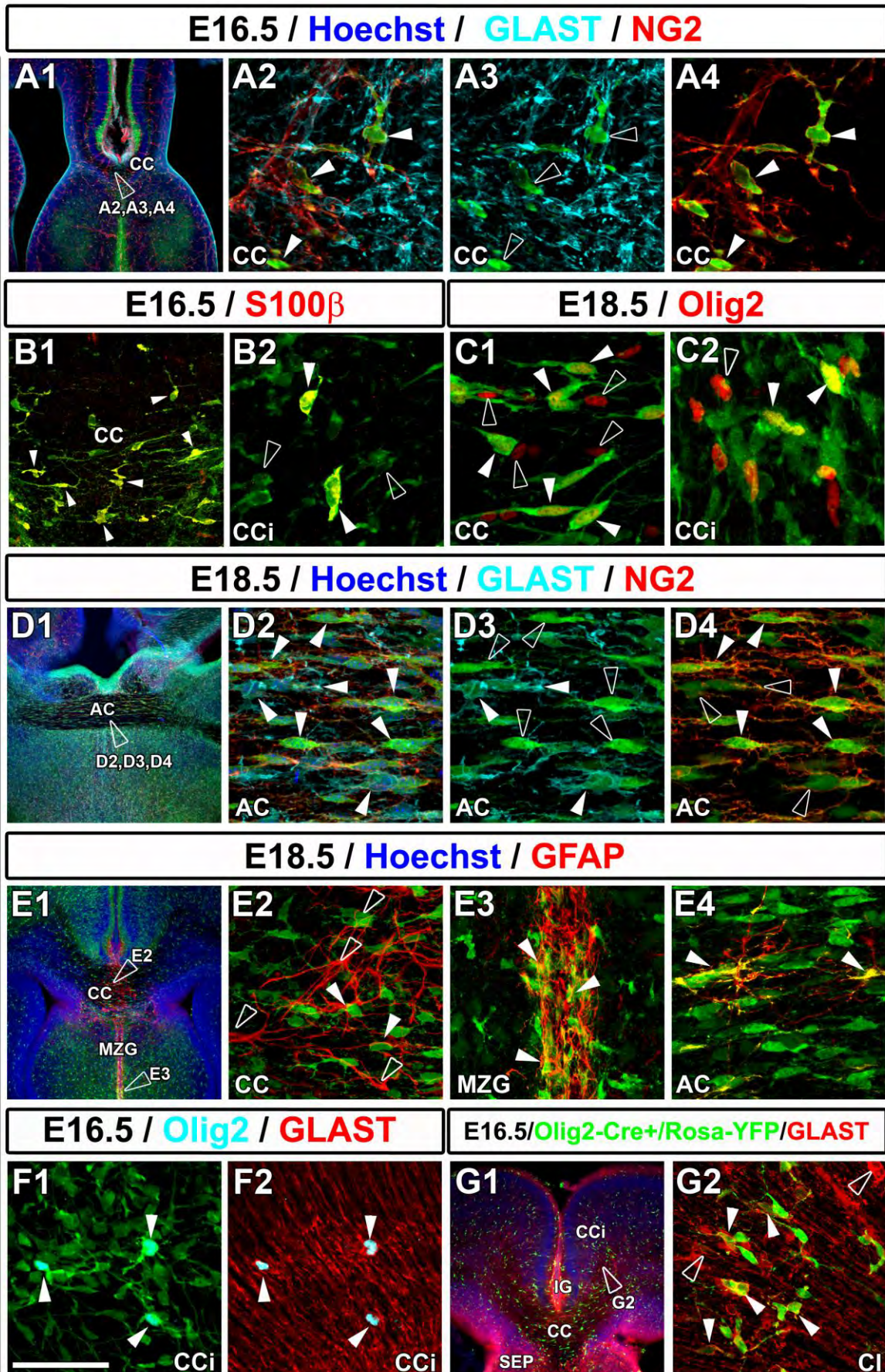


Figure 3. The transcription factor Nkx2.1 regulates different subpopulations of embryonic glial cells, elucidated by the use of *Nkx2.1-Cre⁺/Rosa-YFP* reporter mice.

(A, D and F) Triple immunohistochemistry for the YFP, GLAST and NG2 (A and D) on CC (A) and AC (D) coronal sections from *Nkx2.1-Cre⁺/Rosa-YFP* mice at E16.5 (A1-A4) and at E18.5 (D1-D4) and for the YFP, Olig2 and GLAST on CCi coronal sections of *Nkx2.1-Cre⁺/Rosa-YFP* mice at E16.5 (F1-F2). (B1-B2) Double immunohistochemistry for the YFP and S100 β in CC (B1) and CCi (B2) coronal sections from *Nkx2.1-Cre⁺/Rosa-YFP* mice at E16.5; (C1-C2) for the YFP and Olig2 in CC (C1) and CCi (C2) coronal sections from *Nkx2.1-Cre⁺/Rosa-YFP* mice at E18.5; and (E1-E4) for the YFP and GFAP in CC (E1 and E2), MZG (E3) and AC (E4) coronal sections from *Nkx2.1-Cre⁺/Rosa-YFP* mice at E18.5. (G1-G2) Double immunohistochemistry for the YFP and GLAST in CCi coronal sections from *Olig2-Cre⁺/Rosa-YFP* mice at E16.5. Cell nuclei were counterstained in blue with Hoechst (A1, D1, E1 and G1). Colocalization between the green and the red channel is highlighted in yellow (B1, B2, E3, E4 and G2). A2, A3, A4, D2, D3, D4, E2, E3 and G2 are high magnified views of the regions indicated by an open arrowhead in A1, D1, E1 and G1, respectively. (A, B and F) At E16.5, the Cre-mediated recombination induced under the control of the Nkx2.1 promoter (visualized in green by the YFP) is visible in NG2⁺ polydendrocytes of the CC (white arrowheads in A2 and A4), in a majority of S100 β ⁺ glial cells of the CC and the CCi (white arrowheads in B1 and B2; open arrowheads are indicating cells that do not colocalize in B2), as well as in Olig2⁺/GLAST⁺ glial cells of the CCi (white arrowheads in F1-F2). However, the Cre-mediated recombination did not occur in the GLAST⁺ glial cells of the CC (open arrowheads in A3). (C, D and E) At E18.5, Nkx2.1 promoter-mediated Cre recombinase expression visualized by the YFP signal was found in some of the Olig2⁺ glia of the CC and the CCi (white arrowheads in C1 and C2) while some other Olig2⁺ cells were not co-expressing YFP and thus, did not constitute a part of the *Nkx2.1*-derived cell population (open arrowheads in C1 and C2). (D1-D4) In the AC, Cre-mediated recombination regulated by the Nkx2.1 promoter occurred in both GLAST⁺ (in light blue) and NG2⁺ (in red) glial cells (white arrowheads in D2-D4) which constitute two mutually exclusive populations of glia (open arrowheads in D3 indicate *Nkx2.1*-derived cells that did not express GLAST in D3 but expressed NG2 in D4, and open arrowheads in D4 indicate cells that did not express NG2 in D4 but expressed GLAST in D3). (E1-E4) Some *Nkx2.1*-derived glial cells co-expressed GFAP⁺ in the CC (white arrowheads in E2), and in the MZG and the AC (white arrowheads in E3 and E4). (G1-G2) At E16.5, the Cre-mediated recombination under the direct control of the Olig2 promoter, was visualized by the YFP signal in numerous GLAST⁺ glial cells of the CI (white arrowheads in G2; open arrowheads indicate GLAST⁺/Olig2⁻ cells). (AC) anterior commissure; (CC) corpus callosum; (CCi) cingulate cortex; (CI) cingulate bundle; (IG) indusium griseum; (MZG) midline zipper glia; (SEP) septum. Bar = 675 μ m in A1, D1, E1 and G1; 100 μ m in B1; 60 μ m in E2, E3, F1, F2 and G2; 50 μ m in A2, A3, A4, B2, C1, C2, D2, D3, D4 and E4.

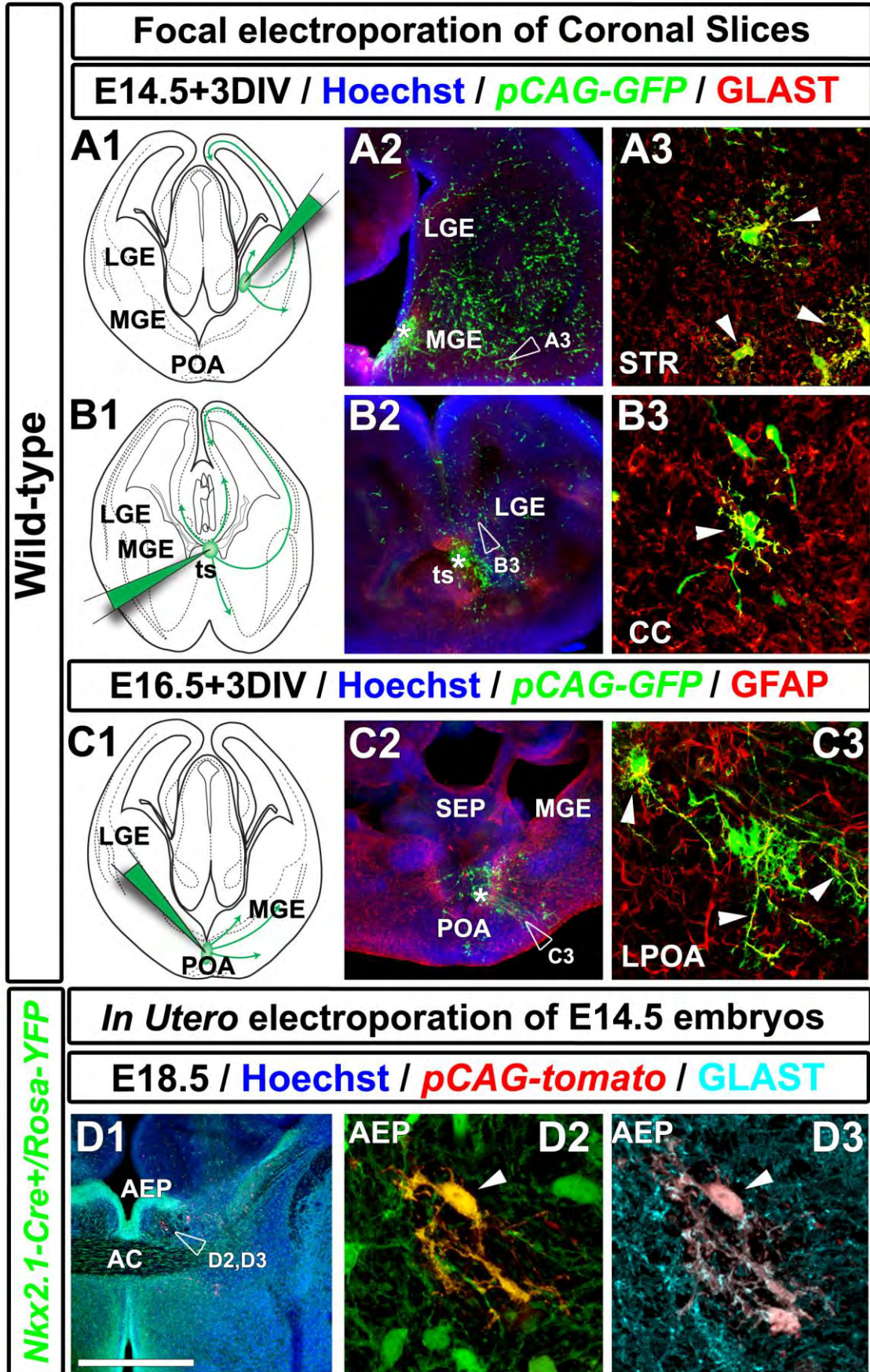


Figure 4. Subpallial origin of *Nkx2.1*-derived GLAST⁺/GFAP⁺ embryonic astroglial cells.

(A-C) *In vitro* focal electroporation of coronal slices from wild-type embryonic brains at E14.5 (**A1-A3** and **B1-B3**) and at E16.5 (**C1-C3**). **(D)** *In utero* electroporation of *Nkx2.1-Cre⁺/RosaYFP* embryonic brains at E14.5 (**D1-D3**). **A1**, **B1** and **C1** are schematic representations of the focal injections of a *pCAG-GFP* plasmid into the three *Nkx2.1*-regulated subpallial ventricular regions namely the MGE, the ts and the POA (indicated by white stars in **A2**, **B2** and **C2**). **A3**, **B3**, **C3**, **D2** and **D3** are high magnified views of the regions indicated by an open arrowhead in **A2**, **B2**, **C2** and **D1**, respectively. Cell nuclei were counterstained in blue with Hoechst (**A2**, **B2**, **C2** and **D1**). Colocalization between the green and the red channel is highlighted in yellow (**A3**, **B3**, **C3** and **D2**). **(A1-A3** and **B1-B3)** *In vitro* focal injection and electroporation of a *pCAG-GFP* plasmid into the MGE and the ts of wild-type E14.5 brains gave rise to GLAST⁺ glial cells (in red) that migrated to the STR and the CC (colocalization depicted in yellow and white arrowheads in **A3** and **B3**), and a similar injection into the POA (**C1-C3**) at E16.5 gave rise to GFAP⁺ glial cells (in red) that migrated to the LPOA (yellow colocalization and white arrowheads in **C3**). **(D1-D3)** *In utero* injection of a *pCAG-tomato* plasmid into the lateral ventricles and electroporation towards the subpallium of E14.5 *Nkx2.1-Cre⁺/RosaYFP* brains, gave rise to *Nkx2.1*⁺ (visualized in green with the YFP signal) and GLAST⁺ (in light blue) glial cells migrating from the AEP (white arrowhead in **D2** and **D3**). **(AC)** anterior commissure; **(AEP)** anterior entopeduncular area; **(CC)** corpus callosum; **(LGE)** lateral ganglionic eminence; **(LPOA)** lateral POA; **(MGE)** medial ganglionic eminence; **(POA)** preoptic area; **(SEP)** septum; **(STR)** striatum; **(ts)** triangular septal nucleus. Bar = 675 μ m in **A2**, **B2**, **C2** and **D1**; 60 μ m in **A3**, **B3** and **C3**; 40 μ m in **D2** and **D3**.

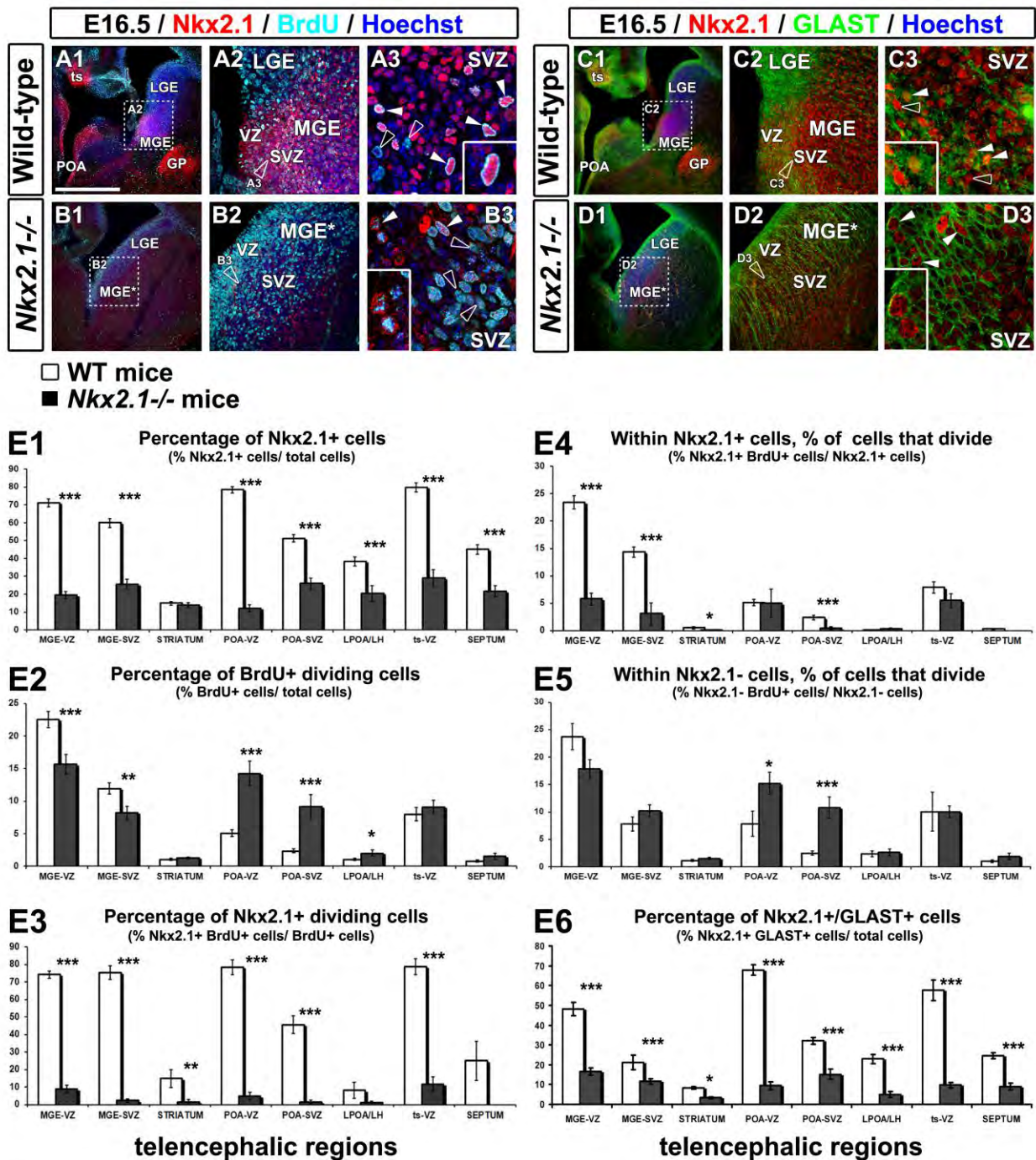


Figure 5. Regulation of the subpallial precursors division and differentiation by *Nkx2.1*. (A-D) Double immunohistochemical staining for Nkx2.1 and 5-bromo-2'-deoxy-uridine (BrdU) (A-B) and Nkx2.1 and GLAST (C-D) on telencephalic coronal sections from wild-type (A1-A3 and C1-C3) and *Nkx2.1*^{-/-} (B1-B3 and D1-D3) mice brains at E16.5. Cell nuclei were counterstained in blue with Hoechst (A1-A3, B1-B3, C1 and D1). A2, B2, C2 and D2 are higher power views of the squared regions seen in A1, B1, C1 and D1. A3, B3, C3 and D3 are higher magnifications of the MGE seen in A2, B2, C2 and D2, respectively.

(A1-A3) In the VZ and the SVZ of the wild-type MGE, AEP/POA and ts, numerous Nkx2.1⁺ precursors (in red) were dividing at E16.5 since they were co-labelled for BrdU (in light blue in **A1-A3**; white arrowheads and inset in **A3**), while other BrdU⁺ dividing cells were not labelled by Nkx2.1 (open arrowheads in **A3**). **(B1-B3)** In the VZ and the SVZ of the *Nkx2.1*^{-/-} MGE (MGE*) AEP/POA and ts, numerous precursors were also seen to divide since they were co-labelled by the BrdU (open arrowheads in **B3**), but only few dividing cells were expressing the mutated Nkx2.1 protein (white arrowheads and inset in **B3**). **(C1-C3)** In the germinal regions of the wild-type telencephalon, numerous Nkx2.1⁺ progenitors were also GLAST⁺ (white arrowheads and inset in **C3**), while some other were GLAST⁻ (open arrowheads in **C3**). **(D1-D3)** In *Nkx2.1*^{-/-} germinal regions, some GLAST⁺ progenitors expressed the mutated Nkx2.1 protein (white arrowheads and inset in **D3**). **(E1-E6)** Bars (mean ± SEM from a sample ranging between n=13-75 sections in WT and n=8-68 sections in *Nkx2.1*^{-/-} depending on the telencephalic region studied) represent the percentage of Nkx2.1⁺ cells (**E1**); the percentage of BrdU⁺ dividing cells (**E2**); the percentage of BrdU⁺ dividing cells which are also Nkx2.1⁺ (**E3**); the percentage of Nkx2.1⁺ cells that have undergone division (**E4**); the percentage of Nkx2.1⁻ cells that have divided (**E5**); and the percentage of Nkx2.1⁺/GLAST⁺ precursors and glial cells (**E6**) compared between *Nkx2.1*^{-/-} versus wild-type (WT) subpallial germinal (MGE, POA and ts: VZ and SVZ) and parenchymal (Striatum, LPOA/LH, septum) telencephalic regions at E16.5. The quantifications revealed significant variabilities in the *Nkx2.1*^{-/-} mice when compared to the WT mice, which are as follows: **(E1)** the number of Nkx2.1⁺ precursors and post-mitotic cells was drastically decreased in all the telencephalic regions, except in the striatum; **(E2)** a significant decrease of the BrdU⁺ dividing precursors in the VZ and SVZ of the MGE balanced by a significant increase of BrdU⁺ dividing precursors in the VZ, SVZ and parenchyma of the POA; **(E3)** there was a drastic and significant decrease in the dividing cells which expressed Nkx2.1 in all regions except those in the LPOA/LH and the septum; **(E4)** the cells that did express Nkx2.1, lost their capacity to divide in the VZ and SVZ of the MGE, the striatum and the SVZ of the POA; **(E5)** by contrast, the cells that did not express Nkx2.1, displayed significantly increased capacity to divide in the VZ and SVZ of the POA; **(E6)** the number of precursors and post-mitotic glial cells that co-expressed Nkx2.1 and GLAST were strongly and significantly decreased in all the regions of the subpallium. **(GP)** globus pallidus; **(LGE)** lateral ganglionic eminence; **(LPOA/LH)** lateral POA/lateral hypothalamus; **(MGE)** medial ganglionic eminence; **(MGE*)** mutant medial ganglionic eminence; **(POA)** preoptic area; **(SEP)** septum; **(STR)** striatum; **(SVZ)** subventricular zone; **(ts)** triangular septal nucleus, **(VZ)** ventricular zone. Bar = 675 µm in **A1, B1, C1** and **D1**; 160 µm in **B2** and **D2**; 100 µm in **A2** and **C2**; 45 µm in **A3, B3, C3** and **D3**.

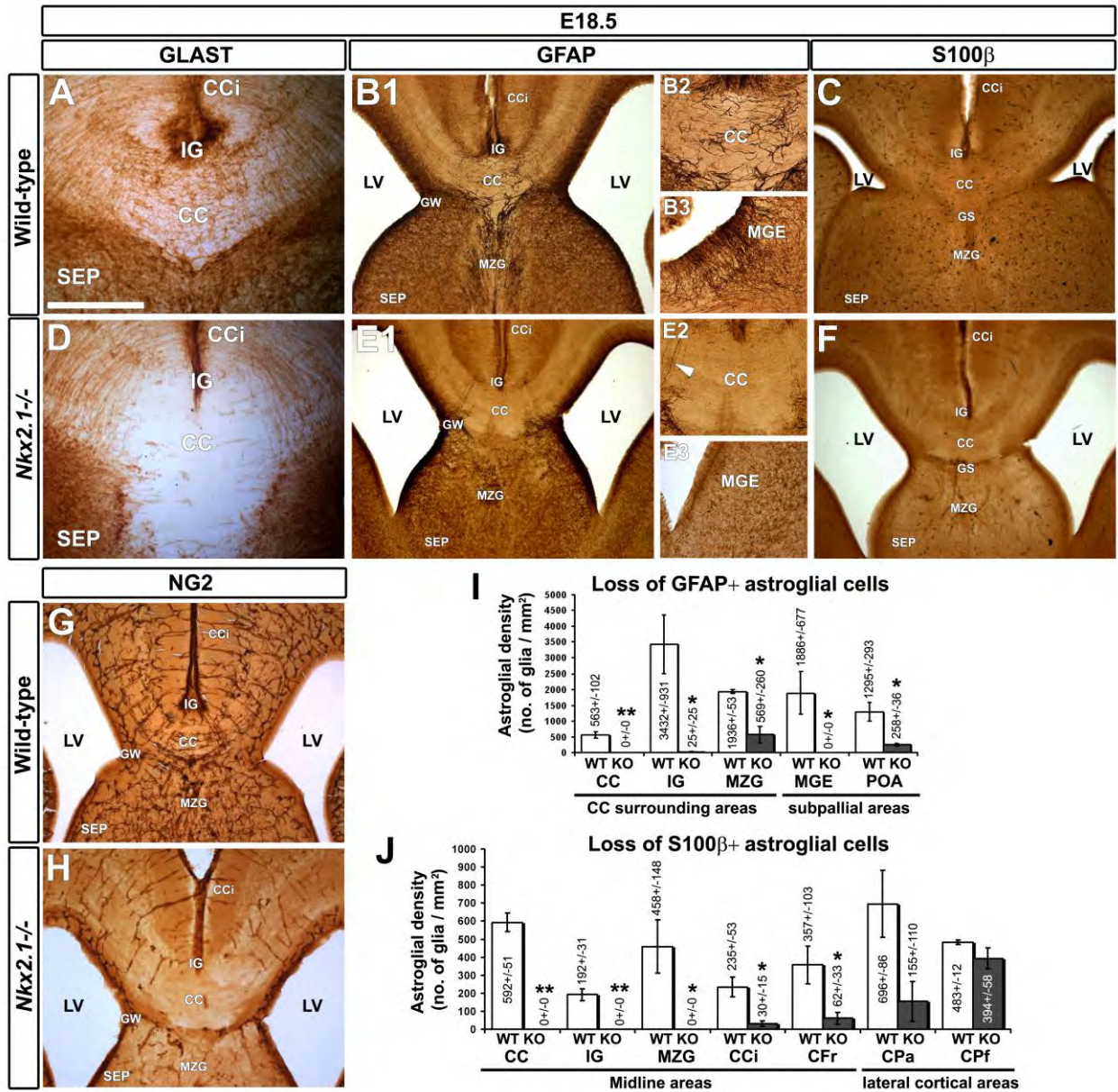


Figure 6. Loss of different glial cell types in the CC, medial cortical areas and subpallium of *Nkx2.1*^{-/-} mice brains.

DAB staining for GLAST (**A** and **D**), GFAP (**B1-B3** and **E1-E3**), S100 β (**C** and **F**), and NG2 (**G** and **H**) on CC and MGE coronal sections from wild-type (**A**, **B1-B3**, **C** and **G**) and *Nkx2.1*^{-/-} (**D**, **E1-E3**, **F** and **H**) mice at E18.5. **B2** and **E2** are higher power views of the CC region seen in **B1** and **E1**, respectively. **B3** and **E3** are higher power views of the MGE region. DAB staining for GLAST, GFAP, S100 β and NG2 revealed a complete loss of these glial cell types from the CC and surrounding areas and from the MGE of the *Nkx2.1*^{-/-} mice compared to wild-type mice (compare **D** with **A**, **E1** with **B1**, **E2** with **B2**, **E3** with **B3**, **F** with **C** and **H** with **G**). Only the GFAP⁺ radial glial cells originating from the Nkx2.1⁺ GW and bordering the CC remained (white arrowhead in **E2**). (**I** and **J**) Bars (mean \pm SEM from a sample of n=3 brains in WT and n=3 brains in *Nkx2.1*^{-/-}) represent the cell densities of GFAP⁺ or S100 β ⁺ glial cells/mm². The quantification of the GFAP⁺ or S100 β ⁺ glial cell density showed a drastic and significant loss of these cells in the CC and surrounding areas, medial cortical areas, as well as, in the germinal subpallial areas but not in the lateral cortical areas of the *Nkx2.1*^{-/-} brain compared to the wild-type brains. (**CC**) corpus callosum; (**CCi**) cingulate cortex; (**CFr**) frontal cortex; (**CPa**) parietal cortex; (**CPf**) piriform cortex; (**GW**) glial wedge; (**IG**) induseum griseum; (**LV**) lateral ventricle; (**MZG**) midline zipper glia; (**MGE**) medial ganglionic eminence; (**POA**) preoptic area; (**SEP**) septum. Bar = 500 μ m in **B1**, **E1**, **C**, **F**, **G** and **H**; 250 μ m in **A**, **D**, **B2**, **B3**, **E2** and **E3**.

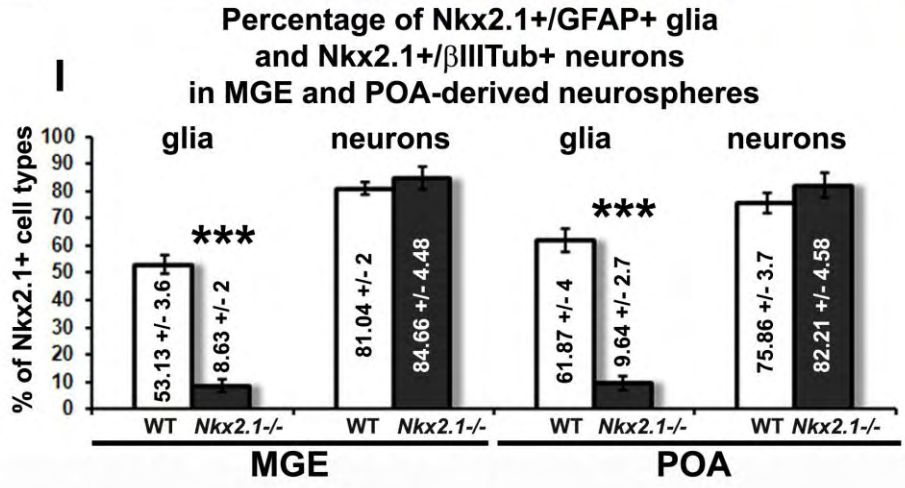
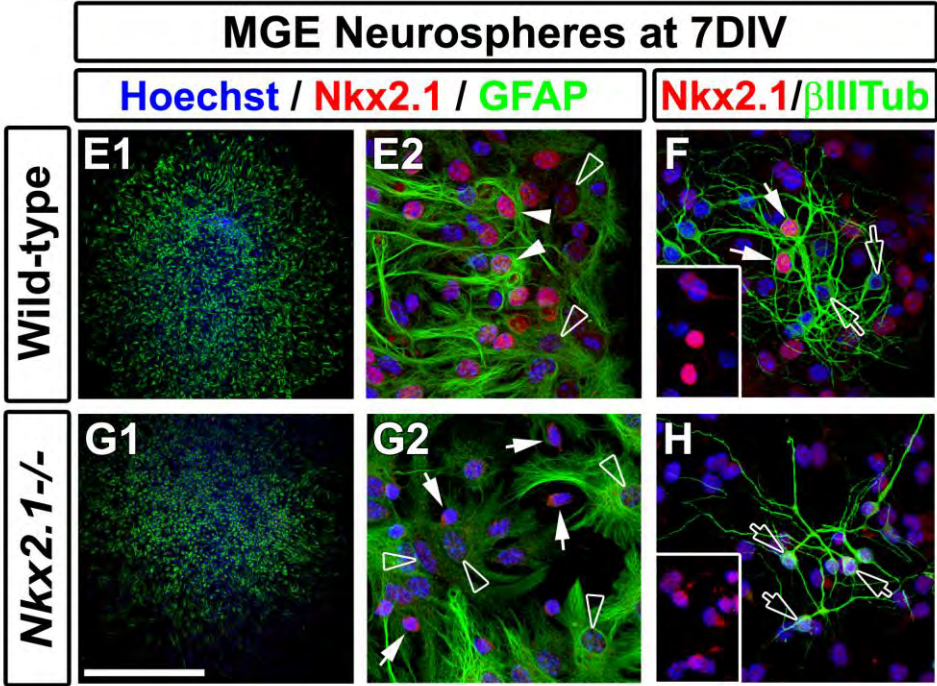
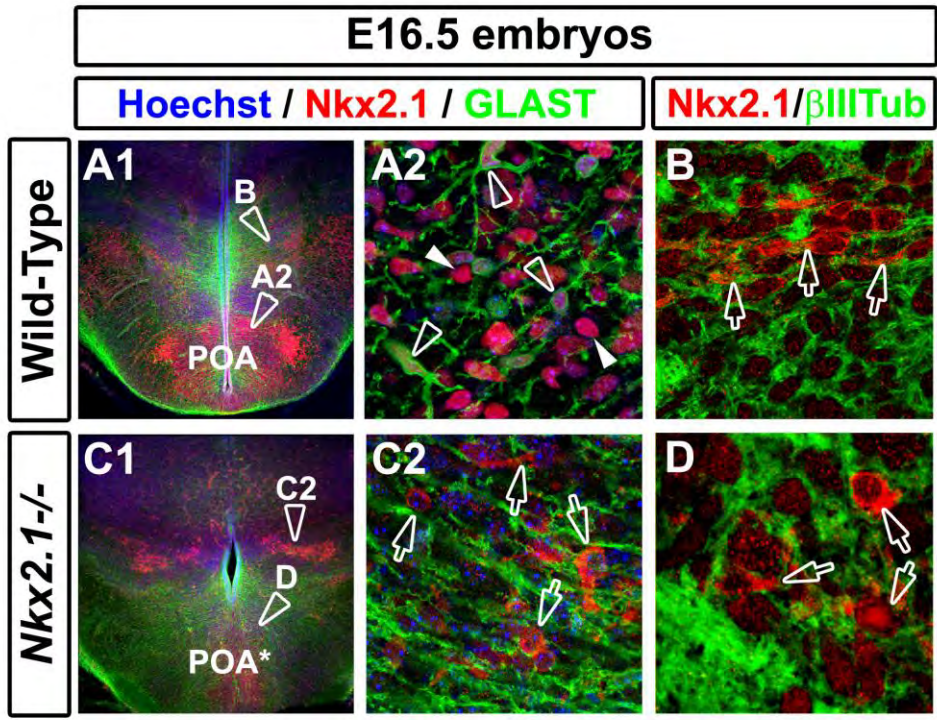


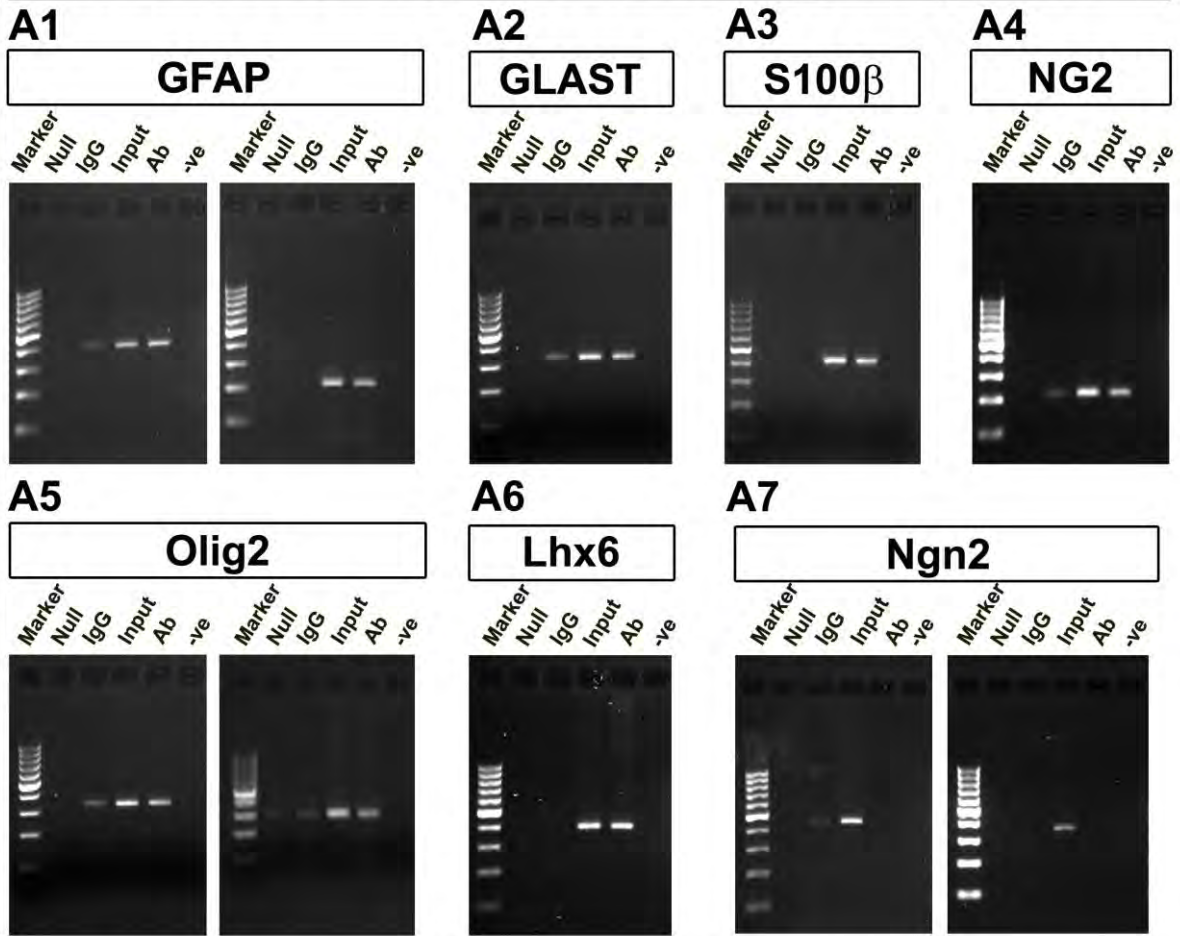
Figure 7. *In vivo* and *in vitro* analyses displayed the incapacity of Nkx2.1⁺ precursors to generate astrocytes in *Nkx2.1*^{-/-} mice brains.

(A1-A2 and C1-C2) Double immunohistochemical staining for Nkx2.1 and GLAST on POA coronal sections from wild-type (A1-A2) and *Nkx2.1*^{-/-} (C1-C2) mice at E16.5 and (B and D) for Nkx2.1 and β III tubulin on POA coronal sections from wild-type (B) and *Nkx2.1*^{-/-} (D) mice at E16.5. (E-H) Double immunocytochemistry for Nkx2.1 and GFAP (E1-E2 and G1-G2), and Nkx2.1 and β III tubulin (F and H) on MGE-derived neurospheres from wild-type (E1-E2 and F) and *Nkx2.1*^{-/-} (G1-G2 and H) mice brains at E14.5 incubated for 7 DIV. (I) Graph representing the quantification results for the percentage of Nkx2.1⁺/GFAP⁺ glia and Nkx2.1⁺/ β III tubulin⁺ neurons in the MGE- and POA- derived neurospheres between wild-type and *Nkx2.1*^{-/-} mice brains at E16.5. Cell nuclei were counterstained in blue with Hoechst (A, C, E-H). A2, B, C2, D, E2, F, G2 and H are higher power views of the regions seen in A1, C1, E1 and G1 respectively. (A1-A2 and B) In the parenchyma of the wild-type POA, many GLAST⁺ glial cells (open arrowheads in A2) and neurons co-expressed Nkx2.1 in their nuclei (white arrowheads in A2) while neurons, in addition, displayed cytoplasmic expression of Nkx2.1, too (open arrows in B). (C1-C2 and D) In the parenchyma of *Nkx2.1*^{-/-} POA (POA*), only few neurons expressed the mutated Nkx2.1 protein in the cytosol (open arrows in C2 and D).

In neurospheres derived from wild-type MGE, several GFAP⁺ astrocytes were labelled for Nkx2.1 (white arrowheads in E2), while some others were not (open arrowheads in E2). In addition, β III tubulin⁺ neurons were also either Nkx2.1⁺ (white arrows and inset in F) or Nkx2.1⁻ (open arrows in F). By contrast, in neurospheres derived from *Nkx2.1*^{-/-} MGE, the GFAP⁺ astrocytes were never observed to be co-labelled for Nkx2.1 (open arrowheads in G2), but the β III tubulin⁺ neurons did express low levels of the mutated Nkx2.1 protein in their nuclei and cytosol (white arrows in G2, and open arrows and inset in H). (I) Bars (mean \pm SEM from a sample of n=21-34 WT neurospheres and n=22-28 *Nkx2.1*^{-/-} neurospheres) represent the percentage of Nkx2.1⁺ GFAP⁺ astrocytes and β III tubulin⁺ neurons in MGE or POA-derived neurospheres from wild-type and *Nkx2.1*^{-/-} mice brains. The quantification revealed that the neurospheres coming from *Nkx2.1*^{-/-} brains were not able to produce Nkx2.1⁺ astrocytes whereas they were able to generate neurons. (MGE) medial ganglionic eminence; (POA) preoptic area; (POA*) mutant preoptic area. Bar = 675 μ m in A1, C1, E1 and G1; 50 μ m in A2, B, C2, E2, F, G2 and H; 40 μ m in D.

Nkx2.1 binding to conserved consensus sequences in the promoter region of various regulatory genes

Chromatin Immunoprecipitation on E16.5 brains



Nkx2.1 activates the expression of GFAP promoter reporter

Transfection of HEK293 cells

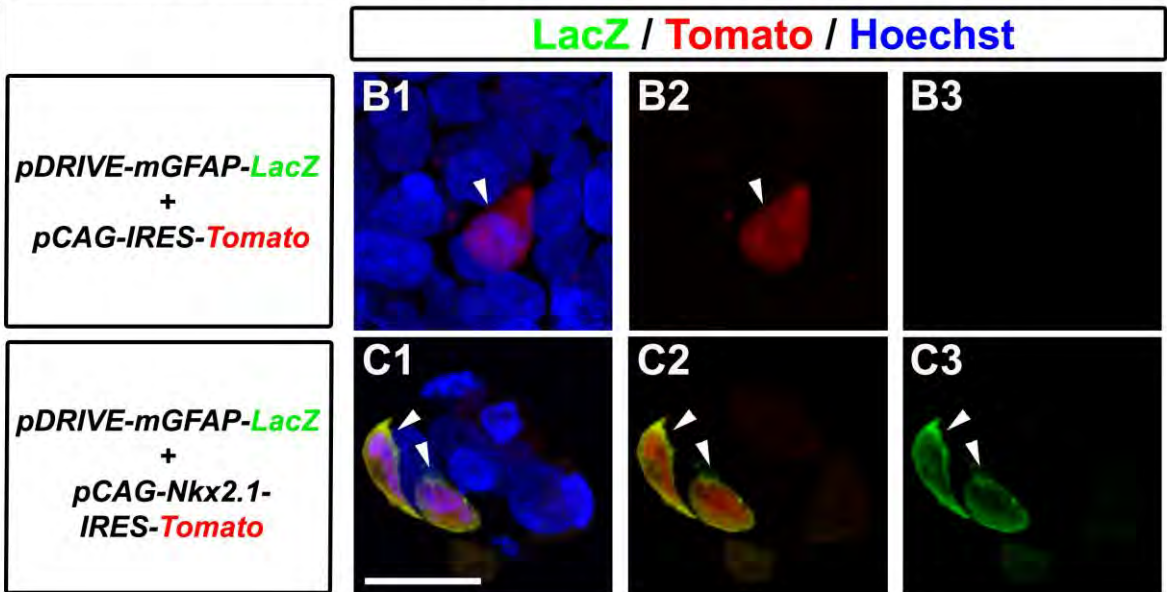
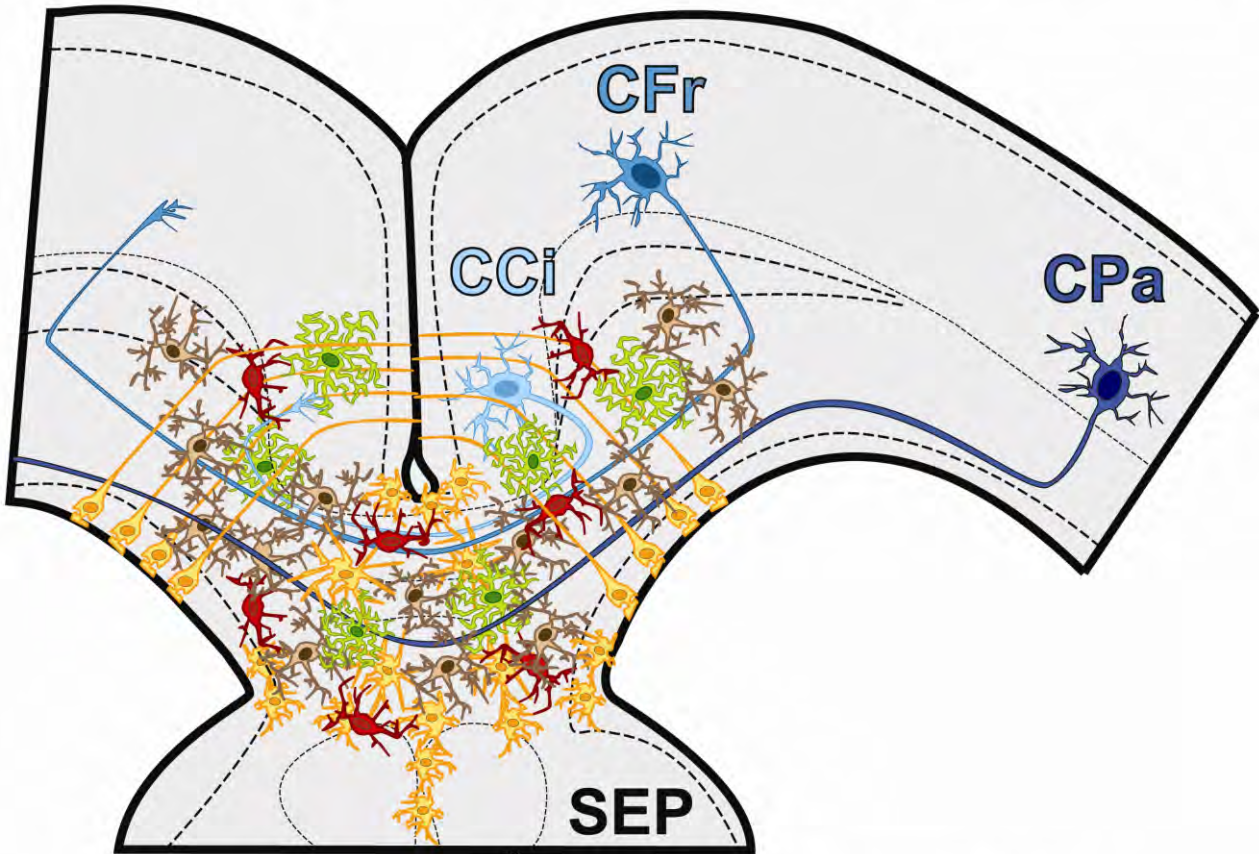


Figure 8. Binding of Nkx2.1 to conserved consensus binding sequences in the promoters of various glial regulatory genes.

Amplification of the Nkx2.1 consensus binding sequences located in two, 412 bp and 216 bp, PCR products within the GFAP promoter (**A1**), in a 363 bp PCR fragment within the GLAST promoter (**A2**), in a 417 bp PCR fragment within the S100 β promoter (**A3**), in a 205 bp PCR fragment within the NG2 promoter (**A4**), in two, 340 bp and 334 bp, PCR products within the Olig2 promoter (**A5**), in a 391 bp PCR fragment within the Lhx6 promoter (**A6**) was positive for the brain samples chromatin immunoprecipitated with the Nkx2.1 antibody. Input DNA was added as the positive loading control as it contains the crosslinked sonicated genomic DNA taken before chromatin immunoprecipitation with the Nkx2.1 antibody, and a strong signal was observed for all the promoter regions. No amplification of the Nkx2.1 core consensus sequence (tcaag) located in two, 410 bp and 352 bp, PCR products within the Ngn2 promoter was detected (**A7**). No signal was detected in the null control, wherein no antibody was added for chromatin immunoprecipitation and in the negative control, wherein no DNA was added while performing the PCR (**A1-7**). A very faint signal was detected in some of the samples immunoprecipitated with non-specific control IgG (**A1, A2, A4, A5** and **A7**) but there intensity was much lower than the intensity of the Input DNA and the test DNA (containing promoter region). These results suggest that Nkx2.1 binds the promoter regions of various glial regulatory genes at a highly conserved Nkx2.1 consensus binding sequence *in vivo*. The figure represents one of the three independently performed assays. Identical results were also obtained for the same glial regulatory genes in the E14.5 brain samples.

As a control, the human embryonic kidney 293 (HEK293) cells were co-transfected with 2.0 μ g of two reporter constructs, namely, the *pDRIVE-mGFAP-LacZ* expression plasmid containing the LacZ reporter under the control of the mouse 1679 bp upstream GFAP promoter sequence, and the *pCAG-IRES-Tomato* plasmid constitutively expressing the Tomato reporter under the control of the pCAG promoter (**B1-B3**). To test the binding of the Nkx2.1 to the GFAP promoter sequence, the HEK293 cells were co-transfected with 2.0 μ g of two reporter constructs, namely, the *pDRIVE-mGFAP* expression plasmid, and the *pCAG-Nkx2.1-IRES-Tomato* plasmid expressing Nkx2.1 protein tagged with Tomato under the control of the constitutive promoter pCAG (**C1-C3**). Cell nuclei were counterstained in blue with Hoechst. Overexpression of the LacZ reporter was seen upon addition of expression vector of Nkx2.1 protein, thus, depicting direct binding of Nkx2.1 to the consensus binding sequence in the promoter region of GFAP. Bar = 50 μ m.

Nkx2.1-derived embryonic glial cell types



Astrocyte-like

Polydendrocyte-like



GLAST+
GFAP+
S100β-
NG2-
Olig2-
Nkx2.1+

GLAST+
GFAP-
S100β-
NG2-
Olig2+
Nkx2.1+

GLAST-
GFAP-
S100β+
NG2+
Olig2+
Nkx2.1-

GLAST-
GFAP-
S100β-
NG2+
Olig2+
Nkx2.1-

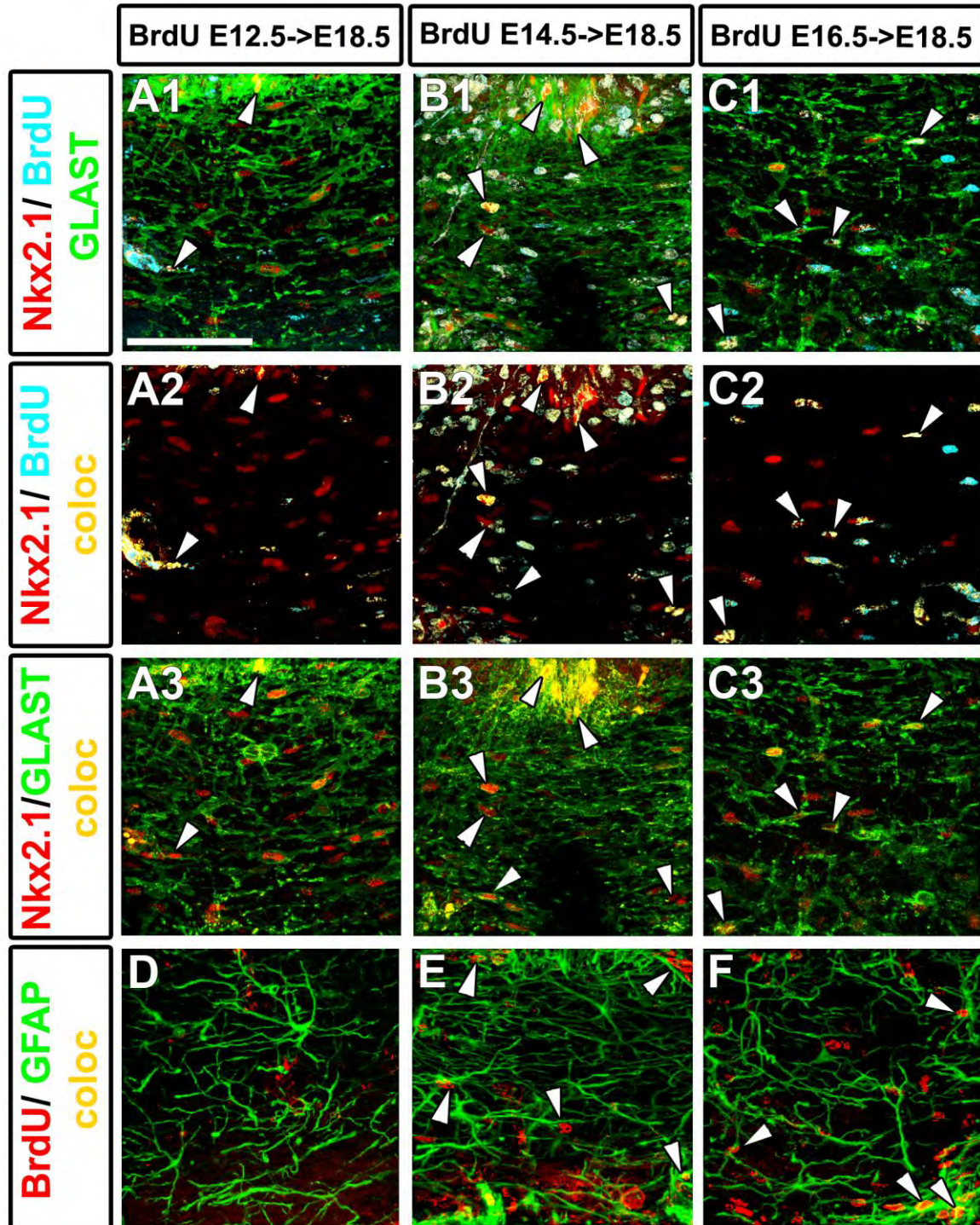
Nkx2.1-derived cells + Nkx2.1-derived cells +

Nkx2.1-derived cells +

Nkx2.1-derived cells +

Supplementary figure S1. Four subtypes of *Nkx2.1*-derived glial cells.

The schema represents a coronal view of the CC at E18.5, and summarizes the different types of *Nkx2.1*-derived glial populations visualized in our experiments. The callosal projection neurons from the CCI (light blue), the CFr (blue) and the CPa (dark blue) were seen to project their axons through a complex environment composed of four different subtypes of *Nkx2.1*-derived glial cells. Two types of astrocyte-like cell populations are shown: in yellow, the GLAST⁺/GFAP⁺ cells and in green, the GLAST⁺/Olig2⁺ cells. Two types of polydendrocyte-like cells are shown; in red, the S100β⁺/NG2⁺/Olig2⁺ cells, and in brown, the NG2⁺/Olig2⁺ cells. Under each glial cell-type category, the expression profile of the different glial markers, employed to identify and characterize the glial cells, used in combination with the Nkx2.1 antibody, is presented. The (+) sign indicates that the glial cell type was positively labelled by the listed marker, whereas the (–) sign indicates that the glial cell type was not labelled by the listed marker. **(CCi)** cingulate cortex, **(CFr)** frontal cortex, **(CPa)** parietal cortex.

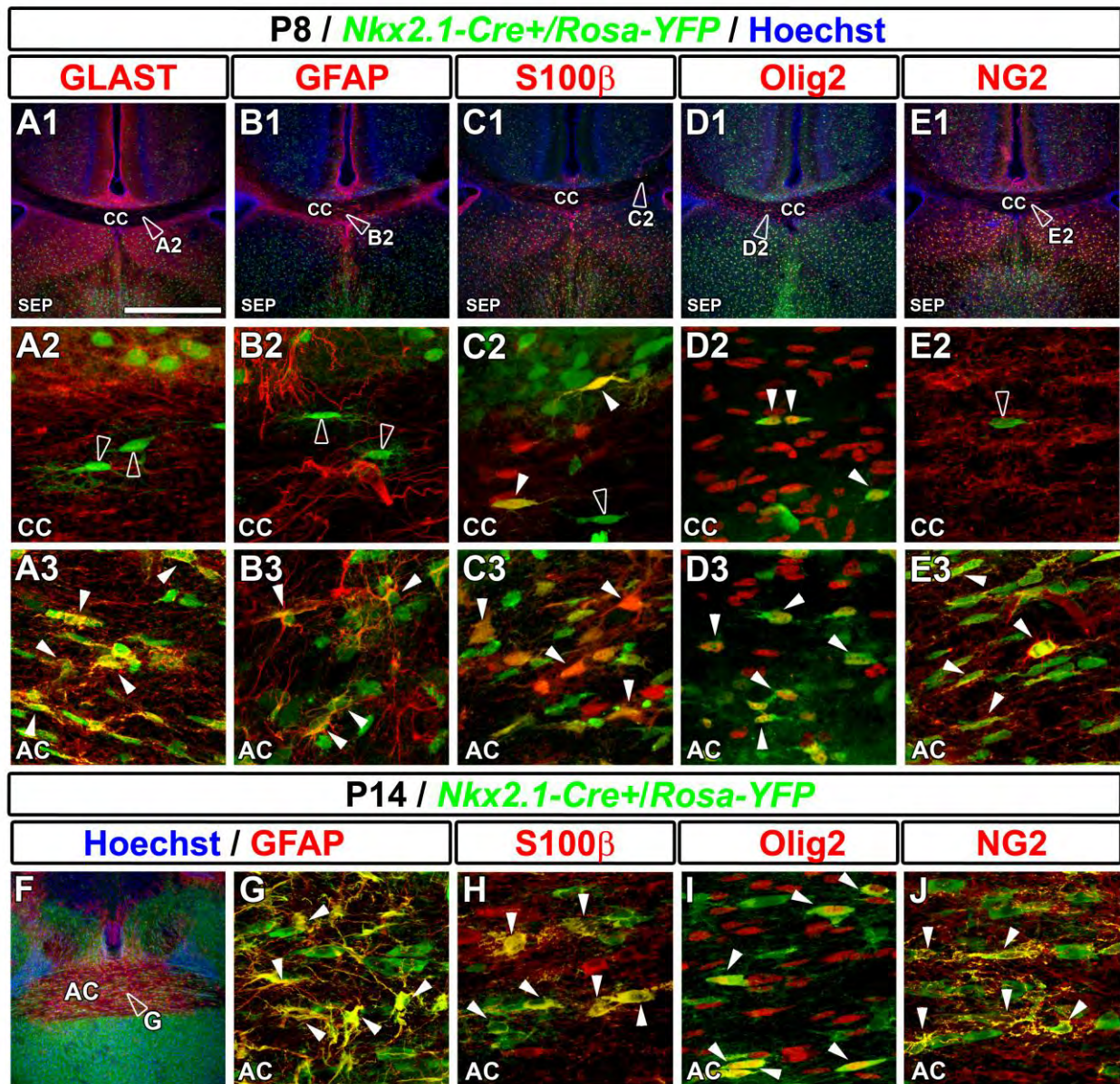


Supplementary figure S2. Nkx2.1-positive glial cells of the CC are generated between E14.5 and E16.5.

(A-C) Triple immunohistochemistry for Nkx2.1, 5-bromo2'-deoxy-uridine (BrdU), and GLAST, and **(D-F)** double immunohistochemistry for BrdU and GFAP on CC coronal sections from wild-type mice brains at E18.5 injected at E12.5 (**A1-A3** and **D**), E14.5 (**B1- B3** and **E**) and E16.5 (**C1- C3** and **F**).

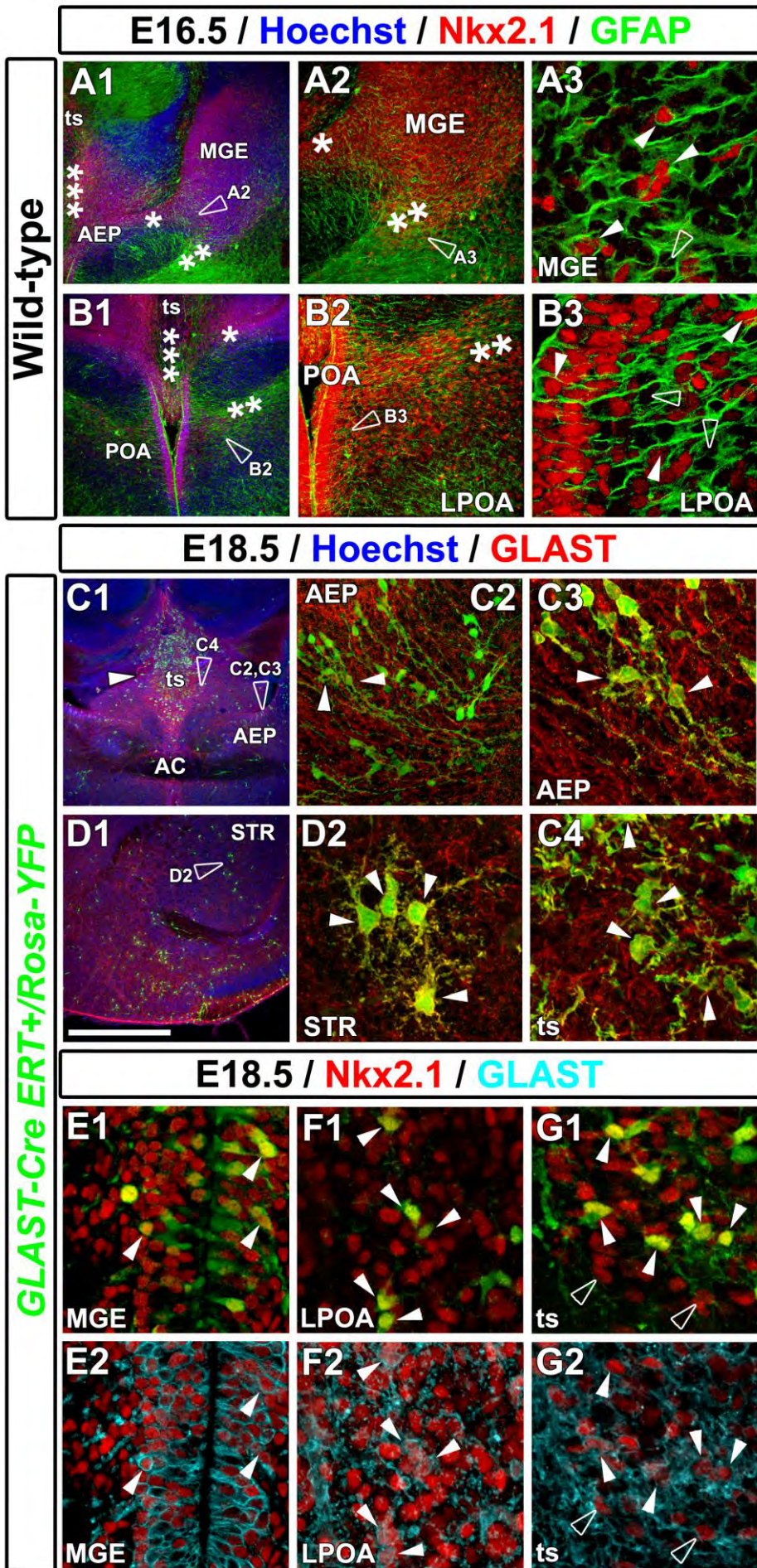
(A-C) At E18.5, several GLAST⁺ glial cells (green) expressing Nkx2.1 (red) are present in the CC midline. **(A2, B2** and **C2)** Colocalization between the blue (BrdU) and the red (Nkx2.1) channel is highlighted in yellow. **(A3, B3,** and **C3)** Colocalization between the green (GLAST) and the red (Nkx2.1) channel is highlighted in yellow. The white arrowheads point towards the Nkx2.1⁺/GLAST⁺/BrdU⁺ cells revealing that the bulk of division for the Nkx2.1⁺ glial cells of the CC occurs at E14.5 (**B2**) and declines at E16.5 (**C2**).

(D-F) Numerous GFAP⁺ astroglial cells (in green) are also present in the CC midline. Colocalization between the green (GFAP) and the red (BrdU) channel is highlighted in yellow. The white arrowheads are pointing on the GFAP⁺/BrdU⁺ cells depicting that the bulk of division for the GFAP⁺ glial cells of the CC occurs also at E14.5 (**E**). Bar = 60 μm in **A1-A3, B1-B3, C1-C3, D, E** and **F**.



Supplementary figure S3. The *Nkx2.1*-regulated glial cells are transient and progressively disappear from the dorsal pallium and then from the subpallium, postnatally.

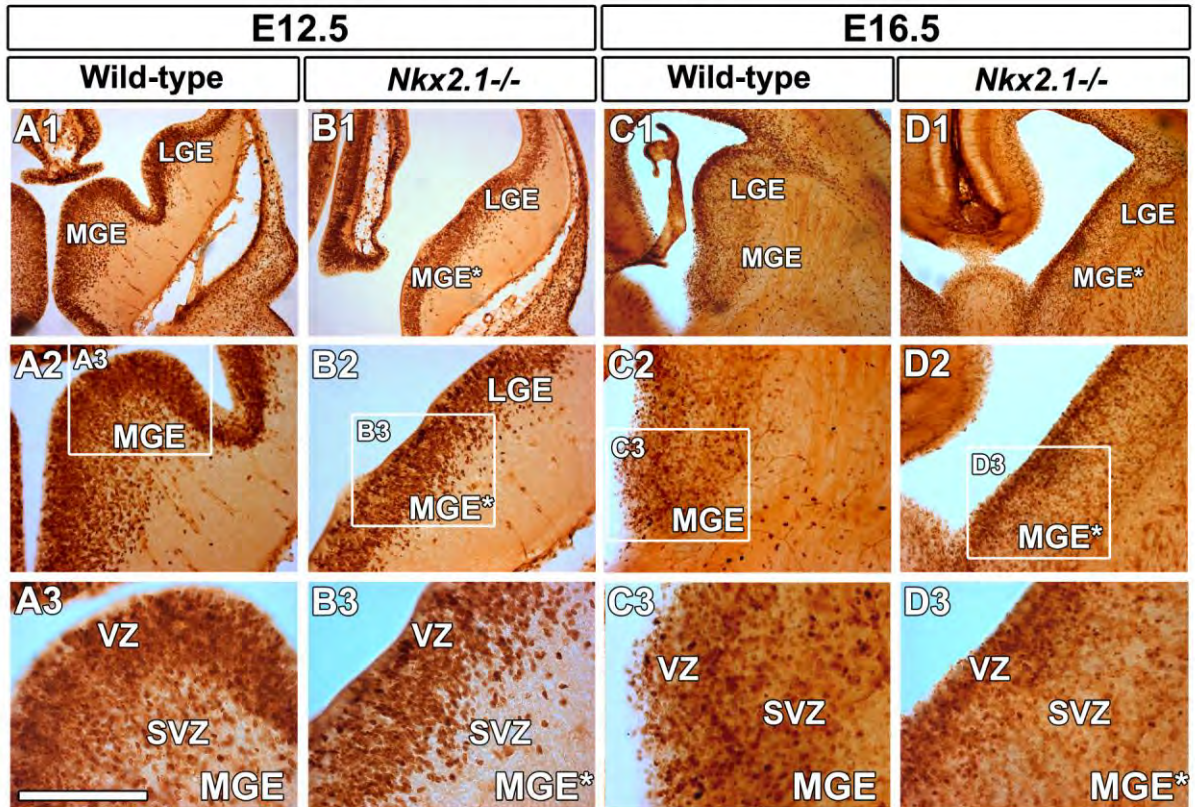
Double immunohistochemical staining for YFP together with GLAST (**A1-A3**), GFAP (**B1-B3**, **F** and **G**), S100 β (**C1-C3** and **H**), Olig2 (**D1-D3** and **I**) and NG2 (**E1-E3** and **J**) on CC (**A1-A2**, **B1-B2**, **C1-C2**, **D1-D2** and **E1-E2**) and AC (**A3**, **B3**, **C3**, **D3**, **E3**, **F**, **G**, **H**, **I** and **J**) coronal sections from *Nkx2.1-Cre⁺/Rosa-YFP* mice at P8 (**A-E**) and P14 (**F-J**). Cell nuclei were counterstained in blue with Hoechst (**A1**, **B1**, **C1**, **D1**, **E1** and **F**). Colocalization between the green and the red channel is highlighted in yellow. **A2**, **B2**, **C2**, **D2** and **E2** are high power views of the CC region seen in **A1**, **B1**, **C1**, **D1** and **E1**, respectively, and **G** is a higher power view of the AC seen in **F**. In the CC of *Nkx2.1-Cre⁺/Rosa-YFP* mice brains at P8, only very few S100 β ⁺ or Olig2⁺ *Nkx2.1*-derived glial cells remained (white arrowheads in **C2** and **D2**). None of the *Nkx2.1*-derived cells found in this region were labelled by GLAST, GFAP or NG2 (open arrowheads in **A2**, **B2** and **E2**). By contrast, in the AC and the subpallium of *Nkx2.1-Cre⁺/Rosa-YFP* mice brains at P8 and P14, numerous *Nkx2.1*-derived glial cells, expressing all types of glial markers, were still present (yellow colocalization and white arrowheads in **A3**, **B3**, **C3**, **D3**, **E3**, **G**, **H**, **I** and **J**). (AC) anterior commissure; (CC) corpus callosum; (SEP) septum. Bar = 675 μ m in **A1**, **B1**, **C1**, **D1**, **E1** and **F**; 40 μ m in **A2-A3**, **B2-B3**, **C2-C3**, **D2-D3**, **E2-E3**, **F**, **G**, **H**, **I** and **J**.



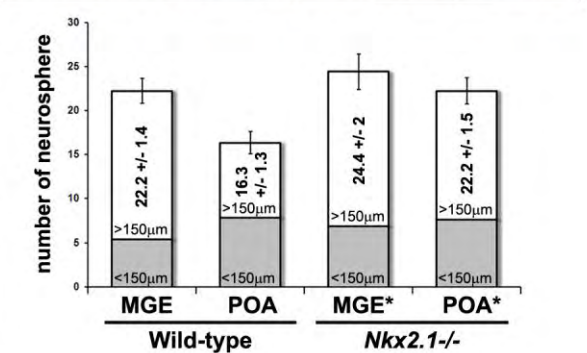
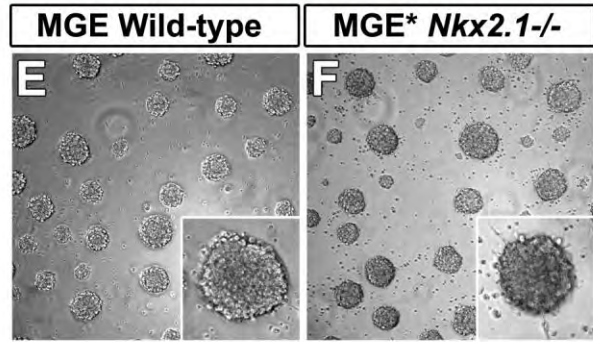
Supplementary figure S4. Three subpallial sites of origin for *Nkx2.1*-derived astroglial cells.

(A-B) Double immunohistochemical staining for *Nkx2.1* and GFAP, on ts (A1 and B1), MGE (A2-A3) and POA (B2-B3) coronal sections from wild-type mice at E16.5; (C-D) for the YFP and GLAST on ts (C1, C4), AEP (C2, C3) AC (C1) and striatum (D1-D2) coronal sections from *GLAST-Cre ERT⁺/Rosa-YFP* mice at E18.5. (E-G) Triple immunohistochemistry for the YFP, *Nkx2.1* and GLAST on MGE (E), LPOA (F) and ts (G) coronal sections from *GLAST-Cre ERT⁺/Rosa-YFP* mice at E18.5. Cell nuclei were counterstained in blue with Hoechst (A1, B1, C1 and D1). Colocalization between the green and the red channel is highlighted in yellow (C2-C4, D2, E1, F1 and G1). A2, A3, B2, B3, C2, C3, C4 and D2 are high power views of the regions seen in A1, A2, B1, B2, C1 and D1, respectively. In E16.5 wild-type mice brains, several *Nkx2.1*⁺ (in red) radial glial precursors expressing the GFAP (in green) were found in the VZ of three different subpallial germinal regions, namely the ts (A1 and B1), the MGE (A2-A3) and the AEP/POA (B2-B3), as well as in regions connecting the MGE to the AEP/POA (*), the POA to the MGE (**), and the ts to the AEP/POA (***). (A3 and B3) White arrowheads indicate *Nkx2.1*⁺ GFAP⁺ astroglial cells while open arrowheads indicate *Nkx2.1*⁻ cells. (C-D) In E18.5 *GLAST-Cre ERT⁺/Rosa-YFP* inducible mice in which the Cre-mediated recombination was induced at E16 by a tamoxifen injection, several GLAST⁺ glial cells were observed to originate from the ts (C1, and white arrowheads in C4) and the AEP (C1, and white arrowheads in C2 and C3). These cells were also observed to migrate to parenchymal regions such as the striatum (STR) (D1, and white arrowheads in D2) (E-G) The GLAST⁺ glial cells (in light blue) generated at E16 and visualized by the YFP (white arrowheads in E1-E2, F1-F2, and G1-G2) were also observed to express *Nkx2.1* (in red) at E18.5, in the SVZ of the MGE (E1-E2), the LPOA (F1-F2) and the ts (G1-G2). Some GLAST⁺ glial cells also regulated by *Nkx2.1* were not co-labelled for the YFP (open arrowheads in G1 and G2). (AC) anterior commissure; (AEP) anterior entopeduncular area; (LPOA) lateral preoptic area; (MGE) medial ganglionic eminence; (POA) preoptic area; (STR) striatum; (ts) triangular septal nucleus. Bar = 675 μ m in C1 and D1; 320 μ m in A1 and B1; 160 μ m in A2, B2 and C2; 45 μ m in A3, B3, C3, C4, D2, E1, E2, F1, F2, G1 and G2.

DAB immunostaining for BrdU



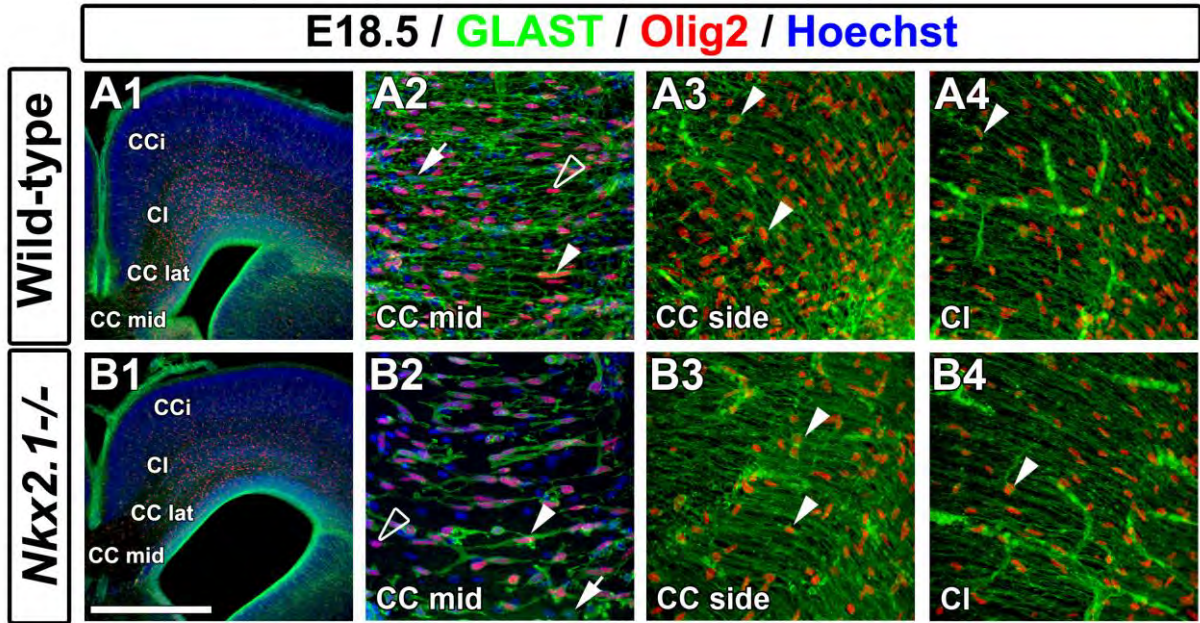
Secondary neurospheres at 10 DIV **G Self-renewal capacity of spheres**



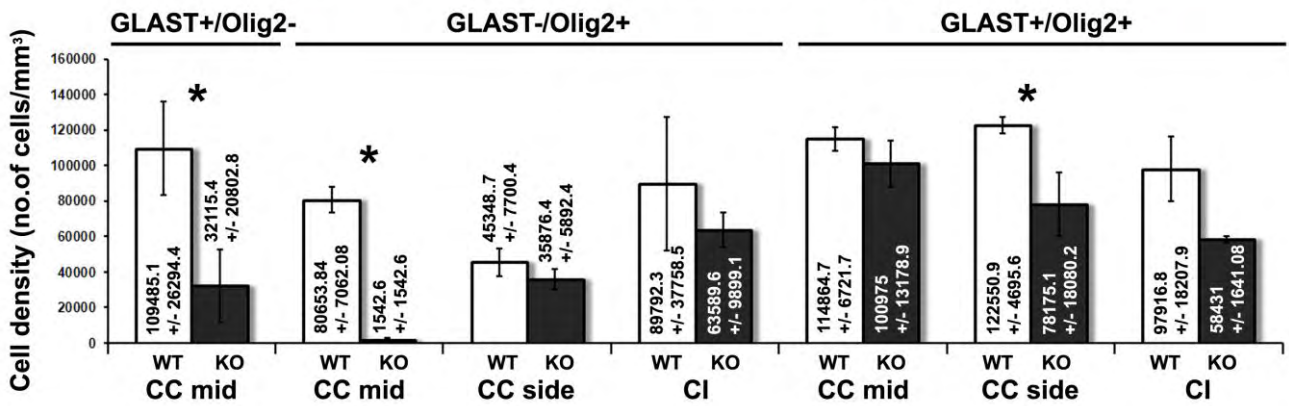
Supplementary figure S5. *In vivo* and *in vitro* study of the dividing capacity and self-renewal of $Nkx2.1^+$ MGE and POA progenitors.

(A-D) DAB staining for the BrdU on E12.5 **(A-B)** and E16.5 **(C-D)** wild-type **(A1-A3** and **C1-C3)** and $Nkx2.1^{-/-}$ **(B1-B3** and **D1-D3)** telencephalic coronal sections. **A2, B2, C2** and **D2** are higher power views of the MGE and MGE* seen in **A1, B1, C1** and **D1** and, **A3, B3, C3** and **D3** are higher magnified views of the squared regions seen in **A2, B2, C2** and **D2**, respectively. At E12.5 and at E16.5, in both the VZ and the SVZ of the wild-type versus the mutant MGE (MGE*), the total amount of BrdU-stained cells seemed to be unchanged but the allocation of the BrdU⁺ cells within the VZ and the SVZ was different. **(E-F)** Pictures and insets are showing *in vitro* secondary neurospheres grown after 10 DIV in a 96-well plate, which are derived from wild-type **(E)** and $Nkx2.1^{-/-}$ **(F)** MGE.

(G) Bars (mean \pm SEM from a sample of n=60-77 wells from the wild-type and n=36-44 wells from $Nkx2.1^{-/-}$) represent an absolute number of secondary neurospheres per well, derived from one dissociated primary neurosphere obtained from, wild-type and $Nkx2.1^{-/-}$, MGE and POA. The grey area represents the portion of spheres which had a diameter smaller than 150 μm , whereas the white area represents the portion of spheres which had a diameter bigger than 150 μm . The quantification revealed no significant differences between the self-renewal capacity of neurospheres derived from $Nkx2.1^{-/-}$ MGE and POA compared to the wild-type MGE and POA respectively. **(LGE)** lateral ganglionic eminence; **(MGE)** medial ganglionic eminence; **(MGE*)** mutant medial ganglionic eminence; **(POA)** preoptic area; **(SVZ)** subventricular zone; **(VZ)** ventricular zone. Bar = 700 μm in **A1, B1, C1** and **D1**; 400 μm in **E** and **F**; 350 μm in **A2, B2, C2** and **D2**; 175 μm in **A3, B3, C3** and **D3**.



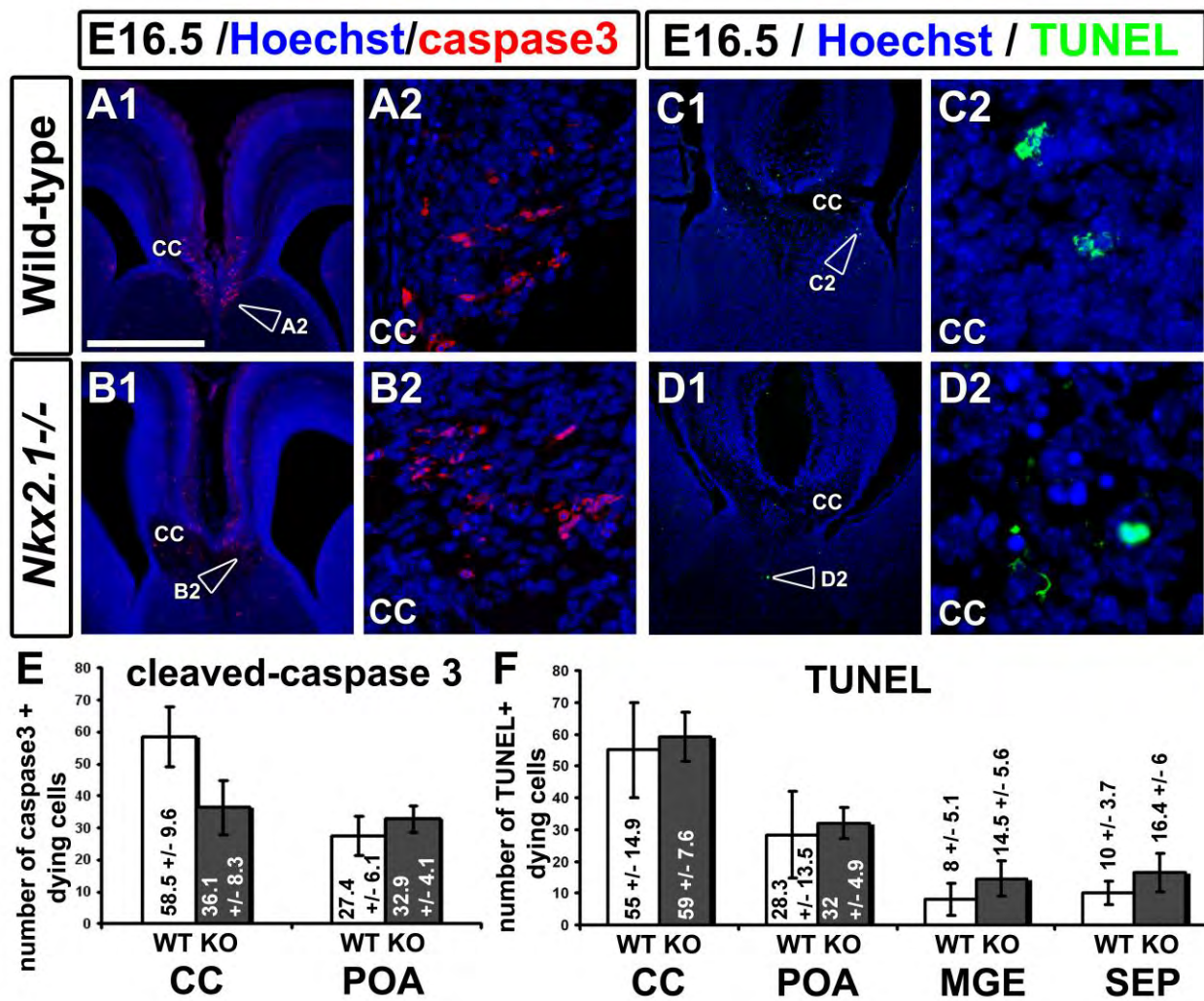
C Loss of astroglia in the CC and cingulate bundle



Supplementary figure S6. Loss of GLAST⁺/Olig2⁻, GLAST⁻/Olig2⁺ and GLAST⁺/Olig2⁺ glial cells in the CC and cingulate bundle of *Nkx2.I*^{-/-} mutant mice.

(A-B) Double immunohistochemical staining for Olig2 and GLAST on CC coronal sections from wild-type (**A1-A4**) and *Nkx2.I*^{-/-} (**B1-B4**) mice at E18.5. Cell nuclei were counterstained in blue with Hoechst (**A1-A2** and **B1-B2**). **A2, A3, A4, B2, B3** and **B4** are higher power views of the regions seen in **A1** and **B1**, respectively. (**A2** and **B2**) In the CC midline of *Nkx2.I*^{-/-} mice, there was a significant loss of GLAST⁺/Olig2⁻ (white arrows) and GLAST⁻/Olig2⁺ (open arrowheads) but not of GLAST⁺/Olig2⁺ (white arrowheads) glial cells compared to the wild-type mice. (**A3** and **B3**) In the side of the CC of *Nkx2.I*^{-/-} mice, there was a significant loss of GLAST⁺/Olig2⁺ (white arrowheads) but not of GLAST⁻/Olig2⁺ glial cells compared to the wild-type mice. (**A4** and **B4**) In the CI of *Nkx2.I*^{-/-} mice, there was a decrease of GLAST⁻/Olig2⁺ and GLAST⁺/Olig2⁺ glial cells (white arrowheads) compared to the wild-type mice.

(C) Bars (mean ± SEM from a sample of n=2 sections in the wild-type and n=2 sections in *Nkx2.I*^{-/-}) represent the density (number of cells/mm³) of GLAST⁺/Olig2⁻, GLAST⁻/Olig2⁺ and GLAST⁺/Olig2⁺ glial cells in the CC midline (**CC mid**), the side of the CC (**CC side**) and the cingulate bundle (**CI**) of *Nkx2.I*^{-/-} (KO) compared to wild-type (WT) mice at E18.5. The quantification revealed a significant decrease of the GLAST⁺/Olig2⁻ and GLAST⁻/Olig2⁺ glia in the CC mid, and of GLAST⁺/Olig2⁺ glia in the CC side of *Nkx2.I*^{-/-} compared to wild-type mice. (**CC**) corpus callosum; (**CCi**) cingulate cortex. Bar = 675 μm in **A1** and **B1**; 100 μm in **A2, A3, A4, B2, B3** and **B4**.



Supplementary figure S7. Cell death in *Nkx2.1*^{-/-} mice brains at E16.5.

(**A1-A2** and **B1-B2**) Single immunohistochemical staining for the cleaved-caspase 3 and (**C1-C2** and **D1-D2**) TUNEL staining on CC coronal sections from wild-type (**A1-A2** and **C1-C2**) and *Nkx2.1*^{-/-} mice (**B1-B2** and **D1-D2**) at E16.5. Cell nuclei were counterstained in blue with Hoechst. **A2**, **B2**, **C2** and **D2** are higher magnified views of the CC region seen in **A1**, **B1**, **C1** and **D1**, respectively. (**E** and **F**) Bars (mean ± SEM from a sample of n=4-16 sections in the wild-type and n=5-22 sections in *Nkx2.1*^{-/-} mice depending on the region studied) represent the number of dying cells labelled by the cleaved-caspase 3 or by the TUNEL staining and displaying pyknotic nuclei per section (surface area/section=24119.332 μm²), in the CC, POA, MGE and SEP of *Nkx2.1*^{-/-} (KO) compared to wild-type (WT) mice. No significant differences were observed in the number of dying cells in *Nkx2.1*^{-/-} mice brains compared to the wild-type. (**CC**) corpus callosum; (**MGE**) medial ganglionic eminence; (**POA**) preoptic area; (**SEP**) septum; Bar = 675 μm in **A1**, **B1**, **C1** and **D1**; 60 μm in **A2** and **B2**; 40 μm in **C2** and **D2**.

RESULTS

SECTION 2:

GUIDANCE OF COMMISSURAL AXONS IN THE EMBRYONIC TELEENCEPHALON: A ROLE FOR NKX2.1-POSITIVE CELLS

NUMEROUS PROGENITORS AND ASTROGLIAL CELLS REGULATED BY NKX2.1 ARE STRATEGICALLY PLACED TO AID AXONAL GUIDANCE IN THE CORPUS CALLOSUM AND THE ANTERIOR COMMISSURE.

Our previous results have shown that the glial cells situated in the CC midline originated from the $Nkx2.1^+$ precursors of the subpallium (results: section 1). Therefore, in order to further study in details the heterogeneity of the population of glial cells which are originating from $Nkx2.1^+$ germinal regions, we made use of several transgenic mice strains such as *Nkx2.1-Cre* (Kessaris, Fogarty et al. 2006), *NG2-Cre* (Jackson Laboratory: B6;FVB-Tg(Cspg4-cre)1Akik/J) and *GLAST-Cre ERTTM* (Jackson Laboratory: Tg(Slc1a3-cre/ERT)1Nat/J)) which were crossed with the reporter *Rosa26R–Yellow fluorescent protein (Rosa-YFP)* mice (Srinivas, Watanabe et al. 2001). The heterogeneous population of glia visualized at the midline commissures in wild-type (WT) mice were labeled with specific glial markers such as GLAST (Astrocyte-specific glutamate and aspartate transporter), GFAP (glial fibrillary acidic protein), Olig2 (Oligodendrocyte precursor bHLH transcription factors 2) and NG2 (Nerve/glial antigen 2 or CSPG for chondroitin sulfate proteoglycan) (Fig. 1). At E16.5, $Nkx2.1$ labeled the precursors at three subpallial sites of origin, i.e. the medial ganglionic eminence (MGE), the entopeduncular/preoptic area (AEP/POA) and the triangular septal nucleus (ts) (Fig. 1a, 1f and results: section 1 Supplementary Fig. S4a-b) and also the numerous astroglial cells that were seen surrounding the CC and the anterior commissure (AC) (Fig. 1d, 1f and results: section1 Fig. 1c-d). $GLAST^+$ precursors at the sites of origin at E16.5, and some of the $GLAST^+$ astroglial cells in the CC and the AC at E18.5, in addition to co-expressing $Nkx2.1$ (Fig. 1a, 1d and 1f), were also labeled by the astroglial marker, GFAP (Fig. 1b). The GLAST-derived astroglial cells, visualized with the YFP signal in the CC and the AC of the *GLAST-Cre ERTTM/Rosa-YFP* mice, were co-labeled for GLAST and $Nkx2.1$ (Fig. 1d). These results corroborated our previous results, that many $GLAST^+$ astroglial cells co-express $Nkx2.1$ (Fig. 1a, 1d and 1f). We also distinguished a second class of $GLAST^+$ astroglial population that did not express $Nkx2.1$ but was co-labeled for Olig2. Thereafter, using the *Nkx2.1-Cre⁺/Rosa-YFP* mice, we found that the *Nkx2.1*-derived cells labeled by the YFP signal were either immunolabeled for the astrocytic marker, GLAST or for the polydendrocytic marker, NG2. On the other hand, the use of the *NG2-Cre⁺/Rosa-YFP* mice revealed that the NG2-derived cells visualized by the YFP signal were not co-labeled for GLAST and were not expressing $Nkx2.1$ anymore outside the germinal zones. In these

experiments, the markers, GLAST and NG2, were found to be mutually exclusive and the $Nkx2.1^+$ glial cells were co-labeled only for GLAST. Thus, from this study, we could determine the presence of two major different populations of glial cells, which, additionally, comprised of two subpopulations each, that originated from the $Nkx2.1^+$ sites (Fig. 1 and results: section 1 Fig 1, Fig. 2 and Supplementary Fig. S1) and migrated to occupy the entire embryonic telencephalon specifically regions surrounding the CC and the AC. One population was characterized as $GLAST^+/GFAP^+/Nkx2.1^+/Olig2^-$ (Fig. 1b and not shown) or $GLAST^+/GFAP^-/Nkx2.1^+/Olig2^+$ (Fig. 1c and not shown), and was classified as an astrocyte-like group of cells. Additionally, the other subpopulation identified was $NG2^+/Olig2^+/Nkx2.1^-/S100\beta^+$ (Fig. 1e and f and not shown) or $NG2^+/Olig2^-/Nkx2.1^-/S100\beta^-$ (results: section 1 Fig 1, Fig. 2 and Supplementary Fig. S1), and was classified as a polydendrocyte-like group of cells.

Altogether, the $Nkx2.1^+$ precursors and glial post-mitotic cells were strategically situated within and around both commissures at an appropriate time to play a role in guiding commissural axons.

NKX2.1 REGULATES GABAERGIC NEURONS THAT ACT AS GUIDEPOST CELLS IN THE FORNIX AND THE ANTERIOR COMMISSURE

In our previous work on axonal guidance in the CC, we have described the role of glutamatergic and GABAergic interneurons that act as guidepost cells to aid the navigation of callosal axons through the midline commissure (Niquille, Garel et al. 2009) (Niquille, Minocha et al., submitted). Since we found that half of the GABAergic neurons of the CC originate from the *Nkx2.1*-regulated MGE, we crossed *Nkx2.1^{+/-}* mice with heterozygous *GAD67-GFP* knock-in mice, described in this work as *GAD67-GFP* mice (Donahoo and Richards 2009). The sequential crosses allowed us to generate *Nkx2.1^{+/+}:GAD67-GFP* and *Nkx2.1^{-/-}:GAD67-GFP* mice which were used to visualize the *GAD67-GFP⁺* GABAergic interneurons in WT and mutant brains labeled by the GFP antibody. In *Nkx2.1^{-/-}:GAD67-GFP* embryos, we observed a drastic loss of about 75% of *GAD67-GFP⁺* neurons at the CC midline (mid), and a significant loss of about 50% in the lateral sides of the CC. Additionally, we observed a nearly complete loss of *GAD67-GFP⁺* neurons within the growing AC tract on the lateral sides (side) (Fig. 2b, 2g, 2k and 2l). We were not able to quantify the *GAD67-GFP⁺* neurons at the AC midline since, in the absence of *Nkx2.1*, the commissure failed to form (Fig. 2g1).

Additionally, in order to study the possible involvement of *Nkx2.1*-derived GABAergic neurons in guiding axons, we visualized the commissural axons of the CC, of the AC, as well

as the hippocampal axons of the fornix by using an immunohistochemical staining for L1 (L1CAM cell adhesion protein) on both *Nkx2.1^{+/+}:GAD67-GFP* and *Nkx2.1^{-/-}:GAD67-GFP* mice (Fig. 2f, Fig. 2g and Fig. 3a, 3b, 3f, 3g). In *Nkx2.1^{-/-}:GAD67-GFP* mice, though we could observe only mild guidance defects in the CC, much stronger defects were found in the fornix in which the hippocampal axons were not fasciculated to the same extent as those in the control fornix (Compare Fig. 3b to Fig. 3a). To further analyze the axonal guidance defects in the CC and the fornix of the *Nkx2.1^{-/-}* mice, we also performed injections of fluorescent carbocyanide dye DiI (1,1'-dioctadecyl 3,3',3',3'-tetramethylindocarbocyanine perchlorate) or DiA (4-[4-(dihexadecyl amino)styryl]N-methyl-pyridinium iodide) in WT and *Nkx2.1^{-/-}* mice (Fig. 4). By placing a DiA crystal in the frontal cortex (CFr) of E18.5 telencephalic coronal slices and a DiI crystal in the lateral side of the hippocampus caudally from the hippocampal commissure (HIC), we were able to reliably label the callosal axons and the axons of the fornix distinctly (Fig. 4 a-d). By this means, we observed that in the *Nkx2.1^{-/-}* brains, some of the callosal axons were misrouted ventrally (Compare Fig. 4 b1-b2 with 4a1-a2) and the axons of the fornix were forming distinct bundles in the septum (Compare Fig. 4 b1, b3 with 4a1, a3). In addition, we also performed *in utero* electroporation of a *pCAG-IRES-Tomato* plasmid into *Nkx2.1^{+/+}:GAD67-GFP* and *Nkx2.1^{-/-}:GAD67-GFP* embryos in order to study the interactions of growing callosal axons and GAD67-GFP⁺ interneurons (Fig. 5). This experiment allowed us to detect that the callosal axons were displaying subtle differences between the mutant and the control. While *Nkx2.1^{-/-}:GAD67-GFP* mice exhibited an enlarged CC, the general callosal axon navigation paths seemed to be preserved in the mutant compared to the WT brains. However, high magnification views revealed that the tomato-labeled callosal axons were not properly fasciculated (midline) and displayed aberrant branching pattern (postcross) (Fig. 5c, open arrowheads). Confocal time-lapse video microscopy unraveled that growth cones of callosal axons in the *Nkx2.1^{-/-}:GAD67-GFP* CC still responded to the remaining GAD67-GFP⁺ GABAergic neurons of the CC and progressed along their normal tracks (Fig. 5d-e). However, they formed branched extensions that grew slowly and in a disoriented manner compared to the WT axonal branches. Interestingly, in the *Nkx2.1^{-/-}* AC, the axonal guidance defects were so strong that the axons were no longer able to reach the midline. The AC tracts from each hemisphere were deflected ventrally and were never able to find their targets at the midline (Fig. 2g and Fig. 3g).

In *Nkx2.1^{-/-}* mice, it is also known that the mutant MGE* doesn't form normally and that the precursors of the MGE change their identity and are re-specified to a more dorsal LGE fate (Sussel, Marin et al. 1999). In order to assess more specifically the potential involvement of the *Nkx2.1*-derived GAD67-GFP⁺ neurons in guiding axons of the AC, we made use of a specific cell ablation strategy that does not interfere with the MGE formation. We crossed

Nkx2.1-Cre mice with the *Rosa-DTA* mice (Brockschnieder, Pechmann et al. 2006) that express the highly potent diphtheria toxin fragment A (DTA) under the control of the *Nkx2.1* promoter to principally ablate the *Nkx2.1*-derived post-mitotic cells. The study of the *Nkx2.1*⁺ precursors at E16.5, in the four germinal zones that generate *Nkx2.1*-derived cells (MGE, AEP, POA and ts, see results: section 1), in the *Nkx2.1-Cre*⁺/*Rosa-DTA* indicated that there was no obvious reduction of the *Nkx2.1* labeling in the MGE the AEP/POA and the ts, (compare Fig. 6a with 6b and results: sections 3 Supplementary Fig. S1). Thus, the added advantage of these mutant mice was that we did not interfere with the *Nkx2.1*⁺ precursors of the subpallium. In addition, the MGE precursors were not re-specified to another fate (not shown) and the MGE was formed normally. Upon quantification of the *GAD67-GFP*⁺ interneurons, we found a loss of more than 80% at the CC midline and more than 70% at the AC midline of *Nkx2.1-Cre*⁺/*Rosa-DTA*:*GAD67-GFP* mice (Fig. 2c, 2h, 2k-l). In *Nkx2.1-Cre*⁺/*Rosa-DTA*:*GAD67-GFP* mice, while we did not detect any guidance defects at the CC midline, the axons of the fornix displayed bundle anomalies similar to those observed in *Nkx2.1*^{-/-}:*GAD67-GFP* mice (Compare Fig. 3c with 3a and 3b). Interestingly, unlike the *Nkx2.1*^{-/-} brains, the MGE still formed in the *Nkx2.1-Cre*⁺/*Rosa-DTA* mice and the axons of the AC could reach the midline but thereafter, the commissural tract was split into two or three tracts (compare Fig. 3h with 3f and 3g). One of the tracts was deflected dorsally towards the ts and the hippocampus, and the other two tracts were misrouted medially and ventrally where they stopped abruptly before reaching the midline (Fig. 2h and Fig. 3h).

In the absence of *Nkx2.1*, there is a significant loss of the GABAergic interneurons at both midline commissures, the CC and the AC and in the septum. As a result, the callosal axons are deflected from their normal trajectories as they use the GABAergic interneurons as guides, and thus, afflicting the proper formation of the tracts especially of the fornix and the AC.

NKX2.1⁺ PRECURSORS AND NKX2.1-DERIVED GLIA HELP IN GUIDING THE COMMISSURAL AXONS

However, based on our previous results, we know that the transcription factor *Nkx2.1* also regulates the proliferation and the specification of several subpopulations of glial cells (Fig. 1 and results: section 1) and directly binds to the promoter region of several glial regulatory genes (results: section 1 Fig 8). We have also shown that there was nearly a complete loss of astroglia and polydendrocytes in the medial telencephalic regions of *Nkx2.1*^{-/-} mice (results: section 1 Fig.6 and Supplementary Fig. S6). Moreover, astroglial cells situated in the region surrounding the CC (IG, GS and GW) have been shown to play a key role in axonal guidance

(Silver, Lorenz et al. 1982; Silver, Edwards et al. 1993; Shu and Richards 2001; Shu, Puche et al. 2003; Shu, Sundaresan et al. 2003; Smith, Ohkubo et al. 2006). Similarly, an astroglial cell population, that surrounds the AC and the fornix, known as “tunnel” has been proposed to be involved in the guidance of axons throughout the commissure but functional evidences are still missing to prove the direct involvement of these glia (Pires-Neto, Braga-De-Souza et al. 1998; Lent, Uziel et al. 2005). Finally, a recent study on polydendrocytes suggests that these cells may play a role in guiding callosal axons (Yang, Suzuki et al. 2006). Therefore, it is possible that, in addition to the observed loss of GABAergic neurons, the unavailability of the *Nkx2.1*-derived glial cells could also account for the guidance defects we have observed in the *Nkx2.1*^{-/-} mice brain commissures.

First, in order to better visualize the loss of astroglial cells and associated guidance defects in the CC and the AC midline of both *Nkx2.1*^{-/-} and *Nkx2.1-Cre⁺/Rosa-DTA* mutant mice, we performed several double immunolabellings. The stainings for the astroglial marker GFAP combined with the neuronal marker Calretinin confirmed our previous results showing that in the CC of *Nkx2.1*^{-/-} mice at E18.5, there was a complete loss of GFAP⁺ astrocytes in the IG, midline, GS and MZG. The Calretinin⁺ neurons were spatially misplaced at the midline as compared to the WT brains (compare Fig. 7b with 7a) where they formed three separate stripes that served as boundaries to separate the callosal axons into two separate, dorsal and ventral, paths (Niquille, Garel et al. 2009). Additionally, the staining for Neuropilin-1 (Nrp-1), a guidance receptor for the semaphorins that labels the callosal axons of the dorsal path, corroborated our previous results on *Nkx2.1*^{-/-} mice brains showing that the dorsal path displayed strong axonal guidance defects in the CC (compare Fig. 7e with 7d, white arrowheads). The Nrp-1⁺ axons from the dorsal path were mis-oriented and penetrated the ventral path and formed haphazard bundles (Fig. 7e2). In addition to the mis-orientation of the CC axons, the axons of the fornix formed bundles and displayed altered fasciculation pattern (Fig. 7e1). By contrast, in *Nkx2.1-Cre⁺/Rosa-DTA* mice, only the GFAP⁺ astrocytes within the CC white matter could be depleted but those of the IG and the subcallosal glial sling (GS) still remained as the Cre-mediated recombination was not complete in these regions (Compare Fig.7c with 7b and 7a). Moreover, the Calretinin⁺ neurons were well positioned and formed three stripes as in the WT (compare Fig.7c with 7a and 7f with 7d). Consequently, the Nrp-1⁺ callosal axons of the CC dorsal path developed normally as in the control brains. Thereby, this implies that the glial cells at the boundaries of the CC are more crucial for guidance than those within the CC. In addition, this suggests that the loss of GAD67-GFP⁺ neurons of the CC at the midline may not be sufficient to explain the CC defects noticed in the *Nkx2.1*^{-/-}.

Thereafter, to further detail the possible involvement of glia in axonal guidance of the commissural axons of the AC, we performed double immunostainings for L1 and GFAP, and

for L1 and GLAST in *Nkx2.1-Cre⁺/Rosa-DTA* mice and the corresponding control *Nkx2.1-Cre⁻/Rosa-DTA* mice. As described previously, in the mutant, the axons forming the AC were observed to be split into two evident tracts, and one of the tracts was deflected dorsally and penetrated the ts region. Interestingly, we noticed that the GLAST⁺/GFAP⁺ astrocytes of the tunnel (*) forming a palisade surrounding the AC were Nkx2.1⁺ (Fig. 6a). We have already shown previously (results: section1), that the ts, situated just above the AC and rostro-ventral to the hippocampus, is one of the germinal subpallial regions regulated by Nkx2.1. A close examination of this region revealed that the ts contained newly generated *Nkx2.1*-derived GABAergic neurons and glia that had just left the ventricular zone of the ts (Fig. 3d, Fig. 6a, 6c, 6f and 6h). Interestingly, the astroglia of the tunnel were seen to originate from the ts and the AEP and were in continuity with this structure (results: section 1 Fig. 4 and Supplementary Fig. S4). In *Nkx2.1-Cre⁺/Rosa-DTA* brains, the number of GLAST⁺/GFAP⁺ and GLAST⁺/Olig2⁺ astrocytes that emanated and migrated from the ts and the AEP was reduced, and there was also less *Nkx2.1*-derived astroglia forming the tunnel-like astroglial structure of the AC (Compare Fig 6b to 6a white arrowheads, and compare Fig.6d to 6c, 6g to 6f and 6i to 6h). Some GLAST⁺/GFAP⁺ astrocytes that were still left at the AC midline, were completely disorganized (Compare Fig. 6g and 6f). Finally, in order to better characterize the loss of astroglial cells in the mutant, we quantified the number of GLAST⁺ and Olig2⁺ glia remaining within the AC midline of *Nkx2.1-Cre⁺/Rosa-DTA* mice. After quantification, we found that more than 60% of the GLAST⁺ astroglial cells were actually depleted within the AC (only 28.73±10.47% of GLAST⁺/Olig2⁻ and 33.56±7.52 % of GLAST⁺/Olig2⁺ remaining cells; p<0.01; n=5 sections) (Fig. 6e).

Altogether, these results indicate that the depletion of the astroglial cells that form boundaries surrounding the CC (IG, GS) and the AC (ts precursors and tunnel-like astrocytes) can be directly correlated with the axonal guidance defects previously described.

NKX2.1-DERIVED INTERNEURONS AND ASTROCYTES SYNERGISTICALLY COOPERATE TO GUIDE GROWING COMMISSURAL AXONS OF THE ANTERIOR COMMISSURE

Thereafter, we wanted to unravel the extent of defects potentiated by the precursors, the glial and the neuronal ablation separately. Thus, for this purpose, we made use of the neuron-specific enolase (NSE)-stop-DTA (*NSE-DTA*) mice (Kobayakawa et al., 2007) in which the expression of the DTA is induced from the neuron-specific enolase locus, and crossed them with the *Nkx2.1-Cre* mice which resulted in the specific ablation of the *Nkx2.1*-derived neurons only. Comparatively to the *Nkx2.1-Cre⁺/Rosa-DTA:GAD67-GFP* mice, the *Nkx2.1-Cre⁺/NSE-DTA:GAD67-GFP* mice displayed slightly reduced disappearance of GAD67-GFP⁺ neurons with a loss of $63 \pm 8.1\%$ neurons at the CC midline and of $63.83 \pm 6.73\%$ neurons at the AC midline (Fig. 2d, 2i, 2k-l). In addition, since the NSE promoter is highly specific for the postmitotic neuronal cells, we never observed any loss of precursors, GFAP⁺ astrocytes and NG2⁺ polydendrocytes in the *Nkx2.1-Cre⁺/NSE-DTA:GAD67-GFP* brains (not shown and results section 3: Supplementary Fig. S3).

To analyze the effects of these two different cell-ablating strategies on axonal guidance, we performed immunostaining with the axonal markers L1 and Nrp-1 on *Nkx2.1-Cre⁺/NSE-DTA:GAD67-GFP* mice and compared the results with previous observations made in the *Nkx2.1-Cre⁺/Rosa-DTA:GAD67-GFP* mice (Fig. 2 and Fig. 3). Interestingly, in *Nkx2.1-Cre⁺/NSE-DTA:GAD67-GFP* mice, the axonal guidance defects were less stronger than those visualized with *Nkx2.1-Cre⁺/Rosa-DTA:GAD67-GFP* mice. At rostral levels, the axons of the CC were observed to navigate appropriately and the axons of the fornix were optimally well fasciculated too, when compared to WT mice brains (not shown and Fig. 2d). By contrast, at more caudal level the axons of the fornix were deflected from their normal trajectory and penetrated the entire septum, as well as the ts where we noticed a drastic loss of the GAD67-GFP⁺ neurons that were born in this region (compare Fig. 3i with 3d). In *Nkx2.1-Cre⁺/NSE-DTA:GAD67-GFP* mice, the axons of the AC exhibited different types of defects: (1) in some cases, they did not cross correctly and were misrouted towards the ts where they intermixed with the axons of the fornix (compare Fig. 3i with 3d) and (2) in other cases, they were able to cross the midline but the AC tract appeared to be narrower than in the control (compare Fig. 2i with 2f). Thus, we measured the surface area of the AC at the midline and in the lateral sides, and found that the tract was indeed thinner by about 30% in *Nkx2.1-Cre⁺/NSE-DTA:GAD67-GFP* mice compared to the control (Fig. 2m). Consequently, these results indicated that the *Nkx2.1*-derived GABAergic neurons played an important role towards the guidance of the AC. Since the defects were stronger in *Nkx2.1-Cre⁺/Rosa-DTA:GAD67-GFP* when ts precursors,

glia and neurons were depleted than, in *Nkx2.1-Cre⁺/NSE-DTA:GAD67-GFP* mice, where only neurons were ablated, it can be deciphered that all cells play synergic actions and that the *Nkx2.1* precursors and glia have also a major role to play in axonal guidance in the AC.

Subsequently, since *Nkx2.1* regulates two different subclasses of glial cells, namely the astrocytes and the polydendrocytes; we made use of the elimination strategy to determine if the loss of one or both has a role to play in the guidance defects visualized in the *Nkx2.1-Cre⁺/Rosa-DTA* mutant brains. To this purpose, we crossed *NG2-Cre* mice with *Rosa-DTA* mice to selectively deplete the *NG2⁺* polydendrocytes. In *NG2-Cre⁺/Rosa-DTA:GAD67-GFP* mice, we verified that *GAD67-GFP⁺* neurons and astrocytes were normal in the CC and the AC and we did not notice any axonal guidance defects within both commissures (Fig. 2e, 2j, 2k and 2l and Fig. 3e and 3j) and thus, implying that the loss of the other subclass of glia, the astrocytes and possibly of the ts precursors, accounts for the significant guidance defects visualized in the mutant brains (see also results: section 2, table 1; for a summary of guidance defects observed in all types of mutants).

Altogether, these results demonstrate that *Nkx2.1*-derived GABAergic neurons, ts precursors and astrocytes synergistically cooperate to guide the growing axons of the AC through the correct path and help them to reach their respective targets during development.

NKX2.1+ PRECURSORS FROM THE TRIANGULAR SEPTAL NUCLEUS MIGHT CHANNEL THE AXONS OF THE AC THROUGH A SLIT2-DEPENDENT MECHANISM.

Our aforementioned results directly implicated the involvement of *Nkx2.1*-derived precursors, astroglia and neurons towards the guidance of the axons through the commissures, and thus, looking for a potential guidance cue required to mediate the said action, we performed *in situ* hybridization for *Slit2* mRNA in wild-type, *Nkx2.1-Cre⁺/Rosa-DTA* and *Nkx2.1^{-/-}* coronal slices at E16.5. *Slit2*, most likely through Robo receptors, has been previously implicated to play the role of a secreted chemorepellant cue important for the proper development of major forebrain tracts through its guiding action on the migrating axons and cells (Rothberg, Hartley et al. 1988; Rothberg, Jacobs et al. 1990; Kidd, Brose et al. 1998; Brose, Bland et al. 1999; Kidd, Bland et al. 1999; Rajagopalan, Nicolas et al. 2000). Moreover, *Slit2* mutants exhibit abnormal development of the axonal trajectories and formation of ventrally projecting bundles of fibres in the telencephalon at the level of AC, and two large bundles on either side of the CC resembling Probst bundles (Bagri, Marin et al. 2002; Plump, Erskine et al. 2002). The labeling revealed that the WT *Nkx2.1*-regulated precursors of the subpallium, including the ts,

the AEP and the POA, strongly expressed the repellent guidance molecule Slit2 (Fig. 8 and Fig. 9a). Indeed, the AC tract extends plausibly into a Slit2⁻ permissive path which is completely encircled by the Slit2⁺ repulsive progenitor cells of the AEP, the ts and the POA. Moreover, in both *Nkx2.1-Cre⁺/Rosa-DTA* and in *Nkx2.1^{-/-}* mice at E16.5 (Fig. 9b and 9c), we could observe that the expression of Slit2 in the Nkx2.1⁺ progenitors was reduced compared to the WT brains in the atrophied regions. The reduction was clearly observed in the POA, the ts and the IG (Compare Fig. 9b with 9a and 9c with 9a). However, in accordance with the absence of Nkx2.1 in the radial glia of the GW, Slit2 was not affected in the Nkx2.1⁻ progenitors of the GW (Fig. 9b1 and 9c1).

Consequently, these results tend to indicate that the *Nkx2.1*-regulated precursors of the ts and the AEP/POA by expressing the repellent molecule Slit2, are participating, in addition to the tunnel-like astroglia, towards the guidance by forming boundaries responsible for the formation of the AC into one unique axonal tract which crosses the midline. When the expression of Slit2 is decreased in these structures, like in *Nkx2.1-Cre⁺/Rosa-DTA* mutant mice, the AC tract is split into two tracts which are deflected ventrally and dorsally and penetrate the POA and the ts instead of crossing the midline.

Taken together, our results indicate that the *Nkx2.1*-derived cells, that constitute GABAergic neurons, ts precursors and astrocytes, have a vital role to play towards the guidance and formation of the normal axonal trajectories in telencephalon (see also results: section 2, table 1; for a summary of guidance defects observed in all types of mutants). These actions could be due to the function of Nkx2.1 on glial proliferation/specification and their subsequent regulation, as glia have been, since long, implicated to act as potential intermediate targets or guidance decision points. This guidance forces may be mediated through the expression of the repellent molecule, Slit2 by the *Nkx2.1*-regulated precursors of the ts and the AEP/POA that aids in maintaining aptly directed axonal growth. The depletion of the either of the *Nkx2.1*-derived cells, or more severely all, leads to axonal targeting defects in the CC and the fornix, and abnormal or absent formation of the AC.

FIGURES of section 2:

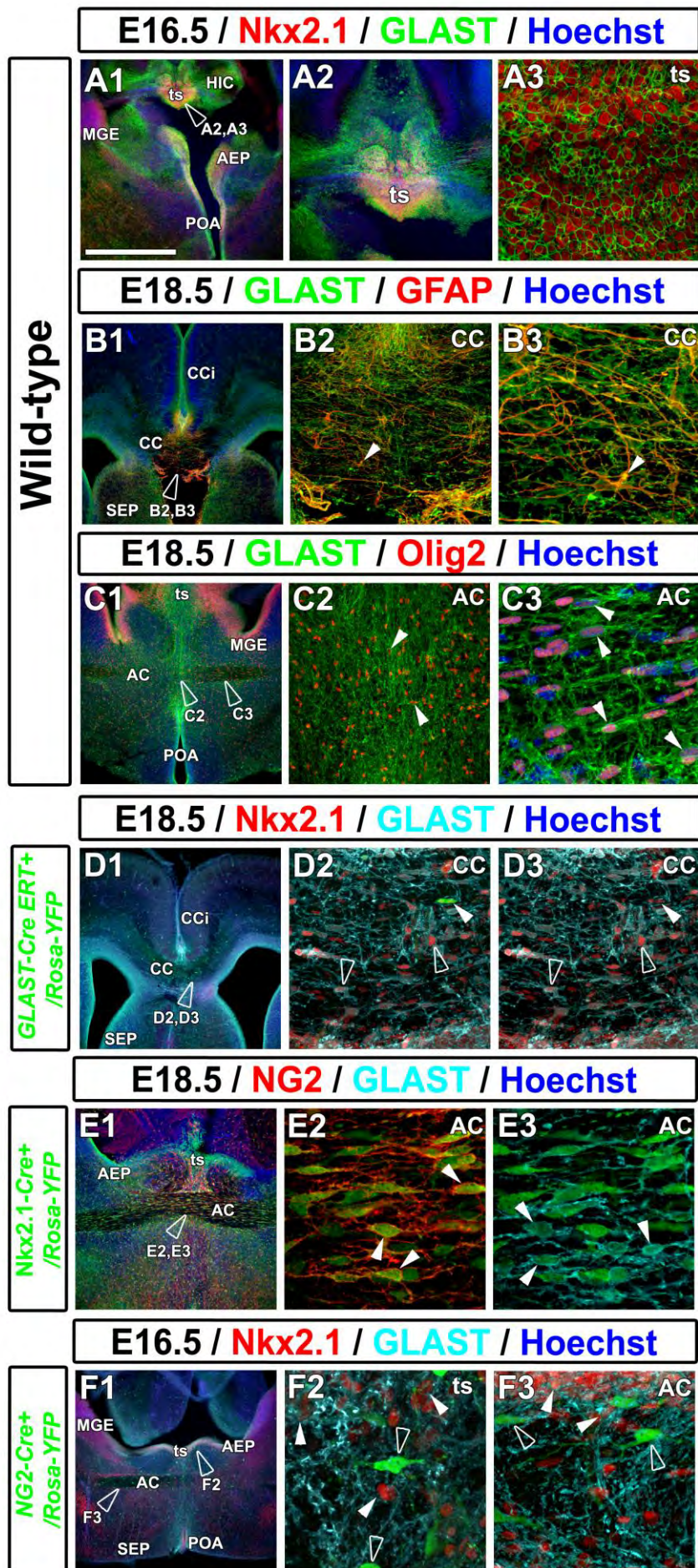


Figure 1. *Nkx2.1*-regulated embryonic glial cells in the CC and the AC.

(A, B and C) Double immunohistochemistry for *Nkx2.1* and GLAST (A1-A3), for GLAST and GFAP (B1-B3), and for GLAST and Olig2 (C1-C3) on coronal slices from wild-type (A-C) mice brains at E16.5 (A, B) and E18.5 (C). (D, E and F) Triple immunohistochemistry for the YFP, *Nkx2.1* and GLAST (D and F) and for the YFP, NG2 and GLAST (E) on coronal sections from E18.5 *GLAST-Cre ERT⁺/Rosa-YFP* (D); E18.5 *Nkx2.1-Cre⁺/Rosa-YFP* (E) and E16.5 *NG2-Cre⁺/Rosa-YFP* (F) mice brains. Cell nuclei were counterstained in blue with Hoechst (A1, A2, B1, C1, C3, D1, E1 and F1). B2, B3, D2 and D3, are higher magnified views of the CC seen in B1 and D1; C2, C3, E2, E3 and F3 are high magnification views of the AC seen in C1, E1 and F1; and A2, A3 and F2 are higher magnified views of the ts seen in A1 and F1.

(A, B and C) In wild-type coronal sections of the telencephalon at E16.5, numerous GLAST⁺ glial cells were found to originate from *Nkx2.1*⁺ germinal regions of the subpallium, namely the triangular septal nucleus (ts), the MGE and the AEP/POA (A1-A3). At E18.5, these glial cells were also found in the CC and AC where they were co-expressing GFAP (B1-B3, white arrowheads) and Olig2 (C1-C3, white arrowheads). (D, E and F) The use of coronal sections from E18.5 *GLAST-Cre ERT⁺/RosaYFP*, E18.5 *Nkx2.1-Cre⁺/Rosa-YFP* and E16.5 *NG2-Cre⁺/Rosa-YFP* mice, confirmed the presence of numerous *Nkx2.1*-derived GLAST⁺ astroglial cells (white and open arrowheads in D2-D3; white arrowheads in E3 and F2-F3), as well as NG2⁺ polydendrocytes (E1-E2 and F1-F3) which were also regulated by *Nkx2.1* (white arrowheads in E2) but displayed down-regulated *Nkx2.1* expression soon after they escaped the ventricular zone (open arrowheads in F2-F3).

(C, E and F) The *Nkx2.1*-derived GLAST⁺ glial cells populated the path through which the axons of the AC were channelled (white arrowheads in F3). (E and F) The NG2⁺ cells never co-expressed GLAST which indicates that they are two mutually exclusive sub-populations of glia (E2 and E3; open arrowheads in F2-F3). (AC) anterior commissure; (AEP) anterior entopeduncular area; (CC) corpus callosum; (CCi) cingulate cortex, (MGE) medial ganglionic area; (POA) preoptic area; (SEP) septum; (ts) triangular septal nucleus. Bar = 675 μ m in A1, B1, C1, D1, E1 and F1; 320 μ m in A2; 180 μ m in C2, 100 μ m in B2; 50 μ m in B3, D2 and D3; 40 μ m in A3, C3, E2, E3, F2 and F3.

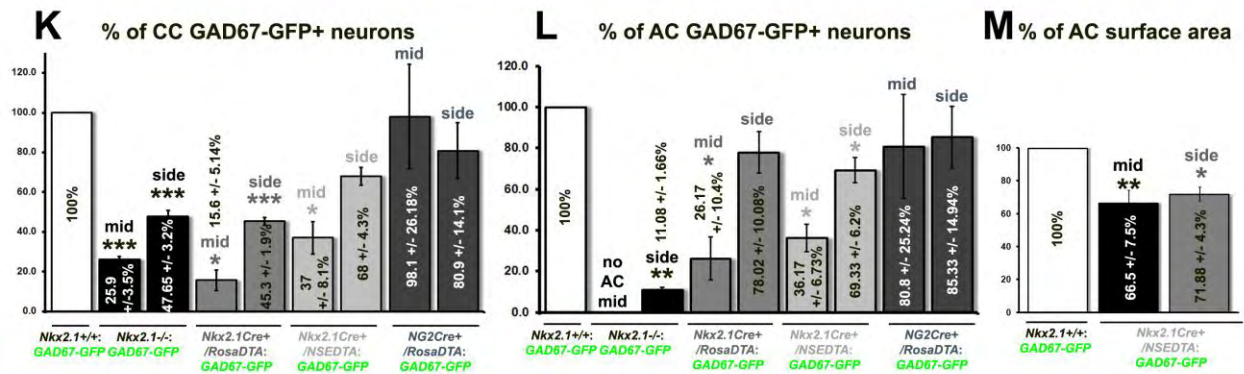
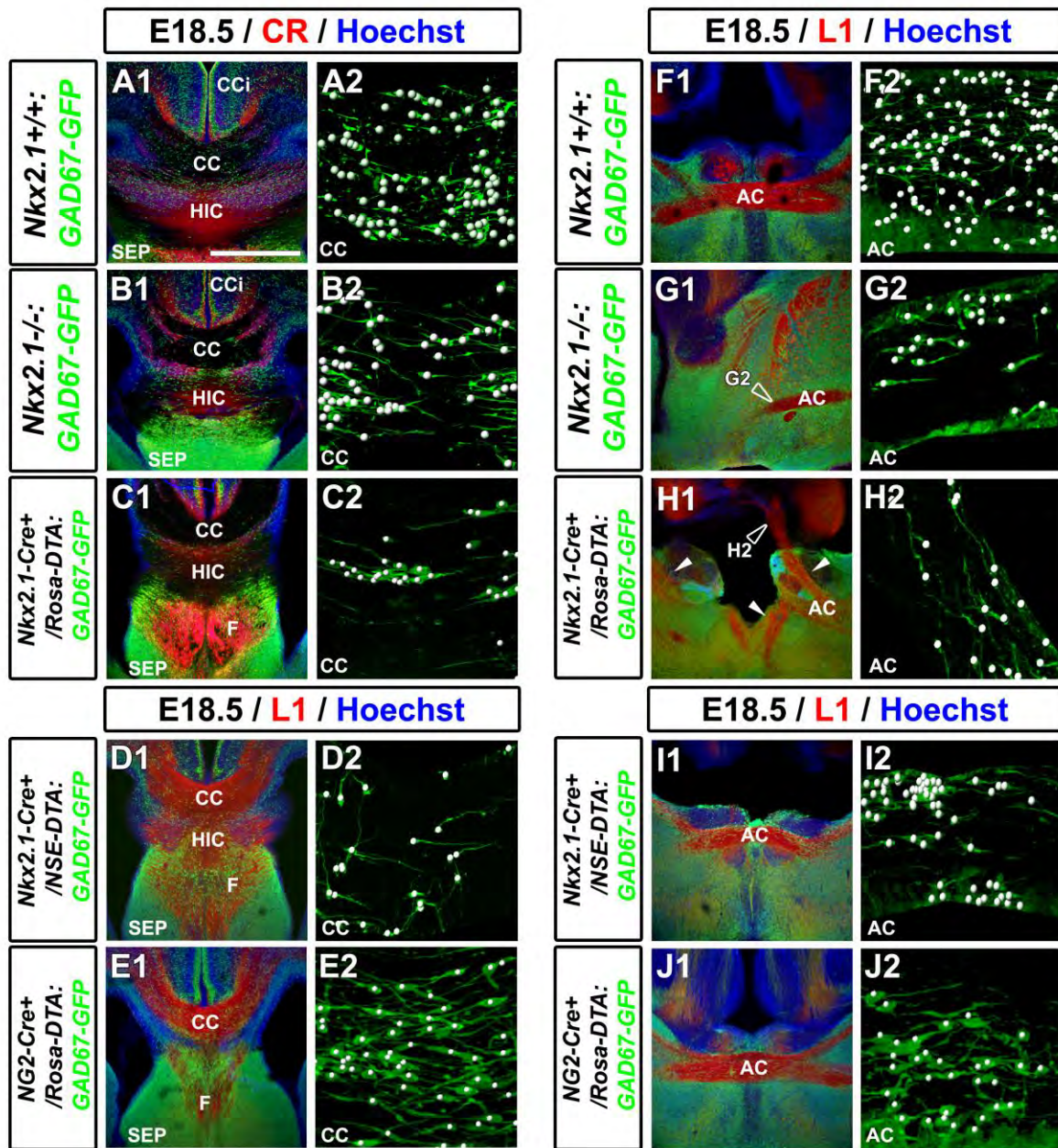


Figure 2. Loss of *GAD67-GFP*⁺ interneurons and axonal guidance defects in *Nkx2.1*^{-/-}:*GAD67-GFP*, *Nkx2.1-Cre*⁺/*Rosa-DTA:GAD67-GFP* and *Nkx2.1-Cre*⁺/*NSE-DTA:GAD67-GFP* mutant mice brains.

(A-H) Double immunohistochemical staining for the GFP and CR (A-C) and for the GFP and L1 (D-J) on CC (A-E) and AC (F-I) coronal sections from *Nkx2.1*^{+/+}:*GAD67-GFP* (A and E), *Nkx2.1*^{-/-}:*GAD67-GFP* (B and F), *Nkx2.1-Cre*⁺/*Rosa-DTA:GAD67-GFP* (C and G), *Nkx2.1-Cre*⁺/*NSE-DTA:GAD67-GFP* (D and H) and *NG2-Cre*⁺/*Rosa-DTA:GAD67-GFP* mice brains at E18.5. Cell nuclei were counterstained in blue with Hoechst (A1, B1, C1, D1, E1, F1, G1, H1, I1 and J1). A2, B2, C2, D2, E2, F2, G2, H2, I2 and J2 are higher power views showing the quantification of the *GAD67-GFP*⁺ interneurons (white spots) within the CC and AC seen in A1, B1, C1, D1, E1, F1, G1, H1, I1 and J1 respectively. (A1-A2 and F1-F2) In the CC and AC of *Nkx2.1*^{+/+}:*GAD67-GFP* mice, numerous *GAD67-GFP*⁺ interneurons (in green) were populating the midline. (B1-B2 and G1-G2) In *Nkx2.1*^{-/-}:*GAD67-GFP* mice, the number of *GAD67-GFP*⁺ interneurons was drastically reduced in both the CC (compare B2 with A2) and AC (compare G2 with F2). (C1-C2 and H1-H2) In *Nkx2.1-Cre*⁺/*Rosa-DTA:GAD67-GFP* mice, the *GAD67-GFP*⁺ interneurons were drastically depleted from the CC (compare C2 with A2) and AC (compare H2 with F2). (D1-D2 and I1-I2) In *Nkx2.1-Cre*⁺/*NSE-DTA:GAD67-GFP* mice, the *GAD67-GFP*⁺ interneurons were also strongly depleted from the CC (compare D2 with A2) and the AC (compare I2 with F2). (E1-E2 and J1-J2) In *NG2-Cre*⁺/*Rosa-DTA:GAD67-GFP* mice, the *GAD67-GFP*⁺ interneurons were similar in number to those observed in the WT mice in both CC (compare E2 with A2) and AC (compare J2 with F2). (K and L) Bars (mean ± SEM from a sample of n=3 sections in *Nkx2.1*^{+/+}:*GAD67-GFP*, n=3 sections in *Nkx2.1*^{-/-}:*GAD67-GFP*, n=3 sections in *Nkx2.1-Cre*⁺/*Rosa-DTA:GAD67-GFP*, n=3 sections in *Nkx2.1-Cre*⁺/*NSE-DTA:GAD67-GFP*, n=3 sections in *NG2-Cre*⁺/*Rosa-DTA:GAD67-GFP*) represent the percentage of *GAD67-GFP*⁺ interneurons, in the middle (mid) and on the sides (side) of the CC (K) and AC (L). The results show that there is a drastic and significant decrease of *GAD67-GFP*⁺ neurons (which is more pronounced in the middle than on the side) in all *Nkx2.1* mutant mice strains compared to wild-type. (M) Bars (mean ± SEM from a sample of n=3 sections *Nkx2.1-Cre*⁺/*NSE-DTA:GAD67-GFP*) represent the AC surface area in the *Nkx2.1-Cre*⁺/*NSE-DTA:GAD67-GFP* mutant compared to *Nkx2.1*^{+/+}:*GAD67-GFP*. Quantification reveals a significant reduction of the AC surface area in the mutant compared to wild-type. (AC) anterior commissure; (CC) corpus callosum; (CCi) cingulate cortex; (F) fornix; (HIC) hippocampal commissure; (SEP) septum. Bar = 675 μm in A1, B1, C1, D1, E1, F1, G1, H1, I1 and J1; 100 μm in A2, B2, C2, D2, E2, F2, G2, H2, I2 and J2.

E18.5 / L1 / Hoechst

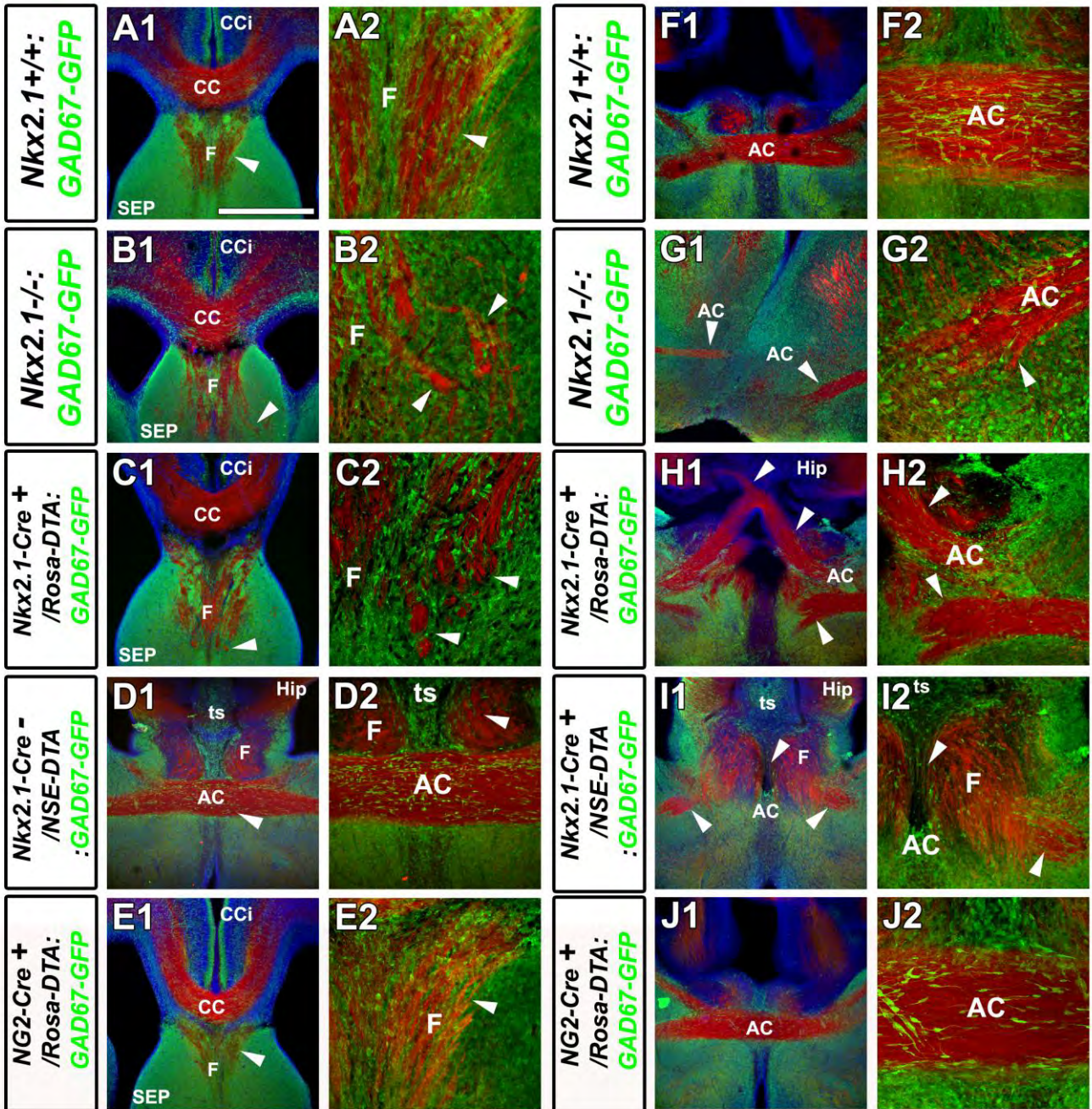


Figure 3. *Nkx2.1*-regulated glial cells and neurons function as guidepost cells for axonal guidance in the CC, fornix and AC.

(A-J) Double immunohistochemical staining for the GFP and L1 on CC (**A-C** and **E**) and AC (**D** and **F-J**) coronal sections from *Nkx2.1^{+/+}:GAD67-GFP* (**A1-A2** and **F1-F2**), *Nkx2.1^{-/-}:GAD67-GFP* (**B1-B2** and **G1-G2**), *Nkx2.1-Cre⁺/Rosa-DTA:GAD67-GFP* (**C1-C2** and **H1-H2**), *Nkx2.1-Cre⁻/NSE-DTA:GAD67-GFP* (**D1-D2**), *Nkx2.1-Cre⁺/NSE-DTA:GAD67-GFP* (**I1-I2**) and *NG2-Cre⁺/Rosa-DTA:GAD67-GFP* (**E1-E2** and **J1-J2**) mice brains at E18.5. Cell nuclei were counterstained in blue with Hoechst (**A1, B1, C1, D1, E1, F1, G1, H1, I1** and **J1**). **A2, B2, C2** and **E2** are higher power views of the fornix seen in **A1, B1, C1** and **E1**, and **D2, F2, G2, H2, I2** and **J2** are higher power views of the AC seen in **D1, F1, G1, H1, I1** and **J1**, respectively.

(A1-A2 and F1-F2) In the CC, the fornix and the AC of *Nkx2.1^{+/+}:GAD67-GFP* mice, the GAD67-GFP⁺ interneurons (in green) were well positioned and the axons labelled by L1 (in red) were properly fasciculated. **(B1-B2 and G1-G2)** In *Nkx2.1^{-/-}:GAD67-GFP* mice, there was a loss of GAD67-GFP⁺ interneurons in the CC (**B1-B2**) and AC (**G1-G2**) while the remaining neurons were mispositioned. The axons of the fornix were unfasciculated and were forming Probst bundles invading the septum (white arrowheads in **B1-B2**), while the axons of the AC failed to cross the midline (white arrowheads in **G1-G2**). **(C1-C2 and H1-H2)** In *Nkx2.1-Cre⁺/Rosa-DTA:GAD67-GFP* mice, GAD67-GFP⁺ interneurons were also missing and the others were mispositioned within the CC which was enlarged compared to the wild-type (compare **C1** with **A1**). The axons of the fornix were forming bundles as well (**C1-C2**), and the AC was divided into two tracts which were misrouted either ventrally or dorsally where part of the axons invaded the hippocampus, while part of the tract crossed the midline (white arrowheads in **H1-H2**). **(I1-I2)** In *Nkx2.1-Cre⁺/NSE-DTA:GAD67-GFP* mice, some of the GAD67-GFP⁺ interneurons were depleted in the AC. The axons of the fornix were forming bundles and those from the AC crossed the midline but the AC tract was thinner than in *Nkx2.1-Cre⁻/NSE-DTA:GAD67-GFP* mice (compare **I1-I2** with **D1-D2**), and the interneurons were also depleted (white arrowheads in **I1-I2**). **(E1-E2 and J1-J2)**. In *NG2-Cre⁺/Rosa-DTA:GAD67-GFP* mice, no axonal guidance defects were detectable within the fornix (compare **E2** with **A2**) despite a partial loss of GAD67-GFP⁺ interneurons in the AC (compare **J2** with **F2**). (AC) anterior commissure; (CC) corpus callosum; (CCi) cingulate cortex; (F) fornix; (PB) Probst bundles; (SEP) septum. Bar = 675 μ m in **A1, B1, C1, D1, E1, F1, G1, H1, I1** and **J1**; 320 μ m in **D2, H2** and **I2**; 160 μ m in **A2, B2, C2, E2, F2, G2** and **J2**.

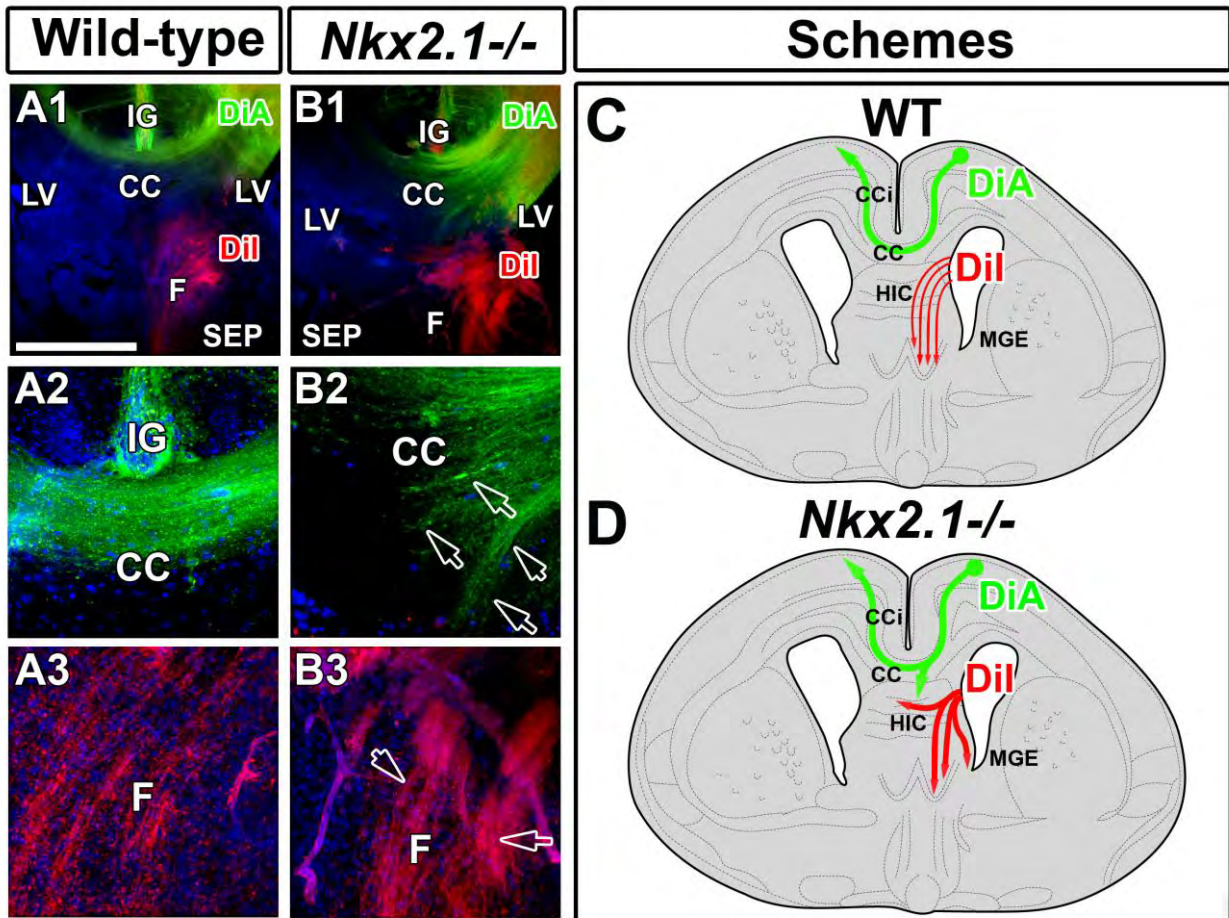
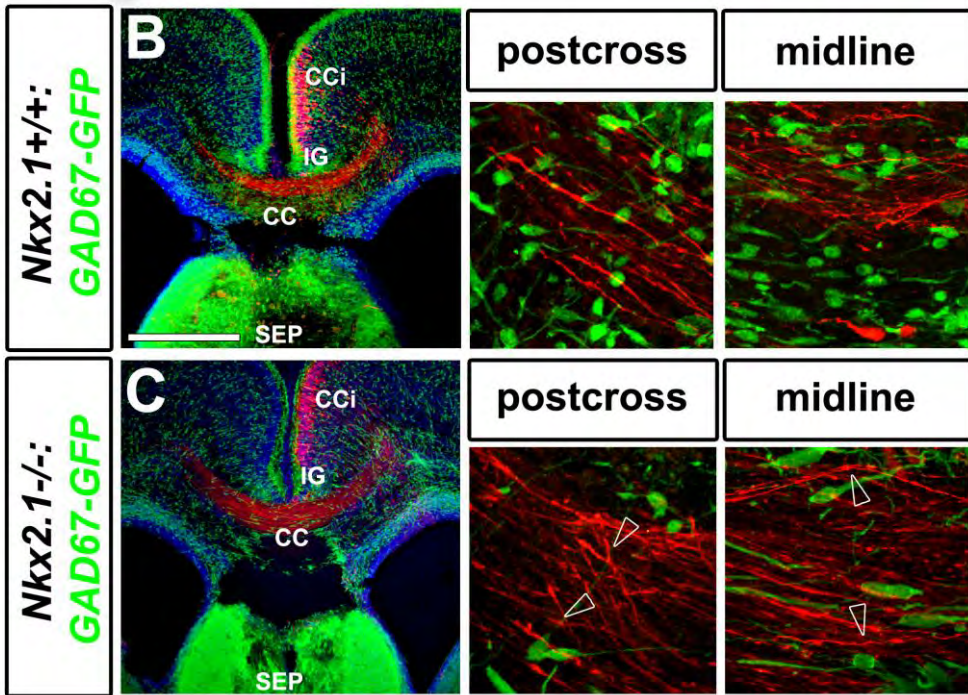
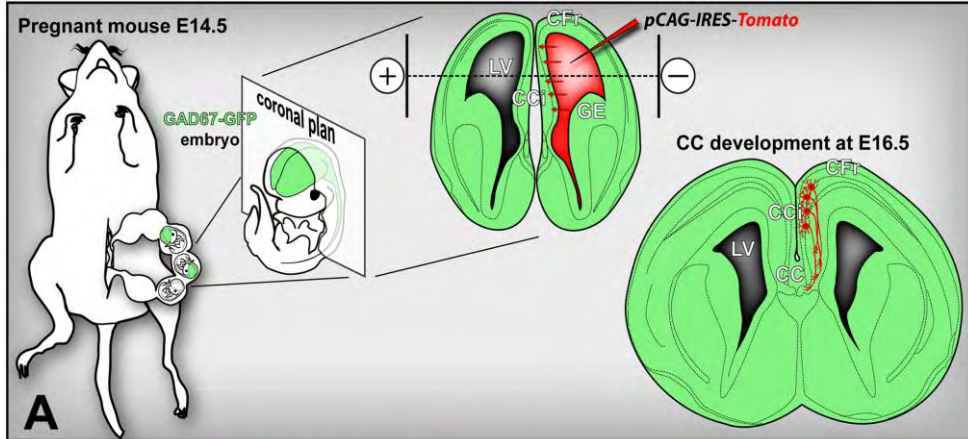


Figure 4. DiA and DiI injections reveal guidance defects in commissural axons of *Nkx2.1*^{-/-} mice brains.

DiA (in green) and DiI (in red) injections were made in the frontal cortex (CFr) and the hippocampal axons, in both wild-type (**A1-A3**) and *Nkx2.1*^{-/-} (**B1-B3**) mice brains, at E18.5. Cell nuclei were counterstained in blue with Hoechst. (**C** and **D**) Schematics representing the direction of growth of the commissural axons labelled by DiA (in the CC) and DiI (in the HIC) injections in wild-type (**C**) and *Nkx2.1*^{-/-} (**D**) brains. (**A1, A2** and **C**) In the wild-type, the axons from the callosal projecting neurons situated in the CFr, labelled by the DiA, are properly fasciculated in the dorsal path of the CC and cross the midline, while the hippocampal axons, labelled by the DiI are well organized in the fornix (**A1, A3** and **C**). In *Nkx2.1*^{-/-}, the callosal axons (in green) are misrouted from their normal trajectory towards the ventral path of the CC and the HIC (**B1**, open arrows in **B2** and **D**), while the hippocampal axons are unfasciculated and form bundles in the fornix (**B1**, open arrows in **B3** and **D**). (**CC**) corpus callosum; (**CCi**) cingulate cortex; (**F**) fornix; (**IG**) indusium griseum; (**HIC**) hippocampal commissure; (**LV**) lateral ventricle; (**MGE**) medial ganglionic eminence; (**SEP**) septum. Bar = 675 μ m in **A1** and **B1**; 160 μ m in **A2, A3, B2** and **B3**.

I.U. electroporation of *pCAG-Tomato* in *GAD67-GFP+* embryos



E16.5 *pCAG-Tomato* I.U. electroporation + 1DIV Time-lapse

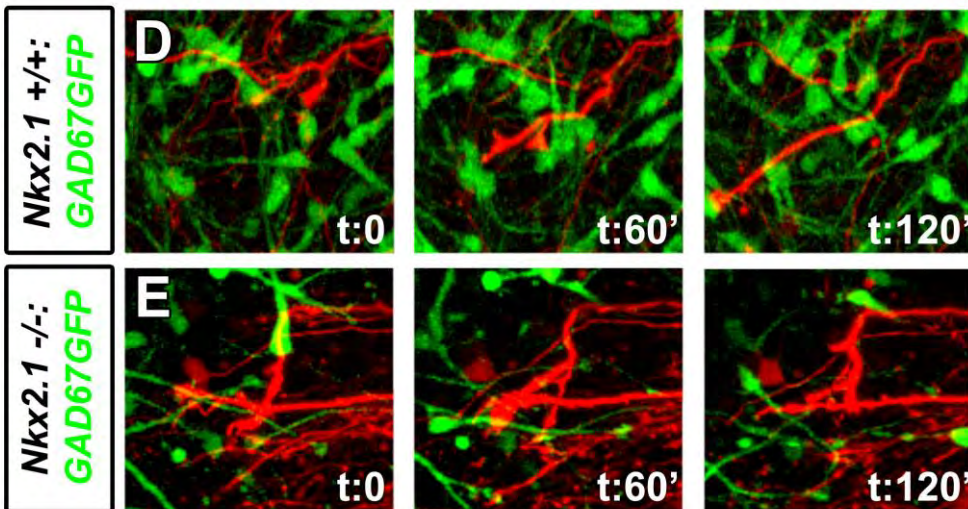
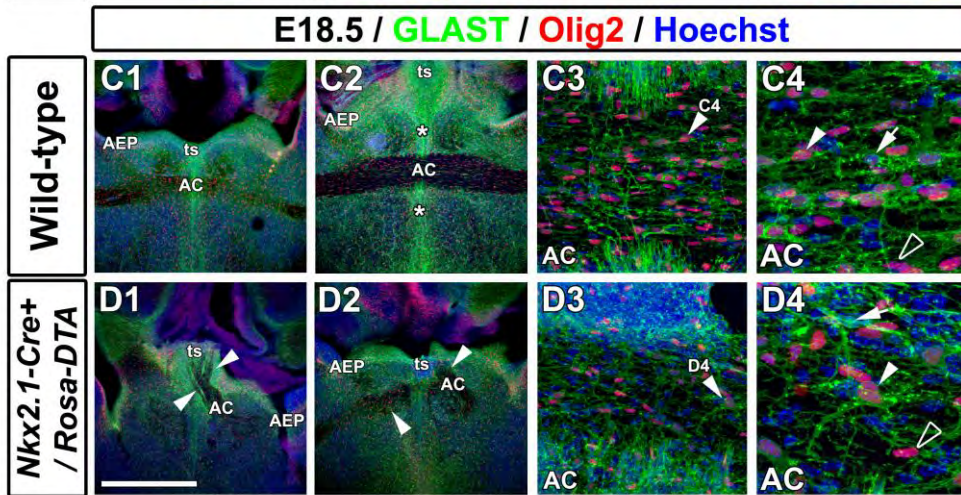
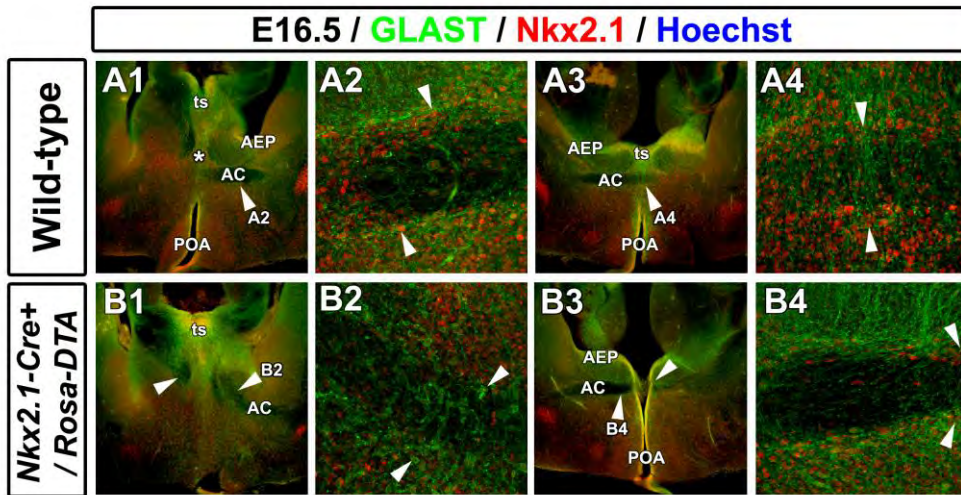


Figure 5. *In utero* electroporation of a *pCAG-tomato* plasmid reveals guidance defects in the callosal axons of *Nkx2.1*^{-/-}:*GAD67-GFP* mice brains.

(A) Experimental paradigm used to study cell interactions between callosal pioneering axons labelled with the red fluorescent protein Tomato and *GAD67-GFP*⁺ CC neurons. A *pCAG-Ires-Tomato* plasmid was injected into the lateral ventricle and electroporated into the dorsal pallium, to label the callosal projecting neurons, of E14.5 *GAD67-GFP*⁺ living embryos that were allowed to develop until E18.5. (B and C) Double immunohistochemistry for the GFP and the tomato on CC coronal sections from *Nkx2.1*^{+/+}:*GAD67-GFP*⁺ (B) and *Nkx2.1*^{-/-}:*GAD67-GFP*⁺ (C) mice brains at E18.5. Cell nuclei were counterstained in blue with Hoechst. The general callosal axon navigation seems to be preserved in the mutants compared to WT brains (compare C with B). Postcross and midline panels are showing higher magnifications of the callosal axons (in red) and the *GAD67-GFP*⁺ interneurons (in green). In the *Nkx2.1*^{-/-}:*GAD67-GFP*⁺ CC, there was a loss of *GAD67-GFP*⁺ neurons and the axons were not properly fasciculated and made aberrant branches that extended in wrong directions (open arrowheads). (D-E) High power views of *in vitro* time-lapse sequences over a period of 120 minutes (at 20 minute intervals) of Tomato-labeled callosal axons and *GAD67-GFP*⁺ neurons on coronal CC slices of E16.5 *Nkx2.1*^{+/+}:*GAD67-GFP*⁺ and *Nkx2.1*^{-/-}:*GAD67-GFP*⁺ embryos. In the *Nkx2.1*^{-/-} brains, though the callosal axons progressed along normal path, they displayed slower and disoriented branch extensions. (CC) corpus callosum; (CCi) cingulate cortex; (CFr) frontal cortex; (IG) indusium griseum; (LV) lateral ventricle; (SEP) septum. Bar = 500 μ m in B and C; 40 μ m in postcross and midline panels; 25 μ m in D and E.



E Loss of GLAST+/Olig2-, GLAST-/Olig2+ and GLAST+/Olig2+ glia in the AC

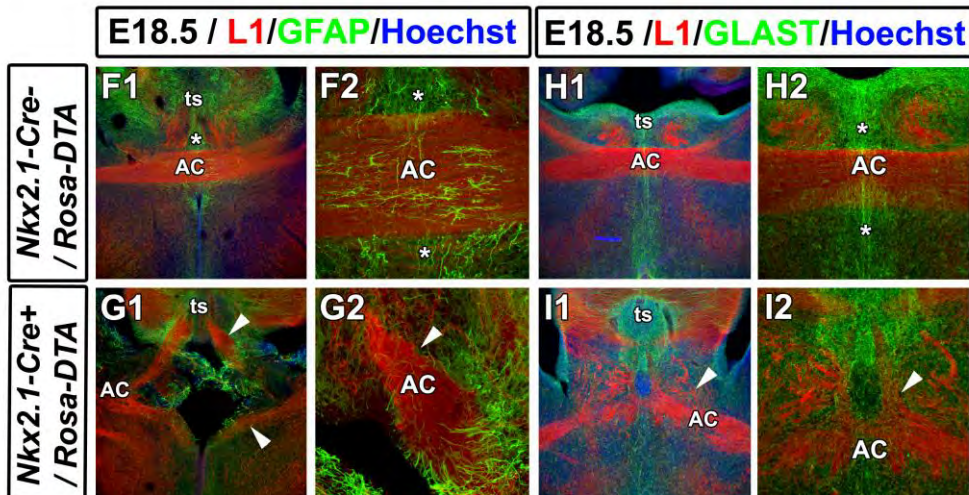
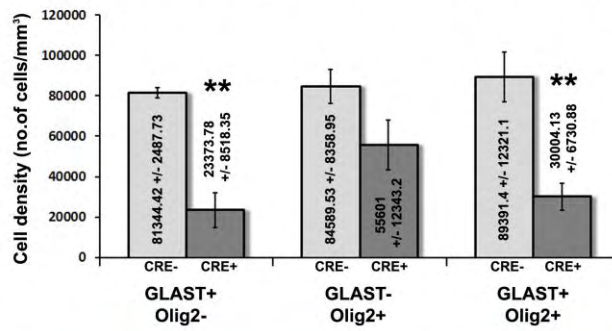


Figure 6. Guidance defects in the AC of *Nkx2.1-Cre⁺/Rosa-DTA* mice due to the loss of GLAST⁺ glia

(A-D) Double immunocytochemistry for GLAST and Nkx2.1 **(A-B)** and GLAST and Olig2 **(C-D)** on AC coronal slices from wild-type **(A1-A4 and C1-C4)** and *Nkx2.1-Cre⁺/Rosa-DTA* **(B1-B4 and D1-D4)** mice at E16.5 **(A-B)** and E18.5 **(C-D)**. **(E)** Quantification of the GLAST⁺/Olig2⁻, GLAST⁻/Olig2⁺ and GLAST⁺/Olig2⁺ glial cells in *Nkx2.1-Cre⁻/Rosa-DTA* and *Nkx2.1-Cre⁺/Rosa-DTA* mice. **(F-I)** Double immunohistochemical staining for L1 and GFAP **(F-G)** and for L1 and GLAST **(H-I)** on AC coronal sections from *Nkx2.1-Cre⁻/Rosa-DTA* **(F1-F2 and H1-H2)** and *Nkx2.1-Cre⁺/Rosa-DTA* **(G1-G2 and I1-I2)** mice brains at E18.5. Cell nuclei were counterstained in blue with Hoechst **(C1-D4, F1, G1, H1 and I1)**.

(A1-A4 and B1-B4) In wild-type animals **(A1-A4)** as well as in *Nkx2.1-Cre⁺/Rosa-DTA* **(B1-B4)** mice, the GLAST⁺ precursor cells of the ts, the AEP and the POA are regulated by Nkx2.1. In the wild-type, the AC tract is surrounded by numerous Nkx2.1⁺/GLAST⁺ glial cells (white arrowheads in **A3-A4**). However, in *Nkx2.1-Cre⁺/Rosa-DTA* **(B1-B4)** mice, the AC axons are misrouted towards the ts (white arrowheads in **B1** and **B3**). A closer look to the AC tract reveals a loss of Nkx2.1⁺/GLAST⁺ glia forming a palisade encircling the AC axons (white arrowheads in **B2** and **B4**). **(C1-C4)** In wild-type mice, the ts being a germinal region generates numerous GLAST⁺/Olig2⁻ (white arrow in **C4**), GLAST⁻/Olig2⁺ (open arrowhead in **C4**) and GLAST⁺/Olig2⁺ (white arrowhead in **C4**) glial cells. The AC axons are well fasciculated and cross the midline. **(D1-D4)** In *Nkx2.1-Cre⁺/Rosa-DTA* mice, the GLAST⁺/Olig2⁻ (white arrow in **D4**), GLAST⁻/Olig2⁺ (open arrowhead in **D4**) and GLAST⁺/Olig2⁺ (white arrowhead in **D4**) glial cells of the ts are still partially generated but the AC axons are deflected towards the ts and penetrate that region instead of crossing the midline (white arrowheads in **D1** and **D2**).

(E) The quantification of the GLAST⁺/Olig2⁻, GLAST⁻/Olig2⁺ and GLAST⁺/Olig2⁺ glial cells in the midline of the AC, revealed a significant decrease of GLAST⁺ cells in *Nkx2.1-Cre⁺/Rosa-DTA* mice compared to control mice. Bars (mean ± SEM from a sample of n=5 sections in *Nkx2.1-Cre⁻/Rosa-DTA*, n=5 sections *Nkx2.1-Cre⁺/Rosa-DTA*).

(F1-F2 and H1-H2) In *Nkx2.1-Cre⁻/Rosa-DTA* mice, the L1⁺ axons of the AC (in red) were well fasciculated and properly crossing the midline **(F1-F2 and H1-H2)**, while the GFAP⁺ **(F1-F2)** or GLAST⁺ **(H1-H2)** astroglial cells (in green) were equally dispersed throughout the AC midline **(F2 and H2)**. **(G1-G2 and I1-I2)** In *Nkx2.1-Cre⁺/Rosa-DTA* mice, the AC was divided into two tracts which were misrouted either ventrally or dorsally where part of the axons invaded the hippocampus, while few others were able to cross the midline (white arrowheads in **G1-G2 and I1-I2**). The GFAP⁺ and GLAST⁺ astroglial cells were completely mispositioned (compare **G1-G2** with **F1-F2** and compare **I2** with **H2**). **(AC)** anterior commissure; **(AEP)** anterior entopeduncular area; **(GW)** glial wedge; **(POA)** preoptic area; **(ts)** triangular septal nucleus. Bar = 675 µm in **A1, A3, B1, B3, C1, C2, D1, D2, F1, G1, H1 and I1**; 320 µm in **F2 and G2**; 160 µm in **H2 and I2**; 100 µm in **A2, A4, B2, B4, C3 and D3**; 50 µm in **C4 and D4**.

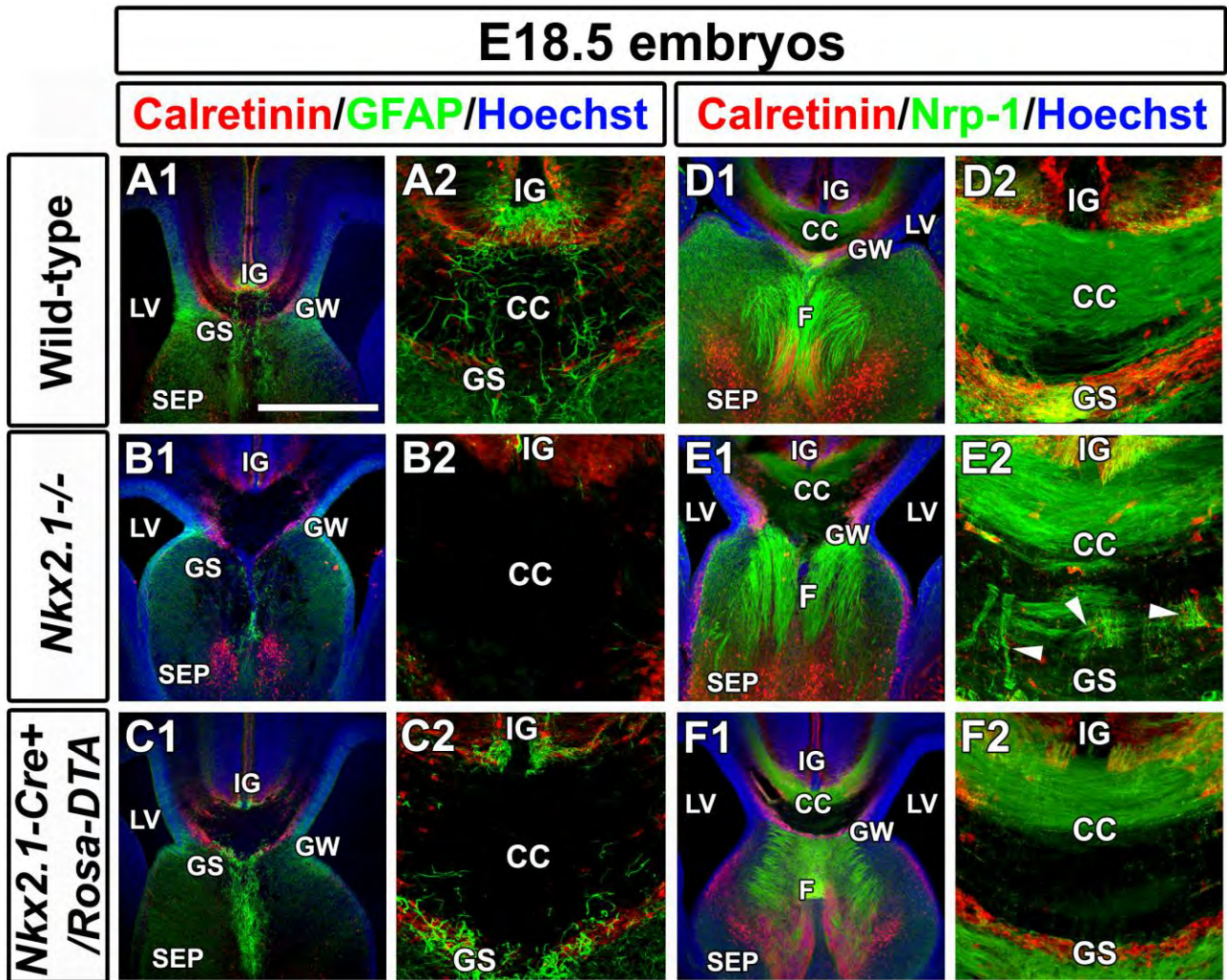


Figure 7. Loss of astroglial cells and axonal guidance defects in *Nkx2.1*^{-/-} and *Nkx2.1-Cre*⁺/*Rosa-DTA* mutant mice brains.

(A-H) Double immunohistochemical staining for Calretinin and GFAP **(A-C)** and for Calretinin and Nrp-1 **(D-F)** on CC coronal sections from wild-type **(A1-A2 and D1-D2)**, *Nkx2.1*^{-/-} **(B1-B2 and E1-E2)**, and *Nkx2.1-Cre*⁺/*Rosa-DTA* **(C1-C2 and F1-F2)** mice brains at E18.5. Cell nuclei were counterstained in blue with Hoechst **(A1, B1, C1, D1, E1 and F1)**. **A2, B2, C2, D2, E2 and F2** are higher power views of the CC seen in **A1, B1, C1, D1, E1 and F1** respectively.

(A1-A2 and D1-D2) In the CC of wild-type mice brains, the Calretinin⁺ neurons (in red) were properly positioned in three stripes delineating the dorsal and the ventral path of the CC. The ventral strip was situated at the level of the GS. Numerous GFAP⁺ astroglial cells (in green) were populating the IG, the GS and the CC midline **(A1-A2)**. The callosal axons from the dorsal path, labelled by Nrp-1 (in green), were properly fasciculated and crossed the midline **(D1-D2)**. **(B1-B2 and E1-E2)** In *Nkx2.1*^{-/-} mice, the Calretinin⁺ neurons lost their proper position especially within the GS. **(B1-B2)** The GFAP⁺ astroglial cells of the IG, the GS and the CC midline were completely lost, which was accompanied by the misrouting of dorsal Nrp-1⁺ callosal axons towards the ventral path of the CC in which they were forming bundles **(E1 and white arrowheads in E2)**. The axons of the fornix were also unfasciculated (compare **E1** with **D1**). **(C1-C2 and F1-F2)** In *Nkx2.1-Cre*⁺/*Rosa-DTA* mice, the CR⁺ neurons were properly positioned and the Nrp-1⁺ callosal axons from the dorsal path were well fasciculated (compare **F1-F2** with **D1-D2**) despite the depletion of the GFAP⁺ astroglial cells from the CC midline (compare **C1-C2** with **A1-A2**). The CC was enlarged compared to the wild-type (compare **C1-C2** with **A1-A2** and **F1-F2** with **D1-D2**). **(AC)** anterior commissure; **(CC)** corpus callosum; **(F)** fornix; **(GS)** glial sling; **(GW)** glial wedge; **(IG)** indusium griseum; **(LV)** lateral ventricle; **(SEP)** septum; **(ts)** triangular septal nucleus. Bar = 675 μm in **A1, B1, C1, D1, E1 and F1**; 160 μm in **A2, B2, C2, D2, E2 and F2**

E16.5 / Slit2 / GFAP / Hoechst

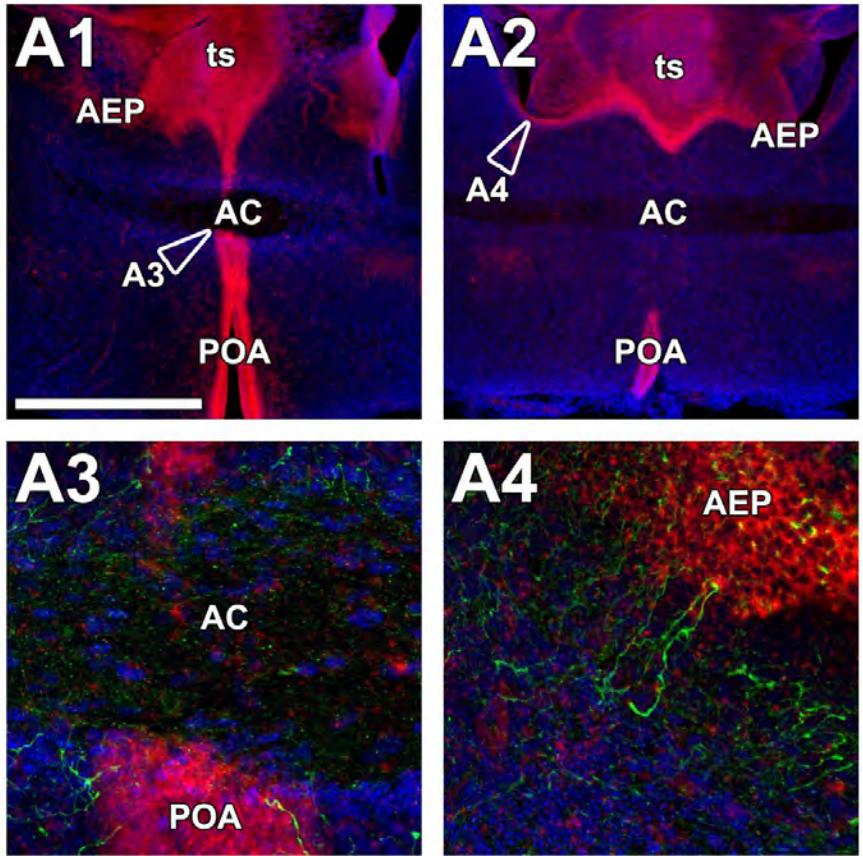
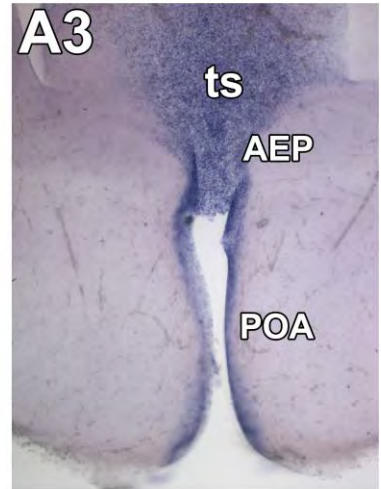
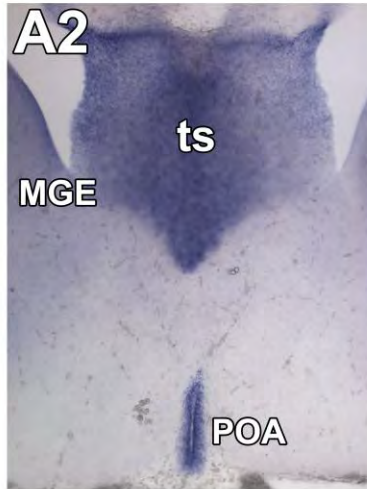
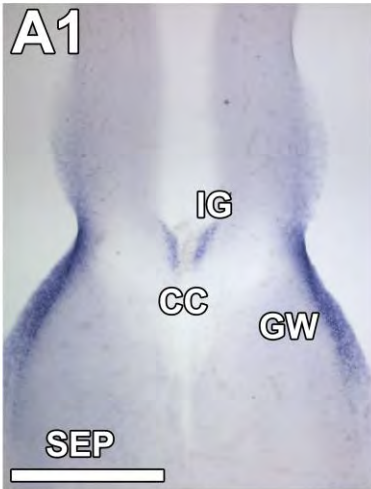


Figure 8. Expression of Slit2 by the Nkx2.1⁺ precursors of the ts, the AEP and the POA.

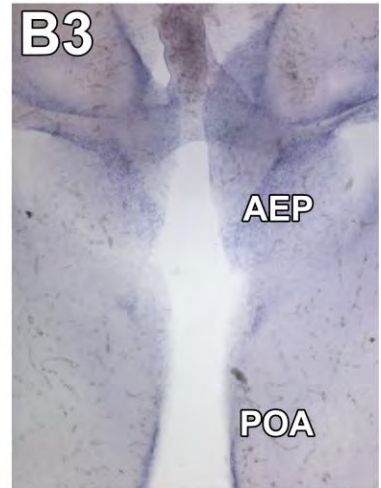
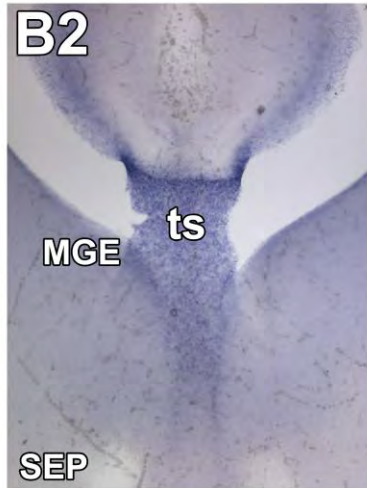
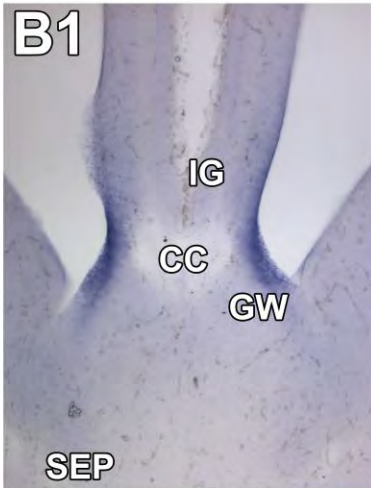
In situ hybridization for Slit2 (**A1-A2**) and Slit2 and GFAP (**A3-A4**) on AC coronal slices from wild-type mice at E16.5. Cell nuclei were counterstained in blue with Hoechst. The Nkx2.1 regulated precursors of the ts, the AEP and the POA strongly express the repulsive molecule Slit2. The radial precursors close to the sub-ventricular zone of the POA (**A3**) and those close to the AEP (**A4**) have begun to express GFAP. (**AC**) anterior commissure; (**AEP**) anterior entopeduncular area; (**POA**) preoptic area; (**ts**) triangular septal nucleus. Bar = 675 μ m in **A1** and **A2**; 50 μ m in **A3** and **A4**.

E16.5 / Slit2

Wild-type



Nkx2.1^{-/-}



Nkx2.1-Cre⁺/Rosa-DTA

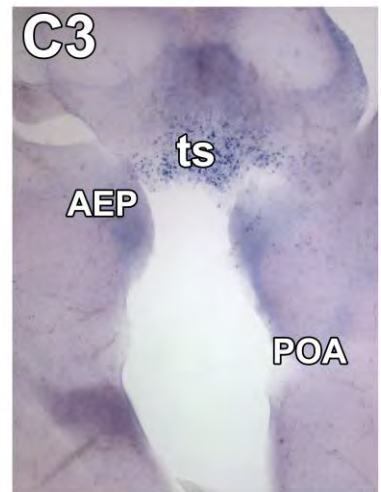
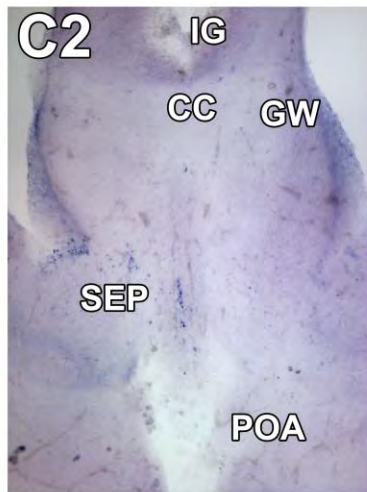
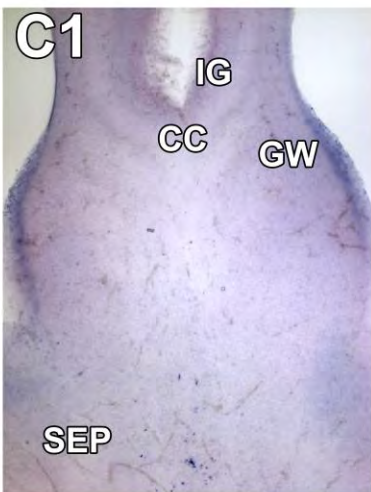


Figure 9. Slit2 expression in Nkx2.1⁺ precursors is strongly decreased in *Nkx2.1*^{-/-} and *Nkx2.1-Cre*⁺/*Rosa-DTA* compared to control.

(A-D) *In situ* hybridization for Slit2 on coronal slices from wild-type **(A1-A3)**, *Nkx2.1*^{-/-} **(B1-B3)**, and *Nkx2.1-Cre*⁺/*Rosa-DTA* **(C1-C3)** mice at E16.5.

(A1-A3) In wild-type mice, the Nkx2.1⁺ precursors of the IG, the MGE, the AEP, the POA and the ts strongly express the mRNA for the repellent guidance molecule Slit2. It is also expressed in the VZ of the GW which is *Nkx2.1*-negative **(A1)**. In *Nkx2.1*^{-/-} **(B1-B3)** and *Nkx2.1-Cre*⁺/*Rosa-DTA* **(C1-C3)** mice, the expression of Slit2 mRNA is reduced in the IG, the ts, the AEP and the POA compared to control mice. Only the precursors of the GW express a normal level of Slit2 **(B1 and C1)**. **(AEP)** anterior entopeduncular area; **(CC)** corpus callosum; **(GW)** glial wedge; **(IG)** indusium griseum; **(MGE)** medial ganglionic eminence; **(POA)** preoptic area; **(SEP)** septum, **(ts)** triangular septal nucleus. Bar = 500 μm in **A-C**.

Table 1:

	Loss of cells and commissural guidance defects in the mutants		
commissures	CC	fornix	AC
<i>Nkx2.1</i>^{-/-}	loss of ~75% of GABAergic interneurons, loss and mispositioning of CR+ glutamatergic neurons, complete loss of GFAP+ astrocytes in the IG, CC midline and GS, loss of GLAST+/Olig2- and GLAST-/Olig2+ glia, the axons of the dorsal path of the CC are deflected ventrally, making aberrant branches, growing slowly, in wrong directions and the CC tract is enlarged	loss of GABAergic interneurons, loss of CR+ glutamatergic neurons, loss of GFAP+ astrocytes of the MZG, the axons are unfasciculated and forming Probst bundles in the septum	loss of ~89% of GABAergic interneurons, nearly complete loss of all glia of the midline, the axons of the AC tract are not able to reach the midline and are deflected ventrally
<i>Nkx2.1-Cre⁺/Rosa-DTA</i>	loss of ~84% of GABAergic interneurons, partial loss of GFAP+ astrocytes only in the CC midline, the general navigation of the callosal axons looks normal but the CC tract is enlarged	no loss of the GFAP+ astrocytes of the MZG, the hippocampal axons of the fornix are unfasciculated and forming Probst bundles in the septum	loss of ~84% of GABAergic interneurons, partial loss and complete disorganization of the GFAP+ astrocytes of the palisade, loss of ~65% of the GLAST+/Olig2- and GLAST+/Olig2+ glia in the tract, the tract is split into two or three tracts which are misrouted either ventrally or dorsally towards the ts where the AC axons invade the hippocampus and only few axons are able to cross the midline
<i>Nkx2.1-Cre⁺/NSE-DTA</i>	loss of ~63% of GABAergic interneurons, no loss of GFAP+ astrocytes, the general navigation of the callosal axons looks normal	no loss of GFAP+ astrocytes of the MZG, at rostral level the hippocampal axons of the fornix are well fasciculated	loss of ~63% of GABAergic interneurons, no loss of the GFAP+ astrocytes of the palisade, the surface area of the AC tract is ~30% reduced, at caudal levels some axons of the AC intermingled with the axons of the fornix
<i>NG2-Cre⁺/Rosa-DTA</i>	loss of ~55% of NG2+ polydendrocytes, no significant loss of GABAergic interneurons, no loss of GFAP+ astrocytes, the general navigation of the callosal axons looks normal	no loss of GFAP+ astrocytes of the MZG, the hippocampal axons of the fornix are well fasciculated	loss of ~55% of NG2+ polydendrocytes, no significant loss of GABAergic interneurons, no loss of the GFAP+ astrocytes of the palisade, the general navigation of the axons of the AC tract looks normal

RESULTS

SECTION 3:

TRANSIENT *NKX2.1*-DERIVED POLYDENDROCYTES ARE REQUIRED FOR VESSEL NETWORK FORMATION DURING EMBRYONIC DEVELOPMENT

We have discovered that during embryonic development polydendrocytes of the telencephalon originate from the ventral telencephalon instead of the dorsal telencephalon. While the *Nkx2.1* homeobox gene is known to be required for the specification of GABAergic interneurons in the ventral telencephalon, we have found that, in addition, it controls polydendrocyte specification and differentiation. Interestingly, *Nkx2.1*-derived polydendrocytes were found to regulate brain angiogenesis (vascular morphology and branching). Altogether, our study reveals novel functions of transient *Nkx2.1*-derived polydendrocytes in vascular development and brings new perspectives about the role of these glial cells in these processes.

IDENTIFICATION OF TRANSIENT *NKX2.1*-DERIVED POLYDENDROCYTES IN EMBRYONIC TELENCEPHALON

Polydendrocytes are considered as a distinct population of cells different from neurons, mature oligodendrocytes, astrocytes and microglia (Nishiyama, Watanabe et al. 2002; Nishiyama, Komitova et al. 2009). They express NG2 (Nerve/glia antigen 2 or CSPG for chondroitin sulfate proteoglycan) and Olig2 (Oligodendrocyte precursor bHLH transcription factors 2) but not GFAP (glial fibrillary acidic protein) and GLAST (Astrocyte-specific glutamate and aspartate transporter). They display complex highly branched morphology and are uniformly distributed within the grey and white matter throughout all layers. They generate oligodendrocytes *in vitro* and have been considered since a long time as oligodendrocyte progenitor cells (Nishiyama, Lin et al. 1996; Nishiyama, Lin et al. 1996; Polito and Reynolds 2005; Zhu, Bergles et al. 2008; Zhu, Hill et al. 2008; Nishiyama, Komitova et al. 2009). However, recently polydendrocytes have also been shown to differentiate into neurons and protoplasmic astrocytes in the grey matter as well as in the white matter (Rivers, Young et al. 2008; Zhu, Bergles et al. 2008; Zhu, Hill et al. 2008). Furthermore, electrophysiological studies indicate that polydendrocytes receive synaptic input from neurons, and probably participate to the neuronal network (Butt, Hamilton et al. 2005; Paukert and Bergles 2006). In this study, we first characterized the molecular identity and source of polydendrocytes that populate the telencephalon during embryonic development. Therefore, to selectively fate map the polydendrocytes, we crossed *NG2-Cre* mice (Xu, Tam et al. 2008; Zhu, Bergles et al. 2008) with the reporter *Rosa26-lox-STOP-lox-YFP* (*Rosa-YFP*) mice (Srinivas, Watanabe et al. 2001; Nakagawa, Oshima et al. 2006). Using *NG2-Cre⁺/Rosa-YFP* mice, we were able to trace the polydendrocytes within the dorsal telencephalon from

embryonic day 16.5 (E16.5) to E18.5 (Fig. 1a-e). At the midline, they populated the corpus callosum (CC), the cingulate bundle (CI) and the cingulate (CCi) and frontal (CFr) cortices. We found that the majority of the cell population visualized by the YFP signal co-expressed the transcription factors Olig2 and NG2, two well known markers for polydendrocytes, and also S100 β which is generally considered as a marker for astrocytes (Fig. 1a, 1b and 1c). The YFP signal in *NG2-Cre⁺/Rosa-YFP* mice was detected in a majority of NG2⁺ embryonic polydendrocytes of the dorsal telencephalon (71.7 \pm 14.6 % in the CC, 57 \pm 3.8 % in the CI and 69 \pm 5.3 % in the CCi at E16.5, n=3) (Supplementary Figure S1a). As expected, NG2-derived YFP⁺ polydendrocytes did not express the astrocytic markers GLAST and GFAP (Fig. 1d and 1e). On the other hand, the Cre-mediated recombination did not occur properly in the PDGFR- β ⁺ (Platelet-derived growth factor receptor beta) pericytes adjacent to the vessels. As a result, though NG2 is known to be expressed by pericytes (Levine and Nishiyama 1996; Stallcup 2002; Virgintino, Girolamo et al. 2007), we found only very few PDGFR- β ⁺ pericytes labeled for the YFP in the cerebral cortex of *NG2-Cre⁺/Rosa-YFP* mice (Fig. 2a).

We then looked at the possible subpallial origin of embryonic polydendrocytes since *Nkx2.1*-regulated precursors have been shown in embryos to produce transient oligodendrocytes in addition to giving rise to GABAergic interneurons (Nery, Wichterle et al. 2001; Kessaris, Fogarty et al. 2006). Using *Nkx2.1-Cre⁺/Rosa-YFP* mice, we were able to fate map multiple types of cells, generated by *Nkx2.1*⁺ subpallial domains, which populated the telencephalon from E16.5 to early postnatal ages (Fig. 1f-j). We found that the *Nkx2.1*-derived precursors produced YFP⁺/NG2⁺ polydendrocytes that migrate tangentially to the cortex, the CI and the CC (Fig. 1f). The YFP signal was detected in all NG2⁺ embryonic polydendrocytes of the dorsal telencephalon. *Nkx2.1*-derived polydendrocytes also expressed the Olig2 marker (Fig. 1g) and therefore, most probably corresponded to the transient oligodendrocyte population described previously (Nery, Wichterle et al. 2001; Kessaris, Fogarty et al. 2006). While expressing S100 β (Fig. 1h), *Nkx2.1*-derived YFP⁺ glia of the dorsal telencephalon did not express GLAST or GFAP (Fig. 1i and 1j). *Nkx2.1*-derived YFP⁺/NG2⁺ polydendrocytes were transient in nature since they disappeared abruptly from the cortex between P2 and P8 (Supplementary Fig. S2b and S2c). Interestingly, we never detected any YFP signal in the endothelial cells of the cerebral vasculature and in the pericytes surrounding the vessels (Fig. 2b and 2f). Therefore, in the dorsal telencephalon, the Cre-mediated recombination under the control of the *Nkx2.1* promoter takes place in GABAergic neurons and polydendrocytes only. To ascertain that the embryonic polydendrocytes of the telencephalon are derived from *Nkx2.1*⁺ domains, we studied the potential loss of polydendrocytes in the cortex (CCi) of *Nkx2.1*^{-/-} mice. Coherently with fate mapping results, we observed a complete loss of NG2⁺

polydendrocytes in the cortex of the *Nkx2.1*^{-/-} mice (Supplementary Fig. S3a and S3b). This confirms that subpallial domains are sites for early polydendrocytes genesis, a process under the regulation of Nkx2.1.

These results altogether unravel that, in embryos, transient polydendrocytes of the dorsal telencephalon are derived from Nkx2.1⁺ progenitors of the subpallium.

SPATIAL ASSOCIATION BETWEEN EMBRYONIC NKX2.1⁺ POLYDENDROCYTES AND DEVELOPING VESSELS

Interestingly, using *NG2-Cre⁺/Rosa-YFP* and *Nkx2.1-Cre⁺/Rosa-YFP* mice, we observed that during embryonic development YFP⁺/NG2⁺ polydendrocytes formed a complex cellular network around the cortico-cerebral vessels outlined by NG2, PECAM, Isolectin or PDGFR-β labeling (Fig. 2a-c, 2f, 2i and Supplementary Fig. S1b). We then aimed to determine if the distribution of the polydendrocytes is temporally and spatially consistent with their potential contribution towards the formation of the vascular network. Hence, we undertook a longitudinal analysis of this population during development to establish their relationship with the vessels in the cerebral cortex.

While at E12.5, absolutely no YFP⁺/NG2⁺ polydendrocytes were observed within the entire telencephalon, at E14.5, the first YFP⁺/NG2⁺ polydendrocytes were seen to emerge from the AEP and populated the primordium of the anterior commissure. Only at E16.5, the first YFP⁺/NG2⁺ polydendrocytes pioneers originating from the subpallium were entering the cortex, migrating within the marginal zone (MZ), subplate, intermediate zone (IZ) and sub-ventricular zone (SVZ) of the lateral cortical areas (not shown). From E16.5 to E18.5, YFP⁺/NG2⁺ polydendrocytes reached the midline and penetrated the CFr and the CCI (Fig. 1, 2 and Supplementary Fig. S1b). As such, they occupied the cortical areas four days after the blood vessels, since the blood vessels had already invaded the dorsal telencephalon by E12.5. Therefore, polydendrocytes were only present throughout the cerebral cortex during the late phase of angiogenesis when the vessels have sprout laterally and have formed new branches that have to fuse together to create the complex and final vascular network (Fig. 2). They were not localized specifically at sprouting tip cells or at branches fusion points but all along the vessel walls. A careful analysis using highly-magnified 3D confocal pictures combined with isosurface representations revealed that polydendrocytes make multiple close contacts with different cortical blood vessels and create bridges between neighboring vessels (Fig. 2f). Polydendrocytes in the cerebral cortex disappeared at P8, a time correlating with the final establishment of the vascular network.

Therefore, their location and timing of appearance raises the possibility that transient Nkx2.1⁺ polydendrocytes actively participate in the final branching and refinement of the cerebral vasculature.

NON-CELL AUTONOMOUS FUNCTION OF NKX2.1 IN CONTROLLING BRAIN ANGIOGENESIS

Angiogenesis is a complex process that implements the formation of the vascular network and involves multiple steps such as: sprouting, outgrowth and guidance of endothelial tip cells followed by stalk endothelial cells proliferation and lumen formation (Adams and Alitalo 2007). Moreover, this is accompanied by the formation of new branches and fusion between separate vessels. During this process, guidepost cells secrete growing or guidance factors to direct endothelial tip cells outgrowth and new branch formation (Carmeliet and Tessier-Lavigne 2005; Eichmann, Makinen et al. 2005). Interestingly, Nkx2.1 has been found to control brain angiogenesis in embryos by regulating endothelial precursor division in a cell autonomous manner (Vasudevan and Bhide 2008; Vasudevan, Long et al. 2008). However, in view of our results showing close association of Nkx2.1⁺ polydendrocytes with cortical vessels, we wondered whether the *Nkx2.1*-derived polydendrocytes are also involved in regulating brain angiogenesis in addition to the cell autonomous function of Nkx2.1. To test this hypothesis and to further discriminate between the cell- and non-cell- autonomous function of Nkx2.1 in regulating angiogenesis, we performed a cell ablating strategy.

Nkx2.1 has been found to specify the medial ganglionic eminence (MGE), the anterior entopeduncular area (AEP) and the anterior preoptic area (POA). In *Nkx2.1*^{-/-} mice, the progenitors originating from the MGE and AEP are re-specified to a more dorsal fate and are comparable to those of the LGE (Sussel, Marin et al. 1999). In addition to *Nkx2.1*^{-/-} mice, we used mice expressing a “floxed” diphtheria toxin gene that allows selective ablation of cells in the whole brain (*Rosa-DTA*) (Brockschneider, Pechmann et al. 2006). By crossing *Nkx2.1-Cre* mice with *Rosa26-DTA* mice that express the diphtheria toxin under the control of the Nkx2.1 promoter, only Nkx2.1-expressing cells were depleted. *Nkx2.1-Cre*⁺/*Rosa-DTA* mice compared to *Nkx2.1*^{-/-} mice allowed a more selective ablation of *Nkx2.1*-derived post-mitotic cells, since the diphtheria toxin expression under the control of Nkx2.1 promoter took several days. Nkx2.1⁺ precursors were not affected in *Nkx2.1-Cre*⁺/*Rosa-DTA* progenitor zones, while they exhibited a drastic reduction in *Nkx2.1*^{-/-} progenitor zones (Supplementary Fig. S1e-g). In both *Nkx2.1*^{-/-} and *Nkx2.1-Cre*⁺/*Rosa-DTA* dorsal telencephalon, *Nkx2.1*-derived post mitotic GABAergic neurons were depleted. A severe loss of at least 50% of GAD67-GFP⁺ GABAergic neurons was noticed in the medial cortex of *Nkx2.1*^{-/-}:*GAD67-GFP* and of

Nkx2.1-Cre⁺/Rosa-DTA:GAD67-GFP mice (Supplementary Fig. S4a-c and S4e-f). Additionally, staining for NG2 revealed a complete loss of polydendrocytes in the medial cortical areas of both *Nkx2.1^{-/-}* and of *Nkx2.1-Cre⁺/Rosa-DTA* mice compared to control mice (Supplementary Fig. S3a-c). In *Nkx2.1-Cre⁺/Rosa-DTA* mice, contrary to *Nkx2.1^{-/-}*, endothelial cells were not affected in an intrinsic manner, since there was no Cre-mediated recombination in these cell types after crossing *Nkx2.1-Cre* mice with *Rosa-DTA* mice. These results are in accordance with the absence of YFP expression in the vascular endothelial cells of *Nkx2.1-Cre⁺/Rosa-YFP* mice (Fig. 2b and 2f).

To verify the involvement of Nkx2.1 in regulating brain angiogenesis, firstly, we carefully studied the organization of the vascular network in *Nkx2.1^{-/-}* and *Nkx2.1-Cre⁺/Rosa-DTA* cortical preparations. We observed that brain vessels stained for vessel markers (NG2, PECAM or Isolectin) formed a poorly developed cortical vascular network in both *Nkx2.1^{-/-}* and *Nkx2.1-Cre⁺/Rosa-DTA* mice compared to WT mice (Fig. 2d, 2g-h and Supplementary Fig. S3a-c and S5a-b). Both mutant mice exhibited a drastic reduction of ramifications and connections between radially organized cortical vessels. Due to the absence of connectivity, the regular alveolar vascular pattern found in WT cortex was not observed any more in mutants, in which vessels formed only isolated units (Fig. 2g-h, Fig 3b and Supplementary Fig. S3a-c and S5a-b). After co-staining for Isolectin and Lymphocyte antigen LY-76 marker (Ter119) allowing the visualization of erythrocytes, analyses on 250 μ m thick sections revealed that the cortical vessels in *Nkx2.1-Cre⁺/Rosa-DTA* mice lost their regular diameter (Fig. 2g-h, arrowheads). Interestingly, erythrocytes were observed to accumulate at the level of enlarged vessel segments (Fig. 2h, Fig.3e and Supplementary Fig. S5e). Quantification using DAB staining that unravels the distribution of erythrocytes within the cerebral vascular network, confirmed that erythrocytes agglomerate inside poorly developed vessels of *Nkx2.1^{-/-}* and *Nkx2.1-Cre⁺/Rosa-DTA* mice (% of increase of erythrocytes clusters in the CI of *Nkx2.1^{-/-}* compared to WT: 107.14 ± 20.64 %, $p < 0.001$, $n = 9$ sections; % of increase of erythrocytes clusters in the CI of *Nkx2.1-Cre⁺/Rosa-DTA* compare to WT: 96.96 ± 39.80 %, $p < 0.05$, $n = 12$ sections) (Fig. 3h and table 2). Furthermore, we found a significant decrease in the number of individual erythrocytes in cortex of *Nkx2.1^{-/-}* mice compared to WT mice (Fig. 3h). These results strongly suggest blood circulation dysfunction in *Nkx2.1^{-/-}* and *Nkx2.1-Cre⁺/Rosa-DTA* mice. While the reduction of the vascular density was stronger in *Nkx2.1^{-/-}* than in *Nkx2.1-Cre⁺/Rosa-DTA* mice, similarities in nature and extent of vascular defects in both mice point out the non-cell autonomous function of Nkx2.1.

Since recent studies have shown that GABAergic interneurons regulate vessel dynamics (Cauli, Tong et al. 2004; Kocharyan, Fernandes et al. 2008), we wondered whether

the loss of cortical GABAergic interneurons noticed in *Nkx2.1^{-/-}* and in *Nkx2.1-Cre⁺/Rosa-DTA* mice might participate to the observed vascular defects. To test this hypothesis, we used mice expressing the “floxed” diphtheria toxin gene under the enolase neuronal promoter (*NSE-DTA*) that allows selective ablation of neuronal cells only (Kobayakawa et al., 2007). In the medial cortex of *Nkx2.1-Cre⁺/NSE-DTA:GAD67-GFP* mice, we noticed a severe depletion of GAD67-GFP⁺ GABAergic neurons equivalent to what we found in *Nkx2.1^{-/-}:GAD67-GFP* and *Nkx2.1-Cre⁺/Rosa-DTA:GAD67-GFP* mice (Supplementary Fig. S4d and S4e-f). In accordance with the neuronal specificity of the NSE promoter, the polydendrocytes were not affected in *Nkx2.1-Cre⁺/NSE-DTA* mice contrary to *Nkx2.1-Cre⁺/Rosa-DTA* mice (Supplementary Fig. S3). The loss of GAD67-GFP⁺ GABAergic interneurons in the *Nkx2.1-Cre⁺/NSE-DTA* cortex was never accompanied by any developmental defects of the vascular network (Supplementary Fig. S5c and S5f). Both cortical vessel densities highlighted by PECAM and erythrocytes distribution outlined after DAB staining in *Nkx2.1-Cre⁺/NSE-DTA*, equalled to that in WT mice, indicating that GABAergic interneurons did not participate at all in brain angiogenesis.

Altogether, these results strongly suggest that the loss of *Nkx2.1*-derived cells, most probably polydendrocytes, was responsible for a major part of the observed vascular ramification and network defects.

NKX2.1 CONTROLS CORTICAL BRAIN ANGIOGENESIS VIA THE ACTION OF NKX2.1-DERIVED POLYDENDROCYTES

To determine whether polydendrocytes may play a role as guidepost cells in the establishment of the vascular network, firstly, we used *NG2-Cre⁺/Rosa-DTA* mice in which only polydendrocytes were depleted (Fig. 2e, Supplementary Fig. S1c-d and S3d). We found a drastic loss of more than 50% of polydendrocytes in the cortex of *NG2-Cre⁺/Rosa-DTA* mutant embryos (NG2⁺ polydendrocytes: 18.96 ± 0.98 polydendrocytes in CCi sections of wild-type mice versus 8.52 ± 1.06 polydendrocytes in CCi sections of *NG2-Cre⁺/Rosa-DTA* mice, n=3 sections, p<0.01) (Supplementary Figure S1c and S1d). Consistent with the very low level of Cre-mediated recombination in the brain vessel pericytes of *NG2-Cre⁺/Rosa-YFP* mice, we did not notice any obvious loss of PDGFR- β ⁺ pericytes in the *NG2-Cre⁺/Rosa-DTA* cortex (compare Fig. 2e and Fig. 2c). Our analysis further showed that the loss of polydendrocytes gave rise to major alterations of brain vessels development (compare Fig. 2e and Fig. 2c, compare Fig. 3c and Fig. 3a and see Supplementary Fig. S1b and c). In *NG2-Cre⁺/Rosa-DTA* cerebral cortex, the vessels network was simplified and lost its regular alveolar organization due to the decrease of ramifications and connections between adjacent

radial vessels. Additionally, cortical vessels in mutants exhibited irregular diameters with an alternation of vessel segments that were larger or thinner than in WT mice. Quantifications after reconstruction of the vascular network on cortical sections, using the NeuroLucida software, confirmed that the vessels in *NG2-Cre⁺/Rosa-DTA* mice displayed a significant decrease in the number of intersections (nodes) and branches and the total length and volume of the vascular network were reduced compared to WT mice (% of reduction of nodes in *NG2-Cre⁺/Rosa-DTA* compare to *WT*: $16.23 \pm 4.33\%$, $p < 0.05$, $n = 8$ sections; % of reduction of branches in *NG2-Cre⁺/Rosa-DTA* compare to *WT*: $12.93 \pm 2.37\%$, $p < 0.05$, $n = 8$ sections ; % of reduction of the total length of the vascular network in *NG2-Cre⁺/Rosa-DTA* compare to *WT*: $16.5 \pm 1.88\%$, $p < 0.05$, $n = 8$ sections; % of reduction of the total volume of the vascular network in *NG2-Cre⁺/Rosa-DTA* compare to *WT*: $21.8 \pm 1.98\%$, $p < 0.05$, $n = 8$ sections; Fig. 3g and table 1). Moreover, DAB staining indicated that erythrocytes aggregated inside *NG2-Cre⁺/Rosa-DTA* cortical vessels (Compare Fig. 3f to 3d). After quantification, we found a significant increase in the number of erythrocyte aggregates in the cortex of *NG2-Cre⁺/Rosa-DTA* mice compared to WT mice (% increase of erythrocyte clusters in the CI of *NG2-Cre⁺/Rosa-DTA* compare to *WT*: $156.3 \pm 30.34\%$, $p < 0.0001$, $n = 20$ sections) (Fig. 3h and table 2).

To confirm the role of *Nkx2.1*-derived polydendrocytes in controlling vessel formation, we then carefully compared vascular defects in *Nkx2.1-Cre⁺/Rosa-DTA* and *NG2-Cre⁺/Rosa-DTA* mice. Interestingly, stainings with PECAM, Isolectin and PDGFR- β showed that in both mice, vascular development was impaired in a similar way while pericytes and endothelial cells remained intact (Fig. 2c-e and Fig. 3a-c). Vessels in *Nkx2.1-Cre⁺/Rosa-DTA* mice lost their regular diameter similar to those in *NG2-Cre⁺/Rosa-DTA* mice (Fig. 2g-h). Quantifications made after reconstructing the vascular network indicated that vessels in *Nkx2.1-Cre⁺/Rosa-DTA* displayed the same significant density reduction as in *NG2-Cre⁺/Rosa-DTA* mice with an equally significant decrease in the number of intersections/branches and in the length/volume of the vascular network (% reduction of nodes in *Nkx2.1-Cre⁺/Rosa-DTA* compare to *WT*: $14.1 \pm 4.8\%$, $p < 0.05$, $n = 8$ sections; % reduction of branches in *Nkx2.1-Cre⁺/Rosa-DTA* compare to *WT*: $14.7 \pm 4.9\%$, $p < 0.5$, $n = 8$ sections; % reduction of the total length of the vascular network in *Nkx2.1-Cre⁺/Rosa-DTA* compare to *WT*: $15.93 \pm 4.6\%$, $p < 0.5$, $n = 8$ sections; % reduction of the total volume of the vascular network in *Nkx2.1-Cre⁺/Rosa-DTA* compare to *WT*: $17.78 \pm 4.33\%$, $p < 0.5$, $n = 8$ sections; Fig. 3g and table 1). Finally, observations made at high magnification after Isolectin staining in both mutant mice did not reveal any defect in tip cell induction, sprouting and in macrophages recruitment, two processes required for vessels anastomosis (Adams and Alitalo 2007; Fantin,

Vieira et al. 2010) (Fig. 2i-j). The exactly similar vascular defects noticed in *Nkx2.1-Cre⁺/Rosa-DTA* mice and in *NG2-Cre⁺/Rosa-DTA* mice confirmed the involvement of transient *Nkx2.1*-derived polydendrocytes in controlling brain angiogenesis.

Our results, altogether, reveal that brain angiogenesis requires, in addition to the cell autonomous function of *Nkx2.1*, the presence of *Nkx2.1*-derived polydendrocytes. This study shows for the first time that polydendrocytes play a major role in brain angiogenesis. *Nkx2.1⁺* transient polydendrocytes form a dense cellular network that closely interacts with vessels, stimulates vessel branching/outgrowth and allows vessel connections. These cells may act as guidepost cells by secreting growing factors or guidance molecules required for the proper development and function of brain vessels.

FIGURES of section 3:

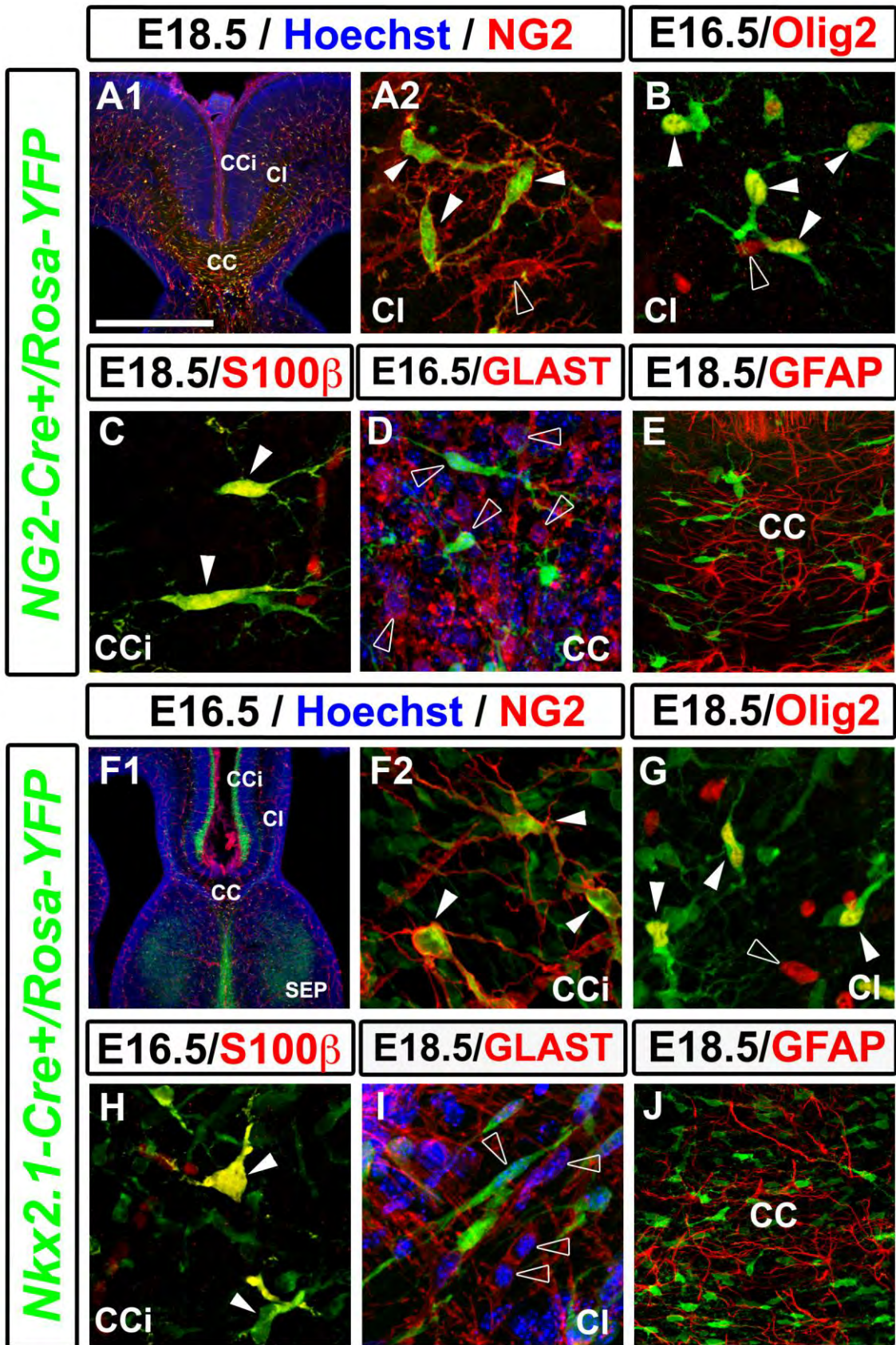


Figure 1. Fate mapping of polydendrocytes in the dorsal telencephalon of *NG2-Cre⁺/Rosa-YFP* and *Nkx2.1-Cre⁺/Rosa-YFP* embryos.

(A-E) Double immunohistochemistry for the YFP and NG2 (**A1-A2**), the YFP and Olig2 (**B**), the YFP and S100 β (**C**), the YFP and GLAST (**D**), and the YFP and GFAP (**E**) on telencephalic coronal slices of *NG2-Cre⁺/Rosa-YFP* mice at E16.5 (**B** and **D**) and E18.5 (**A1**, **A2**, **C** and **E**).

(F-J) Double immunohistochemistry for the YFP and NG2 (**F1-F2**), the YFP and Olig2 (**G**), the YFP and S100 β (**H**), the YFP and GLAST (**I**), and the YFP and GFAP (**J**) on telencephalic coronal slices of *Nkx2.1-Cre⁺/Rosa-YFP* mice at E16.5 (**F1**, **F2** and **H**) and E18.5 (**G**, **I** and **J**). In both *NG2-Cre⁺/Rosa-YFP* and *Nkx2.1-Cre⁺/Rosa-YFP* embryos, the Cre-mediated recombination occurs in NG2⁺, Olig2⁺ and S100 β ⁺ polydendrocytes (white arrowheads), whereas the recombination doesn't occur in GLAST⁺ (open arrowheads in **D** and **I**) and GFAP⁺ (**E** and **J**) astrocytes. (**CC**) corpus callosum; (**CCi**) cingulate cortex; (**CI**) cingulate bundle; (**SEP**) septum.

Bar = 675 μ m in **A1** and **F1**; 100 μ m in **E** and **J**; 50 μ m in **A2**, **B**, **C**, **D**, **F2**, **G**, **H** and **I**.

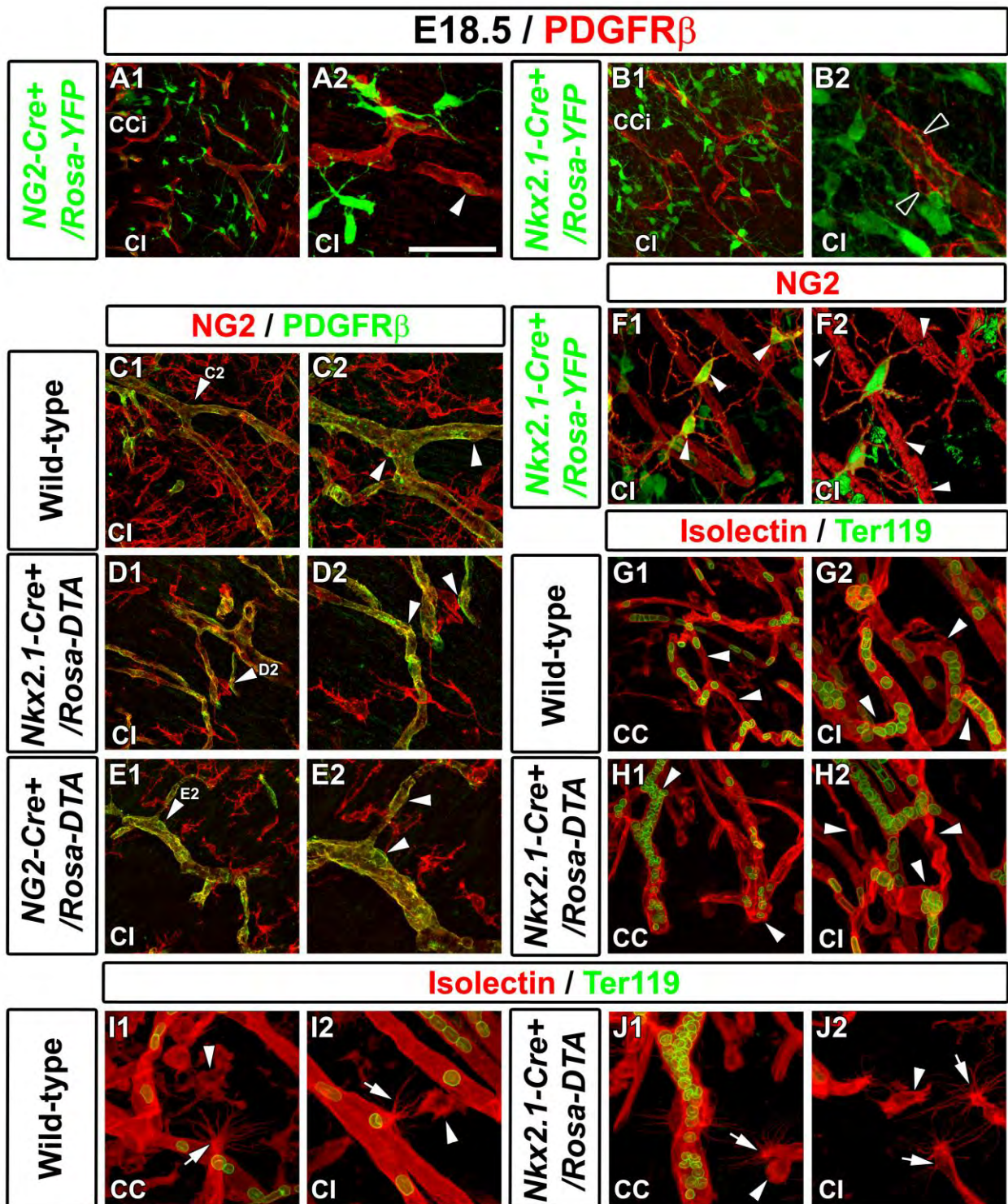


Figure 2. *Nkx2.1*-derived NG2⁺ polydendrocytes but not pericytes control blood vessels formation.

(A-B) Double immunohistochemistry for the YFP and PDGFR β on coronal cingulate cortex (CCi) and cingulate bundle (CI) sections of *NG2-Cre⁺/Rosa-YFP* (**A1-A2**) and *Nkx2.1-Cre⁺/Rosa-YFP* (**B1-B2**) mice at E18.5. The Cre-mediated recombination, visualized by the YFP signal, can be observed in few pericytes surrounding blood vessels in *NG2-Cre⁺/Rosa-YFP* mice (**A1** and arrowhead in **A2**), but not in *Nkx2.1-Cre⁺/Rosa-YFP* mice (**B1** and open arrowheads in **B2**).

(C-E) Double immunohistochemistry for NG2 and PDGFR β on coronal CI sections in wild-type (**C1-C2**), *Nkx2.1-Cre⁺/Rosa-DTA* (**D1-D2**) and *NG2-Cre⁺/Rosa-DTA* (**E1-E2**) mice at E18.5. The DTA under the control of *Nkx2.1* (**D1-D2**) and *NG2* (**E1-E2**) promoters selectively depletes NG2⁺ polydendrocytes but not pericytes (arrowheads in **C2**, **D2** and **E2**).

(F) Double immunohistochemistry for the YFP and NG2 on coronal CI sections in *Nkx2.1-Cre⁺/Rosa-YFP* (**F1**) mice at E18.5. **F2** is an isosurface reconstruction of the labeling seen in **F1**. The processes of the YFP⁺/NG2⁺ polydendrocytes are in close contact with adjacent blood vessels (arrowheads in **F1** and **F2**).

(G-J) Double immunohistochemistry for Isolectin and Ter119 on coronal CC and CI sections in wild-type (**G1-G2** and **I1-I2**) and *Nkx2.1-Cre⁺/Rosa-DTA* (**H1-H2** and **J1-J2**) mice at E18.5.

Both blood vessels morphology, as well as, the erythrocytes distribution are impaired in *Nkx2.1-Cre⁺/Rosa-DTA* mice (**H1-H2**) compared to wild-type (**G1-G2**). In the corpus callosum (CC) and the CI (**H1-H2**) of *Nkx2.1-Cre⁺/Rosa-DTA* mice, the blood vessels have a twisted shape and the erythrocytes are clustered (arrowheads in **H1** and **H2**) compared to the wild-type vessels that formed a regular network (arrowheads in **G1** and **G2**). In the CC and the CI of both wild-type (**I1-I2**) and *Nkx2.1-Cre⁺/Rosa-DTA* mice (**J1-J2**), guidepost macrophages labeled by the isolectin (arrowheads in **I1-I2** and **J1-J2**) are found in the close vicinity of the tip cells (arrows in **I1-I2** and **J1-J2**). The tip cells exhibit the same morphology and same number of filopodia with similar length in both circumstances.

Bar = 100 μ m in **A1** and **B1**; 60 μ m in **G1** and **H1**; 50 μ m in **C1**, **D1**, **E1** and **F1**; 40 μ m in **A2**, **B2**, **C2**, **D2**, **E2**, **F2**, **G2**, **H2**, **I1**, **I2**, **J1** and **J2**.

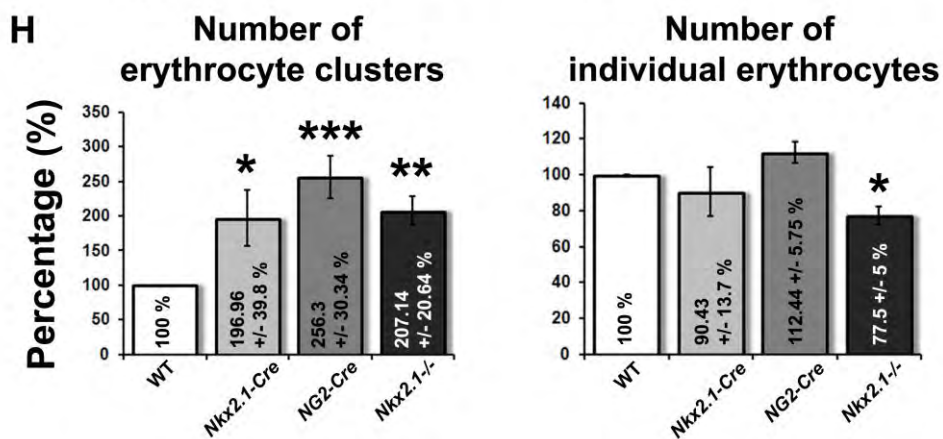
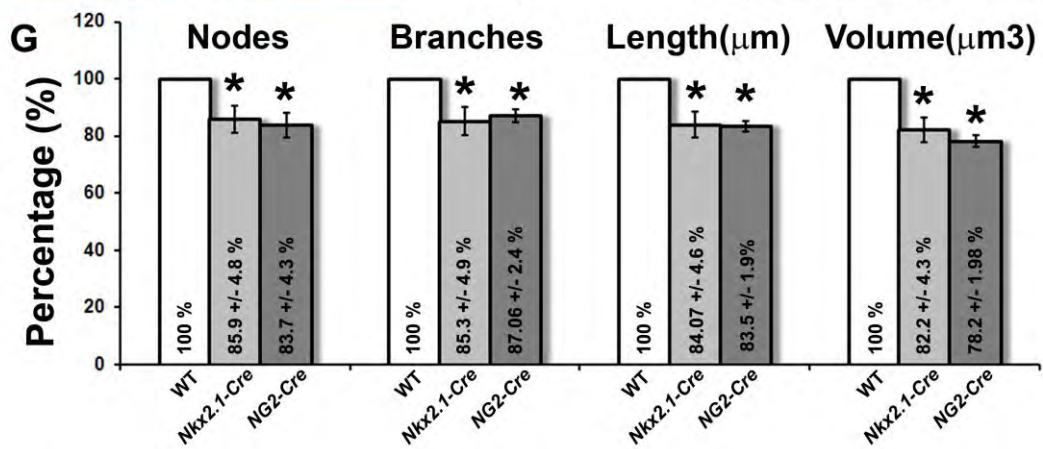
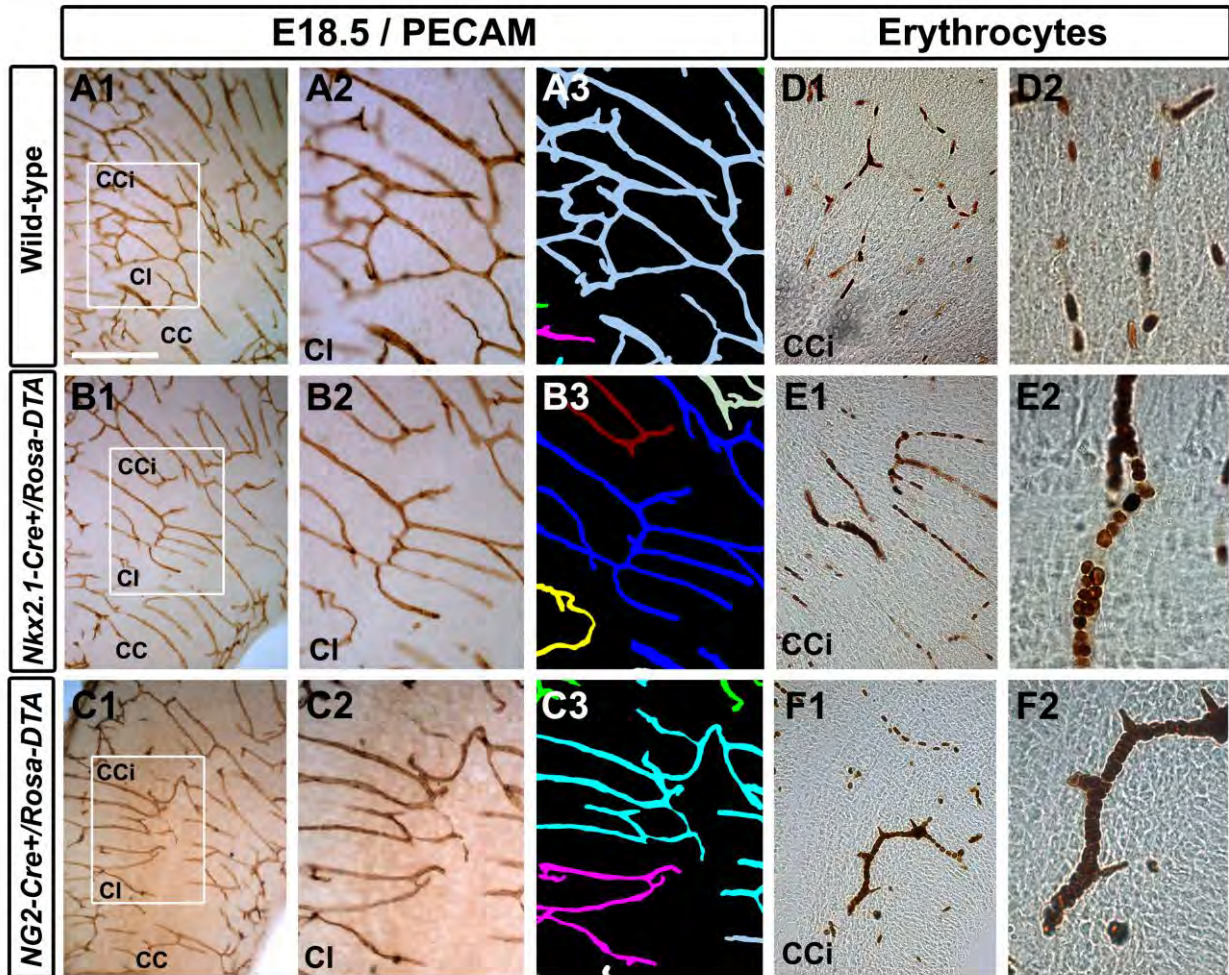


Figure 3. Blood vessels branches/network and erythrocytes distribution are impaired in *NG2-Cre⁺/Rosa-DTA* and *Nkx2.1Cre⁺/Rosa-DTA* mice.

(A-C) DAB staining for PECAM and reconstitution of the vascular network using the NeuroLucida tracing tool in wild-type (**A1-A3**), *Nkx2.1-Cre⁺/Rosa-DTA* (**B1-B3**), and *NG2-Cre⁺/Rosa-DTA* (**C1-C3**) cortical coronal sections at E18.5. **A2**, **B2** and **C2** are higher magnified views of the squared regions seen in **A1**, **B1** and **C1** respectively.

(D-F) DAB staining for erythrocytes in wild-type (**D1-D2**), *Nkx2.1-Cre⁺/Rosa-DTA* (**E1-E2**), and *NG2-Cre⁺/Rosa-DTA* (**F1-F2**) cortical coronal sections at E18.5.

(G) Bars (means \pm SEM from a sample of n=8 sections in WT, n=8 sections in *Nkx2.1-Cre⁺/Rosa-DTA* and n=8 sections in *NG2-Cre⁺/Rosa-DTA*) represent the percentages of vessel nodes, vessel branches, the length and volume of the vascular network in mutant mice compared to WT. The respective absolute values corresponding to the number of nodes, the number of branches, the length and the volume of the vascular network per CCi section (surface area/section = $5'707'280 \mu\text{m}^2$) are given in **table 1**. The number of vessel nodes and branches as well as the full length and volume of the vascular network are significantly decreased in *Nkx2.1-Cre⁺/Rosa-DTA* and *NG2-Cre⁺/Rosa-DTA* mice compared to wild-type.

(H) Bars (means \pm SEM from a sample of n=11 sections in WT, n=12 sections in *Nkx2.1-Cre⁺/Rosa-DTA*, n=20 sections in *NG2-Cre⁺/Rosa-DTA* and n=9 sections in *Nkx2.1^{-/-}*) represent the percentage of erythrocyte clusters and individual erythrocytes in mutant mice compared to WT. The respective absolute values corresponding to the number of erythrocyte clusters and the number of individual erythrocytes per CCi section (surface area/section = $20'150'800 \mu\text{m}^2$), are given in **table 2**. The number of erythrocyte clusters showed a significant increase in *Nkx2.1-Cre⁺/Rosa-DTA*, *NG2-Cre⁺/Rosa-DTA*, and *Nkx2.1^{-/-}* mutant mice compared to wild-type. The total number of individual erythrocytes remained unchanged in all mutant mice except for *Nkx2.1^{-/-}* mice in which a significant decrease was observed.

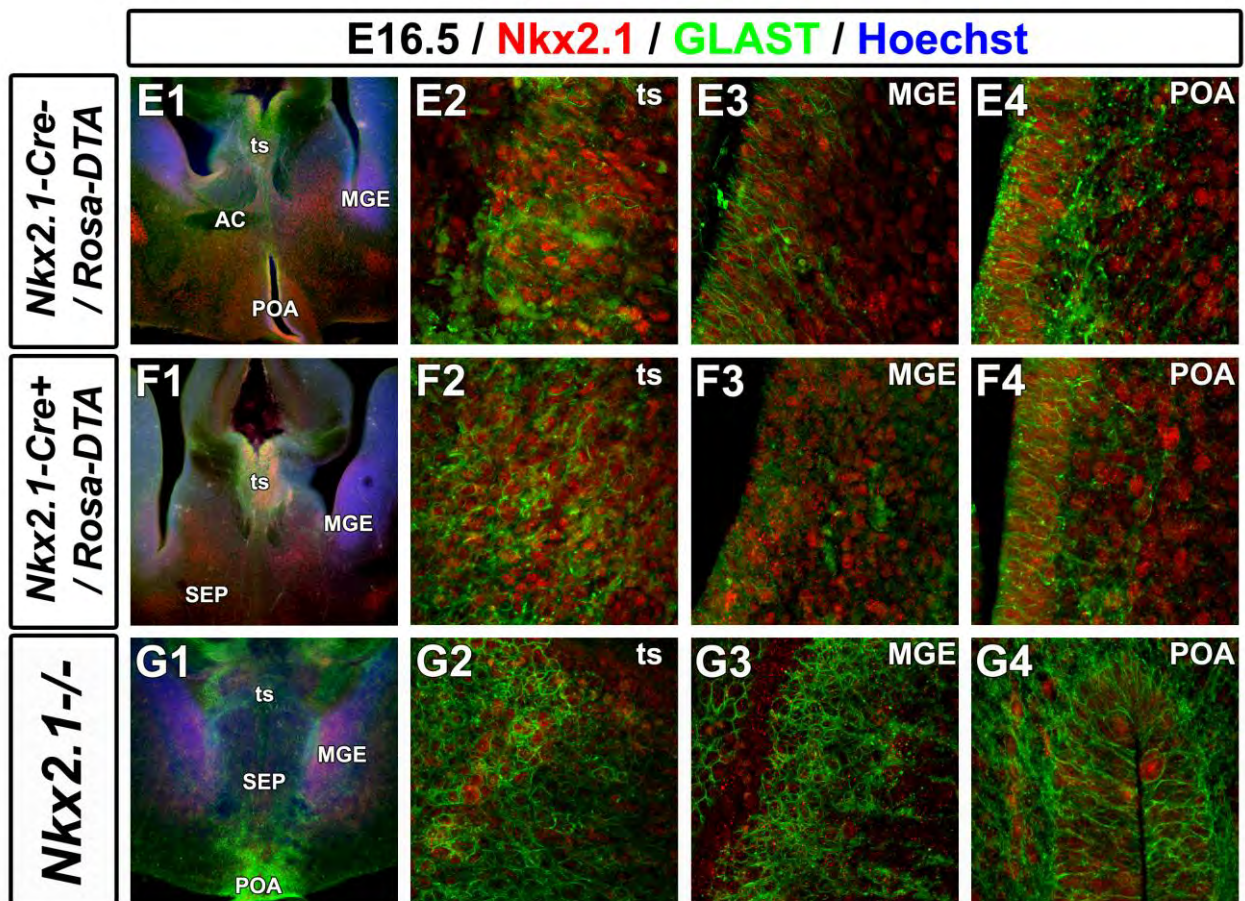
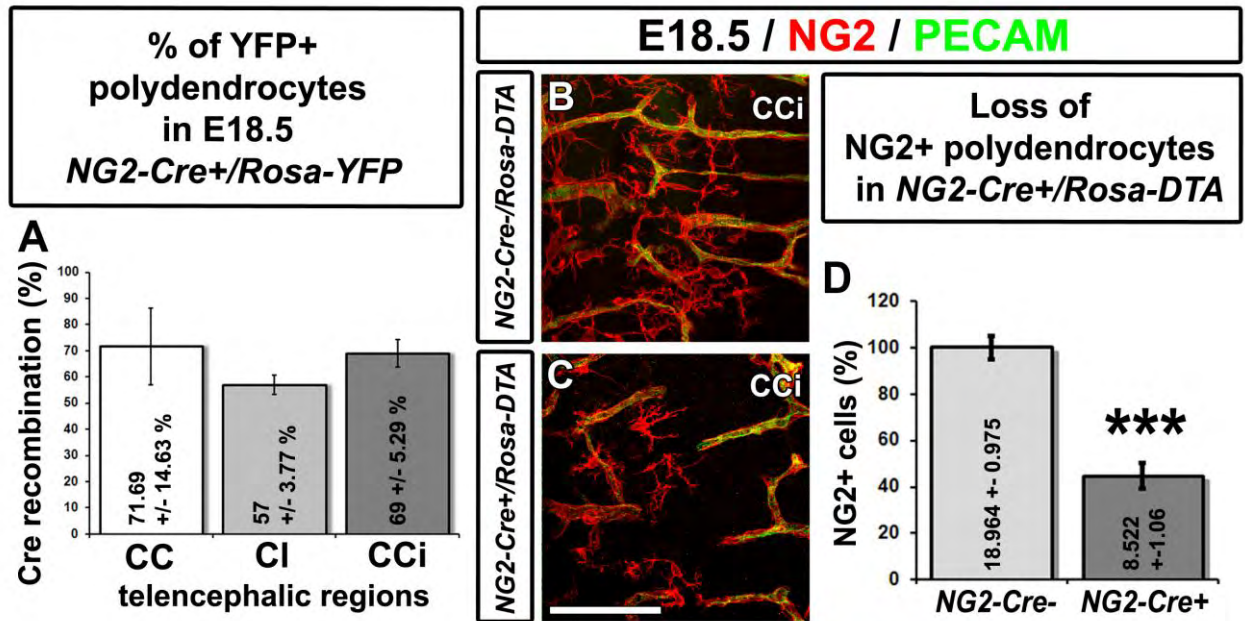
(CC) corpus callosum; **(CCi)** cingulate cortex; **(CI)** cingulate bundle. Bar = 250 μm in **A1**, **B1** and **C1**; 125 μm in **D1**, **E1** and **F1**; 62.5 μm in **A2**, **A3**, **B2**, **B3**, **C2** and **C3**; 50 μm in **D2**, **E2** and **F2**.

	Values (Means \pm SEM) for the vascular network per CCI section			
Genotype	Nodes number	Branches number	Vascular length(μm)	Vascular volume (μm³)
<i>Nkx2.1-Cre⁻/Rosa-DTA</i>	103.44 \pm 7.60	241.77 \pm 14.65	33562.08 \pm 1395.45	20302055.56 \pm 1290760.24
<i>Nkx2.1-Cre⁺/Rosa-DTA</i>	84.63 \pm 6.65	207.75 \pm 11.56	28616.85 \pm 1642.98	16692462.5 \pm 879025.98
<i>NG2-Cre⁻/Rosa-DTA</i>	135.50 \pm 8.60	299.50 \pm 16.89	35942.73 \pm 1072.18	20361275.24 \pm 1429685.42
<i>NG2-Cre⁺/Rosa-DTA</i>	109.25 \pm 6.20	250.87 \pm 13	31293.35 \pm 853.22	15921879.43 \pm 403438.62

Table 1: The values (Means \pm SEM) corresponding to the number of nodes, the number of branches, the length and the volume of the vascular network per CCI section are given for: (1) *Nkx2.1-Cre⁺/Rosa-DTA* mice and their corresponding control *Nkx2.1-Cre⁻/Rosa-DTA* mice and (2) *NG2-Cre⁺/Rosa-DTA* mice and their corresponding control *NG2-Cre⁻/Rosa-DTA* mice.

	Values (Means \pm SEM) per CCI section	
Genotype	Number of erythrocyte clusters per CCI section	Number of individual erythrocytes per CCI section
<i>Nkx2.1-Cre⁻/Rosa-DTA</i>	6.60 \pm 0.88	302.33 \pm 19.12
<i>Nkx2.1-Cre⁺/Rosa-DTA</i>	13.00 \pm 2.62	273.42 \pm 41.44
<i>NG2-Cre⁻/Rosa-DTA</i>	5.833 \pm 0.62	397.80 \pm 18.96
<i>NG2-Cre⁺/Rosa-DTA</i>	14.95 \pm 1.77	447.30 \pm 22.91
<i>Nkx2.1^{+/+}</i>	8.64 \pm 1.74	526.46 \pm 40.73
<i>Nkx2.1^{-/-}</i>	17.86 \pm 1.78	408.00 \pm 26.53

Table 2: The values (Means \pm SEM) corresponding to the number of erythrocyte clusters and the number of individual erythrocytes per CCI section are given for: (1) *Nkx2.1-Cre⁺/Rosa-DTA* mice and their corresponding control *Nkx2.1-Cre⁻/Rosa-DTA* mice; (2) *NG2-Cre⁺/Rosa-DTA* mice and their corresponding control *NG2-Cre⁻/Rosa-DTA* mice and (3) *Nkx2.1^{-/-}* mice and their corresponding control *Nkx2.1^{+/+}* mice.

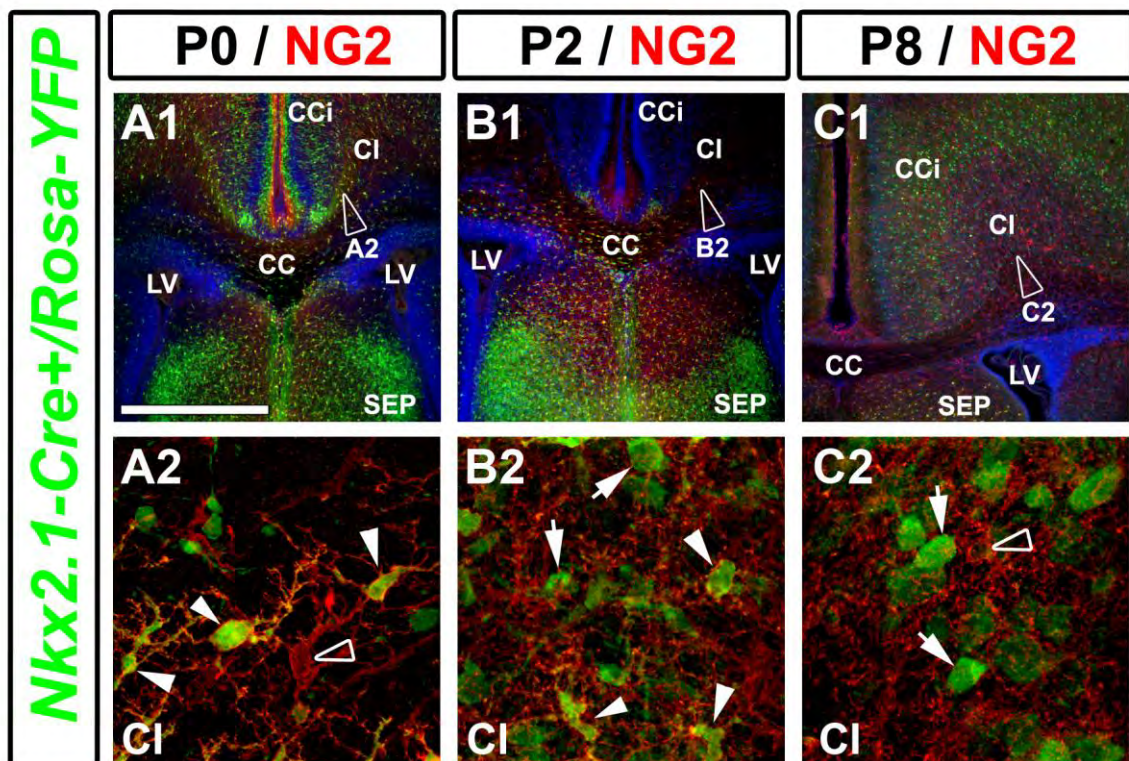


Supplementary figure S1: High level of Cre-mediated recombination in dorsal telencephalon polydendrocytes in *NG2-Cre⁺/Rosa-YFP* mice and drastic loss of *NG2⁺* polydendrocytes in *NG2-Cre⁺/Rosa-DTA* mice.

(A) Bars (means \pm SEM from a sample of n=3 CC sections, n=3 CI sections and n=3 CCI sections) represent the percentage of YFP-labelled polydendrocytes in the telencephalon of E18.5 *NG2-Cre⁺/Rosa-YFP* mice. **(B-C)** Double immunohistochemistry for NG2 and PECAM in CCI coronal sections of *NG2-Cre⁻/Rosa-DTA* **(B)** and *NG2-Cre⁺/Rosa-DTA* **(C)** mutant mice at E18.5. A drastic loss of *NG2⁺* polydendrocytes followed by severe vascular defects was observed in *NG2-Cre⁺/Rosa-DTA* mice **(C)** compared to *NG2-Cre⁻/Rosa-DTA* **(B)**. **(D)** Bars (means \pm SEM from a sample of n=11 sections in *NG2-Cre⁻*, n=11 sections in *NG2-Cre⁺*) represent the percentage of remaining polydendrocytes in the telencephalon of E18.5 *NG2-Cre⁺/Rosa-DTA* mice compared to control mice. A significant loss of about 55% of *NG2⁺* polydendrocytes was noticed in the CCI of *NG2-Cre⁺/Rosa-DTA* mice compared to control mice. The respective absolute values corresponding to the cell density (cell number/mm³) are given within the bars.

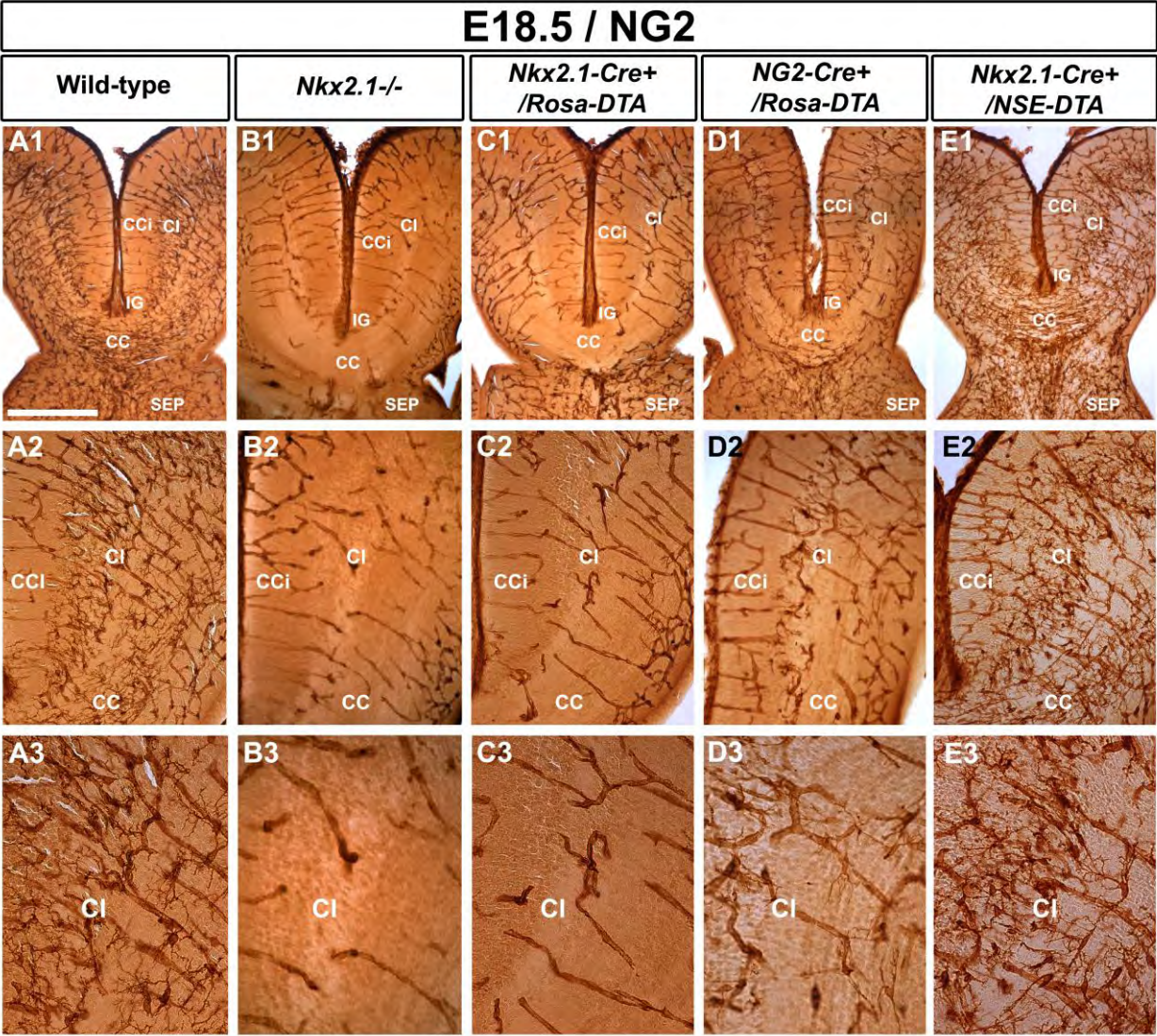
(E-G) Double immunohistochemistry for Nkx2.1 and GLAST on coronal sections from *Nkx2.1-Cre⁻/Rosa-DTA* **(E1-E4)**, *Nkx2.1-Cre⁺/Rosa-DTA* **(F1-F4)** and *Nkx2.1^{-/-}* **(G1-G4)** mice at E16.5. **E2-E4**, **F2-F4** and **G2-G4** are higher power views of the regions seen in **E1**, **F1** and **G1**, respectively.

(CC) corpus callosum; **(CCi)** cingulate cortex; **(CI)** cingulate bundle. Bar = 675 μ m in **E1**, **F1** and **G1**; 50 μ m in **B** and **C**; 40 μ m in **E2**, **E3**, **E4**, **F2**, **F3**, **F4**, **G2**, **G3** and **G4**.

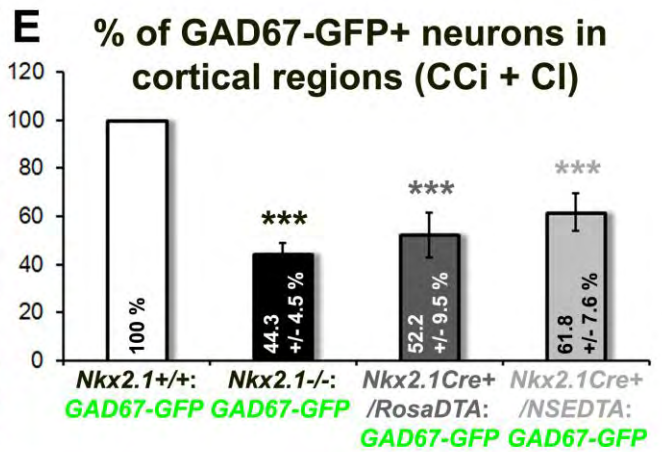
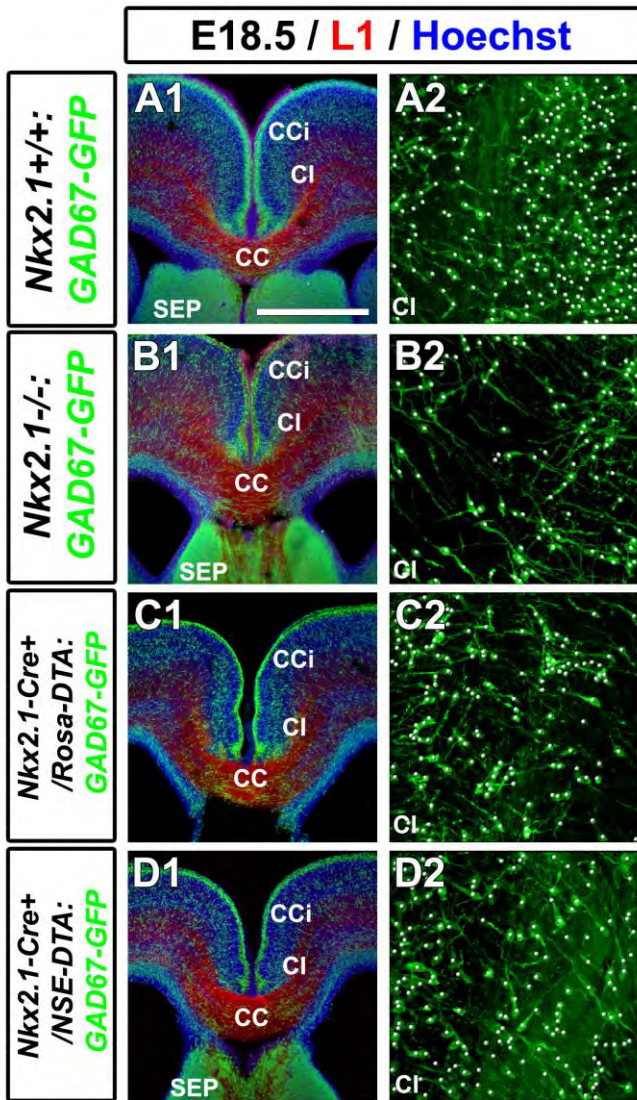


Supplementary figure S2. Polydendrocytes of the cortex disappear at early post-natal ages.

(A-C) Immunohistochemical staining for NG2 (red) in coronal telencephalic sections from *Nkx2.1-Cre⁺/Rosa-YFP* mice (green) at P0 (A1-A2), P2 (B1-B2) and P8 (C1-C2). A2, B2 and C2 illustrate the lateral extensions of the cingulate bundle (CI) seen in A1, B1, and C1, respectively. (C1-C2) At P8, *Nkx2.1⁺/NG2⁺* polydendrocytes (white arrowheads in A2 and B2) have completely disappeared from the CI, only *Nkx2.1⁺* neurons (white arrows in B2 and C2) and *Nkx2.1⁻/NG2⁺* cells (open arrowheads in A2 and C2) remained. (CC) corpus callosum; (CCi) cingulate cortex; (CI) cingulate bundle, (SEP) septum. Bar = 675 μ m in A1, B1 and C1; 45 μ m in A2, B2 and C2.



Supplementary figure S3. Drastic depletion of embryonic NG2⁺ polydendrocytes in *Nkx2.1*^{-/-}, *Nkx2.1-Cre*⁺/*Rosa-DTA* and *NG2-Cre*⁺/*Rosa-DTA* midline dorsal telencephalon. DAB staining for NG2 in wild-type (**A1-A3**), *Nkx2.1*^{-/-} (**B1-B3**), *Nkx2.1Cre*⁺/*Rosa-DTA* (**C1-C3**), *NG2-Cre*⁺/*Rosa-DTA* (**D1-D3**) and *Nkx2.1-Cre*⁺/*NSE-DTA* (**E1-E2**) telencephalic coronal slices at E18.5. (**A-C**) NG2⁺ polydendrocytes were completely depleted from the corpus callosum (**CC**), the cingulate cortex (**CCi**) and cingulate bundle (**CI**) of *Nkx2.1*^{-/-} (**B1-B3**) and *Nkx2.1-Cre*⁺/*Rosa-DTA* (**C1-C3**) mutant mice compared to wild-type mice (**A1-A3**). In *NG2-Cre*⁺/*Rosa-DTA* mutant mice (**D1-D3**), there was also a drastic loss of NG2⁺ cells in medial cortical areas of the dorsal telencephalon with only few remaining cells. In *Nkx2.1-Cre*⁺/*NSE-DTA* (**E1-E3**) mutant mice, there was no loss of polydendrocytes in all the observed regions. (**IG**) indusium griseum; (**SEP**) septum. Bar = 500 μm in **A1, B1, C1, D1** and **E1**; 250 μm in **A2, B2, C2, D2** and **E2**; 125 μm in **A3, B3, C3, D3** and **E3**.

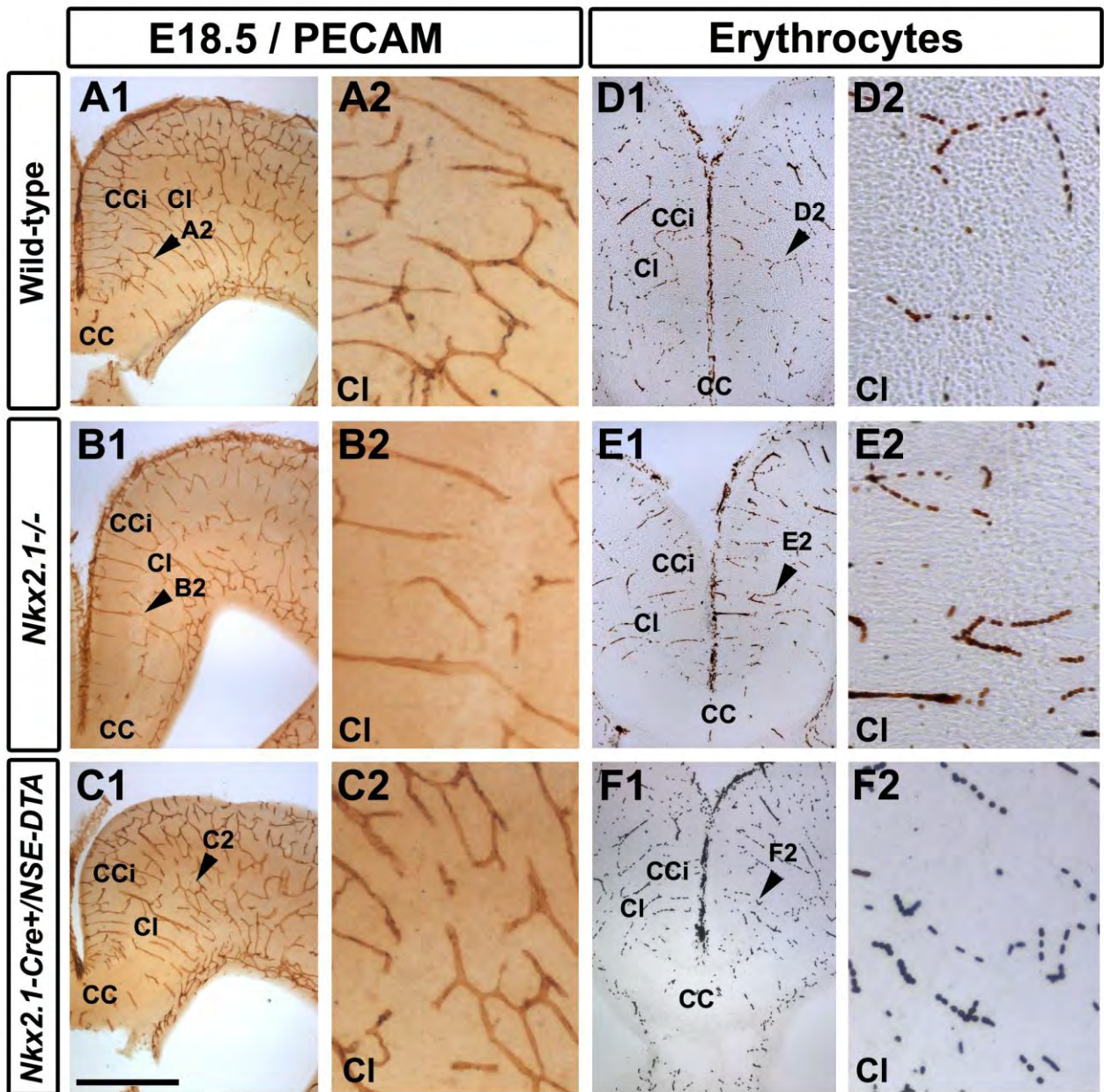


F Respective density values

Genotype	Cell number * 10 ³ /mm ³ (Means ± SEM)
<i>Nkx2.1</i> ^{+/+}	250.86 ± 5.97
<i>Nkx2.1</i> ^{-/-}	110.29 ± 4.48
<i>Nkx2.1</i> ^{Cre-} /Rosa-DTA	274.50 ± 3.88
<i>Nkx2.1</i> ^{Cre+} /Rosa-DTA	143.38 ± 9.53
<i>Nkx2.1</i> ^{Cre-} /NSE-DTA	268.20 ± 6.42
<i>Nkx2.1</i> ^{Cre+} /NSE-DTA	165.83 ± 7.64

Supplementary figure S4. Drastic depletion of GAD67-GFP⁺ neurons in *Nkx2.1*^{-/-}, *Nkx2.1-Cre*⁺/*Rosa-DTA* and *Nkx2.1-Cre*⁺/*NSE-DTA* cingulate bundle.

(A-D) Double immunohistochemistry for the GFP and L1 on coronal CI sections in *Nkx2.1*^{+/+}:*GAD67-GFP* (**A1-A2**), *Nkx2.1*^{-/-}:*GAD67-GFP* (**B1-B2**), *Nkx2.1-Cre*⁺/*Rosa-DTA*:*GAD67-GFP* (**C1-C2**) and *Nkx2.1-Cre*⁺/*NSE-DTA*:*GAD67-GFP* (**D1-D2**) mice at E18.5. **A2**, **B2**, **C2** and **D2** are higher power views showing the quantification of the GAD67-GFP⁺ interneurons (white spots) within the CI region seen in **A1**, **B1**, **C1** and **D1**, respectively. **(E)** Bars (means ± SEM from a sample of n=7 sections in *Nkx2.1*^{+/+}:*GAD67-GFP*, n=7 sections in *Nkx2.1*^{-/-}:*GAD67-GFP*, n=8 sections in *Nkx2.1-Cre*⁺/*Rosa-DTA*:*GAD67-GFP*, n=6 sections in *Nkx2.1-Cre*⁺/*NSE-DTA*:*GAD67-GFP*) represent the percentage of remaining GAD67-GFP⁺ interneurons in the CI of E18.5 *Nkx2.1*^{-/-}:*GAD67-GFP*, *Nkx2.1-Cre*⁺/*Rosa-DTA*:*GAD67-GFP* and *Nkx2.1-Cre*⁺/*NSE-DTA*:*GAD67-GFP* mice compared to *Nkx2.1*^{+/+}:*GAD67-GFP* mice. **(F)** Table of the corresponding cell density values (cell number*10³/mm³). **(CC)** corpus callosum; **(CCi)** cingulate cortex; **(CI)** cingulate bundle, **(SEP)** septum. Bar = 675 μm in **A1**, **B1**, **C1** and **D1**; 100 μm in **A2**, **B2**, **C2** and **D2**.



Supplementary figure S5. Embryonic *Nkx2.1*-derived neurons do not control the proper development and function of cortical blood vessels.

DAB staining for PECAM (**A1, A2, B1, B2, C1 and C2**) and for erythrocytes (**D1, D2, E1, E2, F1 and F2**) in coronal slices of the dorsal telencephalon of E18.5 wild-type (**A1, A2, D1 and D2**), *Nkx2.1*^{-/-} (**B1, B2, E1 and E2**) and *Nkx2.1-Cre*⁺/*NSE-DTA* (**C1, C2, F1 and F2**) mutant mice. (**A2, B2, C2, D2, E2 and F2**) are higher magnified views of the cingulate bundle (**CI**) region pointed with a black arrowhead in (**A1, B1, C1, D1, E1 and F1**) respectively. PECAM and erythrocyte staining revealed drastic vascular defects in the cortex of *Nkx2.1*^{-/-} mice (**B2 and E2**) compared with wild-type (**A2 and D2**). By contrast, the loss of GABAergic neurons in *Nkx2.1-Cre*⁺/*NSE-DTA* mutant mice did not cause vascular anomalies (**C2 and F2**) compared to control mice (**A2 and D2**). (**CC**) corpus callosum; (**CCi**) cingulate cortex. Bar = 500 μm in **A1, B1, C1, D1, E1 and F1**; 125 μm in **A2, B2, C2, D2, E2 and F2**.

DISCUSSION

During the last century, the neuroscientific community has mainly focused his interest on the function of the neurons at the expense of the study of the glial cells. However, this disparity has started to be balanced during the last decades. Indeed, more and more groups have shed light on the respective roles of oligodendrocytes and astrocytes. In the field of the brain development, the main dogma which stipulated that the neurons were first arising, followed by oligodendrocytes and finally by astrocytes, has greatly been improved (Pixley and de Vellis 1984; Mission, Takahashi et al. 1991; Luskin, Parnavelas et al. 1993; Parnavelas 1999; Kriegstein and Gotz 2003; Malatesta, Hack et al. 2003; Noctor, Martinez-Cerdeno et al. 2004; Gotz and Huttner 2005; Guillemot 2005; Hevner 2006; Guillemot 2007; Pinto and Gotz 2007; Kessar, Pringle et al. 2008; Kriegstein and Alvarez-Buylla 2009; Rowitch and Kriegstein 2010; Reillo and Borrell 2011; Reillo, de Juan Romero et al. 2011), making the way for the idea that neuroepithelial cells and radial glial cells can give rise to neurons, oligodendrocytes and astrocytes in a more intermingled manner depending on the location in the brain, and also, that astrocytes proliferate and starts to be differentiated earlier than previously thought. During my thesis work I discovered that, indeed, a heterogeneous population of glial cells composed of astrocytes and polydendrocytes is populating the embryonic telencephalon. Both subpopulations are generated as early as E14.5 and are originating from subpallial domains regulated by the transcription factor *Nkx2.1*. Furthermore, I could demonstrate that the GFAP⁺/GLAST⁺ and the GLAST⁺/Olig2⁺ astrocytes subgroups are implicated in the axonal guidance of the commissures together with other subtypes of neurons previously described by our group (Niquille, Garel et al. 2009), and with Nkx2.1⁺ progenitors which express the chemo-repellant molecule Slit2. I was also able to show that the NG2⁺/Olig2⁺/S100β^{+or-} polydendrocytes might play an important role of “guidepost cells” in angiogenesis. Moreover, the disruption of these glial cells and/or of their signaling pathway results in strong defects in the formation of the commissures as well as impairment in the development of the blood vessels network. Taken together, these results provide new insights on the origin, the heterogeneity, the function and the transient nature of astrocytes and polydendrocytes during brain development. This work thus brings a better understanding of the developmental mechanisms involving glial cells in the mouse telencephalon during the embryonic and early post-natal period.

Early subpallial origin of *Nkx2.1*-regulated astroglial cells

Here we showed that the transcription factor *Nkx2.1*, which was known to specify oligodendrocyte precursor cells (Kessaris, Fogarty et al. 2006; Kessaris, Pringle et al. 2008) and GABAergic interneurons (Anderson, Eisenstat et al. 1997; Casarosa, Fode et al. 1999; Sussel, Marin et al. 1999; Pleasure, Anderson et al. 2000; Super, Del Rio et al. 2000) was also specifying transient astrocytes and polydendrocytes.

By performing immunohistochemistry on *GAD67-GFP*⁺ knock-in mice, we found that in fact, the *Nkx2.1*⁺ cells that were populating the CC at embryonic ages were not GABAergic interneurons, but most of them were GLAST⁺ astroglial cells (results: section 1 Fig. 1). This implies that the astroglial cells of the IG, the GS and the MZG, which were previously described by other groups as guidepost cells secreting guidance molecules for the channeling of callosal axons (Silver, Lorenz et al. 1982; Shu and Richards 2001; Shu, Puche et al. 2003; Shu, Sundaresan et al. 2003; Richards, Plachez et al. 2004; Smith, Ohkubo et al. 2006), are in fact regulated by *Nkx2.1*.

Therefore, we aimed to precisely determine the birth date of the *Nkx2.1*-derived GLAST⁺/GFAP⁺ astroglial cells of the CC and surrounding regions. For this purpose, we performed a BrdU birth-dating study coupled to an immunostaining for *Nkx2.1* and GLAST and for the GFAP which allowed us to confirm results from previous studies unraveling that the bulk of these astroglial cells is generated between E14.5 and E16.5 in the mice (Silver, Edwards et al. 1993; Shu, Puche et al. 2003).

Moreover, it was described in the literature that the transcription factor *Nkx2.1* was expressed in the ventral forebrain, into regions called as the MGE, the AEP/POA, the septum, the hypothalamus and part of the Amygdala (Sussel, Marin et al. 1999; Dickson 2002; Chilton 2006; Dickson and Zou 2010). Therefore, concerning the *Nkx2.1*⁺ germinal sites of origin of the early astroglial cells, we performed diverse double and triple combinations of immuno-labeling for *Nkx2.1* and GLAST, *Nkx2.1* and GFAP, and *Nkx2.1* and the BrdU, into wild-type brains from E14.5 to E18.5.

First, the combination of staining for *Nkx2.1* and the GFAP in wild-type brains at E16.5, allowed us to observe three germinal sites that were *Nkx2.1*⁺, and which were connected to each other by some streams of *Nkx2.1*⁺ cells. After a closer look to these streams, we discovered that they were partially composed of *Nkx2.1*⁺/GFAP⁺ astroglia (results: section 1 Supplementary Fig S4). Then, by combining a fluorescent staining for *Nkx2.1* and three BrdU pulse-chase of one hour, done at E12.5, E14.5 and E16.5 in wild-type brains, which were also revealed by

immunofluorescence, we had the confirmation that the three sites were actively proliferating germinal sites, and that they were regulated by *Nkx2.1* (results: section1 Fig. 5 and not shown).

This allowed us to unravel for the first time that: 1) in addition to the MGE and the AEP/POA, there is a third *Nkx2.1*⁺ site, a ventricular zone bordering the third ventricle, which present a high number of dividing progenitors; 2) this site is situated in the septum, ventro-caudally from the CC, just ventrally from the HIC and dorso–rostrally from the AC; and 3) this site is known as the triangular septal nucleus (ts) but has never been described previously as an *Nkx2.1*⁺ germinal site (results: section1 Fig. 1, 4, 5 and Supplementary Fig. S4).

Consequently, in order to verify that the ts, the MGE and the AEP/POA, were generating astroglial cells, we performed two electroporation assays. Firstly, *in vitro* focal electroporation of *pCAG-EGFP* reporter plasmid on wild-type E14.5 to E16.5 organotypic slices and staining for the GFP and GLAST or the GFAP revealed that the three *Nkx2.1*⁺ germinal regions of the subpallium can generate GLAST⁺ or GFAP⁺ astrocyte-like cells. Secondly, *in utero* injection and electroporation of the *pCAG-GS-Ires-Tomato* plasmid toward the subpallium of E14.5 *Nkx2.1-Cre*⁺/*Rosa-YFP* embryos confirmed this outcome. Numerous GLAST⁺/YFP⁺ astroglial cells were observed to be generated from the AEP/POA and the ts and were observed to migrate and differentiate into mantle regions such as the AC, the striatum, the septum and the lateral part of the POA (results: section 1 Fig. 4 and not shown).

Altogether, these results show that the embryonic astroglial cells of the CC and the midline region are generated as early as E14.5 and are originating from subpallial *Nkx2.1*-regulated germinal sites.

Heterogeneity and origin of the *Nkx2.1*-derived glial cells

We were then able to refine our “*Nkx2.1*-derived glial cells analysis” by using multiple transgenic mice strains. To this purpose, *GLAST-Cre ERT*TM (Jackson Laboratory: Tg(Slc1a3-cre/ERT)1Nat/J), *NG2-Cre* (Jackson Laboratory: B6;FVB-Tg(Cspg4-cre)1Akik/J) (Zhu, Bergles et al. 2008), *Nkx2.1-Cre* (Kessaris, Fogarty et al. 2006; Mori, Tanaka et al. 2006; Fogarty, Grist et al. 2007; Zhu, Bergles et al. 2008; Rubin, Alfonsi et al. 2010) and *Olig2-Cre ERT*TM (Takebayashi, Nabeshima et al. 2002) mice were crossed with *Rosa-YFP* reporter mice (Srinivas, Watanabe et al. 2001). Immunostaining on coronal telencephalic sections of these mice, from E16.5 to E18.5, confirmed the presence of numerous *Nkx2.1*-derived glial cells in the entire telencephalon. We found GLAST⁺, GFAP⁺, S100β⁺, Olig2⁺ and NG2⁺ glial cells that were generated by *Nkx2.1*⁺ progenitors.

Thus, we aimed to distinguish and characterize all the different subpopulations of *Nkx2.1*-derived glial cells, but the complexity of the task was increased by the fact that none of the transgenic mouse strains that we used presented a Cre-mediated recombination rate of 100%. For instance, the *Nkx2.1-Cre* mice were displaying the highest rate of Cre-mediated recombination, but unfortunately, the Cre was hardly to never seen to recombine within the GFAP⁺ or GLAST⁺ glia of the CC and dorsal pallium (results: section 1 Fig. 3). Explanations for that drawback could be that: 1) as soon as these glia end their differentiation, *Nkx2.1* is immediately down-regulated which is too early for the recombination to occur and the reporter gene to be expressed in these cells, or 2) the level of expression of *Nkx2.1* into these astroglial cells is low (as compared as into precursors for NG2⁺ cells or for neuronal cells) and this low level of expression is not sufficient for the Cre recombination to occur.

Moreover, the difficulty to discriminate each glial cell type was raised by the fact that most of the antibodies we had, are produced in rabbits, except the GLAST antibody which is generated in guinea pigs. Consequently, it greatly limited the possible combinations for the labeling of the different glial cell types at a time. However, with this combination of glial marker and transgenic mice, we managed to distinguish four different subpopulations of embryonic glial cells which were regulated by *Nkx2.1* (results: section 1, Supplementary Fig. S1).

The *Nkx2.1*-derived astrocyte-like cells

First, we found GLAST⁺/GFAP⁺/*Nkx2.1*⁺ astrocyte-like cells that were populating the medial regions of the telencephalon, that is, the IG, the CC, the MZG, the ts, the HIC, the AC and the AEP/POA, as well as the VZ of the MGE (results: section 1 Fig. 1, 2, 3, 6 and Supplementary Fig. S1, S2, S3, S4). Moreover, DAB staining for GLAST and the GFAP in wild-type and *Nkx2.1*^{-/-} mice (Flames et al., 2007; Kimura et al., 1996; Sussel et al., 1999) at E16.5 and E18.5 confirmed that these astrocyte-like cells were generated by *Nkx2.1*⁺ progenitors, since these cells were completely depleted from the medial areas, the MGE and the POA in *Nkx2.1*^{-/-} mutant (results: section 1 Fig. 6).

Then, immuno-fluorescent staining revealed that GLAST⁺/Olig2⁺ astrocyte-like cells were also found everywhere in the telencephalon, which includes in addition to the midline regions, the entire cortex, the striatum and the septum (results: section 1 Fig. 3 and Supplementary Fig. S1, S3, S6). Here, studies in *Nkx2.1*^{-/-} mice and *Nkx2.1-Cre*⁺/*Rosa-DTA* mice ascertained that part of these GLAST⁺/Olig2⁺ cells were regulated by *Nkx2.1* since they were partially depleted from the mid and the side of the CC, the CI (results: section 1 Supplementary Fig. S6) and the AC (results: section 2 Fig. 6). Surprisingly, the loss of these glia was more severe in the AC, in the side of the CC and in the CI than in the mid of the CC. From these results, we can conclude that the majority of the

GLAST⁺/Olig2⁺ cells situated in the mid of the CC are not generated from Nkx2.1⁺ precursors. Interestingly, immuno-labeling at E16.5 reveals that, numerous glial cells of the GW, the IG and the ts are positively colocalizing for GLAST and Olig2 (results: section 1 Supplementary Fig. S6 ; results: section 2 Fig.6 and not shown). In addition to the GW, another potential site of origin for these GLAST⁺/Olig2⁺ astroglia might be the IG. Indeed, by performing BrdU pulse-chase studies of two hours at E16.5 in wild-type mice followed by stainings for the BrdU, Nkx2.1 and GLAST we discovered, that in addition to the VZ, numerous cells in the IG are positively stained for the BrdU. Indeed, the IG was a site in which an important number of cells were co-expressing Nkx2.1, GLAST and the BrdU (Figure I).

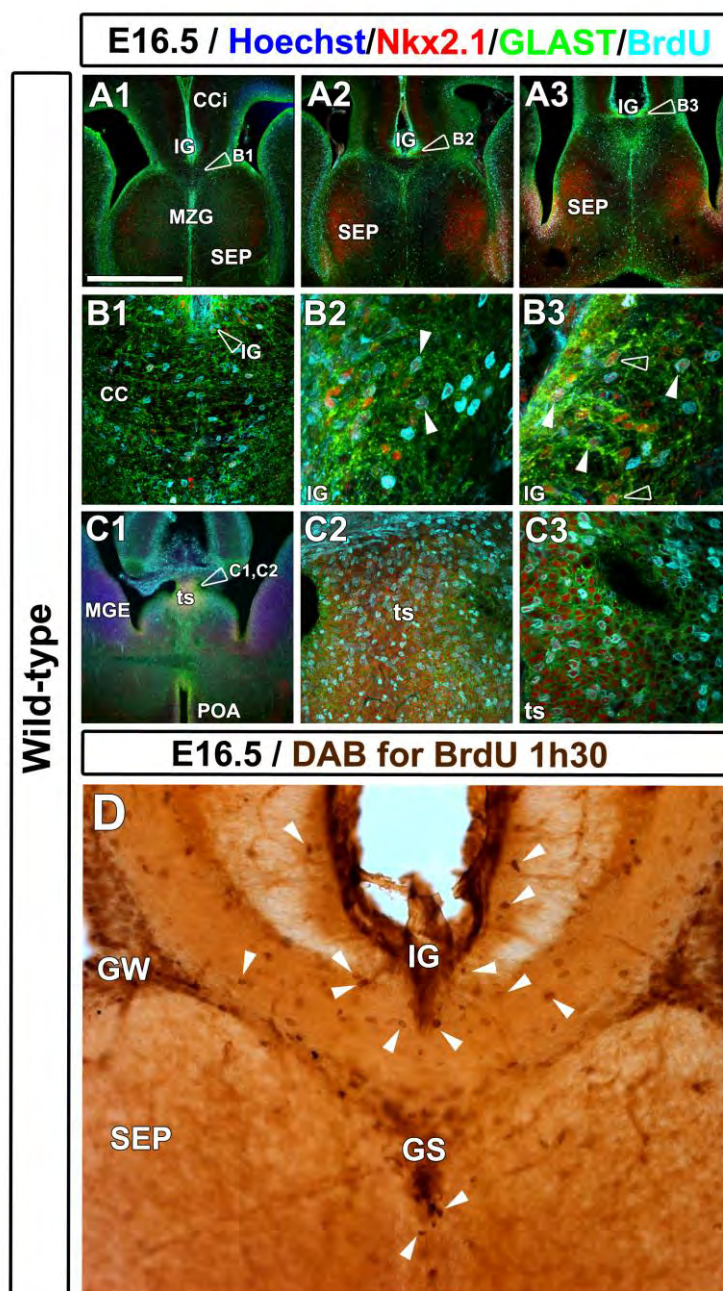


Figure I: $Nkx2.1^+$ /GLAST⁺ cells of the IG and ts are BrdU⁺ dividing cells at E16.5.

(A-C) Triple immunohistochemistry for Nkx2.1, GLAST and BrdU (1h30 pulse-chase) reveals many $Nkx2.1^+$ /GLAST⁺/BrdU⁺ cells originating from the IG (A1-A3 and B1-B3) and the ts (C1-C3) which will populate the CC white matter (B1 and white arrowheads in B2 and B3). (D) DAB staining for the BrdU on a coronal CC section of E16.5 wild-type mouse shows numerous BrdU⁺ cells localized around the IG, in the GS and in the GW. (CC) corpus callosum; (CCi) cingulate cortex; (GS) glial sling; (GW) glial wedge; (IG) indusium griseum; (MGE) medial ganglionic eminence; (MZG) midline zipper glia; (SEP) septum; (ts) triangular septal nucleus. Bar = 675 μ m in A1, A2, A3 and C1; 100 μ m in B1 and C2; 60 μ m in C3 and D; 40 μ m in B2 and B3.

Therefore, it seems plausible that at E16.5, the IG may contain multiple cells in a progenitor state which divide and give birth to new glial cells. Thus, it may be imaginable that the IG may also contain progenitors regulated by Olig2 but not Nkx2.1, which might generate some GLAST⁺/Olig2⁺ but Nkx2.1⁻ glial cells which then migrate to the mid CC and are not depleted in *Nkx2.1^{-/-}* and *Nkx2.1-Cre⁺/Rosa-DTA* mice. Therefore, the GLAST⁺/Olig2⁺ astroglia of the mid CC might also find their origin in this site in addition to the ts and probably, both sites contain precursors giving rise to GLAST⁺/Nkx2.1⁺/Olig2⁻, GLAST⁺/Nkx2.1⁻/Olig2⁺ and GLAST⁺/Nkx2.1⁺/Olig2⁺ cells whereas the GW may contain only precursors for GLAST⁺/Nkx2.1⁻/Olig2⁺ cells since this site is not regulated by Nkx2.1. In addition, we found through the combination of GLAST and Olig2 staining in wild-type and in *Olig2-Cre⁺/Rosa-YFP* brains, that a huge number of GLAST⁺/Nkx2.1⁻/Olig2⁺ cells might be generated from the ventricular zone of dorsal telencephalon and migrate radially through the cortex towards the marginal zone (results: section 1 Supplementary Fig. S6 and Figure II).

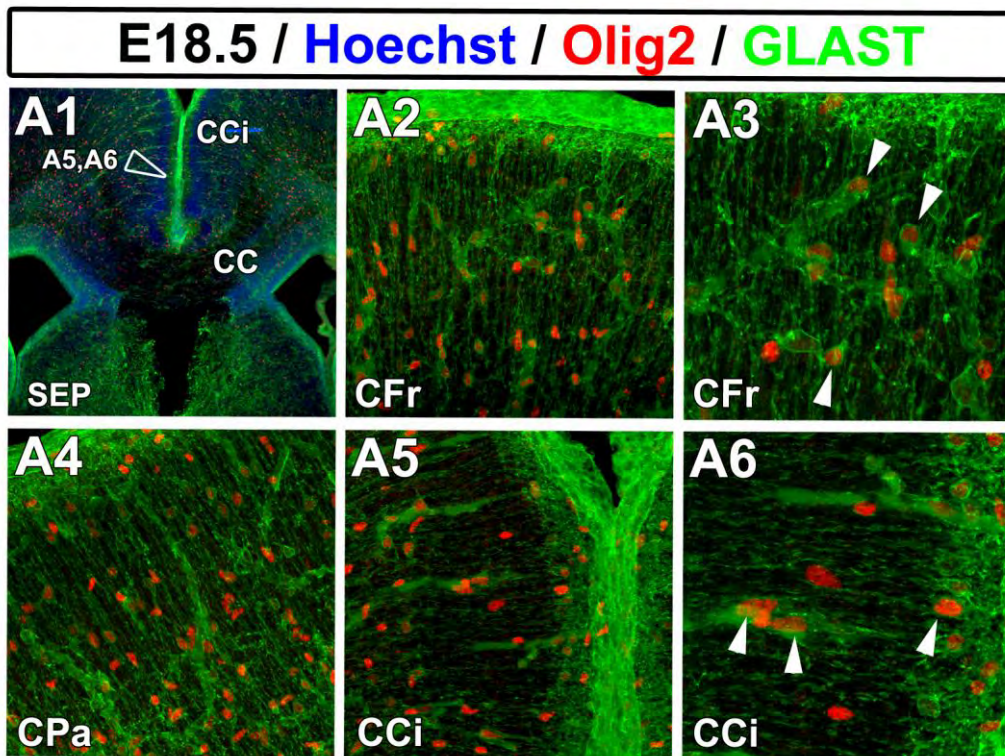


Figure II: $GLAST^{+}/Olig2^{+}$ astrocyte-like cells are uniformly dispersed throughout the entire cortex

(A1-A6) Double immunostaining for Olig2 and GLAST on an E18.5 coronal section of a wild-type brain shows numerous $GLAST^{+}/Olig2^{+}$ astrocyte-like cells (white arrowheads) which are radially migrating along their own glial processes from the VZ of the dorsal telencephalon towards the MZ in the cortex. (CC) corpus callosum; (CCi) cingulate corte; (CFr) frontal cortex; (CPa) parietal cortex; (SEP) septum.

Furthermore, the use of $GLAST-Cre ERT^{TM}$ and $Olig2-Cre ERT^{TM}$ inducible mice crossed to the $Rosa-YFP$ reporter mice allowed us to confirm two points: 1) the early origin of the $GLAST^{+}/GFAP^{+}$ and the $GLAST^{+}/Olig2^{+}$ glial cells, since the tamoxifen induction was made at E15 and E16 for the $GLAST-Cre ERT^{TM}$ and E14.5 for the $Olig2-Cre ERT^{TM}$ and we could see at E18.5 $GLAST^{+}/GFAP^{+}$ (not shown) and at E16.5 $GLAST^{+}/Olig2^{+}$ glial cells which had migrated far from the VZ and were differentiated; 2) the three sites of origin were easily recognizable since we could follow the entire migration trajectory of the $GLAST^{+}$ cells from precursor state in the VZ to the state of differentiated cells in the parenchyma (results: section 1, Fig.1, 3 and Supplementary Fig. S4, and not shown).

Thereafter, the hypothesis of a septal origin for the GLAST⁺/GFAP⁺ astrocyte-like cells was reinforced by the fact that immuno-labeling revealed that all the GFAP⁺ cells of the CC midline and the ts were also expressing the transcription factor Dbx1 which is known to regulate the Cajal-Retzius neurons originating from the septal region (Figure III) (Flames, Pla et al. 2007, Griveau, 2010).

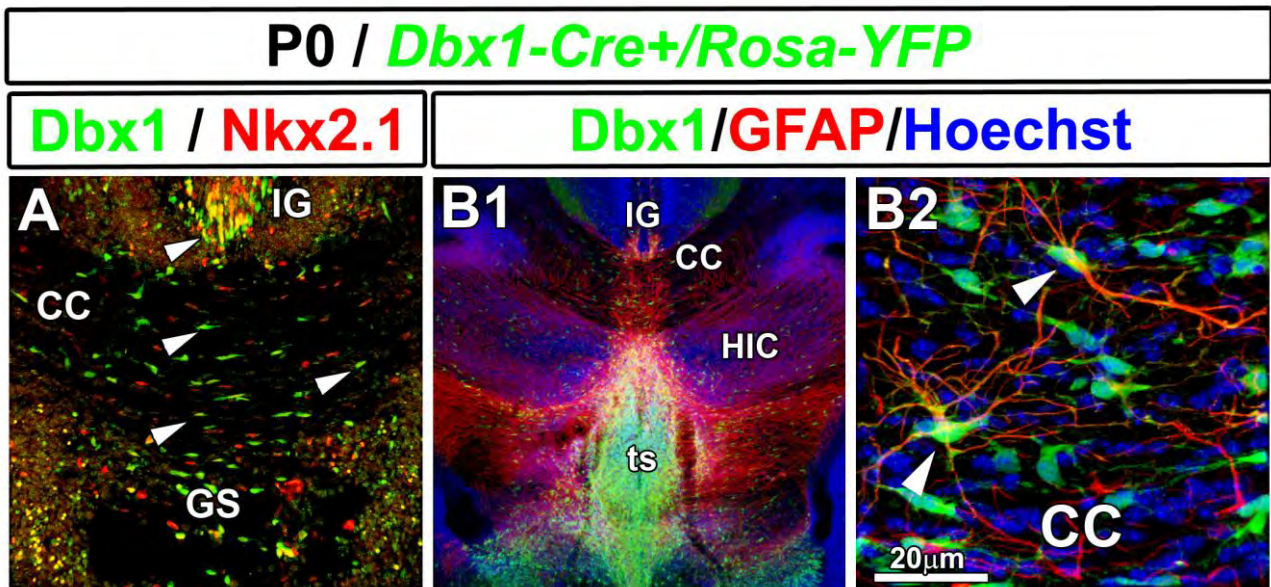


Figure III: Common origin for the Dbx1⁺/Nkx2.1⁺ progenitors of the IG and the ts giving rise to the astrocytes of the CC.

(A) Double immunohistochemistry for the YFP and Nkx2.1 on a coronal CC section of *Dbx1-Cre⁺/Rosa-YFP* mice at P0 showing numerous Nkx2.1⁺/Dbx1⁺ progenitors in the IG and post-mitotic cells in the CC white matter (white arrowheads). (B1-B2) Double immunostaining for the YFP and the GFAP on a coronal CC section of *Dbx1-Cre⁺/Rosa-YFP* mice at P0 reveals that the GFAP⁺ astrocytes of the CC white matter are *Dbx1*-derived cells originating from the ts or the IG (white arrowheads in B2). (CC) corpus callosum; (GS) glial sling; (IG) indusium griseum; (HIC) hippocampal commissure; (ts) triangular septal nucleus. Bar = 500 μm in B1; 80 μm in A and 20 μm in B2.

In addition, the hypothesis of an IG origin might also be reinforced since 1) the IG is also regulated by Dbx1, and 2) as observed in our BrdU pulse-chase analyses, there are numerous Nkx2.1⁺/GLAST⁺/BrdU⁺ dividing cells in the IG at E16.5. Therefore, it could be possible that the IG contains progenitor cells regulated by both Nkx2.1 and Dbx1 which are also GLAST⁺, and which divide to give rise to part of the GLAST⁺/GFAP⁺/Dbx1⁺ astroglia of the mid CC (Figure III; and see results: section 2 Fig.1). Moreover, there is possibly a common origin and common

properties for the cells of the IG, the MZG and the ts. This is clearly visualized on a one hour BrdU pulse-chase experiment done at E14.5 (Figure IV).

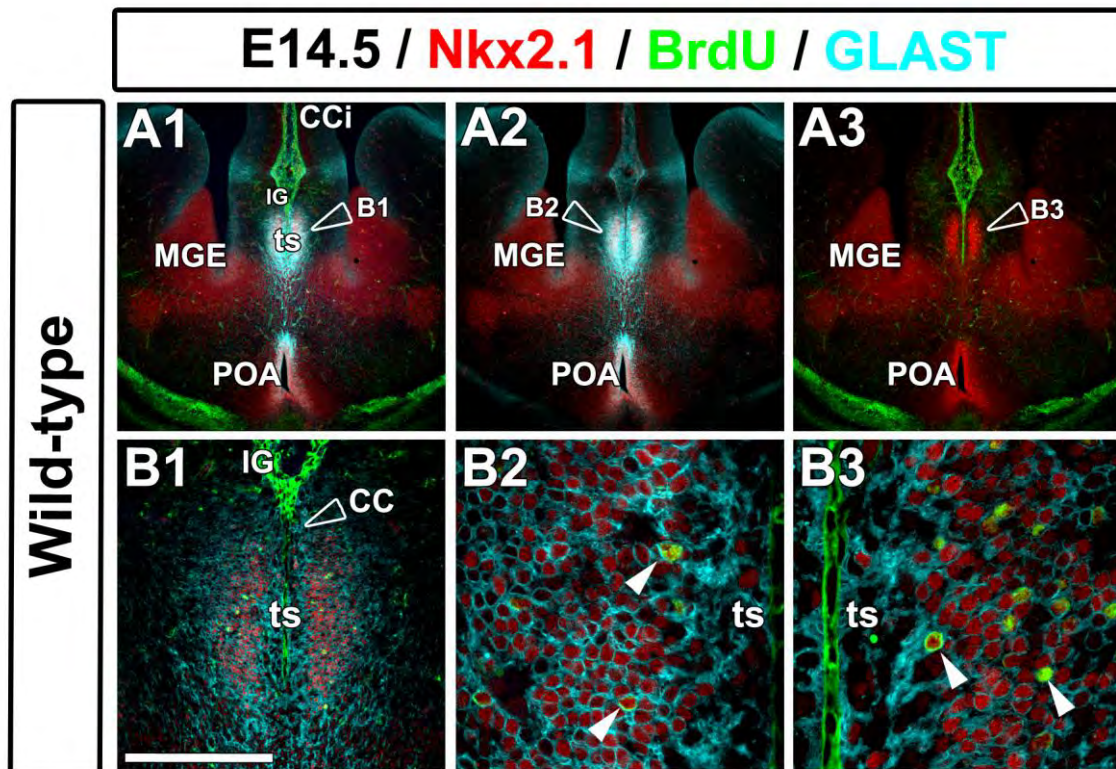


Figure IV: Unique origin for the *Nkx2.1*-derived progenitors of the IG, MZG and the ts.

(A-B) Triple immunostaining for *Nkx2.1*, the BrdU (1 hour pulse-chase), and GLAST on a coronal section of E14.5 wild-type embryo clearly shows that the ts is an *Nkx2.1*⁺ proliferative germinal region situated right under the future IG. (B1-B3) are showing higher magnified views of the ts region seen in A1-A3 and white arrowheads indicate BrdU⁺/*Nkx2.1*⁺/GLAST⁺ dividing progenitors. (CC) corpus callosum; (CCi) cingulate cortex; (IG) indusium griseum; (MGE) medial ganglionic eminence; (POA) preoptic area; (ts) triangular septal nucleus. Bar = 675 μ m in A1, A2 and A3; 100 μ m in B1; 40 μ m in B2 and B3.

Furthermore, it has already been mentioned by Shu and co-authors that the IG and the MZG could originate from the same population which is then split into two by the formation of the CC and the corticoseptal boundary (Shu, Puche et al. 2003). Thus, the IG and the MZG could be considered as the rostral extension of the ts which was split by the formation of the CC tract, and thereby, we can assess that the IG, the MZG and the ts share the same origin and properties.

Moreover, with the use of *GLAST-Cre⁺/Rosa-YFP* mice induced at E14.5, we could directly observe *Nkx2.1⁺/GLAST⁺/YFP⁺* and *GFAP⁺/YFP⁺* glial cells which were positioned as if they were directly arising from the IG itself (Figure V).

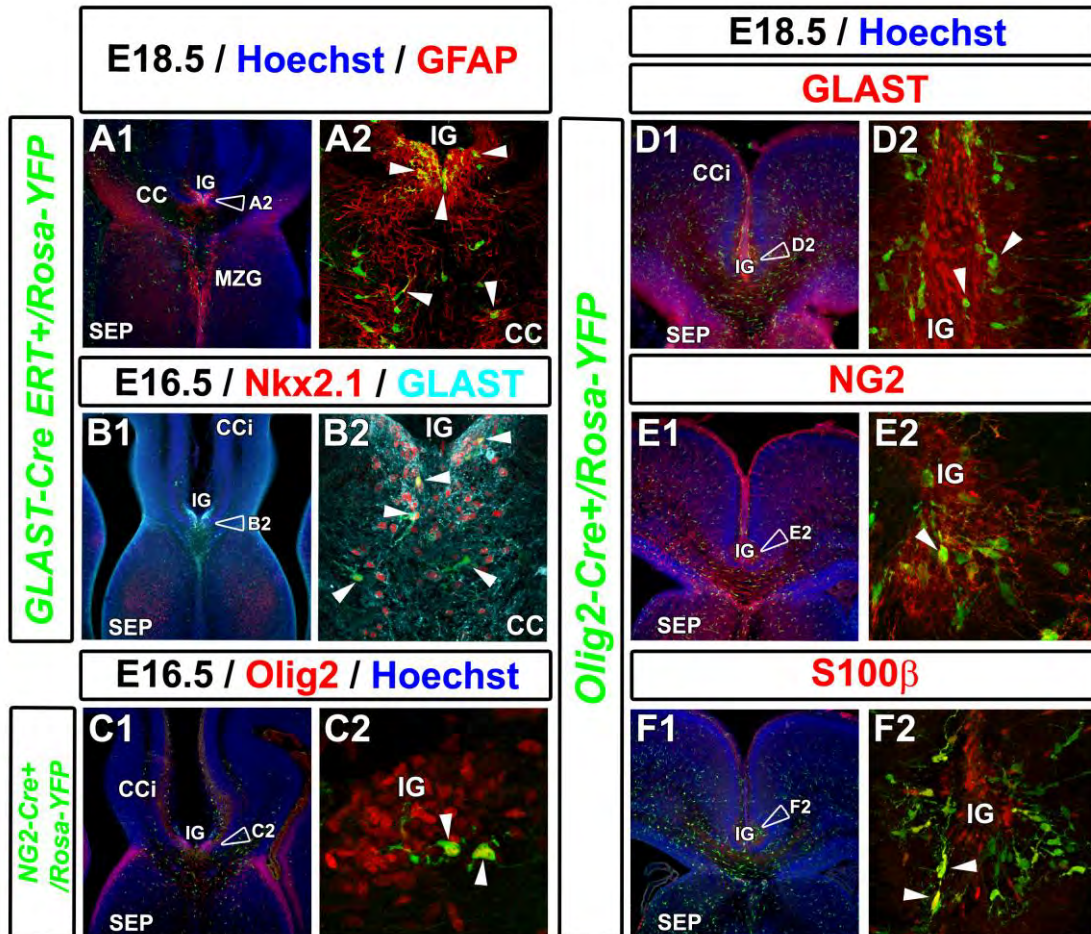


Figure V: IG origin for *GLAST⁺/GFAP⁺* astrocyte-like and *Olig2⁺/NG2⁺/S100β⁺* polydendrocyte-like cells

(A) Double immunostaining for the YFP and the GFAP on E18.5 and (B) triple immunostaining for the YFP, *Nkx2.1* and GLAST on CC coronal sections of E16.5 *GLAST-Cre ERT⁺/Rosa-YFP* mice. (C) Double immunostaining for the YFP and Olig2 on a CC coronal section of E16.5 *NG2-Cre⁺/Rosa-YFP* embryo. (D-F) Double immunostaining for the YFP and GLAST (D), for the YFP and NG2 (E) and for the YFP and S100β (F) on CC coronal sections of E18.5 *Olig2-Cre⁺/Rosa-YFP* mice. White arrowheads indicate *Nkx2.1*-derived *GLAST⁺/GFAP⁺* astrocyte-like cells (A-B); *NG2*-derived *Olig2⁺* polydendrocyte-like cells (C); *Olig2*-derived *GLAST⁺/NG2⁺/S100β⁺* polydendrocyte-like cells (D-F) that could all potentially originate from the IG. (CC) corpus callosum; (CCi) cingulate cortex; (IG) indusium griseum; (MZG) midline zipper glia; (SEP) septum.

Therefore, from these evidences we can hypothesize that: 1) part of the $Nkx2.1^+/GLAST^+/GFAP^+$ astrocytes of the mid CC may be originating from both the ts and the IG that are sites also regulated by *Dbx1*, 2) the $Nkx2.1^+/Olig2^+/GLAST^+$ cells might also come from the ts and the IG, and finally, 3) the $Nkx2.1^+/Olig2^+/GLAST^+$ glial cells might probably originate from the VZ of the GW and the VZ of the dorsal pallium. Nevertheless, these hypothesis need to be further demonstrated by other BrdU pulse-chase studies as well as by time-lapse video microscopy on *GLAST-Cre⁺/Rosa-Tomato* mice induced at E16 for example.

The *Nkx2.1*-derived polydendrocyte-like cells

Afterward, with the use of a combination of NG2 and GLAST markers on *Nkx2.1-Cre⁺/Rosa-YFP* mice and *NG2-Cre⁺/Rosa-YFP* mice, we could see that both markers were labeling two mutually exclusive glial subtypes (results: section 1 Fig. 2 and 3; results: section 2 Fig. 1 and results: section 3 Fig.1) implicating that in addition of the $Nkx2.1^+$ astrocyte-like cells, there was another subpopulation of *Nkx2.1*-derived $NG2^+$ cells. Indeed, it has been unraveled previously that $NG2^+$ cells do not express any of the astrocyte markers such as GFAP, GLAST and GS (Nishiyama, Watanabe et al. 2002). More importantly, it has been shown that part of the $NG2^+$ cells which were previously all considered as OPCs since they were also expressing *Olig2* and *PDGFR α* , are never dividing and differentiating into mature myelinating oligodendrocytes, and since then, they should be considered as a different type of glial cells called as polydendrocytes. Therefore, we chose to term the *Nkx2.1*-derived $NG2^+$ cells, as polydendrocytes (Nishiyama, Watanabe et al. 2002; Butt, Hamilton et al. 2005; Wigley and Butt 2009). Then, we also confirmed that the *Nkx2.1*-derived $NG2^+$ polydendrocytes were always expressing *Olig2* but never GLAST nor GFAP (results: section 1 Fig.2 and results: section 3 Fig.1). Here again, the use of the *NG2-Cre⁺/Rosa-YFP* and *Olig2-Cre⁺/Rosa-YFP* mice allowed us to clearly observe that the *Nkx2.1*-derived $NG2^+$ polydendrocytes were originating from subpallial domains regulated by both *Nkx2.1* and *Olig2*, namely the ts, the MGE and the AEP/POA (results: section 1 Fig.2 ; results: section 3, Fig. 1 and not shown). Furthermore, our results corroborate previous published data describing that $NG2^+$ polydendrocytes were detectable at E15 on *PDGFR α ⁺* cells, when they exit the VZ and that *NG2* was never seen in *PDGFR α ⁺* cells inside the VZ (Trotter, Karram et al. 2010).

The *Nkx2.1*-derived S100 β ⁺ cells

Surprisingly, in this study, we observed first that embryonically, the S100 β ⁺ cells were never co-expressing either GLAST or GFAP (not shown), implicating that in embryos, these cells should not be considered as astrocyte-like cells. Secondly, with the use of *NG2-Cre⁺/Rosa-YFP* and *Olig2-Cre⁺/Rosa-YFP* mice, we found that around 50% of the YFP-labeled polydendrocyte-like cells were co-expressing S100 β (results: section 1 Fig.2 ; results: section 3 Fig.1 and not shown), a marker which was previously known for labeling astrocytes (Malatesta, Hack et al. 2003; Gotz and Barde 2005; Gotz and Huttner 2005; Pinto and Gotz 2007). However, it has been mentioned in very few post-natal studies that some S100 β ⁺ cells were positive also for NG2 (Volterra and Meldolesi 2005). Therefore, we assumed that probably the S100 β ⁺ cells should be considered as polydendrocyte-like cells and not as astrocyte-like cells. Another argument which tends to show that the embryonic S100 β ⁺ cells are probably polydendrocytes, is that in wild-type mice, both S100 β ⁺ and NG2⁺ cells are populating the same parenchymal regions (CTX, CC, AC, SEP and STR), and in *Nkx2.1^{-/-}* mice, both *Nkx2.1*-derived S100 β ⁺ and NG2⁺ cells are depleted from exactly the same regions of the telencephalon, which are the midline and surrounding areas (IG, CC, MZG, CCI, CFr, AC and SEP) (results: section 1 Fig. 6 and not shown).

Paradoxically, in *NG2-Cre⁺/Rosa-YFP* and *Olig2-Cre⁺/Rosa-YFP* mice, even if the majority of the S100 β ⁺ cells were NG2-derived and Olig2-derived cells, a few cells (around 20%) were not. However, since the rate of the Cre-mediated recombination was only reaching a maximum of 70% for the *NG2-Cre⁺/Rosa-YFP* and even less for the *Olig2-Cre⁺/Rosa-YFP* mice (not shown), we cannot rule out the possibility that maybe the S100 β ⁺ cells that were found negative for the YFP signal should have been positive if the recombination was complete. Therefore, it is still unclear whether all the embryonic S100 β ⁺ cells should be considered as NG2⁺ polydendrocytes or if part of them are forming another exclusive S100 β ⁺ group of cells (results: section 1 Fig. 2). Consequently, we propose a model in which four different subpopulations of embryonic glial cells are generated by *Nkx2.1⁺* germinal sites and which populate the entire telencephalon: 1) the GLAST⁺/GFAP⁺/*Nkx2.1⁺* and 2) the GLAST⁺/Olig2⁺/*Nkx2.1⁺* astrocyte-like cells, 3) the S100 β ⁺/NG2⁺/Olig2⁺ and 4) the S100 β ⁻/NG2⁺/Olig2⁺ polydendrocyte-like cells (results: section 1 Supplementary Fig. S1).

***Nkx2.1*-derived glial cells are transient and disappear from the pallium and then from the subpallium post-natally**

Nkx2.1 transcription factor is exclusively expressed during embryonic ages and is abruptly and completely down-regulated at birth (between E19 and P0 in mice), and thus, one of the possibilities is to study the fate of *Nkx2.1*-derived cells through the use of *Nkx2.1-Cre⁺* mice crossed with any reporter mice (Sussel, Marin et al. 1999; Xu, Tam et al. 2008). Therefore, in order to study the post-natal fate of these cells, we performed immunohistochemistry for all the types of glial markers (GLAST, GFAP, S100 β , Olig2 and NG2) on postnatal P0, P2, P8 and P14 *Nkx2.1-Cre⁺/Rosa-YFP* mice brains (not shown and results: section 1 Supplementary Fig. S3; results: section 3 Fig. S2). Indeed, Shu and colleagues had already noticed that the population of GLAST⁺/GFAP⁺ glia of the midline were strongly decreased by P10 (Shu, Puche et al. 2003) and Kessaris and colleagues had also mentioned that at P30 all *Nkx2.1*-derived OLPs that had migrated to the cerebral cortex had disappeared and were replaced by *Gsh2*- or *Emx1*-derived OLPs (Kessaris, Fogarty et al. 2006; Kessaris, Pringle et al. 2008). We confirmed these published results since, at P8, only very few S100 β ⁺, Olig2⁺ and NG2⁺ *Nkx2.1*-derived glial cells were remaining in the CC (results: section 1 Supplementary Fig. S3). Here, few YFP⁺/Olig2⁺ and YFP⁺/S100 β ⁺ cells were also remaining in the CCi (not shown). However, this was not the case in the AC, since a high number of all types of *Nkx2.1*-derived cells were remaining in that tract until P14 (results: section 1 Supplementary Fig. S3). By contrast, at this age, the dorsal telencephalon was already completely devoid of *Nkx2.1*-derived glial cells. In the subpallium, only the septum was still containing a lot of YFP⁺/S100 β ⁺ cells (not shown). The fact that all *Nkx2.1*-regulated glial cells do not all disappear synchronously from the entire telencephalon supports the idea that this population is in fact highly heterogeneous. The specific location of each of these glial subtypes within the telencephalon might be related to a specific function or fate. It is quite interesting to note that these cells tend to disappear first from the pallium at P8, and only after from the subpallium, which suggests that they could have a different function to achieve in these two different locations. Actually, it is still unclear whether these glial cell types disappear post-natally through apoptosis. For instance, it could be interesting to elucidate part of this issue by simply performing a cleaved-caspase3 or TUNEL staining coupled with glial markers on P8, P14 and P21 *Nkx2.1-Cre⁺/Rosa-YFP* brains.

It could be deciphered that the task of the *Nkx2.1*-derived glial cells is coming to an end at birth. They might have a function embryonically which is processed by other cells that replace them post-natally. It could be hypothesized that one week after birth the polydendrocytes have achieved their guidepost function for the blood vessels, and that the astrocyte-like cells also have achieved

their guidepost task for the commissural axons. Consequently, further analysis of the cell fate of the *Nkx2.1*-derived glial cells, would be required to confirm this hypothesis.

Intrinsic regulation of *Nkx2.1*⁺ progenitors for their own division and specification into astroglia

Several groups have already contributed to unravel the multi-functionality of *Nkx2.1* protein in the brain. This transcription factor was known since long for its role in patterning the basal telencephalon (Sussel, Marin et al. 1999; Corbin, Rutlin et al. 2003), in specifying diverse subtypes of interneurons (Marin, Anderson et al. 2000; Xu, Tam et al. 2008) (Du, Xu et al. 2008) (Marin, Valiente et al. 2010), OPCs and oligodendrocytes (Kessaris, Fogarty et al. 2006; Kessaris, Pringle et al. 2008) arising from the MGE (Marin and Rubenstein 2001) and the AEP/POA (Gelman, Griveau et al. 2011), in controlling the migration of post-mitotic interneurons through the repression of the guidance receptor *Nrp-2* (Nobrega-Pereira, Kessaris et al. 2008), and finally in regulating axonal guidance for dopaminergic pathways (Kawano, Horie et al. 2003). Moreover, a recent study done on the transcriptional targets of *Nkx2.1* in lungs, revealed that in pulmonary epithelial cells from mice as well as in human tumoral cells, *Nkx2.1* was affecting the cell cycle progression when its own expression was reduced (Tagne, Gupta et al. 2012). Nevertheless, its involvement in regulating the division of the precursor cells within the VZ and the SVZ of the subpallial germinal regions has never been studied precisely.

Therefore, within the aim of doing it, we performed several BrdU pulse-chase experiments of one to two hours, revealed by a DAB staining, or coupled with a fluorescent staining for *Nkx2.1* at E12.5, E14.5 and E16.5 in wild-type and *Nkx2.1*^{-/-} embryos (not shown and results: section 1 Fig 5 and Supplementary Fig.S5). We also performed phospho-histone 3 (PH3) staining at E12.5, E13.5 and E14.5 to label only mitotic cells (not shown). Firstly, after BrdU injections and DAB staining at E12.5 and E16.5, we found no obvious differences in the number of BrdU dividing cells within the VZ and SVZ of MGE and POA of *Nkx2.1*^{-/-} mice compared to wild-type, but the general distribution of the BrdU⁺ cells was perturbed since the progenitors of the MGE are re-specified to an LGE-like fate in *Nkx2.1*^{-/-} (results: section1 Supplementary Fig. S5). Also, the PH3 staining at E12.5, E13.5 and E14.5 didn't reveal any obvious difference in the general rate of division between the mutant and the wild-type mice (not shown). In addition, these results were again confirmed by an *in vitro* self-renewal capacity analysis by the use of neurospheres (results: section1 Supplementary Fig. S5). There again, both the wild-type and the mutant progenitors which were extracted from the VZ and

SVZ of both the MGE and the POA were displaying an equal capacity to form secondary spheres and therefore, were having an equal capacity to self-renew.

Thus, from these results, we concluded that the mutation of Nkx2.1 was not affecting the dividing capacity of all precursor cells of the subpallium in general.

Thereafter, we performed another BrdU pulse-chase experiment of two hours at E16.5 in both wild-type and in *Nkx2.1*^{-/-} brains, which was revealed by a triple immunohistochemical staining for Nkx2.1, GLAST and BrdU (results: section1 Fig. 5). Thanks to this study and after quantification, we could demonstrate that even if the total number of dividing subpallial progenitors is not decreased in *Nkx2.1*^{-/-} mice, the number of Nkx2.1⁺ cells is diminished, the number of *Nkx2.1*-derived BrdU⁺ dividing progenitor is strongly affected, and finally, the number of BrdU⁺ dividing cells among the remaining Nkx2.1⁺ progenitors is also strongly decreased in *Nkx2.1*^{-/-} mice compared to wild-type. By contrast, the progenitors that are not depending on Nkx2.1, were showing a normal rate of division or were even dividing more frequently in the mutant POA* region (results: section1 Fig. 5). Finally, the GLAST⁺ staining allowed us to unravel that both the number of Nkx2.1⁺ radial glia progenitors of the VZ and the post-mitotic Nkx2.1⁺/GLAST⁺ cells of the parenchyma were decreased in the mutant (results: section1 Fig. 5).

Altogether these results suggest that in *Nkx2.1*^{-/-} mice brains, the progenitor cells which express the mutated Nkx2.1 protein probably possess insufficient capacity to divide completely, which maybe leads to insufficient capacity to give rise to their glial progeny. However, such progenitors are probably replaced by other progenitors which divide but possess other intrinsic properties and which are giving rise to another type of progeny; neurons for instance.

Thereafter, we intended to study the capacity of the mutant Nkx2.1 progenitors to be differentiated into astrocytes. To this purpose, we performed *in vivo* and *in vitro* analyses. First, we combined immuno-fluorescent staining for Nkx2.1, GLAST and β III tubulin on coronal sections from wild-type and *Nkx2.1*^{-/-} brains at E16.5. This allowed us to confirm, that all post-mitotic Nkx2.1⁺ cells which were present in *Nkx2.1*^{-/-} mice brains were β III tubulin⁺ neurons and not glia (results: section 1 Fig.7). Second, we performed also immunocytochemical staining for Nkx2.1 and the GFAP and for Nkx2.1 and the β III tubulin on differentiated neurospheres (results: section 1 Fig. 7). Here again, we found that the mutant neurospheres were quasi exclusively composed of Nkx2.1⁺/ β III tubulin⁺ neurons and Nkx2.1⁻/GFAP⁺ astrocytes, and were devoid of Nkx2.1⁺/GFAP⁺ cells. Therefore, *in vitro* as *in vivo*, the mutant Nkx2.1⁺ progenitors lost their capacity to generate astroglial cells.

Surprisingly, we additionally discovered that the Nkx2.1 protein was frequently found within the cytosol of the neuronal processes instead of within the nucleus. This cytosolic location of Nkx2.1 protein was only found in a small population of neurons migrating from the caudal

extension of the POA (results: section 1 Fig. 7). Interestingly, within differentiated neurospheres, we again found labeling for the Nkx2.1 protein within the nuclei and processes of neurons (results: section 1 Fig. 7). This unexpected cytosolic location for a transcription factor was probably reflecting another yet unstudied function of Nkx2.1. Since that transcription factor has already been shown to be essential for multiple cellular mechanisms, we cannot exclude that Nkx2.1 might have a specific role to play within the neuronal processes. Indeed, a potential effect of Nkx2.1 in neurite elongation has been yet only partially studied by our group and therefore will require to be further investigated.

In conclusion, together these results show that the mutation of Nkx2.1 transcription factor leads to incomplete division capacity and incomplete cell fate specification of the subpallial progenitors.

Nkx2.1 binds the promotor and activates glial specific genes

As a transcription factor, Nkx2.1, also termed TTF-1 for thyroid transcription factor 1 or T/ebp for thyroid-specific enhancer binding protein, is known to bind specific DNA sequences, namely the promotor regions of many genes coding for essential proteins. Indeed, Nkx2.1 regulates the transcription of many genes of the thyroid (Guazzi, Price et al. 1990; Lazzaro, Price et al. 1991) (Sussel, Marin et al. 1999) and activates pulmonary-surfactant (Boggaram 2009), as well as pituitary gland genes (Hamdan, Liu et al. 1998). Moreover, it has been shown *in vitro*, that Nestin, might be a target of *Nkx2.1* (Lonigro, Donnini et al. 2001). Overexpression of *Nkx2.1* lead to the up-regulation of the *Nestin* gene since Nkx2.1 was binding a specific enhancer sequence of *Nestin* (Lonigro, Donnini et al. 2001). Furthermore, recent finding are showing through genome-wide analyses of its transcriptional targets, that Nkx2.1 was binding to many newly identified genes involved in cell proliferation (Tagne, Gupta et al. 2012). Therefore, in addition to the multitude of roles that Nkx2.1 was already shown to play, we hypothesized that, Nkx2.1 was probably also controlling the specification of the subpallial precursors into astrocytes or polydendrocytes by directly regulating the expression of specific astrocytic or polydendrocytic genes such as GLAST, the GFAP, S100 β , Olig2, and NG2. In order to answer this question, we performed a chromatin immuno-precipitation assay (ChIP) and we found that indeed, Nkx2.1 was able to bind consensus sequences in the promoter region of all these glial specific genes (results: section 1 Fig. 8). Afterward, as a control for the potential positive regulation of these glial-specific genes by Nkx2.1, we co-transfected HEK293 cells with two different combinations of reporter constructs. To this purpose, we used: 1) the *pCAG-IRES-Tomato* plasmid for a control of the transfection, 2) a *pDRIVE-mGFAP-LacZ* expression plasmid which contains the LacZ reporter under the control of

GFAP promoter, and 3) a *pCAG-Nkx2.1-IRES-Tomato* to over-express Nkx2.1 (results: section 1 Fig. 8).

Interestingly we found, that when the expression vector of Nkx2.1 protein was added, the LacZ reporter was overexpressed and thus, demonstrating the direct binding of Nkx2.1 to the promoter region of the *GFAP* gene.

Therefore, as previously hypothesized, Nkx2.1 transcription factor is probably directly regulating the differentiation and therefore the specification of the progenitor cells into various types of glial cells by directly up- or down-regulating the expression of specific glial genes. Nevertheless, the direct up-regulation or down-regulation of all the different glial specific genes which we have found to be bound by Nkx2.1, needs yet to be demonstrated.

Guidepost function of Nkx2.1⁺ precursors, interneurons and astroglia for commissural axons

As previously mentioned, one of the multiple role of Nkx2.1 in the developing mouse brain, has been shown to be the guidance of the ascending dopaminergic axons (Kawano, Horie et al. 2003). Indeed, in *Nkx2.1*^{-/-} mice brains, the dopaminergic cells of the mesencephalon were looking to follow a normal development, but the majority of their ascending axons were seen to aberrantly cross the ventral midline of the caudal hypothalamus and to project to the contralateral instead of the ipsilateral striatum (Kawano, Horie et al. 2003).

Importantly, in addition to the previously published results on *Nkx2.1*^{-/-} guidance defects in the mesencephalon, we have discovered in the present study that all the three biggest commissures of the telencephalon were also displaying striking axonal guidance anomalies. For instance, we have found through various immunohistochemical studies (results: section 2 Fig. 2, 3 and 7), DiI and DiA injections (results: section 2 Fig. 4), in utero electroporation and time-lapse video microscopy (results: section 2 Fig. 5), that the axons of the CC were not properly fasciculated in the mid CC, and were making aberrant branching after having crossed the midline. Moreover, some axons of the dorsal path were invading the ventral path of the CC (results: section 2, Fig. 3, 4, 5 and 7). The axons of the hippocampal commissure (HIC) were forming Probst bundles in the region of the fornix which was also completely unfasciculated (results: section 2, Fig. 3, 4, 5 and 7). Finally, the axons of the anterior commissure (AC) were never seen to reach the midline and cross it; they were observed to be deflected ventrally and abruptly stop their growth in ventro-lateral regions (results: section 2, Fig. 2 and 3). Therefore, we aimed to investigate what could be the principal cause of these enormous axonal guidance issues in *Nkx2.1*^{-/-} mice.

First, in our previous study on *Nkx2.1*-derived embryonic glial cells, we had already discovered that both the CC and the AC were populated by numerous transient astrocyte-like and polydendrocyte-like types of cells (results: section 2, Fig 1). In the midline of both commissures, we found GLAST⁺/GFAP⁺ astrocyte-like cells which were born most probably within the ts and the POA, as soon as E14.5 (results: section 1, Supplementary Fig. S1 and section 2, Fig. 1). We found GLAST⁺/Olig2⁺ astrocyte-like cells, within the midline, but also the lateral extensions of both commissures. These cells were partially born from *Nkx2.1*⁺ germinal sites (the ts, the MGE, the AEP/POA) but also from *Nkx2.1*⁻ ventricular regions probably such as the GW (and the VZ of the dorsal pallium for the cells which were populating the dorsal telencephalon only) (results: section 1, Supplementary Fig. S1 and section 2, Fig. 1). We discovered NG2⁺/Olig2⁺/S100β⁺ polydendrocytes also located in the medial and lateral part of the CC and the AC, which were originating from the same *Nkx2.1*-regulated subpallial regions (results: section 1, Supplementary Fig. S1 and section 2, Fig. 1).

Since it was already known from number of studies that the astroglial cells situated at the midline were playing an important role of guidepost cells for channeling the commissural axons (Silver, Lorenz et al. 1982; Silver, Edwards et al. 1993; Shu and Richards 2001; Shu, Puche et al. 2003; Shu, Sundaresan et al. 2003; Smith, Ohkubo et al. 2006) and since our group had already shown that the pioneer GABAergic interneurons of the CC were additionally involved in that function (Niquille, Garel et al. 2009), we aimed to further discriminate which of the two type of cells between *Nkx2.1*-derived interneurons or glia was the key player in axonal guidance.

To this purpose, we performed three different cell ablating strategies from which we compared the axonal guidance issues. First, we used *Nkx2.1-Cre*⁺/*Rosa-DTA* mice in which a majority of *Nkx2.1*-derived post-mitotic cells are selectively ablated. In these mice, the *Nkx2.1*⁺ progenitors are only partially eliminated since the Cre-mediated recombination takes several days to occur (results: section 2, Fig. 6 and results: section 3, Fig. S1). Moreover, contrarily to what happen in *Nkx2.1*^{-/-}, the AC in these mutants is not completely absent from the midline (results section 2 Fig. 2, 3 and 6). This allowed us to better identify what was at the origin of the guidance defects occurring in this region. Second, we used *Nkx2.1-Cre*⁺/*NSE-DTA* mice in which only the *Nkx2.1*-derived post-mitotic neurons are selectively depleted. Finally, we used *NG2-Cre*⁺/*Rosa-DTA* mice in which only the NG2⁺ post-mitotic cells are ablated. This last mutant allowed us to discriminate among the *Nkx2.1*-derived astrocyte-like or polydendrocyte-like, which type of glia was more implicated in axonal guidance.

In order to evaluate the rate of depletion of *Nkx2.1*-derived *GAD67-GFP*⁺ interneurons in these three mutants, we produced them on a *GAD67-GFP*⁺ genetic background. The loss of interneurons was quantified within the midline and the side of both the CC and the AC (results:

section 2, Fig. 2). We found that the loss of interneurons in both *Nkx2.1-Cre⁺/Rosa-DTA* and *Nkx2.1-Cre⁺/NSE-DTA* mice were comparable even if there was a slightly stronger depletion in the *Rosa-DTA* than in the *NSE-DTA* mutant (*Nkx2.1-Cre⁺/Rosa-DTA* : around 85% of loss in the mid CC and 55% in the side CC; 75% loss in the mid AC and 22% in the side AC versus *Nkx2.1-Cre⁺/NSE-DTA* : 63% in the mid CC and 22% in the side CC; 64% loss in the mid AC and 30% in the side AC) (results: section 2, Fig. 2). This small difference might be due to the additional depletion of glial cells in *Nkx2.1-Cre⁺/Rosa-DTA* mice. It has been shown already in the cortex and the cerebellum of rodents that for their proper migration, neurons require the presence of radial glial cells (Marin and Rubenstein 2003; Tabata and Nakajima 2003; Noctor, Martinez-Cerdeno et al. 2004). If we extrapolate these findings to the GABAergic interneurons, it might be possible that also these neurons need the presence of glial cells for their proper migration within the commissural tracts. This could explain why less interneurons were found in both commissures of *Nkx2.1-Cre⁺/Rosa-DTA* compared to *Nkx2.1-Cre⁺/NSE-DTA* mice (results: section 2, Fig. 2). Thereafter, in *NG2-Cre⁺/Rosa-DTA* mice, there was surprisingly a small but anyway insignificant loss of *GAD67-GFP⁺* interneurons which can be indirectly due to the loss of the *NG2⁺* cells or to the loss of some unknown trophic factor that they could maybe secrete (results: section 2, Fig. 2).

When looking at the axonal guidance defects through immunohistochemical staining for L1 and the GFP, we discovered that they were much more severe when both *Nkx2.1*-derived glia and neurons were depleted then when only post-mitotic neurons were ablated (results: section 2, Fig. 2 and 3). In *Nkx2.1-Cre⁺/Rosa-DTA* mice, the axons of the CC were misrouted to a similar extend than in *Nkx2.1^{-/-}* mice, making the CC looking enlarged. The fibers of the fornix were forming Probst bundles within the septum, but the more striking defects were seen at the level of the AC where the tract was split into two/three paths (results: section 2, Fig. 2 and 3). The AC axons were deflected both ventrally and dorsally where a portion of them was still able to cross the midline but where they were also surprisingly invading the hippocampus (results: section 2, Fig. 2 and 3).

By contrast, in *Nkx2.1-Cre⁺/NSE-DTA* mice, more subtle axonal guidance defects were observed in the region of the fornix and the AC. The fibers of the fornix were also seen to form bundles in the septal region and those of the AC were forming a thinner tract crossing the midline and exhibiting a smaller surface area after measurement (results: section 2, Fig. 2), since a part of the axons were deflected dorsally towards the fornix (results: section 2, Fig. 3). Finally, despite recent findings stipulating that *NG2⁺* polydendrocytes may play a role in attracting the callosal axons (Yang, Suzuki et al. 2006), in *NG2-Cre⁺/Rosa-DTA* mice, none of the previously described defects in the CC and the AC were observed. The axonal tracts of the CC, the fornix and the AC were all well channeled and fasciculated indicating that even if the polydendrocytes are depleted

and despite the small loss of *GAD67-GFP*⁺ interneurons found in that mutant, no impairment of axonal pathfinding was visible (results: section 2, Fig. 2 and 3).

Altogether these data unravel that both *Nkx2.1*-derived post-mitotic glial cells and neurons are essential aids for the proper navigation and fasciculation of the growing commissural axons, and also that NG2⁺ polydendrocytes might not be essential in this mechanism since their selective depletion was not sufficient to affect the axonal pathfinding.

Nevertheless, we aimed then to investigate more closely what was happening to the *Nkx2.1*⁺ progenitors and *Nkx2.1*-derived astroglial cells at the midline and around the AC in *Nkx2.1-Cre*⁺/*Rosa-DTA* mutants. Indeed, a “tunnel” structure made of an astroglial cell population that surrounds the AC has been proposed to channel the axons of that tract but functional evidences were missing to prove the direct involvement of these cells (Pires-Neto, Braga-De-Souza et al. 1998; Lent, Uziel et al. 2005). Immunostaining for Nkx2.1 and GLAST revealed that the progenitor cells of the ts, the MGE and the AEP/POA were apparently not ablated. However, the post-mitotic glia seen within the tract and forming a palisade which border the AC, were partially missing (results: section 2, Fig. 6). One explanation for that might be, that only the post-mitotic cells originating from Nkx2.1⁺/GLAST⁺ precursors of the ts and POA are depleted (results: section 2, Fig. 6). Then, knowing from our previous study that a part of the progenitors of the ts and the AEP/POA were also regulated by Olig2, we did quantify the loss of differentiated GLAST⁺/Olig2⁻, GLAST⁻/Olig2⁺, GLAST⁺/Olig2⁺ glia within the AC tract. Indeed, we found that there was an important decrease of these glia in *Nkx2.1-Cre*⁺/*Rosa-DTA* mutants (results: section 2, Fig. 6), indicating once again that the ablation of post-mitotic glia originating from Nkx2.1⁺ germinal sites is directly correlated to the AC axonal guidance issues.

Furthermore, the combination of immunostaining for L1 and the GFAP and for L1 and GLAST allowed us to discover that the GLAST⁺/GFAP⁺ astroglial cells which were remaining at the midline were totally disorganized and therefore were not any more forming structured boundaries encircling the AC. As a result, the axons were deflected dorsally and penetrated the ts (results: section 2 Fig. 6).

Similarly, to study the axonal pathfinding within the CC of *Nkx2.1-Cre*⁺/*Rosa-DTA* embryos, we performed immunostaining for the GFAP⁺ astroglial cells of the midline and the Calretinin⁺ neurons that were previously identified by our group as guidepost neurons funneling the Nrp-1⁺ callosal fibers through the secretion of Sema 3C (Niquille, Garel et al. 2009)(results: section 2, Fig. 7). When compared to *Nkx2.1*^{-/-} mice, only the post-mitotic GFAP⁺ astrocytes situated within the tract were depleted in *Nkx2.1-Cre*⁺/*Rosa-DTA* mice. Moreover, the Calretinin⁺ neurons were not disorganized as in *Nkx2.1*^{-/-}. Consequently, the callosal fibers were not seen to make aberrant branching, or to take wrong trajectories, which seem to indicate that the correct positioning of the

GFAP⁺ glia and Calretinin⁺ neurons is sufficient for a proper axonal pathfinding in the CC. Currently, it is not clear whether the Calretinin⁺ neurons require a proper development of the GFAP⁺ astrocytes of the IG, CC and MZG for their own correct positioning around this area, or whether, in the contrary, the GFAP⁺ astrocytes need the presence of the Calretinin⁺ neurons (Niquille, Garel et al. 2009) (see results: section 2, Fig. 7). It is also interesting to notice that both the GLAST⁺/GFAP⁺ astroglia of the IG and the MZG were not ablated by the diphtheria toxin which supports again the idea that both structures have a common origin with the ts and that these cells might still be partially in a progenitor state, since a lot of them were showing a positive BrdU labeling at E16.5 (discussion: Figure I).

Therefore, our analysis indicates that Nkx2.1⁺ progenitors, post-mitotic glia and interneurons might actively and synergistically participate to the guidance of the commissures.

Finally, we aimed to screen for potential guidance molecules secreted by *Nkx2.1*-regulated precursors, astroglia or neurons implicated in the guidance of the AC. Knowing from the literature that the secreted chemo-repulsive cue Slit2 was playing an important role for the correct formation of major forebrain tracts through interaction with Robo receptors (Rothberg, Hartley et al. 1988; Rothberg, Jacobs et al. 1990; Kidd, Brose et al. 1998; Brose, Bland et al. 1999; Kidd, Bland et al. 1999; Rajagopalan, Nicolas et al. 2000; Shu, Sundaresan et al. 2003; Sabatier, Plump et al. 2004; Andrews, Liapi et al. 2006; Unni, Piper et al. 2012), and also, that the defects observed in *Slit2*^{-/-} and *Nrp-2*^{-/-} mutants were similar to those visualized in *Nkx2.1-Cre⁺/Rosa-DTA* embryos (Chen, Bagri et al. 2000; Bagri, Marin et al. 2002; Plump, Erskine et al. 2002; Unni, Piper et al. 2012), we thus started to screen for guidance molecules and we performed *in situ* hybridizations for Slit2 mRNA in wild-type, *Nkx2.1-Cre⁺/Rosa-DTA* and *Nkx2.1*^{-/-} coronal slices at E16.5 (results: section 2, Fig.8 and 9). This staining revealed that all the precursor cells of the VZ and SVZ of the ts, MGE and AEP/POA were strongly expressing Slit2, consequently probably forming a permissive Slit2⁻ path encircled by a repulsive Slit2⁺ environment (results: section 2, Fig.8). In addition, the level of expression of Slit2 mRNA was looking reduced in both *Nkx2.1-Cre⁺/Rosa-DTA* and *Nkx2.1*^{-/-} compared to wild-type, within all Nkx2.1⁺ germinal regions aforementioned, except within the GW which is not an *Nkx2.1*-regulated site (results: section 2, Fig. 9). Therefore, it may be possible that Nkx2.1⁺ progenitors participate to guide the commissural axons (in addition to their differentiated neuronal and glial progeny) through the secretion of the chemo-repellant molecule Slit2.

Interestingly, it has been demonstrated in another study that the cells surrounding the AC tract, namely the Nkx2.1⁺ progenitors of the ts and AEP/POA, were also expressing high levels of Netrin-1 (Serafini, Colamarino et al. 1996). Moreover, studies of glial cells migration performed within the rat optical tract have shown that astroglial cells were repulsed from their site of origin by a gradient of Netrin-1, which leads to their migration towards the retina (Sugimoto, Taniguchi et al.

2001; Tsai and Miller 2002). It should be therefore interesting to investigate the potential expression of the receptors DCC and Unc5 on the *Nkx2.1*-derived post-mitotic cells.

As a conclusion and in view of our results, it can be deciphered that Nkx2.1 is a novel key regulator of axonal guidance in the commissural plate comprising the CC, the fornix and the AC (Moldrich, Gobijs et al. 2010). The *Nkx2.1*-regulated cells, namely the precursors, the GABAergic interneurons and the astrocytes have a synergistic and essential role to play for the correct formation and development of the axonal tracts. These mechanisms are probably mediated 1) by both the astroglia and the neurons that are known, yet, to act as intermediate targets or guidance decision points, and 2) through the expression of the repellent cue, Slit2 by Nkx2.1-regulated precursors of the ts and the AEP/POA that help maintaining a directed axonal growth. Therefore, the depletion of one type of these actors, or all types, leads to severe axonal targeting defects in the CC and the fornix, and either an abnormal formation or a complete absence of the AC (see also results: section 2; Table 1 p.192).

Role of *Nkx2.1*-derived polydendrocytes in angiogenesis

Really interestingly, in our two previous studies, we have discovered that Nkx2.1 was regulating the division and the specification of embryonic NG2⁺ polydendrocyte-like cells. These cells migrate tangentially from subpallial germinal regions such as the MGE, the ts and the AEP/POA toward the cortex and the CC as OLPs were shown to do (Kessaris, Pringle et al. 2008). These NG2⁺ cells populate the entire telencephalon: white matter and gray matter as previously described, and a large portion of them, the *Nkx2.1*-derived subgroup, will never give rise to mature oligodendrocytes, since they disappear completely from the telencephalon before P30. (Kessaris, Pringle et al. 2008) (Kriegstein and Alvarez-Buylla 2009; Nishiyama, Komitova et al. 2009).

Therefore, the role of this transient population of cells in the developing telencephalon is becoming really intriguing. In our study on the role of *Nkx2.1*-derived glial cells in the axonal guidance of the commissures (results: section 2), we have found that most probably, these NG2⁺ cells were not involved in such mechanisms, since their depletion in *NG2-Cre⁺/Rosa-DTA* mice was not affecting the capacity of commissural axons to find their way through the midline and to find their contralateral targets (results: section 2, Fig. 2 and 3). However, in order to study the function of *Nkx2.1*-regulated polydendrocytes in the telencephalon, we proceeded to a selective fate-mapping study of these cells. To this purpose, we used both *NG2-Cre⁺/Rosa-YFP* and *Nkx2.1-Cre⁺/Rosa-YFP* reporter mice from E14.5 to E18.5 which allowed us to characterize these cells present in the commissures, but also in the gray matter of the entire telencephalon (the entire cortex, septum and striatum). We found that they were all co-expressing Olig2 and in a majority S100 β , but

never GLAST or GFAP (results: section 3, Fig.1). Interestingly, the YFP signal of *Nkx2.1-Cre⁺/Rosa-YFP* mice coupled to a staining for NG2 revealed that the *Nkx2.1*-derived NG2⁺ polydendrocytes were migrating tangentially, with a four day delay after the growing blood vessels, in a ventro-lateral to dorso-medial gradient (Vasudevan, Long et al. 2008), and were strategically situated all along the nascent blood vessels (results: section 3 Fig. 1, 2 and Supplementary Fig. S1 and S3). Moreover, it is interesting to notice, that the pericytes, the mural cells that surrounds the blood vessels and which are known like the vSMCs to elicit the functional hyperemia, also express the NG2 proteoglycan (results: section 3, Fig.2). Indeed, at E18.5, the processes of the *Nkx2.1*-derived polydendrocytes were showing to form close contacts with the pericytes. These contacts were then maintained until the first post-natal week, since the *Nkx2.1*-derived polydendrocytes were seen to disappear abruptly between P2 and P8 (results: section 3, Supplementary Fig. S2).

Moreover, a recent study on brain angiogenesis has designated Nkx2.1 as a regulator of this mechanism in mice embryos. Nkx2.1 is believed to control the proliferation of the endothelial precursors in a cell autonomous manner (Vasudevan and Bhide 2008; Vasudevan, Long et al. 2008). However, in view of our results, the close contacts between *Nkx2.1*-derived polydendrocytes and the cortical vessels show that the former might be additionally implicated in regulating brain angiogenesis. Thus, we aimed to discriminate if there was in addition to the cell-autonomous function of Nkx2.1, a non-cell autonomous function played by the polydendrocytes in regulating angiogenesis.

Surprisingly, using *NG2-Cre⁺/Rosa-YFP* mice, the YFP signal was found in a majority of polydendrocytes of the medial cortex (around 65%) but was only rarely visible in the PDGFR- β ⁺ pericytes, indicating that the Cre-recombination mediated by the NG2 promoter was efficient only into the polydendrocytes (results: section 3, Fig.2). Therefore, we took advantage of that fact to study the potential role of the polydendrocytes on the blood vessels formation. We performed two different selective cell ablating strategy. Thus, by crossing *NG2-Cre* and *Nkx2.1-Cre* mice with the *Rosa-DTA* mice, we were able to selectively deplete nearly 65% of the NG2⁺ polydendrocytes in the first case, and quasi 100% of them in the second case (results: section 3 Supplementary Fig. S1 and S3). As a result, we discovered that in addition to the drastic loss of NG2⁺ polydendrocytes, the blood vessels morphology in both mutants was looking to be impaired in a similar manner (results: section 3 Fig.3). DAB staining for PECAM and erythrocytes as well as, immunofluorescent labeling for Isolectin and for the lymphocyte antigen 76 (Ter119) which respectively stain the endothelial cells of the blood vessels and the erythrocytes, unraveled that: 1) the blood vessels were displaying big variations in their diameter, 2) some vessels were twisted, 3) their secondary branches were stopping to grow abruptly and were exhibiting enlarged flat ends, 4) the erythrocytes were forming aggregates as if they were stuck within the bifurcations, and 5) the blood vessels were unable to

form a regular alveolar pattern (results: section 3 Fig. 2, 3 and Supplementary Fig. S1, S3 and S4). Moreover, the Isolectin staining allowed us to unravel also that in these mutants, the guidepost macrophages were normally present in a close vicinity of the tip cells which were still induced and normally sprouting (Adams and Alitalo 2007; Fantin, Vieira et al. 2010) (results: section 3 Fig. 2). Importantly, in both mutants, the PDGFR- β^+ pericytes were not depleted (results: section 3 Fig. 2).

Taken together, these results thus indicated for the first time that the loss of *Nkx2.1*-derived NG2⁺ polydendrocytes could be correlated to strong defects in the blood vessels development. Thus, to ascertain the truthfulness of these blood vessels defects, we proceeded to a quantification of some criteria that characterize the blood vessels network. We counted a number of nodes, of branches, the total length and volume of the blood vessels network in wild-type, *Nkx2.1-Cre⁺/Rosa-DTA* and *NG2-Cre⁺/Rosa-DTA* telencephalic coronal sections at E18.5. As expected, we found a statistically significant reduced percentage of all the criteria defining the blood vessels morphology (results: section 3, Fig. 3). Furthermore, we quantified also the number of aggregates which were formed by erythrocytes as well as the number of individual erythrocytes which were freely navigating in wild-type, *Nkx2.1-Cre⁺/Rosa-DTA*, *NG2-Cre⁺/Rosa-DTA* and *Nkx2.1^{-/-}* mice. Here again, we unraveled that the erythrocytes were forming significantly more aggregates in all mutants compared to the wild-type, and that *Nkx2.1^{-/-}* mice were displaying less individual erythrocytes as compared to the wild-type (results: section 3, Fig. 3).

Therefore, these results clearly indicate that in all these mutants lacking the majority of the polydendrocytes, the morphology of the blood vessels network is impaired which might lead to a blood flow dysfunction.

Nevertheless, it has been reported by many groups, that in addition to astrocytes which were known to regulate the vasoconstriction and dilation of the vessels (Zonta, Angulo et al. 2003; Metea and Newman 2006; Metea and Newman 2007), some GABAergic interneurons may also play a role in regulating the blood flow (Cauli, Tong et al. 2004; Kocharyan, Fernandes et al. 2008), and since there is a significant loss of more than 55% and 47% of *GAD67-GFP⁺* GABAergic interneurons in the CCi of *Nkx2.1^{-/-}* and *Nkx2.1-Cre⁺/Rosa-DTA* mice respectively, we couldn't rule out the possibility that this loss was not affecting the correct development of blood vessels (results: section 3, Supplementary Fig. S4). In order to resolve this issue, we crossed *Nkx2.1-Cre* mice with *NSE-DTA* mice to selectively deplete the *Nkx2.1*-derived *GAD67-GFP⁺* interneurons. After quantification, we found that around 40% of the interneurons were depleted in the CCi of these mutants (results: section 3, Supplementary Fig. S4). However, after DAB staining for NG2⁺ polydendrocytes, for PECAM and for the erythrocytes in *Nkx2.1-Cre⁺/NSE-DTA* mice, we found that there was absolutely no loss of NG2⁺ polydendrocytes, that the blood vessels morphology was

regular, and that there was no obvious erythrocytes aggregates in *Nkx2.1-Cre⁺/NSE-DTA* mice brains compared to wild-type (results: section 3, Supplementary Fig. S3 and S5).

These results thus show that the defects observed in the blood vessels network and blood flow of *Nkx2.1^{-/-}* and *Nkx2.1-Cre⁺/Rosa-DTA* mice were not due to a loss of *GAD67-GFP⁺* interneurons. Besides, the fact that angiogenesis was affected in a similar way in *Nkx2.1^{-/-}*, *Nkx2.1-Cre⁺/Rosa-DTA* and *NG2-Cre⁺/Rosa-DTA* mice, support the idea that the blood vessels malformations we observe in these mutants are primarily due to the depletion of the NG2⁺ polydendrocytes.

During the last decade, some groups have already reported the angiogenetic guidepost function of specific astrocytes in the retina and of macrophages which secrete VEGF in the mice brain, while some others have mentioned the presence of specific guidepost cells secreting Netrin1 in the zebrafish. (Larrivee, Freitas et al. 2009) (Fantin, Vieira et al. 2010).

Similarly, it could be assessed that the polydendrocytes may play a role of trophic or guidepost cells for the blood vessels during angiogenesis, by secreting some unknown trophic, growth or guidance factors. Some preliminary screening for potential guidance molecules secreted by the NG2⁺ cells has been initiated by our group. Unfortunately, no obvious relation between a guidance molecule and the polydendrocytes has been established yet. However, we carry on our research for other potential molecules which could be secreted by these cells.

Therefore, our results indicate that the transient *Nkx2.1*-derived NG2⁺ polydendrocytes may act as guidepost or trophic cells for the proper development and formation of the blood vessels network in the brain of embryonic mice.

CONCLUSION AND PERSPECTIVES

Through this thesis work, we have been able to bring to light several novel functions for the homeodomain-containing protein Nkx2.1. For the first time, this transcription factor was shown to regulate the dividing capacity of the Nkx2.1⁺ subpallial progenitors. In addition, we demonstrated *in vitro*, that Nkx2.1 was also controlling their specification probably through its direct binding on highly conserved consensus DNA sequences situated in the promoter region of many glial-specific genes. Then, by over-expressing Nkx2.1, we were able to prove that it could directly bind the promoter of the *GFAP*. As a result, the Nkx2.1⁺ progenitors were observed *in vivo*, as well as *in vitro* to give rise to four potentially different subtypes of embryonic and transient glial cells. Two types of astrocyte-like cells: 1) the GLAST⁺/GFAP⁺ astrocytes of the midline and 2) the GLAST⁺/Olig2⁺ astroglia which were found to migrate and populate the entire telencephalon, 3) the polydendrocyte-like cells, which were also dispersed within the entire forebrain and were NG2⁺/Olig2⁺/S100β⁺, and 4), another subpopulation of polydendrocyte-like cells which was not expressing S100β. The only population that had already been well described by other group was the GLAST⁺/GFAP⁺ astrocytes of the midline. Here, the essential novelty that we have discovered is that these astroglial cells are originating from *Nkx2.1*-regulated germinal sites of the ventral telencephalon. There, our study lead to the finding of a new germinal site, located within the septum, called as the triangular septal nucleus (ts). Indeed, the MGE and the AEP/POA were already known, since long, to generate striatal and cortical GABAergic interneurons as well as OPCs or polydendrocytes and future oligodendrocytes. Now, we know that this additional structure is also giving birth to GABAergic neurons, polydendrocytes and diverse astrocyte-like cells. Moreover, in addition to their subpallial origin, this study allowed us to demonstrate the early and transient nature of the astrocyte-like and polydendrocyte-like cells. As a function, we could unravel that *Nkx2.1*-derived astrocyte-like cells together with the GABAergic interneurons and the Nkx2.1⁺ progenitors, probably through the expression of *Slit2* and yet other unknown molecules, were all cooperating in a synergistic manner in the axonal guidance of three major commissural tracts of the forebrain. Finally, we were also able to show, that *Nkx2.1*-derived NG2⁺ polydendrocytes were essential elements potentially acting as guidepost cells during angiogenesis. These specific cells, by secreting some currently unknown growth, trophic or guidance cues, might promote the formation of new nodes and branches and therefore permit to create the final connections between separated growing blood vessels networks.

Nevertheless, the precise mechanisms through which the *Nkx2.1*-derived cells can mediate their guidepost activity in both axonal guidance and angiogenesis will require further investigations to be clarified. Till now, the potential guidance or growth factors which could be involved in

promoting the vascular network formation and which could be secreted by the polydendrocytes is still unknown.

Therefore, it would be interesting to further screen for such molecules, by looking at some potential attractive/repulsive cues such as: Netrin-1 and Netrin-4 that can mediate repulsion through their binding to Unc5B, the Class 3 Semaphorins and the growth factor VEGF which can bind to receptors such as VEGFR, Nrp-1/ Nrp-2 and Plexin D1, the Slit proteins and their Robo1 and Robo4 receptors involved in angiogenesis.

Furthermore, in the case of the AC axonal pathfinding, the possible Slit2 mediated repulsion and channeling of the AC fibers will also require further analyses. First, we plan to perform additional *in situ* hybridizations for Slit2 mRNA on *Nkx2.1-Cre⁺/Rosa-DTA* embryos. Then, the expression of Robo1/Robo2, Nrp2 and Unc5 and DCC should be tested on the cells comprised within the commissural tract or on the axonal fibers composing it. Afterward, it should be possible to produce a double *Slit1^{-/-}/Slit2^{-/-}* mutant mouse strain specific for the *Nkx2.1*-derived cells, by proceeding as follows: with the use of a *Slit1^{+/-}/Slit2^{+/-}* mouse line crossed with an *Nkx2.1-Cre⁺* mouse strain, we probably might be able to produce an *Nkx2.1-Cre⁺/ Slit1^{-/-}/Slit2^{flx/flx}* double mutant mouse to study potential axonal targeting defects similar to those visualized within the AC tract of *Nkx2.1-Cre⁺/Rosa-DTA* mice.

In its integrality, this study has therefore shed light on essential mechanisms occurring in mouse brain during development and moreover, it could potentiate further analyses into new avenues exploring glial involvement in various developmental diseases such as the human Brain-Lung-Thyroid syndrome, and it could also lead to novel strategies for the treatment of human neuropathologies affecting the development of commissures or impairing the vascular network and blood flow.

REFERENCES

- (2011). "Starting the scar: a primary role for pericytes?" *Nat Med* **17**(9): 1052-1053.
- Adams, R. H. and K. Alitalo (2007). "Molecular regulation of angiogenesis and lymphangiogenesis." *Nat Rev Mol Cell Biol* **8**(6): 464-478.
- Aguirre, A., J. L. Dupree, et al. (2007). "A functional role for EGFR signaling in myelination and remyelination." *Nat Neurosci* **10**(8): 990-1002.
- Alifragis, P., A. Liapi, et al. (2004). "Lhx6 regulates the migration of cortical interneurons from the ventral telencephalon but does not specify their GABA phenotype." *J Neurosci* **24**(24): 5643-5648.
- Amselgruber, W. M., M. Buttner, et al. (2006). "The normal cellular prion protein (PrPc) is strongly expressed in bovine endocrine pancreas." *Histochem Cell Biol* **125**(4): 441-448.
- Anastasiades, P. G. and S. J. Butt (2011). "Decoding the transcriptional basis for GABAergic interneuron diversity in the mouse neocortex." *Eur J Neurosci* **34**(10): 1542-1552.
- Anderson, S., M. Mione, et al. (1999). "Differential origins of neocortical projection and local circuit neurons: role of Dlx genes in neocortical interneuronogenesis." *Cereb Cortex* **9**(6): 646-654.
- Anderson, S. A., D. D. Eisenstat, et al. (1997). "Interneuron migration from basal forebrain to neocortex: dependence on Dlx genes." *Science* **278**(5337): 474-476.
- Anderson, S. A., O. Marin, et al. (2001). "Distinct cortical migrations from the medial and lateral ganglionic eminences." *Development* **128**(3): 353-363.
- Andrews, W., A. Liapi, et al. (2006). "Robo1 regulates the development of major axon tracts and interneuron migration in the forebrain." *Development* **133**(11): 2243-2252.
- Andrews, W. D., M. Barber, et al. (2007). "Slit-Robo interactions during cortical development." *J Anat* **211**(2): 188-198.
- Ang, E. S., Jr., T. F. Haydar, et al. (2003). "Four-dimensional migratory coordinates of GABAergic interneurons in the developing mouse cortex." *J Neurosci* **23**(13): 5805-5815.
- Angevine, J. B., Jr. and R. L. Sidman (1961). "Autoradiographic study of cell migration during histogenesis of cerebral cortex in the mouse." *Nature* **192**: 766-768.
- Anthony, T. E., C. Klein, et al. (2004). "Radial glia serve as neuronal progenitors in all regions of the central nervous system." *Neuron* **41**(6): 881-890.
- Anthony, T. E., H. A. Mason, et al. (2005). "Brain lipid-binding protein is a direct target of Notch signaling in radial glial cells." *Genes Dev* **19**(9): 1028-1033.
- Arlotta, P., B. J. Molyneaux, et al. (2005). "Neuronal subtype-specific genes that control corticospinal motor neuron development in vivo." *Neuron* **45**(2): 207-221.
- Arsenijevic, Y., J. G. Villemure, et al. (2001). "Isolation of multipotent neural precursors residing in the cortex of the adult human brain." *Exp Neurol* **170**(1): 48-62.
- Ascoli, G. A., L. Alonso-Nanclares, et al. (2008). "Petilla terminology: nomenclature of features of GABAergic interneurons of the cerebral cortex." *Nat Rev Neurosci* **9**(7): 557-568.
- Avery, A. M., B. Kaur, et al. (1999). "Substrate specificity of ultraviolet DNA endonuclease (UVDE/Uve1p) from *Schizosaccharomyces pombe*." *Nucleic Acids Res* **27**(11): 2256-2264.
- Bagnard, D., M. Lohrum, et al. (1998). "Semaphorins act as attractive and repulsive guidance signals during the development of cortical projections." *Development* **125**(24): 5043-5053.
- Bagnard, D., N. Thomasset, et al. (2000). "Spatial distributions of guidance molecules regulate chemorepulsion and chemoattraction of growth cones." *J Neurosci* **20**(3): 1030-1035.
- Bagri, A., O. Marin, et al. (2002). "Slit proteins prevent midline crossing and determine the dorsoventral position of major axonal pathways in the mammalian forebrain." *Neuron* **33**(2): 233-248.
- Baldwin, L., L. Price, et al. (1992). "Spurious euglycaemia in severe diabetic ketoacidosis." *Lancet* **340**(8832): 1407-1408.

- Bashaw, G. J. and R. Klein (2010). "Signaling from axon guidance receptors." Cold Spring Harb Perspect Biol **2**(5): a001941.
- Bellion, A., J. P. Baudoin, et al. (2005). "Nucleokinesis in tangentially migrating neurons comprises two alternating phases: forward migration of the Golgi/centrosome associated with centrosome splitting and myosin contraction at the rear." J Neurosci **25**(24): 5691-5699.
- Ben-Ari, Y., I. Khalilov, et al. (2004). "Interneurons set the tune of developing networks." Trends Neurosci **27**(7): 422-427.
- Bentley, D. and M. Caudy (1983). "Navigational substrates for peripheral pioneer growth cones: limb-axis polarity cues, limb-segment boundaries, and guidepost neurons." Cold Spring Harb Symp Quant Biol **48 Pt 2**: 573-585.
- Bentley, D. and M. Caudy (1983). "Pioneer axons lose directed growth after selective killing of guidepost cells." Nature **304**(5921): 62-65.
- Berry, M. and A. W. Rogers (1965). "The migration of neuroblasts in the developing cerebral cortex." J Anat **99**(Pt 4): 691-709.
- Bertrand, N., D. S. Castro, et al. (2002). "Proneural genes and the specification of neural cell types." Nat Rev Neurosci **3**(7): 517-530.
- Bielle, F., A. Griveau, et al. (2005). "Multiple origins of Cajal-Retzius cells at the borders of the developing pallium." Nat Neurosci **8**(8): 1002-1012.
- Bielle, F., P. Marcos-Mondejar, et al. (2011). "Slit2 activity in the migration of guidepost neurons shapes thalamic projections during development and evolution." Neuron **69**(6): 1085-1098.
- Bishop, K. M., S. Garel, et al. (2003). "Emx1 and Emx2 cooperate to regulate cortical size, lamination, neuronal differentiation, development of cortical efferents, and thalamocortical pathfinding." J Comp Neurol **457**(4): 345-360.
- Boggaram, V. (2009). "Thyroid transcription factor-1 (TTF-1/Nkx2.1/TITF1) gene regulation in the lung." Clin Sci (Lond) **116**(1): 27-35.
- Borello, U. and A. Pierani (2010). "Patterning the cerebral cortex: traveling with morphogens." Curr Opin Genet Dev **20**(4): 408-415.
- Borrell, V., Y. Yoshimura, et al. (2005). "Targeted gene delivery to telencephalic inhibitory neurons by directional in utero electroporation." J Neurosci Methods **143**(2): 151-158.
- Bowtell, D. D., B. E. Kimmel, et al. (1989). "Regulation of the complex pattern of sevenless expression in the developing Drosophila eye." Proc Natl Acad Sci U S A **86**(16): 6245-6249.
- Breedveld, G. J., J. W. van Dongen, et al. (2002). "Mutations in TITF-1 are associated with benign hereditary chorea." Hum Mol Genet **11**(8): 971-979.
- Brockschneider, D., Y. Pechmann, et al. (2006). "An improved mouse line for Cre-induced cell ablation due to diphtheria toxin A, expressed from the Rosa26 locus." Genesis **44**(7): 322-327.
- Brose, K., K. S. Bland, et al. (1999). "Slit proteins bind Robo receptors and have an evolutionarily conserved role in repulsive axon guidance." Cell **96**(6): 795-806.
- Bruner, M. K., K. K. Hilgers, et al. (2005). "Graduate orthodontic education: the residents' perspective." Am J Orthod Dentofacial Orthop **128**(3): 277-282.
- Brunet, I., C. Weinl, et al. (2005). "The transcription factor Engrailed-2 guides retinal axons." Nature **438**(7064): 94-98.
- Buck, K. B. and J. Q. Zheng (2002). "Growth cone turning induced by direct local modification of microtubule dynamics." J Neurosci **22**(21): 9358-9367.
- Burns, K. A., B. Murphy, et al. (2009). "Developmental and post-injury cortical gliogenesis: a genetic fate-mapping study with Nestin-CreER mice." Glia **57**(10): 1115-1129.
- Bush, J. O. and P. Soriano (2009). "Ephrin-B1 regulates axon guidance by reverse signaling through a PDZ-dependent mechanism." Genes Dev **23**(13): 1586-1599.
- Butt, A. M., N. Hamilton, et al. (2005). "Synantocytes: the fifth element." J Anat **207**(6): 695-706.
- Butt, S. J., M. Fuccillo, et al. (2005). "The temporal and spatial origins of cortical interneurons predict their physiological subtype." Neuron **48**(4): 591-604.

- Cai, J., Y. Chen, et al. (2007). "A crucial role for Olig2 in white matter astrocyte development." Development **134**(10): 1887-1899.
- Campbell, K. and M. Gotz (2002). "Radial glia: multi-purpose cells for vertebrate brain development." Trends Neurosci **25**(5): 235-238.
- Cancedda, L., H. Fiumelli, et al. (2007). "Excitatory GABA action is essential for morphological maturation of cortical neurons in vivo." J Neurosci **27**(19): 5224-5235.
- Carmeliet, P. and M. Tessier-Lavigne (2005). "Common mechanisms of nerve and blood vessel wiring." Nature **436**(7048): 193-200.
- Carney, R. S., L. A. Cocos, et al. (2009). "Differential regulation of telencephalic pallial-subpallial boundary patterning by Pax6 and Gsh2." Cereb Cortex **19**(4): 745-759.
- Casarosa, S., C. Fode, et al. (1999). "Mash1 regulates neurogenesis in the ventral telencephalon." Development **126**(3): 525-534.
- Casper, K. B. and K. D. McCarthy (2006). "GFAP-positive progenitor cells produce neurons and oligodendrocytes throughout the CNS." Mol Cell Neurosci **31**(4): 676-684.
- Castellani, V., A. Chedotal, et al. (2000). "Analysis of the L1-deficient mouse phenotype reveals cross-talk between Semaphorin 3A and L1 signaling pathways in axonal guidance." Neuron **27**(2): 237-249.
- Cauli, B., X. K. Tong, et al. (2004). "Cortical GABA interneurons in neurovascular coupling: relays for subcortical vasoactive pathways." J Neurosci **24**(41): 8940-8949.
- Chen, H., A. Bagri, et al. (2000). "Neuropilin-2 regulates the development of selective cranial and sensory nerves and hippocampal mossy fiber projections." Neuron **25**(1): 43-56.
- Chen, H., A. Chedotal, et al. (1997). "Neuropilin-2, a novel member of the neuropilin family, is a high affinity receptor for the semaphorins Sema E and Sema IV but not Sema III." Neuron **19**(3): 547-559.
- Chen, Z. J., M. Negra, et al. (2002). "Oligodendrocyte precursor cells: reactive cells that inhibit axon growth and regeneration." J Neurocytol **31**(6-7): 481-495.
- Chen, Z. J., Y. Ughrin, et al. (2002). "Inhibition of axon growth by oligodendrocyte precursor cells." Mol Cell Neurosci **20**(1): 125-139.
- Chenn, A. and S. K. McConnell (1995). "Cleavage orientation and the asymmetric inheritance of Notch1 immunoreactivity in mammalian neurogenesis." Cell **82**(4): 631-641.
- Chiang, C., Y. Litingtung, et al. (1996). "Cyclopia and defective axial patterning in mice lacking Sonic hedgehog gene function." Nature **383**(6599): 407-413.
- Chilton, J. K. (2006). "Molecular mechanisms of axon guidance." Dev Biol **292**(1): 13-24.
- Clarke, S. and G. M. Innocenti (1986). "Organization of immature intrahemispheric connections." J Comp Neurol **251**(1): 1-22.
- Colamarino, S. A. and M. Tessier-Lavigne (1995). "The axonal chemoattractant netrin-1 is also a chemorepellent for trochlear motor axons." Cell **81**(4): 621-629.
- Corbin, J. G., N. Gaiano, et al. (2000). "The Gsh2 homeodomain gene controls multiple aspects of telencephalic development." Development **127**(23): 5007-5020.
- Corbin, J. G., S. Nery, et al. (2001). "Telencephalic cells take a tangent: non-radial migration in the mammalian forebrain." Nat Neurosci **4 Suppl**: 1177-1182.
- Corbin, J. G., M. Rutlin, et al. (2003). "Combinatorial function of the homeodomain proteins Nkx2.1 and Gsh2 in ventral telencephalic patterning." Development **130**(20): 4895-4906.
- Costa, M. R., O. Buchholz, et al. (2009). "Late origin of glia-restricted progenitors in the developing mouse cerebral cortex." Cereb Cortex **19 Suppl 1**: i135-143.
- Crews, L., A. Adame, et al. (2010). "Increased BMP6 levels in the brains of Alzheimer's disease patients and APP transgenic mice are accompanied by impaired neurogenesis." J Neurosci **30**(37): 12252-12262.
- Dayer, A. G., K. M. Cleaver, et al. (2005). "New GABAergic interneurons in the adult neocortex and striatum are generated from different precursors." J Cell Biol **168**(3): 415-427.
- Dayer, A. G., B. Jenny, et al. (2008). "Recruiting new neurons from the subventricular zone to the rat postnatal cortex: an organotypic slice culture model." Eur J Neurosci **27**(5): 1051-1060.

- de Carlos, J. A., L. Lopez-Mascaraque, et al. (1996). "Dynamics of cell migration from the lateral ganglionic eminence in the rat." *J Neurosci* **16**(19): 6146-6156.
- de Castro, R., Jr., R. Tajrishi, et al. (2005). "Differential responses of spinal axons to transection: influence of the NG2 proteoglycan." *Exp Neurol* **192**(2): 299-309.
- De Felice, M., G. Damante, et al. (1995). "Redundant domains contribute to the transcriptional activity of the thyroid transcription factor 1." *J Biol Chem* **270**(44): 26649-26656.
- Dehay, C. and H. Kennedy (2007). "Cell-cycle control and cortical development." *Nat Rev Neurosci* **8**(6): 438-450.
- Del Rio, J. A., B. Heimrich, et al. (1997). "A role for Cajal-Retzius cells and reelin in the development of hippocampal connections." *Nature* **385**(6611): 70-74.
- Derijck, A. A., S. Van Erp, et al. (2010). "Semaphorin signaling: molecular switches at the midline." *Trends Cell Biol* **20**(9): 568-576.
- Dickson, B. J. (2001). "Rho GTPases in growth cone guidance." *Curr Opin Neurobiol* **11**(1): 103-110.
- Dickson, B. J. (2002). "Molecular mechanisms of axon guidance." *Science* **298**(5600): 1959-1964.
- Dickson, B. J. and Y. Zou (2010). "Navigating intermediate targets: the nervous system midline." *Cold Spring Harb Perspect Biol* **2**(8): a002055.
- Donahoo, A. L. and L. J. Richards (2009). "Understanding the mechanisms of callosal development through the use of transgenic mouse models." *Semin Pediatr Neurol* **16**(3): 127-142.
- Dou, C. L. and J. M. Levine (1994). "Inhibition of neurite growth by the NG2 chondroitin sulfate proteoglycan." *J Neurosci* **14**(12): 7616-7628.
- Du, T., Q. Xu, et al. (2008). "NKX2.1 specifies cortical interneuron fate by activating Lhx6." *Development* **135**(8): 1559-1567.
- Duan, B., Y. Z. Wang, et al. (2011). "Extracellular spermine exacerbates ischemic neuronal injury through sensitization of ASIC1a channels to extracellular acidosis." *J Neurosci* **31**(6): 2101-2112.
- Egea, J. and R. Klein (2007). "Bidirectional Eph-ephrin signaling during axon guidance." *Trends Cell Biol* **17**(5): 230-238.
- Eichmann, A., T. Makinen, et al. (2005). "Neural guidance molecules regulate vascular remodeling and vessel navigation." *Genes Dev* **19**(9): 1013-1021.
- Ericson, J., P. Rashbass, et al. (1997). "Pax6 controls progenitor cell identity and neuronal fate in response to graded Shh signaling." *Cell* **90**(1): 169-180.
- Evans, T. A. and G. J. Bashaw (2010). "Axon guidance at the midline: of mice and flies." *Curr Opin Neurobiol* **20**(1): 79-85.
- Falk, J., A. Bechara, et al. (2005). "Dual functional activity of semaphorin 3B is required for positioning the anterior commissure." *Neuron* **48**(1): 63-75.
- Fan, J. and J. A. Raper (1995). "Localized collapsing cues can steer growth cones without inducing their full collapse." *Neuron* **14**(2): 263-274.
- Fantin, A., J. M. Vieira, et al. (2010). "Tissue macrophages act as cellular chaperones for vascular anastomosis downstream of VEGF-mediated endothelial tip cell induction." *Blood* **116**(5): 829-840.
- Fazeli, A., S. L. Dickinson, et al. (1997). "Phenotype of mice lacking functional Deleted in colorectal cancer (Dcc) gene." *Nature* **386**(6627): 796-804.
- Fietz, S. A., I. Kelava, et al. (2010). "OSVZ progenitors of human and ferret neocortex are epithelial-like and expand by integrin signaling." *Nat Neurosci* **13**(6): 690-699.
- Fish, J. L., C. Dehay, et al. (2008). "Making bigger brains-the evolution of neural-progenitor-cell division." *J Cell Sci* **121**(Pt 17): 2783-2793.
- Fishell, G. and A. R. Kriegstein (2003). "Neurons from radial glia: the consequences of asymmetric inheritance." *Curr Opin Neurobiol* **13**(1): 34-41.
- Flames, N. and O. Marin (2005). "Developmental mechanisms underlying the generation of cortical interneuron diversity." *Neuron* **46**(3): 377-381.

- Flames, N., R. Pla, et al. (2007). "Delineation of multiple subpallial progenitor domains by the combinatorial expression of transcriptional codes." *J Neurosci* **27**(36): 9682-9695.
- Flandin, P., S. Kimura, et al. (2010). "The progenitor zone of the ventral medial ganglionic eminence requires Nkx2-1 to generate most of the globus pallidus but few neocortical interneurons." *J Neurosci* **30**(8): 2812-2823.
- Fode, C., Q. Ma, et al. (2000). "A role for neural determination genes in specifying the dorsoventral identity of telencephalic neurons." *Genes Dev* **14**(1): 67-80.
- Fogarty, M., M. Grist, et al. (2007). "Spatial genetic patterning of the embryonic neuroepithelium generates GABAergic interneuron diversity in the adult cortex." *J Neurosci* **27**(41): 10935-10946.
- Fogarty, M., W. D. Richardson, et al. (2005). "A subset of oligodendrocytes generated from radial glia in the dorsal spinal cord." *Development* **132**(8): 1951-1959.
- Fragkouli, A., N. V. van Wijk, et al. (2009). "LIM homeodomain transcription factor-dependent specification of bipotential MGE progenitors into cholinergic and GABAergic striatal interneurons." *Development* **136**(22): 3841-3851.
- Francis, F., A. Koulakoff, et al. (1999). "Doublecortin is a developmentally regulated, microtubule-associated protein expressed in migrating and differentiating neurons." *Neuron* **23**(2): 247-256.
- Franklin, R. J., S. A. Bayley, et al. (1995). "Differentiation of the O-2A progenitor cell line CG-4 into oligodendrocytes and astrocytes following transplantation into glia-deficient areas of CNS white matter." *Glia* **13**(1): 39-44.
- Fuentealba, L. C., E. Eivers, et al. (2007). "Integrating patterning signals: Wnt/GSK3 regulates the duration of the BMP/Smad1 signal." *Cell* **131**(5): 980-993.
- Furuta, Y., D. W. Piston, et al. (1997). "Bone morphogenetic proteins (BMPs) as regulators of dorsal forebrain development." *Development* **124**(11): 2203-2212.
- Gadea, A., A. Aguirre, et al. (2009). "Endothelin-1 regulates oligodendrocyte development." *J Neurosci* **29**(32): 10047-10062.
- Gaengel, K., G. Genove, et al. (2009). "Endothelial-mural cell signaling in vascular development and angiogenesis." *Arterioscler Thromb Vasc Biol* **29**(5): 630-638.
- Garcia-Moreno, F., N. A. Vasistha, et al. (2012). "Compartmentalization of cerebral cortical germinal zones in a lissencephalic primate and gyrencephalic rodent." *Cereb Cortex* **22**(2): 482-492.
- Garel, S., F. Marin, et al. (1997). "Family of Ebf/Olf-1-related genes potentially involved in neuronal differentiation and regional specification in the central nervous system." *Dev Dyn* **210**(3): 191-205.
- Gaspard, N., T. Bouchet, et al. (2008). "An intrinsic mechanism of corticogenesis from embryonic stem cells." *Nature* **455**(7211): 351-357.
- Gaspard, N. and P. Vanderhaeghen (2010). "Mechanisms of neural specification from embryonic stem cells." *Curr Opin Neurobiol* **20**(1): 37-43.
- Gelman, D., A. Griveau, et al. (2011). "A wide diversity of cortical GABAergic interneurons derives from the embryonic preoptic area." *J Neurosci* **31**(46): 16570-16580.
- Gelman, D. M., F. J. Martini, et al. (2009). "The embryonic preoptic area is a novel source of cortical GABAergic interneurons." *J Neurosci* **29**(29): 9380-9389.
- Ghaffari, M., X. Zeng, et al. (1997). "Nuclear localization domain of thyroid transcription factor-1 in respiratory epithelial cells." *Biochem J* **328** (Pt 3): 757-761.
- Gleeson, J. G., P. T. Lin, et al. (1999). "Doublecortin is a microtubule-associated protein and is expressed widely by migrating neurons." *Neuron* **23**(2): 257-271.
- Goldberg, D. J. and D. W. Burmeister (1986). "Stages in axon formation: observations of growth of Aplysia axons in culture using video-enhanced contrast-differential interference contrast microscopy." *J Cell Biol* **103**(5): 1921-1931.
- Gong, S., C. Zheng, et al. (2003). "A gene expression atlas of the central nervous system based on bacterial artificial chromosomes." *Nature* **425**(6961): 917-925.

- Goodman, C. S. and C. J. Shatz (1993). "Developmental mechanisms that generate precise patterns of neuronal connectivity." *Cell* **72 Suppl**: 77-98.
- Gotz, M. (2010). "Making glutamatergic neurons from GABAergic progenitors." *Nat Neurosci* **13**(11): 1308-1309.
- Gotz, M. and Y. A. Barde (2005). "Radial glial cells defined and major intermediates between embryonic stem cells and CNS neurons." *Neuron* **46**(3): 369-372.
- Gotz, M. and W. B. Huttner (2005). "The cell biology of neurogenesis." *Nat Rev Mol Cell Biol* **6**(10): 777-788.
- Gray, G. E. and J. R. Sanes (1991). "Migratory paths and phenotypic choices of clonally related cells in the avian optic tectum." *Neuron* **6**(2): 211-225.
- Grigoriou, M., A. S. Tucker, et al. (1998). "Expression and regulation of Lhx6 and Lhx7, a novel subfamily of LIM homeodomain encoding genes, suggests a role in mammalian head development." *Development* **125**(11): 2063-2074.
- Griveau, A., U. Borello, et al. (2010). "A novel role for Dbx1-derived Cajal-Retzius cells in early regionalization of the cerebral cortical neuroepithelium." *PLoS Biol* **8**(7): e1000440.
- Grove, E. A., B. P. Williams, et al. (1993). "Multiple restricted lineages in the embryonic rat cerebral cortex." *Development* **117**(2): 553-561.
- Gu, C., E. R. Rodriguez, et al. (2003). "Neuropilin-1 conveys semaphorin and VEGF signaling during neural and cardiovascular development." *Dev Cell* **5**(1): 45-57.
- Guazzi, S., M. Price, et al. (1990). "Thyroid nuclear factor 1 (TTF-1) contains a homeodomain and displays a novel DNA binding specificity." *EMBO J* **9**(11): 3631-3639.
- Guillemot, F. (2005). "Cellular and molecular control of neurogenesis in the mammalian telencephalon." *Curr Opin Cell Biol* **17**(6): 639-647.
- Guillemot, F. (2007). "Cell fate specification in the mammalian telencephalon." *Prog Neurobiol* **83**(1): 37-52.
- Guillemot, F., Z. Molnar, et al. (2006). "Molecular mechanisms of cortical differentiation." *Eur J Neurosci* **23**(4): 857-868.
- Gulacsi, A. and S. A. Anderson (2006). "Shh maintains Nkx2.1 in the MGE by a Gli3-independent mechanism." *Cereb Cortex* **16 Suppl 1**: i89-95.
- Gundersen, R. W. and J. N. Barrett (1979). "Neuronal chemotaxis: chick dorsal-root axons turn toward high concentrations of nerve growth factor." *Science* **206**(4422): 1079-1080.
- Haber, M., S. Vautrin, et al. (2009). "Subtype-specific oligodendrocyte dynamics in organotypic culture." *Glia* **57**(9): 1000-1013.
- Hamdan, H., H. Liu, et al. (1998). "Structure of the human Nkx2.1 gene." *Biochim Biophys Acta* **1396**(3): 336-348.
- Hamilton, N., P. S. Hubbard, et al. (2009). "Effects of glutamate receptor activation on NG2-glia in the rat optic nerve." *J Anat* **214**(2): 208-218.
- Hansen, D. V., J. H. Lui, et al. (2010). "Neurogenic radial glia in the outer subventricular zone of human neocortex." *Nature* **464**(7288): 554-561.
- Hardy, R. J. and V. L. Friedrich, Jr. (1996). "Progressive remodeling of the oligodendrocyte process arbor during myelinogenesis." *Dev Neurosci* **18**(4): 243-254.
- Hatton, J. D., M. H. Nguyen, et al. (1993). "Differential migration of astrocytes grafted into the developing rat brain." *Glia* **9**(2): 113-119.
- Haubensak, W., A. Attardo, et al. (2004). "Neurons arise in the basal neuroepithelium of the early mammalian telencephalon: a major site of neurogenesis." *Proc Natl Acad Sci U S A* **101**(9): 3196-3201.
- He, W., C. Ingraham, et al. (2001). "Multipotent stem cells from the mouse basal forebrain contribute GABAergic neurons and oligodendrocytes to the cerebral cortex during embryogenesis." *J Neurosci* **21**(22): 8854-8862.
- He, Z. and M. Tessier-Lavigne (1997). "Neuropilin is a receptor for the axonal chemorepellent Semaphorin III." *Cell* **90**(4): 739-751.

- Hebert, J. M. and G. Fishell (2008). "The genetics of early telencephalon patterning: some assembly required." *Nat Rev Neurosci* **9**(9): 678-685.
- Heins, N., F. Cremisi, et al. (2001). "Emx2 promotes symmetric cell divisions and a multipotential fate in precursors from the cerebral cortex." *Mol Cell Neurosci* **18**(5): 485-502.
- Heins, N., P. Malatesta, et al. (2002). "Glial cells generate neurons: the role of the transcription factor Pax6." *Nat Neurosci* **5**(4): 308-315.
- Hellstrom, M., M. Kalen, et al. (1999). "Role of PDGF-B and PDGFR-beta in recruitment of vascular smooth muscle cells and pericytes during embryonic blood vessel formation in the mouse." *Development* **126**(14): 3047-3055.
- Hernandez-Montiel, H. L., E. Tamariz, et al. (2008). "Semaphorins 3A, 3C, and 3F in mesencephalic dopaminergic axon pathfinding." *J Comp Neurol* **506**(3): 387-397.
- Hevner, R. F. (2006). "From radial glia to pyramidal-projection neuron: transcription factor cascades in cerebral cortex development." *Mol Neurobiol* **33**(1): 33-50.
- Hevner, R. F., L. Shi, et al. (2001). "Tbr1 regulates differentiation of the preplate and layer 6." *Neuron* **29**(2): 353-366.
- Higginbotham, H. R. and J. G. Gleeson (2007). "The centrosome in neuronal development." *Trends Neurosci* **30**(6): 276-283.
- Himanen, J. P. and D. B. Nikolov (2003). "Eph receptors and ephrins." *Int J Biochem Cell Biol* **35**(2): 130-134.
- Himanen, J. P. and D. B. Nikolov (2003). "Eph signaling: a structural view." *Trends Neurosci* **26**(1): 46-51.
- Hiruma, T., Y. Nakajima, et al. (2002). "Development of pharyngeal arch arteries in early mouse embryo." *J Anat* **201**(1): 15-29.
- Ho, S. K., N. Kovacevic, et al. (2009). "EphB2 and EphA4 receptors regulate formation of the principal inter-hemispheric tracts of the mammalian forebrain." *Neuroscience* **160**(4): 784-795.
- Hochstim, C., B. Deneen, et al. (2008). "Identification of positionally distinct astrocyte subtypes whose identities are specified by a homeodomain code." *Cell* **133**(3): 510-522.
- Hu, Z., X. Yue, et al. (2003). "Corpus callosum deficiency in transgenic mice expressing a truncated ephrin-A receptor." *J Neurosci* **23**(34): 10963-10970.
- Huttner, W. B. and M. Brand (1997). "Asymmetric division and polarity of neuroepithelial cells." *Curr Opin Neurobiol* **7**(1): 29-39.
- Ichikawa, M., T. Shiga, et al. (1983). "Spatial and temporal pattern of postnatal proliferation of glial cells in the parietal cortex of the rat." *Brain Res* **285**(2): 181-187.
- Innocenti, G. M. and D. J. Price (2005). "Exuberance in the development of cortical networks." *Nat Rev Neurosci* **6**(12): 955-965.
- Inta, D., J. Alfonso, et al. (2008). "Neurogenesis and widespread forebrain migration of distinct GABAergic neurons from the postnatal subventricular zone." *Proc Natl Acad Sci U S A* **105**(52): 20994-20999.
- Jacobsen, C. T. and R. H. Miller (2003). "Control of astrocyte migration in the developing cerebral cortex." *Dev Neurosci* **25**(2-4): 207-216.
- Jimenez, D., L. M. Lopez-Masaraque, et al. (2002). "Tangential migration in neocortical development." *Dev Biol* **244**(1): 155-169.
- Jones, L. L., D. Sajed, et al. (2003). "Axonal regeneration through regions of chondroitin sulfate proteoglycan deposition after spinal cord injury: a balance of permissiveness and inhibition." *J Neurosci* **23**(28): 9276-9288.
- Joshi, G., R. Sultana, et al. (2005). "Free radical mediated oxidative stress and toxic side effects in brain induced by the anti cancer drug adriamycin: insight into chemobrain." *Free Radic Res* **39**(11): 1147-1154.
- Jovanov-Milosevic, N., Z. Petanjek, et al. (2010). "Morphology, molecular phenotypes and distribution of neurons in developing human corpus callosum." *Eur J Neurosci* **32**(9): 1423-1432.

- Kaji, T., C. Yamamoto, et al. (2006). "The vascular endothelial growth factor VEGF165 induces perlecan synthesis via VEGF receptor-2 in cultured human brain microvascular endothelial cells." *Biochim Biophys Acta* **1760**(9): 1465-1474.
- Kakita, A. and J. E. Goldman (1999). "Patterns and dynamics of SVZ cell migration in the postnatal forebrain: monitoring living progenitors in slice preparations." *Neuron* **23**(3): 461-472.
- Kanatani, S., M. Yozu, et al. (2008). "COUP-TFII is preferentially expressed in the caudal ganglionic eminence and is involved in the caudal migratory stream." *J Neurosci* **28**(50): 13582-13591.
- Kang, W. and J. M. Hebert (2011). "Signaling pathways in reactive astrocytes, a genetic perspective." *Mol Neurobiol* **43**(3): 147-154.
- Kapchuk, T. J., J. M. Kelley, et al. (2008). "Components of placebo effect: randomised controlled trial in patients with irritable bowel syndrome." *BMJ* **336**(7651): 999-1003.
- Kawano, H., M. Horie, et al. (2003). "Aberrant trajectory of ascending dopaminergic pathway in mice lacking Nkx2.1." *Exp Neurol* **182**(1): 103-112.
- Keeble, T. R., M. M. Halford, et al. (2006). "The Wnt receptor Ryk is required for Wnt5a-mediated axon guidance on the contralateral side of the corpus callosum." *J Neurosci* **26**(21): 5840-5848.
- Keino-Masu, K., M. Masu, et al. (1996). "Deleted in Colorectal Cancer (DCC) encodes a netrin receptor." *Cell* **87**(2): 175-185.
- Kelava, I., I. Reillo, et al. (2012). "Abundant occurrence of basal radial glia in the subventricular zone of embryonic neocortex of a lissencephalic primate, the common marmoset *Callithrix jacchus*." *Cereb Cortex* **22**(2): 469-481.
- Keleman, K., S. Rajagopalan, et al. (2002). "Comm sorts robo to control axon guidance at the *Drosophila* midline." *Cell* **110**(4): 415-427.
- Keleman, K., C. Ribeiro, et al. (2005). "Comm function in commissural axon guidance: cell-autonomous sorting of Robo in vivo." *Nat Neurosci* **8**(2): 156-163.
- Kennedy, T. E., T. Serafini, et al. (1994). "Netrins are diffusible chemotropic factors for commissural axons in the embryonic spinal cord." *Cell* **78**(3): 425-435.
- Kerjan, G. and J. G. Gleeson (2007). "Genetic mechanisms underlying abnormal neuronal migration in classical lissencephaly." *Trends Genet* **23**(12): 623-630.
- Kessaris, N., M. Fogarty, et al. (2006). "Competing waves of oligodendrocytes in the forebrain and postnatal elimination of an embryonic lineage." *Nat Neurosci* **9**(2): 173-179.
- Kessaris, N., F. Jamen, et al. (2004). "Cooperation between sonic hedgehog and fibroblast growth factor/MAPK signalling pathways in neocortical precursors." *Development* **131**(6): 1289-1298.
- Kessaris, N., N. Pringle, et al. (2008). "Specification of CNS glia from neural stem cells in the embryonic neuroepithelium." *Philos Trans R Soc Lond B Biol Sci* **363**(1489): 71-85.
- Kidd, T., K. S. Bland, et al. (1999). "Slit is the midline repellent for the robo receptor in *Drosophila*." *Cell* **96**(6): 785-794.
- Kidd, T., K. Brose, et al. (1998). "Roundabout controls axon crossing of the CNS midline and defines a novel subfamily of evolutionarily conserved guidance receptors." *Cell* **92**(2): 205-215.
- Kim, Y. and M. Nirenberg (1989). "*Drosophila* NK-homeobox genes." *Proc Natl Acad Sci U S A* **86**(20): 7716-7720.
- Kimelberg, H. K. (2004). "The problem of astrocyte identity." *Neurochem Int* **45**(2-3): 191-202.
- Kimura, S., Y. Hara, et al. (1996). "The T/ebp null mouse: thyroid-specific enhancer-binding protein is essential for the organogenesis of the thyroid, lung, ventral forebrain, and pituitary." *Genes Dev* **10**(1): 60-69.
- Kleiner-Fisman, G. and A. E. Lang (2007). "Benign hereditary chorea revisited: a journey to understanding." *Mov Disord* **22**(16): 2297-2305; quiz 2452.

- Kocharyan, A., P. Fernandes, et al. (2008). "Specific subtypes of cortical GABA interneurons contribute to the neurovascular coupling response to basal forebrain stimulation." J Cereb Blood Flow Metab **28**(2): 221-231.
- Koester, S. E. and D. D. O'Leary (1993). "Connectional distinction between callosal and subcortically projecting cortical neurons is determined prior to axon extension." Dev Biol **160**(1): 1-14.
- Kolla, V., L. W. Gonzales, et al. (2007). "Thyroid transcription factor in differentiating type II cells: regulation, isoforms, and target genes." Am J Respir Cell Mol Biol **36**(2): 213-225.
- Kosodo, Y., K. Roper, et al. (2004). "Asymmetric distribution of the apical plasma membrane during neurogenic divisions of mammalian neuroepithelial cells." Embo Journal **23**(11): 2314-2324.
- Kriegstein, A. and A. Alvarez-Buylla (2009). "The glial nature of embryonic and adult neural stem cells." Annu Rev Neurosci **32**: 149-184.
- Kriegstein, A. R. and M. Gotz (2003). "Radial glia diversity: a matter of cell fate." Glia **43**(1): 37-43.
- Kriegstein, A. R. and S. C. Noctor (2004). "Patterns of neuronal migration in the embryonic cortex." Trends Neurosci **27**(7): 392-399.
- Krude, H., B. Schutz, et al. (2002). "Choreoathetosis, hypothyroidism, and pulmonary alterations due to human NKX2-1 haploinsufficiency." J Clin Invest **109**(4): 475-480.
- Kusakabe, T., A. Kawaguchi, et al. (2006). "Thyroid-specific enhancer-binding protein/NKX2.1 is required for the maintenance of ordered architecture and function of the differentiated thyroid." Mol Endocrinol **20**(8): 1796-1809.
- Larrivee, B., C. Freitas, et al. (2009). "Guidance of vascular development: lessons from the nervous system." Circ Res **104**(4): 428-441.
- LaVaute, T. M., Y. D. Yoo, et al. (2009). "Regulation of neural specification from human embryonic stem cells by BMP and FGF." Stem Cells **27**(8): 1741-1749.
- Lavdas, A. A., M. Grigoriou, et al. (1999). "The medial ganglionic eminence gives rise to a population of early neurons in the developing cerebral cortex." J Neurosci **19**(18): 7881-7888.
- Lazzaro, D., M. Price, et al. (1991). "The transcription factor TTF-1 is expressed at the onset of thyroid and lung morphogenesis and in restricted regions of the foetal brain." Development **113**(4): 1093-1104.
- Lebrand, C., E. W. Dent, et al. (2004). "Critical role of Ena/VASP proteins for filopodia formation in neurons and in function downstream of netrin-1." Neuron **42**(1): 37-49.
- Lee, S. H., N. Lumelsky, et al. (2000). "Efficient generation of midbrain and hindbrain neurons from mouse embryonic stem cells." Nat Biotechnol **18**(6): 675-679.
- Lent, R. and R. Z. Guimaraes (1990). "Development of interhemispheric connections through the anterior commissure in hamsters." Braz J Med Biol Res **23**(8): 671-675.
- Lent, R., D. Uziel, et al. (2005). "Cellular and molecular tunnels surrounding the forebrain commissures of human fetuses." J Comp Neurol **483**(4): 375-382.
- Letinic, K., R. Zoncu, et al. (2002). "Origin of GABAergic neurons in the human neocortex." Nature **417**(6889): 645-649.
- Levine, A. J. and A. H. Brivanlou (2007). "Proposal of a model of mammalian neural induction." Dev Biol **308**(2): 247-256.
- Levine, J. M. and A. Nishiyama (1996). "The NG2 chondroitin sulfate proteoglycan: a multifunctional proteoglycan associated with immature cells." Perspect Dev Neurobiol **3**(4): 245-259.
- Levine, J. M., F. Stincone, et al. (1993). "Development and differentiation of glial precursor cells in the rat cerebellum." Glia **7**(4): 307-321.
- Levison, S. W. and J. E. Goldman (1993). "Both oligodendrocytes and astrocytes develop from progenitors in the subventricular zone of postnatal rat forebrain." Neuron **10**(2): 201-212.

- Levitt, P., K. L. Eagleson, et al. (2004). "Regulation of neocortical interneuron development and the implications for neurodevelopmental disorders." *Trends Neurosci* **27**(7): 400-406.
- Li, L., B. I. Hutchins, et al. (2009). "Wnt5a induces simultaneous cortical axon outgrowth and repulsive axon guidance through distinct signaling mechanisms." *J Neurosci* **29**(18): 5873-5883.
- Ligon, K. L., S. Kesari, et al. (2006). "Development of NG2 neural progenitor cells requires Olig gene function." *Proc Natl Acad Sci U S A* **103**(20): 7853-7858.
- Lin, A. C. and C. E. Holt (2007). "Local translation and directional steering in axons." *EMBO J* **26**(16): 3729-3736.
- Lindwall, C., T. Fothergill, et al. (2007). "Commissure formation in the mammalian forebrain." *Curr Opin Neurobiol* **17**(1): 3-14.
- Liodis, P., M. Denaxa, et al. (2007). "Lhx6 activity is required for the normal migration and specification of cortical interneuron subtypes." *J Neurosci* **27**(12): 3078-3089.
- Lodato, S., C. Rouaux, et al. (2011). "Excitatory projection neuron subtypes control the distribution of local inhibitory interneurons in the cerebral cortex." *Neuron* **69**(4): 763-779.
- Long, H., C. Sabatier, et al. (2004). "Conserved roles for Slit and Robo proteins in midline commissural axon guidance." *Neuron* **42**(2): 213-223.
- Long, J. E., I. Cobos, et al. (2009). "Dlx1&2 and Mash1 transcription factors control MGE and CGE patterning and differentiation through parallel and overlapping pathways." *Cereb Cortex* **19 Suppl 1**: i96-106.
- Lonigro, R., D. Donnini, et al. (2001). "Nestin is a neuroepithelial target gene of thyroid transcription factor-1, a homeoprotein required for forebrain organogenesis." *J Biol Chem* **276**(51): 47807-47813.
- Lopez-Bendito, G., A. Cautinat, et al. (2006). "Tangential neuronal migration controls axon guidance: a role for neuregulin-1 in thalamocortical axon navigation." *Cell* **125**(1): 127-142.
- Lopez-Bendito, G., N. Flames, et al. (2007). "Robo1 and Robo2 cooperate to control the guidance of major axonal tracts in the mammalian forebrain." *J Neurosci* **27**(13): 3395-3407.
- Lowery, L. A. and D. Van Vactor (2009). "The trip of the tip: understanding the growth cone machinery." *Nat Rev Mol Cell Biol* **10**(5): 332-343.
- Ludwin, S. K., J. C. Kosek, et al. (1976). "The topographical distribution of S-100 and GFA proteins in the adult rat brain: an immunohistochemical study using horseradish peroxidase-labelled antibodies." *J Comp Neurol* **165**(2): 197-207.
- Lupski, J. R., J. G. Reid, et al. (2010). "Whole-genome sequencing in a patient with Charcot-Marie-Tooth neuropathy." *N Engl J Med* **362**(13): 1181-1191.
- Luskin, M. B., J. G. Parnavelas, et al. (1993). "Neurons, astrocytes, and oligodendrocytes of the rat cerebral cortex originate from separate progenitor cells: an ultrastructural analysis of clonally related cells." *J Neurosci* **13**(4): 1730-1750.
- Magno, L., V. Catanzariti, et al. (2009). "Ongoing expression of Nkx2.1 in the postnatal mouse forebrain: potential for understanding NKX2.1 haploinsufficiency in humans?" *Brain Res* **1304**: 164-186.
- Malatesta, P., M. A. Hack, et al. (2003). "Neuronal or glial progeny: regional differences in radial glia fate." *Neuron* **37**(5): 751-764.
- Mallamaci, A., L. Muzio, et al. (2000). "Area identity shifts in the early cerebral cortex of Emx2^{-/-} mutant mice." *Nat Neurosci* **3**(7): 679-686.
- Mann, F. and G. Rougon (2007). "Mechanisms of axon guidance: membrane dynamics and axonal transport in semaphorin signalling." *J Neurochem* **102**(2): 316-323.
- Marin, O., S. A. Anderson, et al. (2000). "Origin and molecular specification of striatal interneurons." *J Neurosci* **20**(16): 6063-6076.
- Marin, O., J. Baker, et al. (2002). "Patterning of the basal telencephalon and hypothalamus is essential for guidance of cortical projections." *Development* **129**(3): 761-773.

- Marin, O., A. S. Plump, et al. (2003). "Directional guidance of interneuron migration to the cerebral cortex relies on subcortical Slit1/2-independent repulsion and cortical attraction." Development **130**(9): 1889-1901.
- Marin, O. and J. L. Rubenstein (2001). "A long, remarkable journey: tangential migration in the telencephalon." Nat Rev Neurosci **2**(11): 780-790.
- Marin, O. and J. L. Rubenstein (2003). "Cell migration in the forebrain." Annu Rev Neurosci **26**: 441-483.
- Marin, O., M. Valiente, et al. (2010). "Guiding neuronal cell migrations." Cold Spring Harb Perspect Biol **2**(2): a001834.
- Markram, H., M. Toledo-Rodriguez, et al. (2004). "Interneurons of the neocortical inhibitory system." Nat Rev Neurosci **5**(10): 793-807.
- Marshall, C. A. and J. E. Goldman (2002). "Subpallial dlx2-expressing cells give rise to astrocytes and oligodendrocytes in the cerebral cortex and white matter." J Neurosci **22**(22): 9821-9830.
- Martini, F. J., M. Valiente, et al. (2009). "Biased selection of leading process branches mediates chemotaxis during tangential neuronal migration." Development **136**(1): 41-50.
- Masahira, N., H. Takebayashi, et al. (2006). "Olig2-positive progenitors in the embryonic spinal cord give rise not only to motoneurons and oligodendrocytes, but also to a subset of astrocytes and ependymal cells." Dev Biol **293**(2): 358-369.
- Mastracci, T. L., C. L. Wilcox, et al. (2011). "Nkx2.2 and Arx genetically interact to regulate pancreatic endocrine cell development and endocrine hormone expression." Dev Biol **359**(1): 1-11.
- McCarthy, M., D. H. Turnbull, et al. (2001). "Telencephalic neural progenitors appear to be restricted to regional and glial fates before the onset of neurogenesis." J Neurosci **21**(17): 6772-6781.
- McLaughlin, T., R. Hindges, et al. (2003). "Regulation of axial patterning of the retina and its topographic mapping in the brain." Curr Opin Neurobiol **13**(1): 57-69.
- McLaughlin, T., R. Hindges, et al. (2003). "Bifunctional action of ephrin-B1 as a repellent and attractant to control bidirectional branch extension in dorsal-ventral retinotopic mapping." Development **130**(11): 2407-2418.
- Mekki-Dauriac, S., E. Agius, et al. (2002). "Bone morphogenetic proteins negatively control oligodendrocyte precursor specification in the chick spinal cord." Development **129**(22): 5117-5130.
- Metea, M. R. and E. A. Newman (2006). "Glial cells dilate and constrict blood vessels: a mechanism of neurovascular coupling." J Neurosci **26**(11): 2862-2870.
- Metea, M. R. and E. A. Newman (2007). "Signalling within the neurovascular unit in the mammalian retina." Exp Physiol **92**(4): 635-640.
- Metin, C., J. P. Baudoin, et al. (2006). "Cell and molecular mechanisms involved in the migration of cortical interneurons." Eur J Neurosci **23**(4): 894-900.
- Meyer, G. and A. M. Goffinet (1998). "Prenatal development of reelin-immunoreactive neurons in the human neocortex." J Comp Neurol **397**(1): 29-40.
- Meyer, G., J. M. Soria, et al. (1998). "Different origins and developmental histories of transient neurons in the marginal zone of the fetal and neonatal rat cortex." J Comp Neurol **397**(4): 493-518.
- Miller, M. W. (1986). "The migration and neurochemical differentiation of gamma-aminobutyric acid (GABA)-immunoreactive neurons in rat visual cortex as demonstrated by a combined immunocytochemical-autoradiographic technique." Brain Res **393**(1): 41-46.
- Ming, G. L., H. J. Song, et al. (1997). "cAMP-dependent growth cone guidance by netrin-1." Neuron **19**(6): 1225-1235.
- Mission, J. P., T. Takahashi, et al. (1991). "Ontogeny of radial and other astroglial cells in murine cerebral cortex." Glia **4**(2): 138-148.

- Miyata, T., A. Kawaguchi, et al. (2001). "Asymmetric inheritance of radial glial fibers by cortical neurons." *Neuron* **31**(5): 727-741.
- Miyata, T., A. Kawaguchi, et al. (2004). "Asymmetric production of surface-dividing and non-surface-dividing cortical progenitor cells." *Development* **131**(13): 3133-3145.
- Miyoshi, G., S. J. Butt, et al. (2007). "Physiologically distinct temporal cohorts of cortical interneurons arise from telencephalic Olig2-expressing precursors." *J Neurosci* **27**(29): 7786-7798.
- Miyoshi, G. and G. Fishell (2010). "GABAergic Interneuron Lineages Selectively Sort into Specific Cortical Layers during Early Postnatal Development." *Cereb Cortex*.
- Miyoshi, G., J. Hjerling-Leffler, et al. (2010). "Genetic fate mapping reveals that the caudal ganglionic eminence produces a large and diverse population of superficial cortical interneurons." *J Neurosci* **30**(5): 1582-1594.
- Moldrich, R. X., I. Gobius, et al. (2010). "Molecular regulation of the developing commissural plate." *J Comp Neurol* **518**(18): 3645-3661.
- Molyneaux, B. J., P. Arlotta, et al. (2009). "Novel subtype-specific genes identify distinct subpopulations of callosal projection neurons." *J Neurosci* **29**(39): 12343-12354.
- Molyneaux, B. J., P. Arlotta, et al. (2007). "Neuronal subtype specification in the cerebral cortex." *Nat Rev Neurosci* **8**(6): 427-437.
- Monyer, H. and H. Markram (2004). "Interneuron Diversity series: Molecular and genetic tools to study GABAergic interneuron diversity and function." *Trends Neurosci* **27**(2): 90-97.
- Moreno, N., A. Gonzalez, et al. (2009). "Development and evolution of the subpallium." *Semin Cell Dev Biol* **20**(6): 735-743.
- Mori, T., A. Buffo, et al. (2005). "The novel roles of glial cells revisited: the contribution of radial glia and astrocytes to neurogenesis." *Curr Top Dev Biol* **69**: 67-99.
- Mori, T., K. Tanaka, et al. (2006). "Inducible gene deletion in astroglia and radial glia--a valuable tool for functional and lineage analysis." *Glia* **54**(1): 21-34.
- Morrow, T., M. R. Song, et al. (2001). "Sequential specification of neurons and glia by developmentally regulated extracellular factors." *Development* **128**(18): 3585-3594.
- Mueller, L. A., S. D. Tanksley, et al. (2005). "The Tomato Sequencing Project, the first cornerstone of the International Solanaceae Project (SOL)." *Comp Funct Genomics* **6**(3): 153-158.
- Nadarajah, B. and J. G. Parnavelas (2002). "Modes of neuronal migration in the developing cerebral cortex." *Nat Rev Neurosci* **3**(6): 423-432.
- Nakagawa, A., T. Oshima, et al. (2006). "Identification and characterization of a second, inducible promoter of relA in Escherichia coli." *Genes Genet Syst* **81**(5): 299-310.
- Nery, S., G. Fishell, et al. (2002). "The caudal ganglionic eminence is a source of distinct cortical and subcortical cell populations." *Nat Neurosci* **5**(12): 1279-1287.
- Nery, S., H. Wichterle, et al. (2001). "Sonic hedgehog contributes to oligodendrocyte specification in the mammalian forebrain." *Development* **128**(4): 527-540.
- Niquille, M., S. Garel, et al. (2009). "Transient neuronal populations are required to guide callosal axons: a role for semaphorin 3C." *PLoS Biol* **7**(10): e1000230.
- Nishiyama, A., M. Komitova, et al. (2009). "Polydendrocytes (NG2 cells): multifunctional cells with lineage plasticity." *Nat Rev Neurosci* **10**(1): 9-22.
- Nishiyama, A., X. H. Lin, et al. (1996). "Co-localization of NG2 proteoglycan and PDGF alpha-receptor on O2A progenitor cells in the developing rat brain." *J Neurosci Res* **43**(3): 299-314.
- Nishiyama, A., X. H. Lin, et al. (1996). "Interaction between NG2 proteoglycan and PDGF alpha-receptor on O2A progenitor cells is required for optimal response to PDGF." *J Neurosci Res* **43**(3): 315-330.
- Nishiyama, A., M. Watanabe, et al. (2002). "Identity, distribution, and development of polydendrocytes: NG2-expressing glial cells." *J Neurocytol* **31**(6-7): 437-455.

- Nobrega-Pereira, S., N. Kessaris, et al. (2008). "Postmitotic Nkx2-1 controls the migration of telencephalic interneurons by direct repression of guidance receptors." Neuron **59**(5): 733-745.
- Noctor, S. C., A. C. Flint, et al. (2001). "Neurons derived from radial glial cells establish radial units in neocortex." Nature **409**(6821): 714-720.
- Noctor, S. C., A. C. Flint, et al. (2002). "Dividing precursor cells of the embryonic cortical ventricular zone have morphological and molecular characteristics of radial glia." J Neurosci **22**(8): 3161-3173.
- Noctor, S. C., V. Martinez-Cerdeno, et al. (2004). "Cortical neurons arise in symmetric and asymmetric division zones and migrate through specific phases." Nat Neurosci **7**(2): 136-144.
- Norris, C. R. and K. Kalil (1991). "Guidance of callosal axons by radial glia in the developing cerebral cortex." J Neurosci **11**(11): 3481-3492.
- Okada, S., M. Nakamura, et al. (2006). "Conditional ablation of Stat3 or Socs3 discloses a dual role for reactive astrocytes after spinal cord injury." Nat Med **12**(7): 829-834.
- Okada, T., K. Keino-Masu, et al. (2007). "Migration and nucleogenesis of mouse precerebellar neurons visualized by in utero electroporation of a green fluorescent protein gene." Neurosci Res **57**(1): 40-49.
- Ozaki, H. S. and D. Wahlsten (1998). "Timing and origin of the first cortical axons to project through the corpus callosum and the subsequent emergence of callosal projection cells in mouse." J Comp Neurol **400**(2): 197-206.
- Pabst, O., H. Herbrand, et al. (2000). "NKX2 gene expression in neuroectoderm but not in mesendodermally derived structures depends on sonic hedgehog in mouse embryos." Dev Genes Evol **210**(1): 47-50.
- Pabst, O., R. Zweigerdt, et al. (1999). "Targeted disruption of the homeobox transcription factor Nkx2-3 in mice results in postnatal lethality and abnormal development of small intestine and spleen." Development **126**(10): 2215-2225.
- Parnavelas, J. G. (1999). "Glial cell lineages in the rat cerebral cortex." Exp Neurol **156**(2): 418-429.
- Parnavelas, J. G., J. A. Barfield, et al. (1991). "Separate progenitor cells give rise to pyramidal and nonpyramidal neurons in the rat telencephalon." Cereb Cortex **1**(6): 463-468.
- Parras, C. M., C. Hunt, et al. (2007). "The proneural gene Mash1 specifies an early population of telencephalic oligodendrocytes." J Neurosci **27**(16): 4233-4242.
- Pascual, M., E. Pozas, et al. (2005). "Role of class 3 semaphorins in the development and maturation of the septohippocampal pathway." Hippocampus **15**(2): 184-202.
- Pasquale, E. B. (2005). "Eph receptor signalling casts a wide net on cell behaviour." Nat Rev Mol Cell Biol **6**(6): 462-475.
- Paukert, M. and D. E. Bergles (2006). "Synaptic communication between neurons and NG2+ cells." Curr Opin Neurobiol **16**(5): 515-521.
- Pierani, A. and M. Wassef (2009). "Cerebral cortex development: From progenitors patterning to neocortical size during evolution." Dev Growth Differ **51**(3): 325-342.
- Pinto, L. and M. Gotz (2007). "Radial glial cell heterogeneity--the source of diverse progeny in the CNS." Prog Neurobiol **83**(1): 2-23.
- Pires-Neto, M. A., S. Braga-De-Souza, et al. (1998). "Molecular tunnels and boundaries for growing axons in the anterior commissure of hamster embryos." J Comp Neurol **399**(2): 176-188.
- Pires-Neto, M. A. and R. Lent (1993). "The prenatal development of the anterior commissure in hamsters: pioneer fibers lead the way." Brain Res Dev Brain Res **72**(1): 59-66.
- Pixley, S. K. and J. de Vellis (1984). "Transition between immature radial glia and mature astrocytes studied with a monoclonal antibody to vimentin." Brain Res **317**(2): 201-209.

- Pleasure, S. J., S. Anderson, et al. (2000). "Cell migration from the ganglionic eminences is required for the development of hippocampal GABAergic interneurons." *Neuron* **28**(3): 727-740.
- Plump, A. S., L. Erskine, et al. (2002). "Slit1 and Slit2 cooperate to prevent premature midline crossing of retinal axons in the mouse visual system." *Neuron* **33**(2): 219-232.
- Polito, A. and R. Reynolds (2005). "NG2-expressing cells as oligodendrocyte progenitors in the normal and demyelinated adult central nervous system." *J Anat* **207**(6): 707-716.
- Potiron, V. and J. Roche (2005). "Class 3 semaphorin signaling: the end of a dogma." *Sci STKE* **2005**(285): pe24.
- Price, J. and L. Thurlow (1988). "Cell lineage in the rat cerebral cortex: a study using retroviral-mediated gene transfer." *Development* **104**(3): 473-482.
- Provenzano, C., L. Veneziano, et al. (2008). "Functional characterization of a novel mutation in TITF-1 in a patient with benign hereditary chorea." *J Neurol Sci* **264**(1-2): 56-62.
- Puelles, L., E. Kuwana, et al. (2000). "Pallial and subpallial derivatives in the embryonic chick and mouse telencephalon, traced by the expression of the genes *Dlx-2*, *Emx-1*, *Nkx-2.1*, *Pax-6*, and *Tbr-1*." *J Comp Neurol* **424**(3): 409-438.
- Qian, X., Q. Shen, et al. (2000). "Timing of CNS cell generation: a programmed sequence of neuron and glial cell production from isolated murine cortical stem cells." *Neuron* **28**(1): 69-80.
- Raff, M. C., R. H. Miller, et al. (1983). "A glial progenitor cell that develops in vitro into an astrocyte or an oligodendrocyte depending on culture medium." *Nature* **303**(5916): 390-396.
- Rajagopalan, S., E. Nicolas, et al. (2000). "Crossing the midline: roles and regulation of Robo receptors." *Neuron* **28**(3): 767-777.
- Rakic, P. (1972). "Mode of cell migration to the superficial layers of fetal monkey neocortex." *J Comp Neurol* **145**(1): 61-83.
- Rakic, P. (1988). "Specification of cerebral cortical areas." *Science* **241**(4862): 170-176.
- Rakic, P. (2007). "The radial edifice of cortical architecture: from neuronal silhouettes to genetic engineering." *Brain Res Rev* **55**(2): 204-219.
- Rakic, P., L. J. Stensas, et al. (1974). "Computer-aided three-dimensional reconstruction and quantitative analysis of cells from serial electron microscopic montages of foetal monkey brain." *Nature* **250**(461): 31-34.
- Rao, M. S. and M. Mayer-Proschel (1997). "Glial-restricted precursors are derived from multipotent neuroepithelial stem cells." *Dev Biol* **188**(1): 48-63.
- Raper, J. and C. Mason (2010). "Cellular strategies of axonal pathfinding." *Cold Spring Harb Perspect Biol* **2**(9): a001933.
- Raper, J. A. (2000). "Semaphorins and their receptors in vertebrates and invertebrates." *Curr Opin Neurobiol* **10**(1): 88-94.
- Rash, B. G. and L. J. Richards (2001). "A role for cingulate pioneering axons in the development of the corpus callosum." *J Comp Neurol* **434**(2): 147-157.
- Rashid, T., A. L. Upton, et al. (2005). "Opposing gradients of ephrin-As and EphA7 in the superior colliculus are essential for topographic mapping in the mammalian visual system." *Neuron* **47**(1): 57-69.
- Reillo, I. and V. Borrell (2011). "Germinal Zones in the Developing Cerebral Cortex of Ferret: Ontogeny, Cell Cycle Kinetics, and Diversity of Progenitors." *Cereb Cortex*.
- Reillo, I., C. de Juan Romero, et al. (2011). "A role for intermediate radial glia in the tangential expansion of the mammalian cerebral cortex." *Cereb Cortex* **21**(7): 1674-1694.
- Reiner, O., R. Carrozzo, et al. (1993). "Isolation of a Miller-Dieker lissencephaly gene containing G protein beta-subunit-like repeats." *Nature* **364**(6439): 717-721.
- Ren, T., A. Anderson, et al. (2006). "Imaging, anatomical, and molecular analysis of callosal formation in the developing human fetal brain." *Anat Rec A Discov Mol Cell Evol Biol* **288**(2): 191-204.
- Represa, A. and Y. Ben-Ari (2005). "Trophic actions of GABA on neuronal development." *Trends Neurosci* **28**(6): 278-283.

- Reynolds, R. and R. Hardy (1997). "Oligodendroglial progenitors labeled with the O4 antibody persist in the adult rat cerebral cortex in vivo." *J Neurosci Res* **47**(5): 455-470.
- Richards, L. J., C. Plachez, et al. (2004). "Mechanisms regulating the development of the corpus callosum and its agenesis in mouse and human." *Clin Genet* **66**(4): 276-289.
- Riederer, B. M., P. Berbel, et al. (2004). "Neurons in the corpus callosum of the cat during postnatal development." *Eur J Neurosci* **19**(8): 2039-2046.
- Riederer, B. M. and G. M. Innocenti (1992). "MAP2 Isoforms in Developing Cat Cerebral Cortex and Corpus Callosum." *Eur J Neurosci* **4**(12): 1376-1386.
- Rivas, R. J. and M. E. Hatten (1995). "Motility and cytoskeletal organization of migrating cerebellar granule neurons." *J Neurosci* **15**(2): 981-989.
- Rivers, L. E., K. M. Young, et al. (2008). "PDGFRA/NG2 glia generate myelinating oligodendrocytes and piriform projection neurons in adult mice." *Nat Neurosci* **11**(12): 1392-1401.
- Rohm, B., A. Ottemeyer, et al. (2000). "Plexin/neuropilin complexes mediate repulsion by the axonal guidance signal semaphorin 3A." *Mech Dev* **93**(1-2): 95-104.
- Rossi, A., E. Zoico, et al. (2010). "Quantification of intermuscular adipose tissue in the erector spinae muscle by MRI: agreement with histological evaluation." *Obesity (Silver Spring)* **18**(12): 2379-2384.
- Rothberg, J. M., D. A. Hartley, et al. (1988). "slit: an EGF-homologous locus of *D. melanogaster* involved in the development of the embryonic central nervous system." *Cell* **55**(6): 1047-1059.
- Rothberg, J. M., J. R. Jacobs, et al. (1990). "slit: an extracellular protein necessary for development of midline glia and commissural axon pathways contains both EGF and LRR domains." *Genes Dev* **4**(12A): 2169-2187.
- Rouaux, C. and P. Arlotta (2010). "Fezf2 directs the differentiation of corticofugal neurons from striatal progenitors in vivo." *Nat Neurosci* **13**(11): 1345-1347.
- Rowitch, D. H. and A. R. Kriegstein (2010). "Developmental genetics of vertebrate glial-cell specification." *Nature* **468**(7321): 214-222.
- Rubenstein, J. L., S. Martinez, et al. (1994). "The embryonic vertebrate forebrain: the prosomeric model." *Science* **266**(5185): 578-580.
- Rubin, A. N., F. Alfonsi, et al. (2010). "The germinal zones of the basal ganglia but not the septum generate GABAergic interneurons for the cortex." *J Neurosci* **30**(36): 12050-12062.
- Rudy, B., G. Fishell, et al. (2010). "Three groups of interneurons account for nearly 100% of neocortical GABAergic neurons." *Dev Neurobiol.*
- Sabatier, C., A. S. Plump, et al. (2004). "The divergent Robo family protein rig-1/Robo3 is a negative regulator of slit responsiveness required for midline crossing by commissural axons." *Cell* **117**(2): 157-169.
- Sahay, A., M. E. Molliver, et al. (2003). "Semaphorin 3F is critical for development of limbic system circuitry and is required in neurons for selective CNS axon guidance events." *J Neurosci* **23**(17): 6671-6680.
- Samanta, J. and J. A. Kessler (2004). "Interactions between ID and OLIG proteins mediate the inhibitory effects of BMP4 on oligodendroglial differentiation." *Development* **131**(17): 4131-4142.
- Sanchez-Camacho, C. and P. Bovolenta (2009). "Emerging mechanisms in morphogen-mediated axon guidance." *Bioessays* **31**(10): 1013-1025.
- Sapir, T., M. Elbaum, et al. (1997). "Reduction of microtubule catastrophe events by LIS1, platelet-activating factor acetylhydrolase subunit." *EMBO J* **16**(23): 6977-6984.
- Sato, Y., T. Hirata, et al. (1998). "Requirement for early-generated neurons recognized by monoclonal antibody lot1 in the formation of lateral olfactory tract." *J Neurosci* **18**(19): 7800-7810.
- Schaar, B. T. and S. K. McConnell (2005). "Cytoskeletal coordination during neuronal migration." *Proc Natl Acad Sci U S A* **102**(38): 13652-13657.

- Schaefer, A. W., N. Kabir, et al. (2002). "Filopodia and actin arcs guide the assembly and transport of two populations of microtubules with unique dynamic parameters in neuronal growth cones." *J Cell Biol* **158**(1): 139-152.
- Schaefer, A. W., H. Kamiguchi, et al. (1999). "Activation of the MAPK signal cascade by the neural cell adhesion molecule L1 requires L1 internalization." *J Biol Chem* **274**(53): 37965-37973.
- Schmechel, D. E. and P. Rakic (1979). "A Golgi study of radial glial cells in developing monkey telencephalon: morphogenesis and transformation into astrocytes." *Anat Embryol (Berl)* **156**(2): 115-152.
- Schmid, R. S. and P. F. Maness (2008). "L1 and NCAM adhesion molecules as signaling coreceptors in neuronal migration and process outgrowth." *Curr Opin Neurobiol* **18**(3): 245-250.
- Schuurmans, C., O. Armant, et al. (2004). "Sequential phases of cortical specification involve Neurogenin-dependent and -independent pathways." *Embo Journal* **23**(14): 2892-2902.
- Schuurmans, C. and F. Guillemot (2002). "Molecular mechanisms underlying cell fate specification in the developing telencephalon." *Curr Opin Neurobiol* **12**(1): 26-34.
- Schwarz, Q. and C. Ruhrberg (2010). "Neuropilin, you gotta let me know: should I stay or should I go?" *Cell Adh Migr* **4**(1): 61-66.
- Scicolone, G., A. L. Ortalli, et al. (2009). "Key roles of Ephs and ephrins in retinotectal topographic map formation." *Brain Res Bull* **79**(5): 227-247.
- Serafini, T., S. A. Colamarino, et al. (1996). "Netrin-1 is required for commissural axon guidance in the developing vertebrate nervous system." *Cell* **87**(6): 1001-1014.
- Serafini, T., T. E. Kennedy, et al. (1994). "The netrins define a family of axon outgrowth-promoting proteins homologous to *C. elegans* UNC-6." *Cell* **78**(3): 409-424.
- Shen, Q., Y. Wang, et al. (2006). "The timing of cortical neurogenesis is encoded within lineages of individual progenitor cells." *Nat Neurosci* **9**(6): 743-751.
- Shimamura, K., D. J. Hartigan, et al. (1995). "Longitudinal organization of the anterior neural plate and neural tube." *Development* **121**(12): 3923-3933.
- Shimamura, K. and J. L. Rubenstein (1997). "Inductive interactions direct early regionalization of the mouse forebrain." *Development* **124**(14): 2709-2718.
- Shu, T., K. G. Butz, et al. (2003). "Abnormal development of forebrain midline glia and commissural projections in *Nfia* knock-out mice." *J Neurosci* **23**(1): 203-212.
- Shu, T., Y. Li, et al. (2003). "The glial sling is a migratory population of developing neurons." *Development* **130**(13): 2929-2937.
- Shu, T., A. C. Puche, et al. (2003). "Development of midline glial populations at the corticoseptal boundary." *J Neurobiol* **57**(1): 81-94.
- Shu, T. and L. J. Richards (2001). "Cortical axon guidance by the glial wedge during the development of the corpus callosum." *J Neurosci* **21**(8): 2749-2758.
- Shu, T., V. Sundaresan, et al. (2003). "Slit2 guides both precrossing and postcrossing callosal axons at the midline in vivo." *J Neurosci* **23**(22): 8176-8184.
- Shu, T., K. M. Valentino, et al. (2000). "Expression of the netrin-1 receptor, deleted in colorectal cancer (DCC), is largely confined to projecting neurons in the developing forebrain." *J Comp Neurol* **416**(2): 201-212.
- Silver, J., M. A. Edwards, et al. (1993). "Immunocytochemical demonstration of early appearing astroglial structures that form boundaries and pathways along axon tracts in the fetal brain." *J Comp Neurol* **328**(3): 415-436.
- Silver, J., S. E. Lorenz, et al. (1982). "Axonal guidance during development of the great cerebral commissures: descriptive and experimental studies, in vivo, on the role of preformed glial pathways." *J Comp Neurol* **210**(1): 10-29.
- Smart, I. H., C. Dehay, et al. (2002). "Unique morphological features of the proliferative zones and postmitotic compartments of the neural epithelium giving rise to striate and extrastriate cortex in the monkey." *Cereb Cortex* **12**(1): 37-53.

- Smith, K. M., Y. Ohkubo, et al. (2006). "Midline radial glia translocation and corpus callosum formation require FGF signaling." *Nat Neurosci* **9**(6): 787-797.
- Smukler, S. R., S. B. Runciman, et al. (2006). "Embryonic stem cells assume a primitive neural stem cell fate in the absence of extrinsic influences." *J Cell Biol* **172**(1): 79-90.
- Sousa, V. H., G. Miyoshi, et al. (2009). "Characterization of Nkx6-2-derived neocortical interneuron lineages." *Cereb Cortex* **19 Suppl 1**: i1-10.
- Spassky, N., K. Heydon, et al. (2001). "Sonic hedgehog-dependent emergence of oligodendrocytes in the telencephalon: evidence for a source of oligodendrocytes in the olfactory bulb that is independent of PDGFRalpha signaling." *Development* **128**(24): 4993-5004.
- Sretavan, D. W., E. Pure, et al. (1995). "Disruption of retinal axon ingrowth by ablation of embryonic mouse optic chiasm neurons." *Science* **269**(5220): 98-101.
- Srinivas, S., T. Watanabe, et al. (2001). "Cre reporter strains produced by targeted insertion of EYFP and ECFP into the ROSA26 locus." *BMC Dev Biol* **1**: 4.
- Srinivas, S., T. Watanabe, et al. (2001). "Cre reporter strains produced by targeted insertion of EYFP and ECFP into the ROSA26 locus." *BMC.Dev.Biol.* **1**: 4.
- Stallcup, W. B. (2002). "The NG2 proteoglycan: past insights and future prospects." *J Neurocytol* **31**(6-7): 423-435.
- Stein, E. and M. Tessier-Lavigne (2001). "Hierarchical organization of guidance receptors: silencing of netrin attraction by slit through a Robo/DCC receptor complex." *Science* **291**(5510): 1928-1938.
- Stenman, J., H. Toresson, et al. (2003). "Identification of two distinct progenitor populations in the lateral ganglionic eminence: implications for striatal and olfactory bulb neurogenesis." *J Neurosci* **23**(1): 167-174.
- Stoeckli, E. T. (1998). "Molecular mechanisms of commissural axon pathfinding." *Prog Brain Res* **117**: 105-114.
- Stoeckli, E. T. and L. T. Landmesser (1998). "Axon guidance at choice points." *Curr Opin Neurobiol* **8**(1): 73-79.
- Stoykova, A., D. Treichel, et al. (2000). "Pax6 modulates the dorsoventral patterning of the mammalian telencephalon." *J Neurosci* **20**(21): 8042-8050.
- Stuhmer, T., S. A. Anderson, et al. (2002). "Ectopic expression of the Dlx genes induces glutamic acid decarboxylase and Dlx expression." *Development* **129**(1): 245-252.
- Sugimoto, Y., M. Taniguchi, et al. (2001). "Guidance of glial precursor cell migration by secreted cues in the developing optic nerve." *Development* **128**(17): 3321-3330.
- Sugino, K., C. M. Hempel, et al. (2006). "Molecular taxonomy of major neuronal classes in the adult mouse forebrain." *Nat Neurosci* **9**(1): 99-107.
- Sultana, S., S. W. Sernett, et al. (2000). "Intermediate filament protein synemin is transiently expressed in a subset of astrocytes during development." *Glia* **30**(2): 143-153.
- Sun, Y., S. K. Goderie, et al. (2005). "Asymmetric distribution of EGFR receptor during mitosis generates diverse CNS progenitor cells." *Neuron* **45**(6): 873-886.
- Super, H., J. A. Del Rio, et al. (2000). "Disruption of neuronal migration and radial glia in the developing cerebral cortex following ablation of Cajal-Retzius cells." *Cereb Cortex* **10**(6): 602-613.
- Sussel, L., O. Marin, et al. (1999). "Loss of Nkx2.1 homeobox gene function results in a ventral to dorsal molecular respecification within the basal telencephalon: evidence for a transformation of the pallidum into the striatum." *Development* **126**(15): 3359-3370.
- Suter, D. M. and P. Forscher (2000). "Substrate-cytoskeletal coupling as a mechanism for the regulation of growth cone motility and guidance." *J Neurobiol* **44**(2): 97-113.
- Tabata, H. and K. Nakajima (2003). "Multipolar migration: the third mode of radial neuronal migration in the developing cerebral cortex." *J Neurosci* **23**(31): 9996-10001.
- Tagliatalata, P., J. M. Soria, et al. (2004). "Compromised generation of GABAergic interneurons in the brains of Vax1^{-/-} mice." *Development* **131**(17): 4239-4249.

- Tagne, J. B., S. Gupta, et al. (2012). "Genome-wide analyses of Nkx2-1 binding to transcriptional target genes uncover novel regulatory patterns conserved in lung development and tumors." *PLoS One* **7**(1): e29907.
- Takahashi, T., J. P. Misson, et al. (1990). "Glial process elongation and branching in the developing murine neocortex: a qualitative and quantitative immunohistochemical analysis." *J Comp Neurol* **302**(1): 15-28.
- Takahashi, T., F. Nakamura, et al. (1998). "Semaphorins A and E act as antagonists of neuropilin-1 and agonists of neuropilin-2 receptors." *Nat Neurosci* **1**(6): 487-493.
- Takebayashi, H., Y. Nabeshima, et al. (2002). "The basic helix-loop-helix factor olig2 is essential for the development of motoneuron and oligodendrocyte lineages." *Curr Biol* **12**(13): 1157-1163.
- Takeuchi, H., K. Inokuchi, et al. (2010). "Sequential arrival and graded secretion of Sema3F by olfactory neuron axons specify map topography at the bulb." *Cell* **141**(6): 1056-1067.
- Takiguchi-Hayashi, K., M. Sekiguchi, et al. (2004). "Generation of reelin-positive marginal zone cells from the caudomedial wall of telencephalic vesicles." *J Neurosci* **24**(9): 2286-2295.
- Tamagnone, L., S. Artigiani, et al. (1999). "Plexins are a large family of receptors for transmembrane, secreted, and GPI-anchored semaphorins in vertebrates." *Cell* **99**(1): 71-80.
- Tamamaki, N., Y. Yanagawa, et al. (2003). "Green fluorescent protein expression and colocalization with calretinin, parvalbumin, and somatostatin in the GAD67-GFP knock-in mouse." *J Comp Neurol* **467**(1): 60-79.
- Tanaka, D., Y. Nakaya, et al. (2003). "Multimodal tangential migration of neocortical GABAergic neurons independent of GPI-anchored proteins." *Development* **130**(23): 5803-5813.
- Tanaka, D. H., K. Maekawa, et al. (2006). "Multidirectional and multizonal tangential migration of GABAergic interneurons in the developing cerebral cortex." *Development* **133**(11): 2167-2176.
- Tatsumi, K., H. Takebayashi, et al. (2008). "Genetic fate mapping of Olig2 progenitors in the injured adult cerebral cortex reveals preferential differentiation into astrocytes." *J Neurosci Res* **86**(16): 3494-3502.
- Taverna, E. and W. B. Huttner (2010). "Neural progenitor nuclei IN motion." *Neuron* **67**(6): 906-914.
- Tekki-Kessaris, N., R. Woodruff, et al. (2001). "Hedgehog-dependent oligodendrocyte lineage specification in the telencephalon." *Development* **128**(13): 2545-2554.
- Tessier-Lavigne, M. and C. S. Goodman (1996). "The molecular biology of axon guidance." *Science* **274**(5290): 1123-1133.
- Toresson, H., S. S. Potter, et al. (2000). "Genetic control of dorsal-ventral identity in the telencephalon: opposing roles for Pax6 and Gsh2." *Development* **127**(20): 4361-4371.
- Trotter, J., K. Karram, et al. (2010). "NG2 cells: Properties, progeny and origin." *Brain Res Rev* **63**(1-2): 72-82.
- Tsai, H. H. and R. H. Miller (2002). "Glial cell migration directed by axon guidance cues." *Trends Neurosci* **25**(4): 173-175; discussion 175-176.
- Tsai, L. H. and J. G. Gleeson (2005). "Nucleokinesis in neuronal migration." *Neuron* **46**(3): 383-388.
- Unni, D. K., M. Piper, et al. (2012). "Multiple Slits regulate the development of midline glial populations and the corpus callosum." *Dev Biol*.
- Valcanis, H. and S. S. Tan (2003). "Layer specification of transplanted interneurons in developing mouse neocortex." *J Neurosci* **23**(12): 5113-5122.
- Vallstedt, A., J. M. Klos, et al. (2005). "Multiple dorsoventral origins of oligodendrocyte generation in the spinal cord and hindbrain." *Neuron* **45**(1): 55-67.
- Vallstedt, A., J. Muhr, et al. (2001). "Different levels of repressor activity assign redundant and specific roles to Nkx6 genes in motor neuron and interneuron specification." *Neuron* **31**(5): 743-755.

- Vasudevan, A. and P. G. Bhide (2008). "Angiogenesis in the embryonic CNS: a new twist on an old tale." Cell Adh Migr **2**(3): 167-169.
- Vasudevan, A., J. E. Long, et al. (2008). "Compartment-specific transcription factors orchestrate angiogenesis gradients in the embryonic brain." Nat Neurosci **11**(4): 429-439.
- Virgintino, D., F. Girolamo, et al. (2007). "An intimate interplay between precocious, migrating pericytes and endothelial cells governs human fetal brain angiogenesis." Angiogenesis **10**(1): 35-45.
- Vitalis, T. and J. Rossier (2010). "New insights into cortical interneurons development and classification: Contribution of developmental studies." Dev Neurobiol.
- Volterra, A. and J. Meldolesi (2005). "Astrocytes, from brain glue to communication elements: the revolution continues." Nat Rev Neurosci **6**(8): 626-640.
- Vucurovic, K., T. Gallopin, et al. (2010). "Serotonin 3A receptor subtype as an early and protracted marker of cortical interneuron subpopulations." Cereb Cortex **20**(10): 2333-2347.
- Walsh, F. S. and P. Doherty (1997). "Neural cell adhesion molecules of the immunoglobulin superfamily: role in axon growth and guidance." Annu Rev Cell Dev Biol **13**: 425-456.
- Wang, B., R. R. Waclaw, et al. (2009). "Ascl1 is a required downstream effector of Gsx gene function in the embryonic mouse telencephalon." Neural Dev **4**: 5.
- Wang, D. D. and A. R. Kriegstein (2009). "Defining the role of GABA in cortical development." J Physiol **587**(Pt 9): 1873-1879.
- Wang, X., J. W. Tsai, et al. (2011). "A new subtype of progenitor cell in the mouse embryonic neocortex." Nat Neurosci **14**(5): 555-561.
- Wang, Y., C. A. Dye, et al. (2010). "Dlx5 and Dlx6 regulate the development of parvalbumin-expressing cortical interneurons." J Neurosci **30**(15): 5334-5345.
- Wang, Y., J. Zhang, et al. (2006). "Axonal growth and guidance defects in Frizzled3 knock-out mice: a comparison of diffusion tensor magnetic resonance imaging, neurofilament staining, and genetically directed cell labeling." J Neurosci **26**(2): 355-364.
- Ward, M. E., H. Jiang, et al. (2005). "Regulated formation and selection of neuronal processes underlie directional guidance of neuronal migration." Mol Cell Neurosci **30**(3): 378-387.
- Watanabe, K., D. Kamiya, et al. (2005). "Directed differentiation of telencephalic precursors from embryonic stem cells." Nat Neurosci **8**(3): 288-296.
- Wichterle, H., J. M. Garcia-Verdugo, et al. (1999). "Young neurons from medial ganglionic eminence disperse in adult and embryonic brain." Nat Neurosci **2**(5): 461-466.
- Wichterle, H., I. Lieberam, et al. (2002). "Directed differentiation of embryonic stem cells into motor neurons." Cell **110**(3): 385-397.
- Wichterle, H., D. H. Turnbull, et al. (2001). "In utero fate mapping reveals distinct migratory pathways and fates of neurons born in the mammalian basal forebrain." Development **128**(19): 3759-3771.
- Wigley, R. and A. M. Butt (2009). "Integration of NG2-glia (synantocytes) into the neuroglial network." Neuron Glia Biol **5**(1-2): 21-28.
- Willemsen, M. A., G. J. Breedveld, et al. (2005). "Brain-Thyroid-Lung syndrome: a patient with a severe multi-system disorder due to a de novo mutation in the thyroid transcription factor 1 gene." Eur J Pediatr **164**(1): 28-30.
- Wilson, S. W. and C. Houart (2004). "Early steps in the development of the forebrain." Dev Cell **6**(2): 167-181.
- Wilson, S. W. and J. L. Rubenstein (2000). "Induction and dorsoventral patterning of the telencephalon." Neuron **28**(3): 641-651.
- Winberg, M. L., K. J. Mitchell, et al. (1998). "Genetic analysis of the mechanisms controlling target selection: complementary and combinatorial functions of netrins, semaphorins, and IgCAMs." Cell **93**(4): 581-591.
- Windrem, M. S., M. C. Nunes, et al. (2004). "Fetal and adult human oligodendrocyte progenitor cell isolates myelinate the congenitally dysmyelinated brain." Nat Med **10**(1): 93-97.

- Wonders, C. P. and S. A. Anderson (2006). "The origin and specification of cortical interneurons." Nat Rev Neurosci **7**(9): 687-696.
- Xiang, Y., Y. Li, et al. (2002). "Nerve growth cone guidance mediated by G protein-coupled receptors." Nat Neurosci **5**(9): 843-848.
- Xu, Q., I. Cobos, et al. (2004). "Origins of cortical interneuron subtypes." J Neurosci **24**(11): 2612-2622.
- Xu, Q., M. Tam, et al. (2008). "Fate mapping Nkx2.1-lineage cells in the mouse telencephalon." J Comp Neurol **506**(1): 16-29.
- Xu, Q., C. P. Wonders, et al. (2005). "Sonic hedgehog maintains the identity of cortical interneuron progenitors in the ventral telencephalon." Development **132**(22): 4987-4998.
- Yang, Z., R. Suzuki, et al. (2006). "NG2 glial cells provide a favorable substrate for growing axons." J Neurosci **26**(14): 3829-3839.
- Yates, P. A., A. L. Roskies, et al. (2001). "Topographic-specific axon branching controlled by ephrin-As is the critical event in retinotectal map development." J Neurosci **21**(21): 8548-8563.
- Yau, H. J., H. F. Wang, et al. (2003). "Neural development of the neuregulin receptor ErbB4 in the cerebral cortex and the hippocampus: preferential expression by interneurons tangentially migrating from the ganglionic eminences." Cereb Cortex **13**(3): 252-264.
- Ye, P., L. Li, et al. (2002). "Myelination is altered in insulin-like growth factor-I null mutant mice." J Neurosci **22**(14): 6041-6051.
- Yee, K. T., H. H. Simon, et al. (1999). "Extension of long leading processes and neuronal migration in the mammalian brain directed by the chemoattractant netrin-1." Neuron **24**(3): 607-622.
- Yorke, C. H., Jr. and V. S. Caviness, Jr. (1975). "Interhemispheric neocortical connections of the corpus callosum in the normal mouse: a study based on anterograde and retrograde methods." J Comp Neurol **164**(2): 233-245.
- Yoshida, M., S. Assimakopoulos, et al. (2006). "Massive loss of Cajal-Retzius cells does not disrupt neocortical layer order." Development **133**(3): 537-545.
- Yoshida, M., Y. Suda, et al. (1997). "Emx1 and Emx2 functions in development of dorsal telencephalon." Development **124**(1): 101-111.
- Yozu, M., H. Tabata, et al. (2005). "The caudal migratory stream: a novel migratory stream of interneurons derived from the caudal ganglionic eminence in the developing mouse forebrain." J Neurosci **25**(31): 7268-7277.
- Ypsilanti, A. R., Y. Zagar, et al. (2010). "Moving away from the midline: new developments for Slit and Robo." Development **137**(12): 1939-1952.
- Yun, K., S. Garel, et al. (2003). "Patterning of the lateral ganglionic eminence by the Gsh1 and Gsh2 homeobox genes regulates striatal and olfactory bulb histogenesis and the growth of axons through the basal ganglia." J Comp Neurol **461**(2): 151-165.
- Yun, K., S. Potter, et al. (2001). "Gsh2 and Pax6 play complementary roles in dorsoventral patterning of the mammalian telencephalon." Development **128**(2): 193-205.
- Zhou, F. Q., C. M. Waterman-Storer, et al. (2002). "Focal loss of actin bundles causes microtubule redistribution and growth cone turning." J Cell Biol **157**(5): 839-849.
- Zhou, H. F. and R. D. Lund (1992). "Migration of astrocytes transplanted to the midbrain of neonatal rats." J Comp Neurol **317**(2): 145-155.
- Zhou, M., G. P. Schools, et al. (2006). "Development of GLAST(+) astrocytes and NG2(+) glia in rat hippocampus CA1: mature astrocytes are electrophysiologically passive." J Neurophysiol **95**(1): 134-143.
- Zhou, Q. and D. J. Anderson (2002). "The bHLH transcription factors OLIG2 and OLIG1 couple neuronal and glial subtype specification." Cell **109**(1): 61-73.
- Zhou, Y., R. A. Gunput, et al. (2008). "Semaphorin signaling: progress made and promises ahead." Trends Biochem Sci **33**(4): 161-170.
- Zhu, X., D. E. Bergles, et al. (2008). "NG2 cells generate both oligodendrocytes and gray matter astrocytes." Development **135**(1): 145-157.

- Zhu, X., R. A. Hill, et al. (2008). "NG2 cells generate oligodendrocytes and gray matter astrocytes in the spinal cord." Neuron Glia Biol **4**(1): 19-26.
- Zonta, M., M. C. Angulo, et al. (2003). "Neuron-to-astrocyte signaling is central to the dynamic control of brain microcirculation." Nat Neurosci **6**(1): 43-50.
- Zou, Y. and A. I. Lyuksyutova (2007). "Morphogens as conserved axon guidance cues." Curr Opin Neurobiol **17**(1): 22-28.
- Zou, Y., E. Stoeckli, et al. (2000). "Squeezing axons out of the gray matter: a role for slit and semaphorin proteins from midline and ventral spinal cord." Cell **102**(3): 363-375.